ELECTROPHYSIOLOGICAL AND BIOCHEMICAL STUDIES ON THE EFFECTS OF RNA AND PROTEIN SYNTHESIS INHIBITORS ON THE CIRCADIAN RHYTHM OF THE ISOLATED *APLYSIA* EYE

Thesis by

Barry Samuel Rothman

In Partial Fulfillment of the Requirements

for the Degree of

Doctor of Philosophy

California Institute of Technology

Pasadena, California

1976

(Submitted September 16, 1975)

ACKNOWLEDGEMENT

I would like to take this opportunity to thank the people who have helped me in the completion of this Ph.D. thesis:

My parents, Arthur and Claire Rothman, for providing me with the funds necessary to obtain my undergraduate education, and without whose efforts none of the following work would have been possible;

Haverford College, for an introduction to biology and a unique opportunity for personal development;

Nan, my wife, for emotional and financial support, artistry both creative and graphic, and for being my best friend for the past five years;

Prufrockers old and new: Al Jesaitis, Jack Geltosky, John Flory, Jim McArdle, Dave Pollard, Lloyd and Peg Smith, for making Caltech a happier place to be, and teaching me the joys of hiking and bicycling uphill, "torture", and the production of theatrical events; and special appreciation to Dave Armstrong for many good times and absurd conversations and Charlie and Glynn Birdwell for a very special relationship;

My labmates: Steve Arch, Arnold Eskin, Dave Wilson, Bob Sener, Bob Berry, Gerry Audesirk, Duncan Stuart, Jeff Ram, Barbara Keenan, Shelly Rempel, Louise Fletcher, Sandi Smith, Robin Paltis, Reni Alvarez, Jim Gilliam and Floyd Schlechte for happy times in and out of school, and a great amount of scientific assistance;

The McMahon group, Dan, Mark Miller and Chris West for being tremendously cooperative consultants;

Ron Konopka, for many provocative discussions on circadian rhythms and for encouragement during the writing of this Ph. D. thesis;

The Burkes, my new family, for "adopting" me, and special thanks to Anne Burke for typing rough drafts, and Ellen Burke and Mary Burke for able assistance in data analysis;

Harpo, with whom I have spent many long nights, and to whom I wish much happiness upon becoming 55 or 65;

My Thesis Advisory Committee: Seymour Benzer, Eric Davidson, Herschel Mitchell and C.A.G. Wiersma for the guidance they have offered, and special appreciation to Felix Strumwasser for six years of friendship, reasonable advice and excellent laboratory facilities;

And finally the taxpayers of the United States, who provided my stipend and much of my research support funds.

ABSTRACT

The isolated eye of Aplysia californica produces a circadian rhythm of optic nerve activity. In filtered sea water, at 15°C, in constant darkness, the free-running period of the circadian rhythm is 23.4 hrs. Optic nerve activity is recorded by means of suction electrode, and is in the form of spontaneous compound action potentials (CAPs) which vary in frequency from 0 to 200 per hr.

Experiments were designed to test the necessity of macromolecular synthesis for the production of the circadian rhythm. Eyes were given a pulse of an inhibitor of RNA or protein synthesis and the effects on the circadian rhythm, biochemistry or electrophysiology assayed.

When eyes were given a 3 hr pulse of actinomycin D (AMD)(4 ug/ml), the circadian rhythm was inhibited without blocking spontaneous CAP activity altogether. Eyes receiving a 3 hr pulse of aflatoxin B_1 (AFTX) (16 ug/ml) revealed similar effects in half the cases studied, while in the other half a reduced amplitude phase delayed circadian rhythm was found. Eyes given a 12 hr pulse of puromycin (PURO)(20-134 ug/ml) or cycloheximide (CHX)(500-2000 ug/ml) beginning in mid-subjective night had their circadian rhythms phase delayed by 12-16 hrs and 6-12 hrs, respectively, after the drug pulse was washed out. A phase-response curve determined for the effects of a 6 hr PURO (125 ug/ml) pulse showed that maximum phase delays were caused by pulses given in late subjective night, and maximum phase advances caused by pulses given in early subjective day.

In biochemical studies, incorporation of ^{3}H-uridine and ^{14}C-leucine

were measured 1-9, 9-17, 49-57 and 73-81 hrs after the removal of a 3 hr pulse of AFTX (16 ug/ml) or AMD (4 ug/ml). Uridine incorporation was inhibited by 50-75% from 1 to 17 hrs after an AFTX or AMD pulse, while leucine incorporation was inhibited by 40-70% from 1 to 81 hrs after an AFTX pulse, and by about 20% from 49 to 57 hrs after an AMD pulse. At all other times measured, uridine and leucine incorporation were not significantly different from controls. In other biochemical studies the effects of PURO and CHX on leucine incorporation were tested by means of a double-label SDS-polyacrylamide gel system. When eyes were labeled during the last 5 hrs of a 12 hr pulse of PURO (20 ug/ml) or CHX (500 ug/ml), incorporation was inhibited by about 50%. The distribution of label in the gels of PURO-treated eyes showed increasing inhibition of incorporation with increasing molecular weight above 75,000 daltons, while in the gels of CHX-treated eyes, incorporation was almost equally inhibited at all molecular weights. A 12 hr PURO (125 ug/ml) inhibited leucine incorporation by about 85%, while the distribution of label in the gels showed increasing inhibition of incorporation with increasing molecular weight above 12,000 daltons. At 12-20 hrs and 20-28 hrs after the end of the PURO pulse, incorporation was normal except for a small peak at 20,000 daltons.

The electrophysiological properties of eyes were tested by recording spontaneous CAP activity and responses to light pulses at various times before, during and after the administration of a drug pulse. Eight electrophysiological parameters were measured and compared quantitatively between experimental and control eyes. They were the latency,

amplitude and frequency of both the phasic and tonic light responses; and the amplitude and frequency of spontaneous CAP activity. AFTX (3 hrs, 16 ug/ml) induced multiphasic tonic light responses during the drug pulse; and when applied during the peak of an activity cycle, increased the frequency of spontaneous CAP activity by 35% for the remainder of the cycle. AMD (3 hrs, 4 ug/ml) caused a 13% increase in spontaneous CAP amplitude and a 10% decrease in tonic light response latency subsequent to its removal. PURO (12 hrs, 20 ug/ml) increased the amplitude of the tonic light response by 23% when measured more than 7 hrs after the end of the pulse. CHX (12 hrs, 500 ug/ml) caused a 32% increase in the tonic light response frequency measured 0-7 hrs after the end of the pulse, and a 33% decrease in the duration of spontaneous CAP bursts during the pulse.

The results of these experiments indicate that doses of four inhibitors of macromolecular synthesis capable of modifying the circadian rhythm of the eye reduce the incorporation of uridine and/or leucine and cause only small changes in the electrophysiolohy of the eye. These data suggest that the production of the circadian rhythm of the Aplysia eye is dependent on macromolecular synthesis.

TABLE OF CONTENTS

Acknowledgement ii

Abstract iv

Chapter One---Review of Circadian Rhythms

I. Ubiquity of Circadian Rhythms 2

II. Common Properties of Circadian Rhythms 2

A. The Free-Running Rhythm 2

B. Small Dependence of the Period on the Nature of Constant Conditions 3

C. Phase Shifts by Light or Temperature Pulses 4

D. Limited Range of Entrainment 4

III. Mechanism of the Free-Running Circadian Rhythm 5

A. The Endogenous Nature of the Circadian Oscillator 5

B. The Involvement of Macromolecular Synthesis 7

C. Inhibitor Studies 8

1) Inhibitors of Macromolecular Synthesis 8

2) Other Agents 12

D. Control of Circadian Activities 14

E. Clock Mutants 15

IV. Location of the Circadian Oscillator 16

Chapter Two---Review of the Aplysia Eye

I. Gross Aspects of the Aplysia Eye 23

II. Role of the Eye in Aplysia 23

Chapter Two, Continued

III. Anatomy..... 27

IV. Electrophysiology of the Aplysia Eye..... 29

A. Optic Nerve Impulses..... 29

B. Intracellular Recordings..... 30

C. Wiring of the Eye..... 31

V. Properties of the Aplysia Eye Circadian Rhythm..... 35

A. The Free-Running Rhythm..... 35

B. In Vitro Entrainment..... 36

C. The Aplysia Eye in Perspective..... 39

Chapter Three---Review of the Biochemical Effects of Four Inhibitors of Macromolecular Synthesis: Aflatoxin B_1, Actinomycin D, Puromycin and Cycloheximide

I. Aflatoxin B_1..... 57

A. Binding of AFTX-B_1 to DNA, RNA and Protein..... 58

B. Effects of AFTX-B_1 on Transcription and Translation In Vivo..... 65

C. Side Effects..... 72

D. Summary..... 77

II. Actinomycin D..... 79

A. Binding to DNA..... 80

B. Inhibition of RNA and Protein Synthesis In Vivo..... 84

C. Side Effects..... 86

D. Summary..... 90

Chapter Three, Continued

III. Puromycin..... 91

A. Effect on Protein Synthesis..... 91

B. Side Effects..... 94

C. Summary..... 100

IV. Cycloheximide..... 100

A. Effect on Protein Synthesis..... 100

B. Side Effects..... 104

C. Summary..... 110

Chapter Four---Effects of Aflatoxin B_1 and Actinomycin D on the Circadian Rhythm of Spontaneous CAP Activity

I. Introduction..... 126

II. Materials and Methods..... 128

A. Recording of Optic Nerve Activity..... 128

B. Drugs..... 129

C. Periodogram Analysis..... 130

III. Results..... 130

A. Normal Eyes..... 130

B. Drug-Induced Changes in Rhythmicity..... 132

1) Arhythmicity..... 132

2) Reduced Amplitude Circadian Rhythms..... 134

3) Low Amplitude Oscillations of Higher Frequency... 134

4) Prolonged Activity Cycles..... 135

C. Dose-Response Relationships..... 135

Chapter Four, Continued

D. Phase-Response Relationships..... 137

E. Zeitgeber Experiments..... 138

F. Electrophysiology of Drug-Treated Eyes..... 140

IV. Discussion..... 144

A. Inhibition of Circadian Rhythmicity..... 144

B. Electrophysiology of Drug-Treated Eyes..... 145

C. Level of Drug Action..... 147

Chapter Five---The Biochemical Effects of Aflatoxin B_1 and Actinomycin D on the Eye

I. Introduction..... 182

II. Materials and Methods..... 182

A. Double Label Experiments..... 183

B. Single Label Experiments..... 185

III. Results..... 186

IV. Discussion..... 189

A. Inhibition of Uridine and Leucine Incorporation..... 189

V. Appendix I---Supplementary Control Experiments..... 193

A. Incorporation of Label into RNA and Protein..... 193

B. The Source of Incorporation..... 194

C. Specific Activity of Delensed vs. Intact Eyes..... 196

D. Sensitivity to Changes in Amount of Protein..... 197

VI. Appendix II---Leucine Pool Studies..... 201

A. Introduction..... 201

Chapter Five, Continued

B. Materials and Methods..... 202

1) Labeling of Eyes..... 202

2) Dinitrophenylation of Samples..... 202

3) Purification of DNP-Leucine..... 204

a) Two Dimensional Thin Layer Chromatography..... 204

b) One Dimensional Thin Layer Chromatography..... 206

4) Counting of Radioactivity..... 206

C. Results and Discussion..... 207

1) Quantitative Analysis of the ^{14}C-Leucine Content of Eye Supernatants--One Dimensional TLC..... 207

2) Analysis of ^{14}C-Leucine Specific Activity by Two Dimensional TLC..... 209

3) Test of the Sensitivity of the Method to Changes in Specific Activity..... 212

4) Test of Inulin as an Extracellular Marker..... 214

5) Comparison of ^{14}C-Leucine Specific Activities and Incorporation in Pairs of Eyes..... 217

Chapter Six---Effects of Puromycin and Cycloheximide on the Circadian Rhythm of Spontaneous CAP Activity

I. Introduction..... 242

II. Materials and Methods..... 243

A. Recording Optic Nerve Activity..... 243

B. Drug Solutions..... 243

Chapter Six, Continued

III. Results..... 244

A. Normal Eyes..... 244

B. Dose-Response Relationships..... 243

1) During the Drug Pulse..... 246

2) Zero to Seven Hours After the Pulse..... 248

3) More Than Seven Hours After the Drug Pulse..... 249

C. The Effect of Varying Puromycin Pulse Duration..... 253

D. Phase-Response Relationships..... 254

1) During the PURO Pulse..... 255

2) Zero to Seven Hours After the PURO Pulse..... 256

3) More Than Seven Hours After the PURO Pulse..... 256

E. Electrophysiology of Drug-Treated Eyes..... 258

IV. Discussion..... 262

A. The Nature of the Phase Shift..... 262

B. The Electrophysiology of Drug-Treated Eyes..... 264

1) PURO Effects..... 265

2) CHX Effects..... 267

C. Level of Drug Action..... 268

Chapter Seven---The Biochemical Effects of Puromycin and Cycloheximide on the Eye

I. Introduction..... 296

II. Materials and Methods..... 297

A. Labeling of Eyes..... 297

Chapter Seven, Continued

B. Preparation of Gel Samples..... 298

C. Gel Techniques..... 299

III. Results..... 300

A. Control Eyes..... 300

B. Threshold Studies..... 301

C. Kinetics of PURO Inhibition..... 302

IV. Discussion..... 304

A. Control Vs. Control Eyes..... 304

B. Threshold Studies..... 306

C. Kinetics of PURO Inhibition..... 307

V. Appendix I---Behavior of Molecular Weight Standards on SDS-Polyacrylamide Gels..... 311

Chapter Eight---Summary and Discussion of Experimental Results Presented in this Ph.D. Thesis

I. Modification of the Circadian Oscillator..... 334

II. Biochemical Effects of Inhibitors..... 336

III. Side Effects of Inhibitors..... 339

IV. Perspectives..... 344

CHAPTER I

REVIEW OF CIRCADIAN RHYTHMS

I Ubiquity of Circadian Rhythms

A circadian rhythm (CR) is an endogenously controlled oscillation in a biological activity with a period of about 24 hours. Under constant conditions of the appropriate temperature and light intensity, the CR free-runs at its natural frequency. The CR may become entrained to a driving oscillation, such as the light-dark cycle on earth or an artificial cycle in the laboratory, with a period different from its free-running period.

Organisms showing CRs span the eukaryotic phylogeny from Euglena (1) to man (2). Equally diverse is the type of circadian activity. CRs are found in cellular processes such as oxygen evolution (3), luminescence (4), amino acid incorporation (5); electrophysiological activities such as spike frequency and membrane potential oscillations (6); and behavioral activities such as locomotion (6) and phototaxis (1). Even though the organism studied and type of circadian activity may vary, many common properties of CRs have been recognized.

II Common Properties of Circadian Rhythms

The formal properties of CRs have been recently reviewed by both Bünning (7) and Pittendrigh (8). A summary of the four most important properties follows:

A. The Free-Running Rhythm

CRs free-run under constant conditions with a period close to, but usually not equal to, 24 hours. The period of the free-running CR is determined by the genetic make-up of the organism (9,10,11) and

the conditions under which the system is maintained (12,13). Free-running CRs, such as the CR of luminescence in Gonyaulax, can persist for months (dim LL, ? lux) (14), or can damp out in a few cycles [DD (14) or bright LL > 7,300 lux (15)], depending on the organism and conditions of maintenance. When a CR is damped out it can sometimes be (re)initiated by a stimulus (zeitgeber) such as a light pulse (16) or temperature (17) pulse, or a sudden change to a new light (16) or temperature (17) level. In Gonyaulax cultures, a transition to dim LL (970 lux) after maintenance in bright LL (8,600 lux) for more than a year can initiate the CR of luminescence (15).

B. Small Dependence of the Period on the Nature of Constant Conditions

The period of free-running CRs shows a small dependence on the level of light or temperature under which the system is maintained. The Q_{10} of free-running periods usually varies from about 0.85, as found with the CR of luminescence in Gonyaulax (16 to 32°C) (18), to 1.3, as found with the CR of leaf movement in Phaseolus (15 to 35°C) (19). The discovery of both "positive" and "negative" temperature coefficients probably reflects the existence of imperfect temperature compensation mechanisms in the systems studied.

The level of illumination can also influence the period of the free-running CR. Aschoff's rule (12) states that the free-running period of day-active animals is decreased by greater light intensities; whereas the period is increased by greater light intensities in

nocturnal animals. Although it is difficult to classify plants as day or night-active, the free-running period of at least one plant CR, luminescence in Gonyaulax, is decreased by higher light levels (14). Changes in the free-running period caused by changes in light or temperature levels rarely exceed 10% (8).

C. Phase Shifts by Light or Temperature Pulses

Although the constant level of light or temperature has little effect on the free-running period, a pulse change of either parameter can phase shift the CR (8,17). For a given stimulus, the direction and magnitude of the phase shift is phase dependent. Pulses applied during subjective day usually have little effect on the phase of the CR; pulses given during the first half of subjective night tend to cause phase delays, while those applied during the second half of subjective night tend to cause phase advances (13). The phase dependent response of circadian systems to light and temperature pulses accounts for their ability to entrain to periodic light and temperature stimuli (13).

D. Limited Period of Entrainment

The range of periods to which circadian systems can be entrained depends on the organism and the type of driving stimulus employed (16). In Drosophila the range of the LD entrainment period for the eclosion CR is from 14 to 35 hours, whereas a much narrower range of 23 to 25 hours is found for the activity CR of mice (16). Most circadian entrainment limits are within the range of

18 to 30 hours in period (7). Presumably the limits of entrainment are predictable from the magnitude of the maximal phase advance and phase delay found in the phase-response plot (using the appropriate stimuli) of the organism being studied (13).

Outside the range of entrainment the CR may free-run; or when driven by higher frequency oscillations, e.g. LD 2:2 or 6:6 cycles, the CR may exhibit frequency demultiplication by synchronizing to an integral multiple of the driving period, e.g. 24 hours (7,16).

III Mechanism of the Free-Running Circadian Rhythm

Attempts to understand the mechanisms underlying CRs have proceeded on many levels. Such a mechanism is referred to in this discussion as a circadian oscillator (CO). Studies of the interactions between COs in multicellular organisms, and the coupling of COs to both environmental stimuli and overt activities are still being pursued. However the most pertinent area of investigation, in regard to this Ph.D. thesis, has been directed toward an understanding of the biochemical basis of the free-running CO. I will therefore limit the remainder of this chapter to a discussion of the progress made in this area.

A. The Endogenous Nature of the Circadian Oscillator

Evidence to date indicates that free-running CRs are driven by an endogenous process, although no unequivocal proof has been demonstrated. Arguments in favor of the exogenous nature of CRs require special assumptions concerning the transduction of an environmental rhythm into free-running CRs with a different period.

Brown has been a proponent of the theory that free-running CRs are driven by geophysical oscillations. He claims that a variety of organisms including potatoes, fiddler crabs and rats exhibit solar day (24 hour) or lunar day (24.8 hour) rhythms when isolated under "constant conditions". Many of these rhythms have properties that correlate with changes in atmospheric temperature, barometric pressure or level of cosmic radiation. Brown also maintains that magnetic, electrical and gamma ray fields can influence the direction of travel of snails and flatworms. From these data he hypothesizes that geophysical oscillations can be transduced into free-running CRs (of a different period) by means of a constant phase shift each cycle (20,21). Although Brown's experiments raise interesting questions regarding the isolation of circadian systems from, and entrainment by, environmental oscillations, they are not necessarily relevant to free-running CRs. Furthermore, his mechanism would require phase-independent phase shifts, and is thus not supported by available evidence (see section IC, Phase Shifts by Light or Temperature Pulses).

Experiments designed to test the influence of the Earth's rotation on the period of free-running CRs have been conducted at the South Pole. Organisms showing CRs of locomotion, growth or eclosion were placed in light-tight boxes on slowly spinning turntables that allowed rotation relative to the sun to be adjusted to 0, 20.0, 24.0 and 28.8 hours in period. Regardless of the period of

rotation, the period of the free-running CRs was not affected. However the influence of daily rotation around the magnetic pole could not be eliminated (22). Complete isolation from influences of the Earth's rotation may only be possible in outer space. Until a space experiment is conducted the idea of endogenously driven free-running CRs remains a hypothesis.

B. The Involvement of Macromolecular Synthesis

In the broadest sense, macromolecular (RNA, protein) synthesis is necessarily involved in the CO mechanism since genetic control of the period of the free-running CR has been demonstrated in a few cases (9,10,11). However, the manner in which the genome influences the CO is not at all understood.

In a more restricted view, macromolecular synthesis could be directly involved in the time-keeping mechanism. For example, in the chronon model of Ehret and Trucco the transcription and translation of certain genetic information is hypothesized to be the time base for the CO. According to this theory, the circadian escapement mechanism consists of the sequential, linear transcription of polycistronic complexes of DNA (chronons). The rate-limiting steps for the transcription of the entire chronon, however, reside in intercistronic events such as diffusion of mRNA from the nucleus, and translation. These events are necessary for transcription to proceed to the next cistron. When the end of a chronon is reached, the existence of circular chronons, or certain biochemical events such as

the depletion of essential substrates, allow reinitiation of the chronon transcription (23). However, this theory does not deal adequately with the temperature compensation or the phase lability of CRs.

Macromolecular synthesis could be just indirectly involved in circadian rhythmicity. The synthesis of enzymes that produce a CR of substances (24) involved in the expression of an overt circadian activity would be an example. The half-lives of macromolecules indirectly contributing to the CO would determine their degree of involvement. Very long half-lives would make the involvement of macromolecular synthesis very remote, as may be the case in dormant onion seeds. In this system, a free-running CR of gas exchange occurs in DD. It has a Q_{10} lying between 0.83 and 1.17, and is expressed in the absence of detectable DNA, RNA and protein synthesis (25). Whether absolutely no macromolecular synthesis occurs in the dormant seed, however, remains unanswered. Experiments designed to probe the circadian mechanism have taken essentially three different approaches. They are: 1) the use of inhibitors of various cellular processes to disrupt CRs, 2) a search for the controls of circadian biochemical activities, and 3) an analysis of CR mutants. These three approaches are discussed in greater detail below.

C. Inhibitor Studies

(1) Inhibitors of Macromolecular Synthesis

Inhibitors whose primary effects are on RNA or protein synthesis have been used to test the necessity of macromolecular

synthesis in the production of CRs. Actinomycin D (AMD), known to block DNA-dependent RNA synthesis in a variety of organisms (26), has been used most extensively. The most thorough study of the effects of this drug was conducted by Karakashian and Hastings on the CR of glow bioluminescence in the marine dinoflagellate Gonyaulax. Either pulse (8 hours, 0.16 µg/ml) or continuous (0.02 to 0.33 µg/ml) exposure of Gonyaulax cultures to AMD caused irreversible inhibition of the luminescence CR without causing a total block of luminescence activity. By varying the phase of AMD (1.0 µg/ml) administration, it was discovered that AMD had to be given 20 hours or more before the anticipated onset of an activity cycle to block its expression (27,28). Inhibition of circadian rhythmicity by AMD (0.27 to 2.7 µg/ml) has also been found in intact Acetabularia, although the effect occurred after 6 to 16 days of continuous exposure, depending on the dose. The CRs of both photosynthesis and chloroplast shape were similarly affected (29). In neither Gonyaulax nor Acetabularia were the effects on RNA or protein synthesis determined for CR-modifying doses of AMD. (27-29).

Karakashian and Hastings also showed that continuous exposure of Gonyaulax cultures to puromycin (2×10^{-5} M) or mitomycin C (0.52 µg/ml) inhibited the CR of luminescence, whereas exposure to novobiocin (2.6×10^{-4} M), amethopterin (10^{-5} M) or chloramphenicol (3.1×10^{-4} M) allowed at least partial expression of the CR (28). The above agents are thought to have the following biochemical effects, respectively: inhibition of protein synthesis in prokaryotes and

eukaryotes; cross-linking or fragmentation of DNA in prokaryotes and eukaryotes; inhibition of cell wall, DNA, RNA and protein synthesis in prokaryotes; inhibition of purine and thymine nucleotide synthesis in prokaryotes and eukaryotes; inhibition of protein synthesis in prokaryotes, mitochondria and chloroplasts (26).

In one case the period, and in another the phase of a CR have been changed by AMD. Macdowall found that the CR of sap exudation from decapitated stems of Nicotiana tabacum increased in period from about 24 to 28 hours for 3 days in the presence of 0.25 µg/ml AMD. After return to the normal medium, the period of the CR became normal, although the 12 hour phase delay caused by exposure to AMD was maintained (30). Strumwasser has shown that the CR of spike frequency recorded intracellularly from neuron R15 in the isolated abdominal ganglion of Aplysia can be phase shifted by intracellular injection of AMD. When the drug was injected during subjective night, it caused a phase advance. A phase delay was caused by AMD injected during subjective day. Intracellular AMD concentration was estimated to be 1.2 µg/ml (31). The effects of AMD on RNA synthesis were not determined in either of the above experiments.

A lengthening of the CR period has also been caused by cycloheximide (CHX), an inhibitor of protein synthesis (26). Feldman found that cultures of Euglena exposed continuously to 0.2 to 4.0 µg/ml doses of CHX showed an increase in the period of the phototactic motility CR. The lengthening of the period was dose-dependent and reversible,

although the phase of the CR remained different from controls after CHX was removed. Studies of cells exposed to light pulses while being exposed to CHX revealed that the resulting phase shifts were consistent with the longer period CR. Measurement of phenylalanine incorporation one day after the beginning of CHX administration showed that incorporation was inhibited 19 to 80% by CHX doses capable of lengthening the CR period. Although there was a correlation of increasing period length and increasing inhibition of incorporation with increasing CHX doses, the drug had a much greater effect on incorporation than on the CR period (1).

Interpretation of the above studies presents some difficulties. To help establish a connection between biochemical activities and the circadian clock in inhibitor studies, the effects of the inhibitor should be examined on three different levels. First, the inhibitor should be shown to affect the CO. Complete inhibition of circadian rhythmicity is not necessarily indicative of CO disruption, since a block in the connection between the CO and the overt circadian activity could also bring about this effect. In contrast, changes in the phase or the period of a CR are generally considered to reflect changes in the CO mechanism. Given these criteria, of the inhibitor studies mentioned above, only those of Strumwasser, and Macdowall and Feldman have shown changes at the CO level.

Second, the biochemical effect of the inhibitor should be assayed at doses capable of modifying the CO. Only the study of Feldman fulfills this criterion.

Third, the possibility of inhibitor side effects causing the CO lesion should be ruled out. This might be accomplished by the use of an inhibitor specific for only one biochemical process, if such an agent is available. More likely, the inhibitors used are not this specific, so that a number of structurally different inhibitors affecting the same biochemical pathway should be used. Of the above studies, only Karakashian and Hastings tested the effects of a number of inhibitors of macromolecular synthesis on a CR.

None of the above studies meets all three criteria.

(2) Other Agents

In attempts to gain some understanding of the level of CO organization, circadian systems have been treated with a large variety of biologically active chemicals, including inhibitors of respiration, photosynthesis, glycolysis and mitosis (32). Of all agents tested, four have caused consistent results on a variety of organisms. Heavy water (D_2O) and ethanol have caused a lengthening of the CR period; ethanol, valinomycin, and high potassium pulses have caused phase shifts.

Of these agents, heavy water has been the most extensively studied. To date at least two protozoans, three insects, an isopod, six vertebrates and one higher plant have shown lengthened CR periods from doses of 10 to 100% D_2O in their media or drinking water. Typically, heavy water causes a 2 to 7% increase in the free-running period per 10% D_2O administered. In addition, 20 to 30% D_2O has been

shown to lengthen the period of higher frequency biological rhythms such as the electric organ discharge rate (1 msec period) in the fish Stenarchus, the respiratory gill movements of gold fish (12 second period) and the respiratory or cardiac rhythms (∿ 12 second periods) of four marine invertebrates by 3 to 37% (33). Identification of the CR-dependent biochemical processes affected by D_2O has not been attempted because of the large number of solvent and isotope substitution effects expected.

Ethanol (0.25 to 2.5%) has lengthened the free-running period of the activity CR of the isopod Excirolana (34) and the CR of leaf movements in Phaseolus (35). In both cases the CR period was lengthened about 6 to 8% per 1% ethanol in the bathing media. Furthermore, the upper limits of period values induced by ethanol were similar to those induced by heavy water.

Ethanol pulses have been shown to cause phase shifts in Gonyaulax (4 hours, 0.1 to 0.2%) (36) and Phaseolus (2 hours, 5 to 30%) (37). The phase-response plots generated in these experiments were qualitatively similar to those of light-pulse experiments (36,37). In addition, ethanol pulses that caused phase shifts in Gonyaulax also caused a 50% reduction in intracellular potassium concentration($[K_i]$). Both the phase shift and reduction in $[K_i]$ were blocked when the ethanol pulse was delivered with valinomycin (0.1 µg/ml) (36).

Phase-response curves similar to those from light-pulse data have also been found for the effects of high potassium pulses delivered to Phaseolus (4 hours, 100 to 300 mM) (37), and the isolated

Aplysia eye (4 hours, 107 mM) (38), and for *Phaseolus* treated with valinomycin pulses (0.01 µg/ml in 0.1% EtOH) (39). High potassium pulses (4 hours, 110 mM) delivered to *Gonyaulax* had no effect on the free-running CR (36).

A model, proposed by Njus *et al.*, based on the results of the four above treatments, proposes that the cellular membrane is the site of the CO. The CO is hypothesized to result from feedback interactions between ion gradients and transport protein activities. Furthermore, if the activity of transport proteins is dependent on their orientation and mutual interaction in the membrane, then temperature compensation may arise from changes in lipid fluidity. Control of other circadian activities would be mediated by changing intracellular ion concentrations. Presumably this mechanism is only remotely dependent on protein synthesis (40).

D. Control of Circadian Activities

A great many cellular processes showing circadian changes have been discovered. In addition to the CRs mentioned in Section I, a number of CRs of nucleic acid synthesis (41), protein synthesis (5) and enzyme activity (42,43) have been found. Although the existence of these CRs is consistent with the involvement of macromolecular synthesis in the production of CRs, there has been no demonstration of these rhythms being fundamentally involved in the time-keeping mechanism. Elucidation of intracellular controls linking the clock to the expression of these CRs has not been attempted except for a few cases involving circadian enzyme activities.

The CR of luminescence capacity (not to be confused with glow luminescence) in Gonyaulax has been examined for involvement of circadian enzyme activities. A CR of luciferase activity that parallels that of luminescence capacity does not appear to be due to a CR of luciferase extractability (unless covalent binding of the enzyme to cellular debris follows a CR) or the presence of a dissociable activator or inhibitor. At present it cannot be decided whether the luminescence capacity CR is controlled by luciferase synthesis or degradation, or if it is controlled by a tightly bound inhibitor (42).

A search for circadian enzyme activities paralleling photosynthetic CRs in a number of plants has had some promising results. In two species the activity of NADP-dependent glyceraldehyde-3-phosphate dehydrogenase has shown a diurnal variation under constant conditions (44,45) while in a third species it exhibits diurnal activity in LD (46). Another Calvin cycle enzyme, ribulose 1,5-diphosphate carboxylase has consistently failed to exhibit circadian rhythmicity under LD conditions (46-49). Hopefully some of the controls operating in this well known pathway will be elucidated as research continues on these systems.

E. Clock Mutants

Mutants expressing altered free-running periods have been isolated in Drosophila, Neurospora and Chlamydomonas. In Drosophila, a short period mutation, a long period mutation and an arhythmic mutation of circadian locomotor and eclosion activities appear to involve the same functional gene (9). In Neurospora, two short

period mutations and one long-period mutation in the CR of conidiation appear tightly linked to each other, but it has not yet been determined if the mutations are allelic (10). The Chlamydomonas mutations, in contrast, are at different genetic loci, since crosses between long-period mutants produced recombinants with additive period increases (11). The Drosophila, Neurospora and some of the Chlamydomonas mutants retained temperature compensation of the free-running period.

The above systems offer an opportunity for genetic dissection of the clock, and a chance to look for altered biochemistry as a result of single gene clock mutations. These systems are particularly inviting to test the membrane CO model of Njus, Sulzman and Hastings (see Section III C), which predicts the existence of altered lipid or membrane transport protein properties in clock mutants (40).

IV Location of the Circadian Oscillator

CRs have been demonstrated in single unicellular organisms (3,4,14) and are thought to be the result of endogenous intracellular processes. Although no CR has been shown to be the result of interactions among noncircadian cells, the theoretical possibility of a CR derived from mutual inhibitory interactions among ultradian (period < 24 hours) oscillators has been described (50).

At present, the location of the COs in unicellular systems is not clearly understood. In the only case studied, both nuclear and extranuclear control of the CR of oxygen evolution in Acetabularia

has been demonstrated. Acetabularia continue to show an entrainable (51) CR for as long as 40 days after enucleation (52), suggesting an extranuclear CR control. However, experiments in which purified nuclei or basal rhizoids (containing nuclei) are exchanged between cells entrained 180° out of phase from each other revealed that the phase of the free-running CR was determined by the nucleus. In addition, cells whose rhizoids were exposed to an LD schedule 180° out of phase from that of their stalks exhibited a free-running CR in phase with the rhizoid schedule when transferred to constant conditions (52). Furthermore, when treated with AMD, intact Acetabularia become arrhythmic whereas enucleate cells retain circadian rhythmicity (3, 29).

These data suggest that in Acetabularia nuclear and extranuclear COs exist in a hierarchical relationship. When the nucleus is present it inhibits expression of the extranuclear CO, even though its CO is made arrhythmic by AMD. In the absence of the nucleus, the extranuclear CO is fully expressed, and is AMD independent. Hierarchical organization of COs is well known in multicellular organisms (8).

References

1. Feldman, J. F. 1967. Proc. Nat. Acad. Sci. 57: 1080-1087.
2. Aschoff, J. 1965. Science 148: 1427-1432.
3. Schweiger, H. G. in: International Symposium on Circadian Rhythmicity. Wageningen, Netherlands, Pudoc, 1972. Pp. 157-174.
4. Sweeney, B. M. in: International Symposium on Circadian Rhythmicity. Wageningen, Netherlands, Pudoc, 1972. Pp. 137-156.
5. Feldman, J. F. 1968. Science 160: 1454-1456.
6. Strumwasser, F. 1973. The Physiologist 16: 9-42.
7. Bünning, E. in: International Symposium on Circadian Rhythmicity. Wageningen, Netherlands, Pudoc, 1972. Pp. 11-31.
8. Pittendrigh, C. S. in: The Neurosciences Third Study Section, F. O. Schmitt and F. G. Worden, eds. MIT Press, 1974. Pp. 437-458.
9. Konopka, R. J. and S. Benzer. 1971. Proc. Nat. Acad. Sci. 68: 2112-2116.
10. Feldman, J. F. and M. N. Hoyle. 1973. Genetics 75: 605-613.
11. Bruce, V. G. 1972. Genetics 70: 537-548.
12. Aschoff, J. 1960. Cold Spring Harb. Symp. Quant. Biol. 25: 11-28.
13. Pittendrigh, C. S. in: Circadian Clocks, J. Aschoff, ed. North Holland Publ. Co., Amsterdam, 1965. Pp. 277-297.

14. Sweeney, B. M. Rhythmic Phenomena in Plants, Academic Press, New York, 1969. Pp. 18-59.

15. Hastings, J. W. and B. M. Sweeney. 1958. Biol. Bull. 115: 440-458.

16. Bruce, V. G. 1960. Cold Spring Harbor Symp. Quant. Biol. 25: 29-48.

17. Sweeney, B. M. and J. W. Hastings. 1960. Cold Spring Harbor Symp. Quant. Biol. 25: 87-104.

18. Hastings, J. W. and B. M. Sweeney. 1957. Proc. Nat. Acad. Sci. 43: 804-811.

19. Bünning, E. 1931. Jahrb. Wiss. Botan. 75: 439-480.

20. Brown, F. A. in: Circadian Clocks, J. Aschoff, ed. N. Holland Publ. Co., Amsterdam, 1965. Pp. 231-261.

21. Brown, F. A. 1960. Cold Spring Harbor Symp. Quant. Biol. 25: 57-71.

22. Hamner, K. C., J. C. Finn, Jr., G. S. Sirohi, T. Hoshizaki and B. H. Carpenter. 1962. Nature 195: 476-480.

23. Ehret, C. F. and E. Trucco. 1967. J. Theor. Biol. 15: 240-262.

24. Pavlidis, T. and W. Kauzmann. 1969. Arch. Biochem. Biophys. 132: 338-348.

25. Bryant, T. R. 1972. Science 178: 634-636.

26. Gale, E. F., E. Cundliffe, P. E. Reynolds, M. H. Richmond, and M. J. Waring. The Molecular Basis of Antibiotic Action, John Wiley & Sons, New York, 1972. Pp. 278-379.

27. Karakashian, M. W. and J. W. Hastings. 1963. J. Gen. Physiol. 47: 1-12.

28. Karakashian, M. W. and J. W. Hastings. 1962. Proc. Nat. Acad. Sci. 48: 2130-2137.

29. Vanden Driessche, T. 1966. Biophys. Biochim. Acta 126: 456-470.

30. Macdowall, F. D. H. 1964. Canad. J. Bot. 42: 115-122.

31. Strumwasser, F. in: Circadian Clocks, J. Aschoff, ed. N. Holland Publ. Co., Amsterdam, 1965. Pp. 442-462.

32. Hastings, J. W. 1960. Cold Spring Harbor Symp. Quant. Biol. 25: 131-143.

33. Enright, J. T. 1971. Z. vergl. Physiologie 72: 1-16.

34. Enright, J. T. 1971. Z. vergl. Physiologie 75: 332-346.

35. Keller, S. 1960. Z. Botan. 48: 32-57.

36. Sweeney, B. M. 1974. Plant Physiol. 53: 337-342.

37. Bünning, E. and I. Moser. 1973. Proc. Nat. Acad. Sci. 70: 3387-3389.

38. Eskin, A. 1972. J. Comp. Physiol. 80: 353-376.

39. Bünning, E. and I. Moser. 1972. Proc. Nat. Acad. Sci. 69: 2732-2733.

40. Njus, D., F. M. Sulzman and J. W. Hastings. 1974. Nature 248: 116-120.

41. Vanden Driessche, T. and S. Bonotto. 1969. Biophys. Biochim. Acta 179: 58-66.

42. McMurray, L. and J. W. Hastings. 1972. Biol. Bull. 143: 196-206.

43. Sulzman, F. M. and L. N. Edmunds. 1973. Biophys. Biochim. Acta 320: 594-609.

44. Miyata, H. and Y. Yamamoto. 1969. Plant and Cell Physiol. 10: 875-889.

45. Frosch, S., E. Wagner and B. G. Cumming. 1972. Can. J. Botan. 51: 1355-1367.

46. Walther, W. G. and L. N. Edmonds, Jr. 1973. Plant Physiol. 51: 250-258.

47. Pallas, J. E., Y. B. Samish and C. M. Willmer. 1974. Plant Physiol. 53: 907-911.

48. Bush, K. J. and B. M. Sweeney. 1972. Plant Physiol. 50: 446-451.

49. Hellebust, J. A., J. Terbough and G. C. McLeod. 1967. Biol. Bull. 133: 670-678.

50. Pavlidis, T. 1969. J. Theor. Biol. 22: 418-436.

51. Sweeney, B. M. and F. T. Haxo. 1961. Science 134: 1361-1363.

52. Schweiger, E., H. G. Walraff and H. G. Schweiger. 1964. Science 146: 658-659.

CHAPTER II

REVIEW OF THE *APLYSIA* EYE

In this chapter I will summarize the information known about the eye of Aplysia californica. The location, gross anatomy and electrical properties of the eye will be briefly described, after which the role of the eye in the animal will be discussed. The anatomy, electrophysiology and circadian rhythms of the eye will then be reviewed in greater detail.

I Gross Aspects of the Aplysia Eye

Aplysia californica has two eyes located bilaterally in the head region of the animal, anterior to the rhinophores. Each eye is about 700 μ in diameter and consists of a central lens and vitreous humor surrounded by a retina (1) (Figure 1). The lens protrudes through the retina and skin of the animal allowing light to enter the eye. The optic nerve, consisting of thousands of fibers (2), connects each eye to the cerebral ganglion. Each eye is surrounded by a sheath of connective tissue, and receives blood circulated through the cephalic artery (3).

The isolated eye produces a circadian rhythm (CR) of optic nerve impulses when recordings are made in constant darkness (4). When illuminated, the eye fires a transient volley of impulses followed by a sustained tonic discharge at a frequency higher than that in the dark (1,4). The above electrical activity is conducted down the optic nerve into the cerebral ganglion (1).

II Role of the Eye in Aplysia

Light-dark cycles have been shown to influence the CRs of locomotion (5), spike output in neuron R15 of the parietovisceral

ganglion (PVG) (6), and possibly other neurons showing circadian activity in the same ganglion (7). The eye could entrain and/or synchronize these CRs since it both perceives light-dark information and produces an endogenous circadian rhythm. Experimental evidence supporting this view is presented below.

The eyes appear to mediate the entrainment and synchronization of the locomotor rhythm. Animals exposed to a LD 12:12 schedule show locomotor activity during the light portion of the entrainment cycle, and are quiescent during the dark portion (fig. 2) (7,8,9). When both eyes are removed from the animal, and it remains exposed to the same LD schedule, a large, long-lasting decrement in locomotor circadian rhythmicity occurs (Figure 2) (7,8). The locomotor rhythm becomes 'desynchronized', showing many small peaks upon periodogram analysis (7). In freshly blinded animals, a consistent rise in locomotor activity following the onset of light may reveal the contribution of extra-optic entrainment pathways (7,8) presumably mediated by light sensitive neurons in the cerebral ganglion (8,10). All signs of entrainment disappear in 5 to 6 weeks after blinding (7).

Aplysia monitored in LL (280 lux) (9) or DD (7,8) show a free-running locomotor rhythm that persists for as long as 13 days (8). However, animals do not show this free-running rhythm for more than about 8 days after blinding (Figure 3) (7), indicating that the eyes may mediate the synchronization of the free-running locomotor CR, as well as its entrainment.

The influence of the eye on the CR of R15 has been tested both synaptically and humorally. Audesirk (11) showed that the eyes can synaptically influence electrical activity in R15 via a multineuronal route through the cerebral ganglion, the right pleural ganglion and the right connective of the PVG. He based this conclusion, in part, on data that showed correlations between the electrical activity of the eye and R15. When the optic nerve of an isolated Aplysia CNS preparation was stimulated, a particular unitary EPSP (input I of Parnas et al., 1974 (12)) was evoked in R15. In the dark, the unstimulated preparation showed a correlation between troughs of spontaneous optic nerve activity and peaks of input I EPSPs and spikes in R15. When one eye was illuminated, its light response coincided with a decrease in the rate of input I EPSP's observed in R15. When the light was turned off, the eye temporarily ceased activity, while the EPSP frequency in R15 increased. These data show excitatory and inhibitory influences of optic nerve activity on R15.

Audesirk and Armstrong (11) unsuccessfully tried to entrain the CR in R15 by activating input I with electrical stimulation of the right PVG connective. Although stimulation of this connective can evoke both excitatory and inhibitory synaptic potentials in R15 (12), only the excitatory potential was tested. Clearly more types of synaptic stimulation and more sources of synaptic input to R15 must be tested before this route of entrainment can be properly evaluated.

A humoral influence of the eye on the entrainment of R15 has been demonstrated by Audesirk, who compared the circadian rhythm

of R15 from animals that were intact, blinded or sham-operated (11). Immediately after the appropriate operation, all three groups of animals were put on a new LD schedule 6 hours phase-advanced from the original schedule. One to two weeks later, the PVG from each animal was isolated and the spikes in R15 were recorded. The R15 CRs of the intact and sham-operated animals were 6 hours phase advanced relative to the rhythms of the blinded animals. Thus the eyes are necessary for the entrainment of R15.

To distinguish between humoral and synaptic routes of entrainment, Audesirk compared the entrainment of R15 in intact animals with its entrainment in animals in which the two PVG connectives to the head ganglia had been cut. After exposure to the new 6 hour phase-advanced LD schedule, all 5 intact and 5 of 8 operated animals had 6 hour phase-advanced R15 rhythms. Hence, the eyes seem capable of humorally entraining R15 *in vivo*.

Audesirk next tested for *in vitro* entrainment of R15 in isolated PVGs. The two eyes from an animal entrained to a 6 hour, phase-advanced LD schedule were incubated in a small volume of filtered sea water with the PVG of an animal entrained to a normal LD schedule. The CR of R15 became phase-advanced about 6 hours compared to controls. Controls had the eyes and abdominal ganglion from the same animal incubated together, and were themselves almost 4 hours phase-advanced compared to R15s from isolated PVGs. Hence the eye appears to humorally entrain R15 without the mediation of any tissue except the PVG. Whether or not a hypothetical entrainment hormone directly affects R15 is currently being investigated by Stuart and Audesirk in

this laboratory.

The existence of other neurons showing circadian activity has been implicated in the isolated PVG by means of computer assisted spike sorting of long-term recordings from the genital and pericardial nerves (5,7). At least two units showing CRs of spike frequency appear to free-run in organ cultured PVGs. Although the route of light-dark information to these neurons has not yet been determined, it is not unlikely that the eyes serve to entrain such units (7).

III Anatomy

Examination of the Aplysia eye with the light and electron microscopes has allowed identification and location of various cell types.

The retina surrounding the lens is thinnest near its protrusion, and thickest at the base of the eye, where much of the retinal neuropile is located and where the optic nerve joins the eye (Figures 1 and 4) (2). The retina is composed of thousands of cells distributed among at least eight cell types based on location and morphology (13).

The first layer of cells surrounding the lens and vitreous humor consists of receptor cells, pigment cells (2) and type Ia neurons (13) (Figures 3 and 4). Receptor cells (15 to 20 μ in diameter) send microvillous processes into the vitreous humor (Figure 3) (2). Because of this property, and the fact that electrical recordings reveal typical depolarizing receptor cell potentials (1)

(see Section IVB, Intracellular Recordings), these cells are considered to be primary photoreceptors. Throughout the soma and adjacent processes of receptor cells, paracrystalline arrays of clear vessicles, 500 to 750 Å in diameter are seen. Proximal to the soma, a branching process projects into the neuropile region (2). Based on transmission electron microscopy (13) and freeze-fracture studies conducted in this laboratory with the aid of Dr. J.-P. Revel (14), receptor cells are thought to be interconnected by gap junctions, which are considered to be thesites of low resistance electrical coupling between cells in other systems (15). According to counts made by Jacklet (16,17) about 80% of the neurons in the Aplysia eye are receptor cells.

Two types of pigment cells have been found in the Aplysia eye. Large pigment cells (5 to 10 μ in diameter) interdigitate receptor cells and contain distal segments supporting small microvillous and rudimentary ciliary projections at the level of the vitreous humor (Figure 3). Pigment granules are contained in the portion of these cells distal to the nucleus, while proximally a process projects into the neuropile region (Figure 3) (2). Small pigment cells (about 4 μ in diameter) are located among the branching processes of receptor cells (13).

Type Ia neurons (about 4 μ in diameter) are also located among receptor cell processes, and are characterized by the inclusion of many free ribosomes and a poorly organized endoplasmic reticulum (ER) (13).

Two types of presumed higher order neurons are seen surrounding the first retinal layer (Figure 4). Type Ib neurons are similar in size to type Ia neurons, but are distinguished by the inclusion of extensive rough ER. Often type Ib neurons border on blood sinus spaces in the lower retina (13). Type II neurons are identified by their larger size (15 to 20 μ in diameter) and inclusion of irregularly shaped dense-core granules (1000 to 1200 Å in diameter) (2). The similarity between these granules and others found in neurosecretory Aplysia cells (18), and the fact that type II neurons often border blood sinuses at the base of the eye (13) suggest that these cells have a neurosecretory function; perhaps that of secreting the substance that entrains neuron R15 (see Section II, Role of the Eye).

Neuroglial cells are primarily seen at the base of the eye, and have varied appearances. In general they are small in size (2 to 10 μ in diameter) and possess a "watery"-appearing cytoplasm (13). Recently, epithelial cells have been found surrounding the lens where it protrudes from the eye (13).

IV Electrophysiology of the Aplysia Eye

A. Optic Nerve Impulses

The isolated Aplysia eye produces spontaneous and light-evoked impulses as recorded from the optic nerve. The optic nerve discharges are called compound action potentials (CAPs) because they appear to be the result of synchronous firing of a population of fibers in the optic nerve (1). Bursts of 1 to 6 spontaneous CAPs

can be recorded from the optic nerve of eyes kept in darkness. The frequency of these spontaneous CAPs follows a CR (4). When the eye is illuminated (Figure 5), a transient high frequency burst of graded CAPs (phasic light response) occurs, followed by a steady, lower frequency discharge of CAPs (tonic light response). After the light is turned off, a period of silence ensues, and is followed by a resumption of spontaneous CAP activity (1,4).

B. Intracellular Recordings

In an effort to find the sources of the various activities recorded in the optic nerve, Jacklet conducted an intracellular investigation of the intact eye (1). Jacklet compared recordings from single impaled cells with simultaneous extracellular recordings from the optic nerve. He identified at least four different types of intracellular activities.

Most of Jacklet's recordings came from receptor-type cells, which had resting potentials of -40 to -50 mv, and showed a smooth depolarization upon illumination. This receptor potential had about the same duration as the light response recorded from the optic nerve, and was graded with the intensity of the light. An example is seen in Figure 6.

Another type of activity came from cells that fired in synchrony with the optic nerve, during both spontaneous and light-evoked activity. Most likely the neuron firing these spikes sent processes down the optic nerve. Such cells had resting potentials of -20 to -50 mv, but never fired intracellular spikes larger than

5 mv (See Figure 7).

Other units showed low amplitude (5 mv) tonic spiking activity, but did not fire in synchrony with the optic nerve. One type of unit was spontaneously active in the dark, and was inhibited upon illumination. According to Jacklet, the nature of this inhibition was variable; sometimes it was associated with depolarization, sometimes with hyperpolarization. A silent period at the offset of illumination was followed by a resumption of tonic activity, as in Figures 8b and 9.

Another type of unit appeared tonically active in the light, and silent in the dark (Figure 8a).

Identification of the sources of the various electrical activities recorded by Jacklet awaits the study of the Aplysia eye with intracellular marking techniques.

C. Wiring of the Eye

Approaches to the wiring of the Aplysia eye have been based on experiments in which eyes were exposed to solutions designed to block synaptic transmission or to reduce its population of neurons.

Audesirk's model (19) is the result of short term experiments in which eyes were exposed to artificial sea water (ASW) of four varieties: 1) zero calcium ASW; 2) high magnesium (125 mM) - low calcium (1 mM) ASW; 3) lanthanum (0.1 to 4.5 mM) ASW; and 4) propionate (470 mM) (substituted for chloride) ASW. The first three solutions were expected to block chemical transmission (20-24), while the latter was expected to block electrical synapses (25,26). Audesirk found

that high magnesium-low calcium ASW or lanthanum ASW blocked all spontaneous and light-evoked tonic activity in the Aplysia eye. All that remained was the phasic component of the light response. Furthermore, he showed that propionate ASW blocked all recordable responses from the optic nerve. In all solutions, however, the eye maintained a normal electroretinogram (ERG), and conduction mechanism in the optic nerve, suggesting that receptor cells and optic nerve fibers were still functional.

Eyes treated with zero calcium ASW showed intense spontaneous and evoked CAP activity. Audesirk hypothesized that such treatment increased membrane excitability (28,29) in addition to blocking chemical synapses.

The simplest model that could be constructed from the data proposed that receptor cells were electrically coupled to follower (secondary) cells that sent processes down the optic nerve, since the phasic light response was inhibited by agents that blocked electrical, but not chemical synapses (19). A tonic pacemaker (not necessarily circadian) was proposed to drive follower cells through a chemical synapse since lanthanum ASW and low calcium, high magnesium ASW blocked both spontaneous and light-evoked tonic activity. The pacemaker, which could be a cell or group of cells, would be inhibited by light either directly, or through the action of receptor cells. Synchrony among follower cells would result from their being electrically coupled, and would thus account for their ability to fire CAPs

(12). A schematic representation of this model is seen in Figure 10.

A later study by Jacklet raised doubts about the interpretation of chemical synapses mediating tonic CAP activity (30). Jacklet showed that the circadian rhythm of spontaneous CAP activity in the Aplysia eye is expressed in zero calcium ASW and in various low calcium-high magnesium ASW solutions (0.5 mM Ca, 100, 120 mM Mg) (30).

Audesirk (11) later confirmed Jacklet's findings using low calcium-high magnesium ASW (0, 0.5 or 1 mM Ca, 125 mM Mg). However, Audesirk found that the above solutions temporarily blocked all tonic activity for 0.1 to 9.0 hours, a point not mentioned by Jacklet. Eyes kept in 1 mM lanthanum ASW never recovered spontaneous activity. Audesirk proposed that recovery of spontaneous CAP activity is related to an increase in follower cell excitability due to zero or low calcium concentrations. However, proper evaluation of the role of a chemical synapse mediating tonic activity in the Aplysia eye awaits more refined intracellular measurements.

Based on the results of reducing the population of cells in the eye, Jacklet and Geronimo have offered the theory that the circadian pacemaker of the Aplysia eye is composed of a group of electrically coupled ultradian oscillators (16). They base this idea on a model developed by Pavlidis (31), who showed that a group of strongly coupled oscillators could produce a rhythm with a frequency lower than each oscillator in an uncoupled state. The frequency of the coupled population was shown to be a function of the number of

oscillators and their individual frequencies. Jacklet and Geronimo cut eyes symmetrically about the base, leaving less than 20% of the retina attached to the optic nerve, and claimed that in such eyes the normal circadian activity was replaced by higher frequency activity of 1 to 10 hours in period (16). They reasoned that cutting the eye lowered the number of oscillators in the pacemaker population and thus caused a shift toward the shorter periods of the individual oscillators. However, the data on which this claim is based (16,17) (see Figure 11) show no convincing rhythmicity. More likely, these data show a relatively steady level of activity in cut down eyes, comparable to the maximum level of activity in normal eyes. Because Jacklet and Geronimo ignored the possibility that their data were arrhythmic, they did not consider that, by cutting down eyes, they may have removed a population of circadian inhibitory cells that modulated the tonic dark activity. In the absence of this circadian inhibition, only a steady, maximal activity would remain.

Still another complication of these cutting experiments is the difficulty in repeating Jacklet's results. Sener, in this laboratory, has found that eyes trimmed to less than 20% normal size maintained a normal CR (7). Comparison of his number of experiments (N = 13) with Jacklet's (N = 3) strengthens the possibility that Jacklet injured a few key circadian neurons at the base of the eye (7).

One clear result of cutting experiments is that even though over 80% of the cells of the eye have been removed, the CAP amplitude is little disturbed, as shown in Figure 11. This suggests that the

site of coupling for CAP producing units is in the base of the eye or in the optic nerve; and that only a relatively small number of intact cells is needed to fire a full CAP (7).

V Properties of the Aplysia Eye Circadian Rhythm

A. The Free-Running Rhythm

Jacklet was the first to show that the spontaneous CAP activity of the isolated Aplysia eye follows a circadian rhythm when maintained in the dark (4) (Figure 12). Spontaneous CAP activity occurs in bursts of 1 to 6 CAPs; and ranges in frequency from zero to about 300 CAPs per hour when the eyes are kept in filtered sea water (FWS) (4) (Figure 13). In addition, the number of CAPs per burst (4), the frequency of bursts (17), and the CAP amplitude (16,32) express CRs that at least loosely follow the CAP frequency rhythm (Figures 6, 11 and 13) (17). The latter rhythm, however, appears to be the most precise and longest lasting.

For isolated eyes taken from animals entrained to a LD 12:12 schedule and recorded in FSW, the first peak in the CAP frequency rhythm corresponds to the projected dawn (dark-light transition) of the donor animal, while the minimum CAP frequency is reached near projected dusk (light-dark transition) (Figure 12a and Figure 13). Since the eye free-runs with a period of 22 to 24 hours in FSW, the correspondence of activity peaks with the animal's entrainment schedule may become less precise as more cycles are recorded.

Eyes from animals entrained to a LD 12:12 schedule that are maintained in a nutrient medium composed of amino acids, vitamins and 20% Aplysia blood (33) show a CAP frequency rhythm of about 27 hours in period (Figure 12b) (4). Identification of the factor(s) in the bathing medium that influence the length of the free-running period has not been attempted.

Eyes from animals entrained on a LL schedule show low amplitude CRs in the dark (4) (Figure 12a). The light-dark transition following dissection may serve as a 'zeitgeber' (cue for timing) to initiate the rhythm, but this hypothesis has not been tested.

The period of the free-running CR in a nutrient medium is also influenced by the level of illumination maintained during the recording from isolated eyes (32). In agreement with Aschoff's Rule (see Chapter I), the period of the CR appears to be shortened from 26 hours (in the dark) to 25 hours under constant illumination (20 lux) (32), although the statistical significance of this change in period length is questionable (see Chapter IV, Normal Eyes). In addition, the waveform of the rhythm is flattened, and the rhythm may even damp out in constant light $\geq$ 100 lux, while the average CAP frequency is increased (32).

B. In Vitro Entrainment

Eskin has established that the Aplysia eye can be entrained in vitro to a LD 12:12 schedule phase advanced 13 hours from that of the donor animal (34). The time necessary for complete entrainment

is 4 to 5 days, in contrast to *in vivo* entrainment, which is complete in only one day. To account for the differences in the two preparations, Eskin tested the influence of *Aplysia* blood in the medium, or attachment of the eyes to the cerebral ganglion on the speed of entrainment. Neither factor had a significant effect on entrainment, although attachment to the cerebral ganglion did alter the waveform of the CR of the eye.

To test the mechanism of *in vitro* entrainment, Eskin considered the influence of membrane polarization (35). He hypothesized that LD cycles appear as cycles of membrane polarization at the pacemaker region of the eye. Jacklet had already shown that light could evoke depolarization of receptor and output (follower) cells (1). To test his hypothesis, Eskin exposed eyes to 4 hour pulses of high potassium (107 mM) ASW. Since the resting potential of most neurons, including *Aplysia* neurons (36), depends mainly on the potassium gradient across their membranes, a decrease in this gradient will lower their resting potential. By increasing the potassium concentration outside the eye from 10 mM to 107 mM, Eskin caused an estimated 13 to 50 mv depolarization of eye cells (35).

Exposure of eyes to a 4 hour high potassium ASW pulse caused a phase shift in their CRs (35). Examples of a phase delay and a phase advance are seen in Figure 14. Eskin generated a phase-response plot (Figure 15) by testing all contiguous 4 hour periods of a circadian cycle with high potassium ASW pulses. The plot shows that

phase advances are caused by pulses given during early subjective day of the projected LD schedule, while phase delays result from pulses given during subjective night. More recently, Jacklet has described a phase-response plot for light pulses (600 lux) of one hour duration given to the Aplysia eye (32). Although the statistical significance of many of his phase shift values under 2 hours is doubtful (see Chapter IV , Normal Eyes), the phase response plot is qualitatively similar to Eskin's for high potassium pulses.

Eskin further suggested that phase shifts were not mediated by chemical synapses or neurosecretion, since the phase shifts still occurred in high potassium (90 mM) ASW with high magnesium (125 mM) --low calcium (1 mM) concentrations (35). In such a medium, chemical transmission and neurosecretion should have been blocked (37).

Eskin's argument for the direct influence of membrane polarization on the pacemaker of the eye does not take some biochemical changes into account. For example, Ram, in this laboratory, found that high potassium treatment (4 hours, 90 to 110 mM) of the abdominal ganglion in Aplysia caused about 50% reduction of incorporation of ^{3}H-leucine into TCA insoluble material. In addition, when analyzed by SDS-polyacrylamide gel electrophoresis, the label incorporated during high potassium treatment was decreased in high (> 75,000 daltons) molecular weight proteins relative to lower molecular weight ones (38). Hence, the high potassium treatment appears to affect protein synthesis as well as membrane polarization.

C. The Aplysia Eye in Perspective

As a circadian system, the Aplysia eye provides an easily assayed circadian rhythm of large amplitude and low noise. Although the entrainment and free-running properties of the system have been established, not all the usual properties of circadian rhythms have been demonstrated. In particular the temperature dependence and the limits of entrainment remain to be determined.

The Aplysia eye offers the unique opportunity of studying the organization of a CR in an isolated ensemble of neurons. Although the CRs of pigment migration, ERG amplitude or spontaneous activity are known for other invertebrate eyes (39-43), in none of these cases could circulating hormones or neuronal inputs be ruled out as sources of the rhythmicity. Furthermore, the Aplysia eye may serve as a model for the neuronal loci controlling CRs, since both vertebrate (44,45) and invertebrate (7,46-48) CRs appear to be driven by the nervous system.

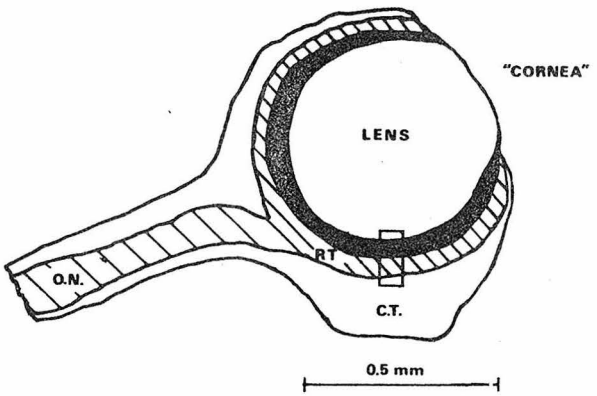

1 . Diagram of the eye and optic nerve (*O.N.*) drawn from a light microscopy section. The central lens (*lens*) is surrounded except at the "cornea" by the retina of which the innermost layer (black) contains the pigmented processes of the receptor and pigmented cells and the outermost layer (cross-hatch) contains the cell bodies and fibers of these elements; the fibers converge to form the optic nerve which goes to the cerebral ganglion. The whole structure is encapsulated by a fibrous (epineural) connective tissue sheath (*ct*). The rectangular area (arrow) is shown enlarged in fig. 3.

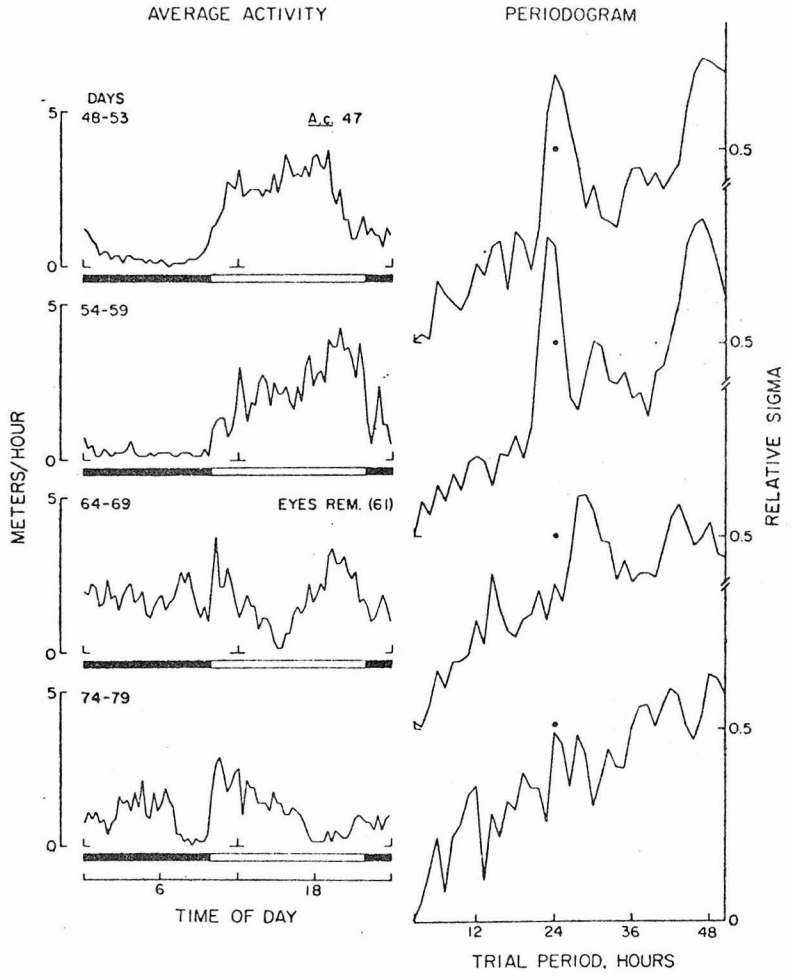

2 The average locomotor activity and periodogram analysis of a sea hare before and after the removal of both eyes. The first two rows of data were taken before removal of the eyes. Twelve inclusive days are contained in this period. This period terminates 2 days prior to eye removal. The experimental data frames began 3 days after eye removal. The light intensity was 350 lux.

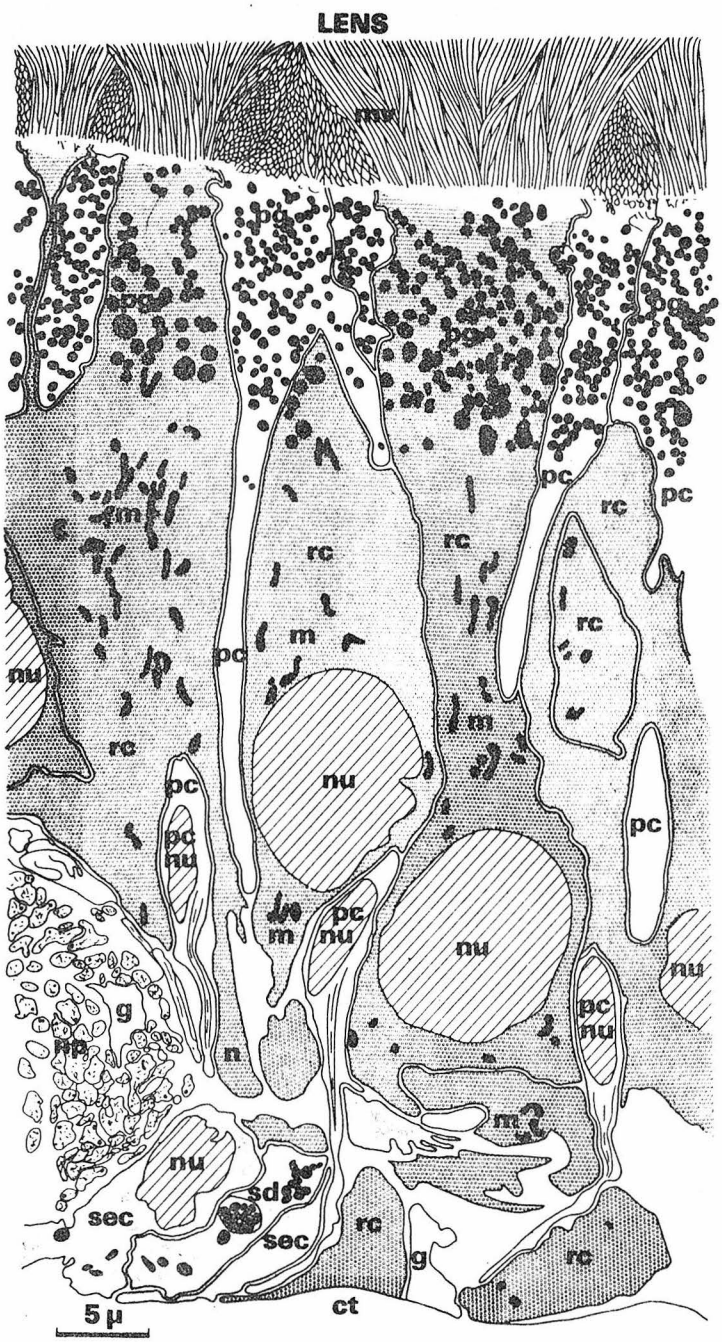

3 . Diagram of a section of the retina approximately in the rectangle of Fig. 1. The diagram was drawn referring to a montage of electron micrographs of the retina from the lens to the connective tissue sheath (*ct*). A receptor cell (*rc*) has a large nucleus (*nu*), many mitochondria (*m*), a neurite (*n*), pigment granules (*pg*), and microvilli (*mv*) arising from the distal segments to form a loosely arranged rhabdomere. The uniform circles indicate the distribution of small vesicles within the cytoplasm of the receptor cells. Interdigitated with the receptor cells are pigment cells (*pc*) containing pigment granules (*pg*) and nuclei (*pcnu*). At the base of the retina, cells (*sec*) containing secretory droplets (*sd*) and glial (*g*) cells are abundant. Their fibers contribute to the fibers of the neuropile (*np*) along with receptor cell neurites. The neuropile (*np*) contains many fibers (in this case cut in cross section).

Figure 4

Saggital section of Aplysia eye fixed in alcoholic Bouin's solution and stained with hematoxylin-eosin. Central lens (L) is surrounded by vitreous humor (V) containing microvillous projections from distal segments of photoreceptor and pigment cells. Nuclear zone (N) contains somas of photoreceptors and large pigment cells as well as type Ia neurons and some small pigment cells. Outer retinal layer contains type II (II) neurons, which lie among processes comprising the neuropile (NP), in addition to type Ib neurons and some small pigment cells. Optic nerve (ON), seen in cross section, is composed of fibers projecting from the neuropile. Sheath of connective tissue (CT) surrounds the entire eye.

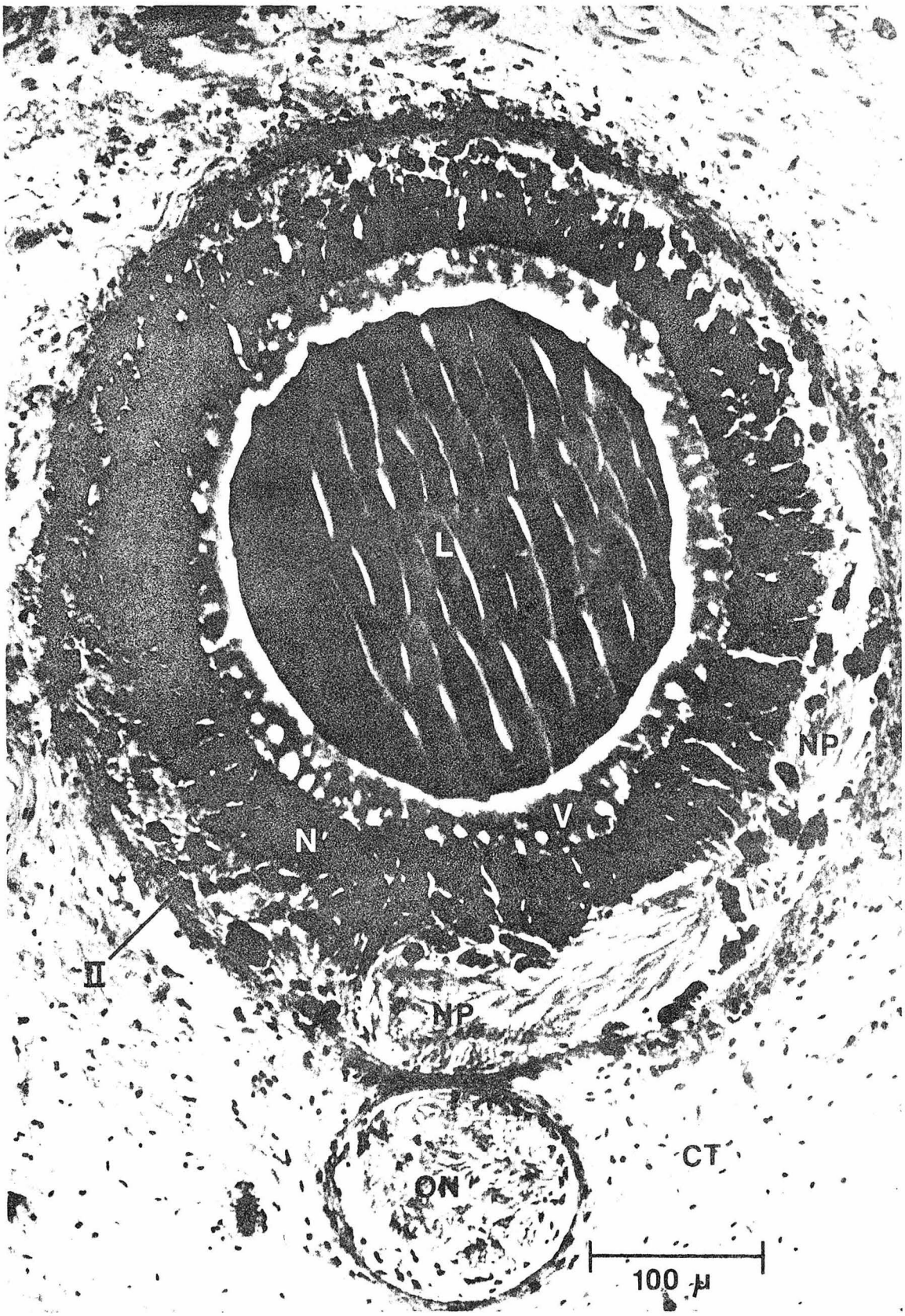
L
NP
V
N
II
NP
CT
ON
100 μ

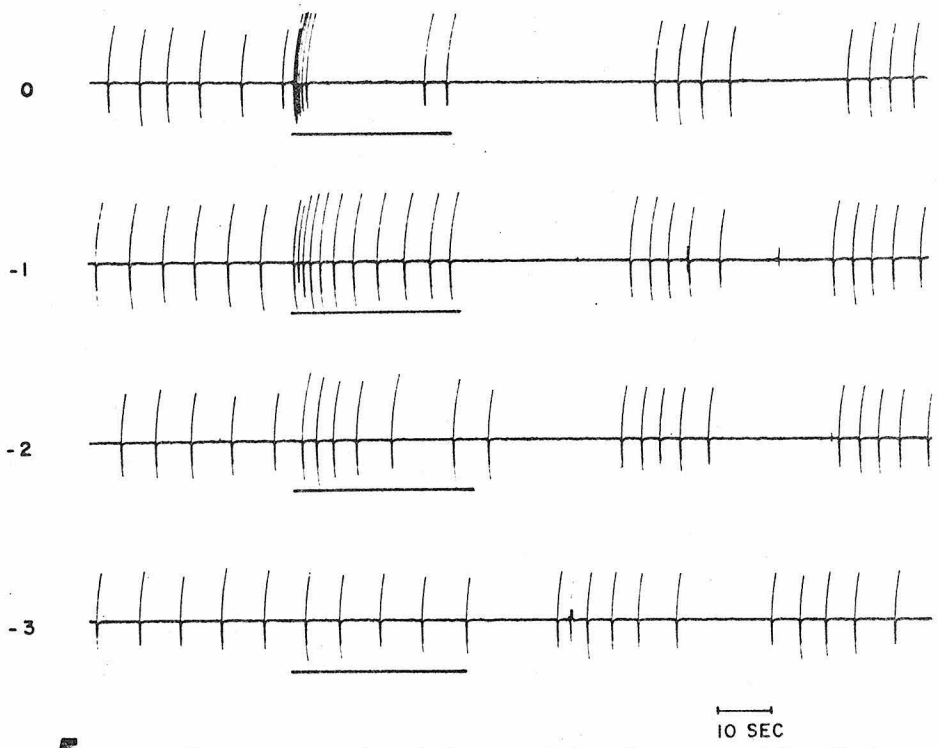

5 Spontaneous and evoked compound optic nerve activity. Optic nerve potentials in response to illumination of the eye at four intensities of white light are shown (the black bars indicate illumination). The 0 intensity is about 600 lux and the remaining intensities successive log units less intense. The spontaneous activity is interrupted by the on response to illumination and resumes after cessation of illumination. The potentials were recorded with a suction electrode on the optic nerve. Spike amplitude is 50 μv, negative upward.

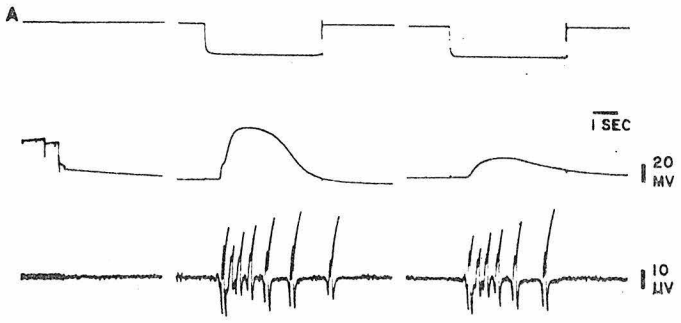

6 Intracellular receptor potentials. A, two successive test illuminations of a receptor cell at 10 min intervals. The top line is a monitor of light; downward deflection indicates illumination of the eye. The second line is a DC record of penetration, 2 min gap, test illumination, 10 min gap, and second test illumination. Line 3 is a simultaneous extracellular record of optic nerve potentials. Note the notch in the rising phase and the apparent overshoot of the graded potential in the first test.

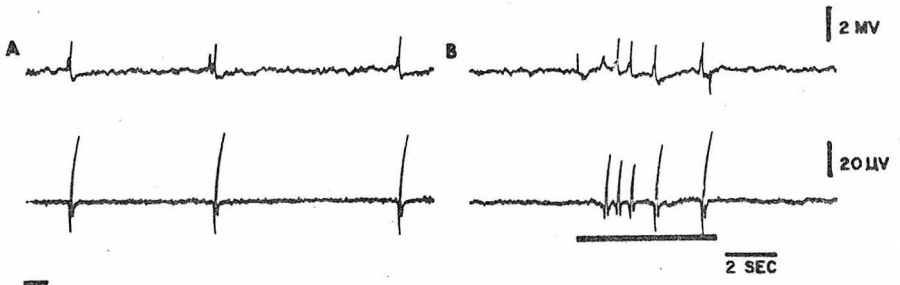

7 Tonic and evoked retinal element activity. A, simultaneous recording of intracellular activity (upper trace) in a retinal element and extracellular optic nerve potentials during dark adaptation. B, illumination of eye causes intracellular spikes correlated with optic nerve potentials. Note the one-to-one relationship in both tonic dark activity and response to illumination.

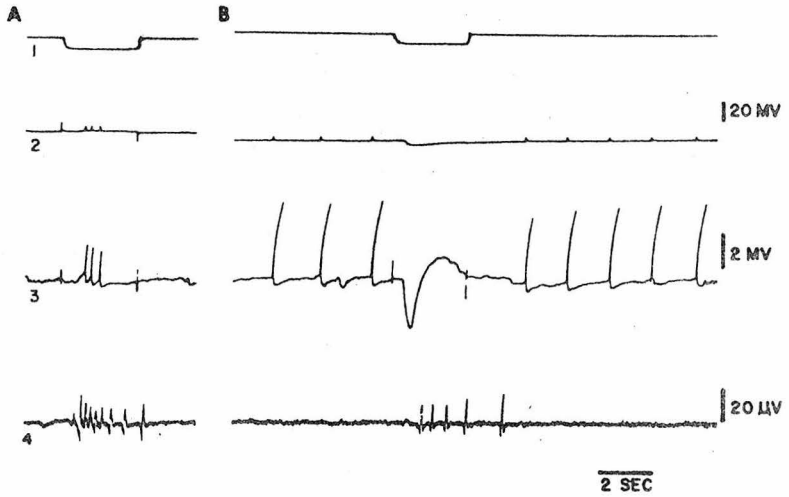

8 Intracellularly recorded responses. A, illumination (1) of eye evokes intracellular on response (2 and 3) in neuron that is not correlated with optic nerve (4) activity. B, hyperpolarization on illumination (1) of an element in the eye (2 and 3). Note this cell's activity does not appear in the optic nerve which shows the typical on response and the increase in optic nerve activity amplitude as the hyperpolarization diminishes. Line 3 is AC-coupled high gain of the DC record in line 2.

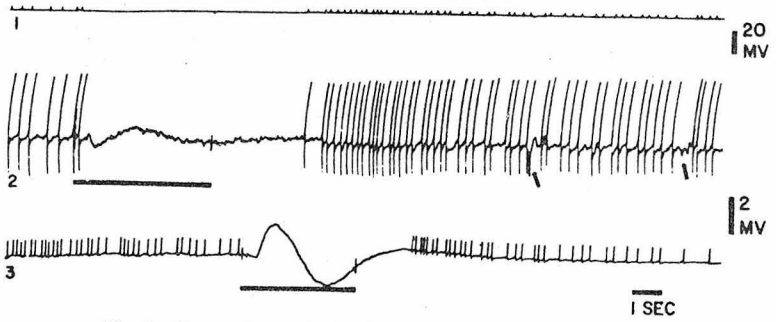

9 Tonically active cell inhibited by illumination. Line 2 is high gain AC-couple duplication of the DC activity in line 1. Illumination of the eye caused hyperpolarization and inhibition of the spike activity which rebounds on cessation of illumination. Ipsp's can be seen at the arrows. Line 3 shows a different preparation (AC-coupled) that is depolarized on illumination but nevertheless inhibits spiking in the cell. Amplifier time constant 0.45 sec.

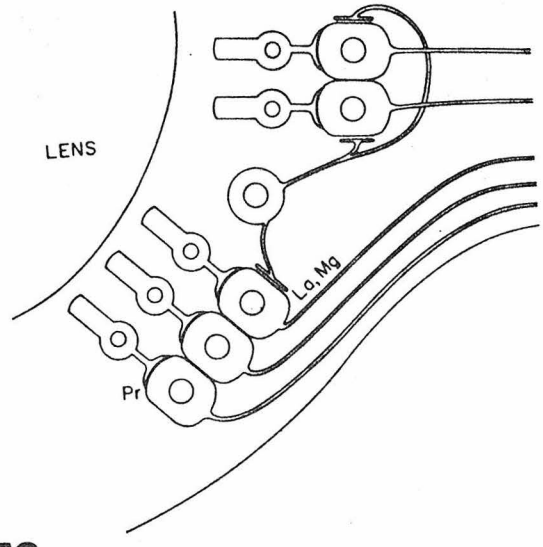

10 A simplified model for the eye of *Aplysia*, showing interrelations among the major cell types. Receptors ring lens, and are electrically coupled (thickened lines) to secondary neurons, whose axons comprise the optic nerve. Round cell in the center represents a pacemaker cell, which chemically synapses on the secondaries (with gap). Secondaries are electrically coupled to one another. Pacemaker may provide input to every secondary (upper) or only to some (lower), with electrotonic coupling providing transmission of excitation to other secondaries. Electrical coupling probably interconnects all secondaries; separation into groups is only for convenience of illustration. Letters near synapses represent types of ions which likely interrupt transmission across them.

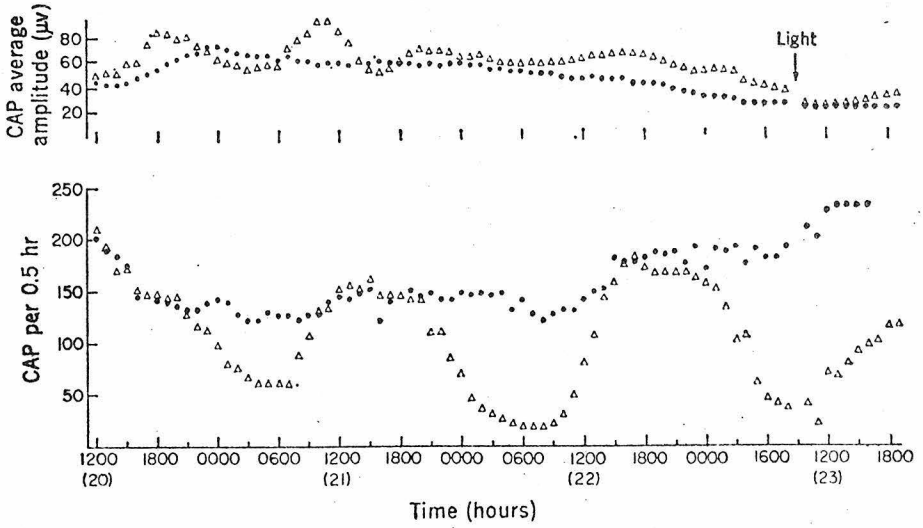

11 Average amplitude and frequency of CAP for each 0.5 hour for several days of continuous recording from both eyes from the same animal, tested in the same culture medium in constant darkness. The whole eye has clear circadian periodicity in CAP frequency; the one-eighth eye does not. The intact *Aplysia* was kept on a daily cycle with light from 0800 to 2000 previous to 20 March 1971. The eyes were then cultured at 14°C in culture medium II. The period of the whole eye (τ) was 28 hours. Times are Eastern standard time. Triangles, whole eye; circles, one-eighth eye. Light refers to a brief light used to test responsiveness of the eye.

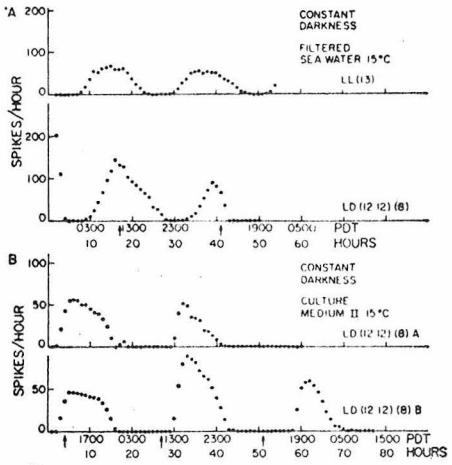

12 Plots of the frequency of impulses over several days in total darkness. (A) The eyes were tested in the same chamber in filtered seawater. The upper graph is that of an LL (13 days) eye; the lower is that of an LD 12:12 (8 days) eye. The black arrows on the time axis indicate the projected DL transition time for the LD eyes in (A) and (B). (B) A pair of LD 12:12 (8 days) eyes from the same animal in culture medium.

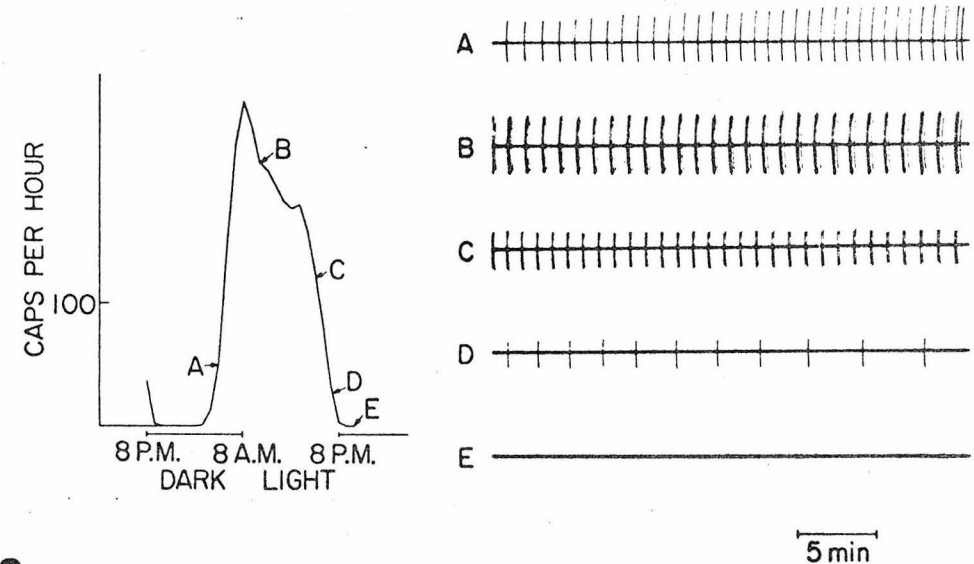

13 **Left:** Plot of the first cycle of optic nerve activity recorded from the isolated Aplysia eye by means of suction electrode. Dissection occurred 4 hours before the beginning of the record. The eye is recorded in filtered sea water supplemented with penicillin and streptomycin in total darkness at 15°C. The donor animal was entrained to a LD 12:12 schedule with lights on at 8 am and lights off at 8 pm. Data is plotted in one hour blocks. The total number of compoumd action potentials (CAPs) occurring each hour is plotted at the beginning of that hour.

Right: Samples of recordings from the optic nerve at various points in the activity cycle. Note that the CAPs change both bursting pattern and amplitude during the cycle.

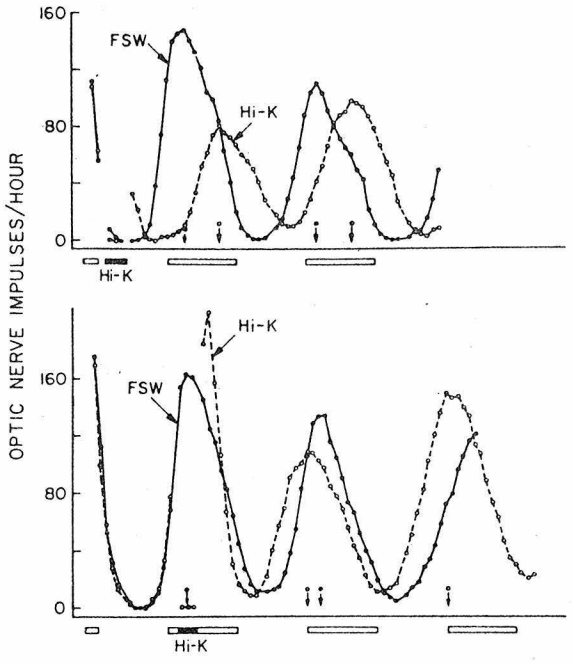

14 Delay phase shift (top curves) and advance phase shift (bottom curves) produced by 4 hour hi-K(I) pulses during the time shown by the solid bars at the bottom of the graphs. In each graph, the two rhythms were obtained from eyes of the same animal recorded under conditions of constant darkness. The peaks of the rhythms were chosen as phase reference points and they are indicated by arrows beneath the curves. The open bars at the bottom of the graphs represent projected light

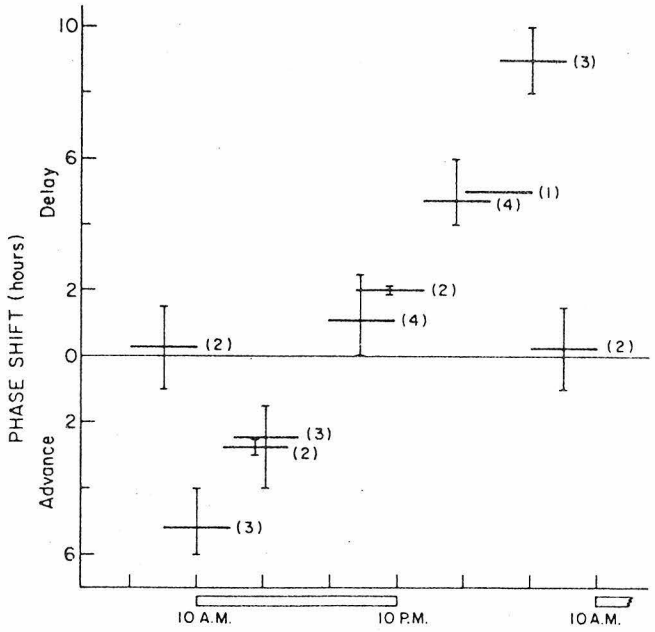

15 Phase shifts of the impulse rhythm as a function of the time of day that the eyes were exposed to 4 hour hi-K(I) pulses. The horizontal bars are mean responses (number of experiments shown in parentheses) and span the time of exposure to hi-K. The vertical bars represent ranges

Sources of Figures in Chapter II

1. Jacklet, Alvarez and Bernstein. 1971. (2)
2. Strumwasser, 1973. (7)
3. Jacklet, Alvarez and Bernstein. 1971. (2)
4. Prepared by R. Alvarez and R. Sener. 1973.
5. Jacklet. 1969. (1)
6. Jacklet. 1969. (1)
7. Jacklet. 1969. (1)
8. Jacklet. 1969. (1)
9. Jacklet. 1969. (1)
10. Audesirk. 1973. (19)
11. Jacklet and Geronimo. 1971. (16)
12. Jacklet. 1969. (4)
13. Prepared by B. Rothman. 1973.
14. Eskin. 1972. (35)
15. Eskin. 1972. (35)

References

1. Jacklet, J. W. 1969. J. Gen. Physiol. 53: 21-41.

2. Jacklet, J. W., R. Alvarez and B. Bernstein. 1971. J. Ultrastr. Res. 38: 24 -261.

3. Eales, N. B. 1921. Proc. Trans. Liverpool Biol. Soc. 35: 183-259.

4. Jacklet, J. W. 1969. Science 164: 562-563.

5. Strumwasser, F. 1967. In: The Neurosciences, ed. Quarton, G. C., T. Melnechuk and F. O. Schmitt. M.I.T. Press, Cambridge, Massachusetts. pp. 516-528.

6. Strumwasser, F. 1965. In: Circadian Clocks, ed. J. Aschoff. Amsterdam: North Holland Publishing Company, pp. 291-319.

7. Strumwasser, F. 1973. The Physiologist 16: 9-42.

8. Block, G. D. and M. E. Lickey. 1973. J. Comp. Physiol. 84: 367-374.

9. Jacklet, J. W. 1972. J. Comp. Physiol. 79: 325-341.

10. Block, G. and J. T. Smith. 1973. Comp. Biochem. Physiol. 46A: 115-121.

11. Audesirk, G. 1974. Ph.D. Thesis, California Institute of Technology.

12. Parnas, I., D. Armstrong and F. Strumwasser. 1974. J. Neurophysiol. 37: 594-608.

13. Strumwasser, F. and R. Alvarez. Personal communication.

14. Alvarez, R. and F. Strumwasser. 1974. Biology Annual Report, California Institute of Technology, pp. 225-226.

15. Bennett, M. V. L. 1973. Fed. Proc. 32: 65-75.

16. Jacklet, J. W. and J. Geronimo. 1971. Science 174: 299-302.

17. Jacklet, J. W. 1971. In: Neurobiology of Invertebrates, Tihany. ed. J. Salanki Akademiai Kaido, Budapest. pp. 313-380.

18. Coggeshall, R. E. 1967. J. Neurophysiol. 30: 1263-1287.

19. Audesirk, G. 1973. Brain Res. 59: 229-242.

20. Harvey, A. M. and F. C. MacIntosh. 1940. J. Physiol. 97: 408-416.

21. Del Castillo, J. and L. Engbaek. 1954. J. Physiol. 124: 370-384.

22. Miledi, R. 1966. Nature 212: 1233-1234.

23. Heuser, J. and R. Miledi. 1971. Proc. Royal Soc. B. 179: 247-260.

24. Miledi, R. 1971. Nature 229: 410-411.

25. Asada, Y. and M. V. L. Bennett. 1971. J. Cell Biol. 49: 159-172.

26. Pappas, G. D., Y. Asada and M. V. L. Bennett. 1971. J. Cell Biol. 49: 173-188.

27. Adrian, E. D. and S. Gelfan. 1933. J. Physiol. 78: 271-287.

28. Bronk, D. W., M. G. Larrabee, J. B. Taylor and F. Brink, Jr. 1938. Amer. J. Physiol. 123: 24-25.

29. Kishimoto, U. 1966. Plant Cell Physiol. 7: 547-558.

30. Jacklet, J. W. 1973. J. Comp. Physiol. 87: 329-338.

31. Pavlidis, T. 1969. J. Theoret. Biol. 22: 418-436.

32. Jacklet, J. W. 1974. J. Comp. Physiol. 90: 33-45.

33. Strumwasser, F. and R. Bahr. 1966. Fed. Proc. 25: 512.

34. Eskin, A. 1971. Z. vergl. Physiol. 74: 353-371.

35. Eskin, A. 1972. J. Comp. Physiol. 80: 353-376.

36. Carpenter, D. O. and B. O. Alving. 1968. J. Gen. Physiol. 52: 1-21.

37. Arch, S. 1972. J. Gen, Physiol. 59: 47-59.

38. Ram, J. L. 1974. Brain Res. 76: 281-296.

39. Jahn, T. L. and F. Crescitelli. 1940. Biol. Bull. 78: 42-52.

40. Arechiga, H. and C. A. G. Wiersma. 1969. J. Neurobiol. 1: 71-85.

41. Welsh, J. 1938. Quart. Rev. Biol. 13: 123-139.

42. Welsh, J. 1941. J. Exper. Zool. 86: 35-49.

43. Fingerman, M. and M. Lowe. 1957. J. Cell Comp. Physiol. 50: 371-379.

44. Moore, R. Y. 1974. In: The Neurosciences Third Study Program, ed. F. O. Schmitt and F. G. Worden, M.I.T. Press, Cambridge, Massachusetts. pp. 537-542.

45. Menaker, M. 1974. In: The Neurosciences Third Study Program, ed. F. O. Schmitt and F. G. Worden, M.I.T. Press, Cambridge, Massachusetts. pp. 479-489.

46. Arechiga, H. 1974. In: The Neurosciences Third Study Program, ed. F. O. Schmitt and F. G. Worden, M.I.T. Press, Cambridge, Massachusetts. pp. 517-523.

47. Truman, J. W. 1974. In: The Neurosciences Third Study Program, ed. F. O. Schmitt and F. G. Worden, M.I.T. Press, Cambridge, Massachusetts. pp. 525-529.

48. Konopka, R. J. and S. Benzer. 1971. Proc. Nat. Acad. Sci. 68: 2112-2116.

CHAPTER III

REVIEW OF THE BIOCHEMICAL EFFECTS OF FOUR INHIBITORS OF MACROMOLECULAR SYNTHESIS: AFLATOXIN B_1, ACTINOMYCIN D, PUROMYCIN AND CYCLOHEXIMIDE

I Aflatoxin-B_1

Aflatoxin-B_1 (AFTX-B_1) is a potent hepatocarcinogen produced by the fungus Aspergillus flavus. Of the group of naturally occurring aflatoxins, which include AFTX-B_2, AFTX-G_1 and AFTX-G_2, AFTX-B_1 is the most potent carcinogen and inhibitor of transcription (AFTX-B_1> AFTX-G_1> AFTX-B_2> AFTX-G_2). Aflatoxins are characterized by dihydrofurofuran and O-methyl coumarin moieties, the latter being attached to an additional 5- or 6-membered ring (fig. 1). Potency is dependent, in part, on the existence of the C(2)-C(3) double bond (AFTX-B_1, AFTX-G_1 vs AFTX-B_2, AFTX-G_2) in the terminal furan, and a 5-membered cyclic ketone (AFTX-B_1, AFTX-B_2 vs AFTX-G_1, AFTX-G_2) at the other end of the molecule. Reduction of the ketone (aflatoxicol) or removal of the dihydrofurofuran moiety lowers potency, whereas hydroxylation of the furan bridge carbon (AFTX-M_1) does not (1).

The mechanism of tumor induction by AFTX-B_1 is not clearly understood. Since the relative amount of DNA binding activity generally parallels the carcinogenicity of the aflatoxins, their interaction with DNA has been considered a possible explanation of tumor induction (1). This interpretation has received more support recently by the discovery that microsomal metabolites of AFTX-B_1, and of many other polycyclic aromatic hydrocarbons known to be carcinogenic, could cause reversion of frame-shift mutations in Salmonella (2). However, there has been no direct demonstration of transformation caused by the interaction of aflatoxins with DNA.

Its carcinogenic properties notwithstanding, AFTX-B_1 is a potent inhibitor of RNA and protein synthesis. It was because of these inhibitory properties that AFTX-B_1 was used in the experiments conducted on the Aplysia eye described in this Ph.D. thesis. The following discussion on the primary action of AFTX-B_1 will therefore be limited to its effects on macromolecular synthesis.

A. Binding of AFTX-B_1 to DNA, RNA and Protein

Binding studies have demonstrated that AFTX-B_1 interacts weakly with DNA *in vitro*. Sporn *et al.* showed that the absorption spectrum of AFTX-B_1 was changed when it was mixed with native or denatured calf thymus DNA. The wavelength of maximum absorption in the range of 340-390 nm shifted from 362-364 nm to 366-368 nm, while absorbance from 340 to 370 nm decreased by about 25%. Calculations based on equilibrium binding studies showed that more AFTX-B_1 was bound to denatured DNA than to native DNA (3). In similar spectral studies King and Nicholson calculated that one AFTX-B_1 molecule was bound to every 80 nucleotides of denatured calf thymus DNA, with an association constant of $4 \times 10^{-4} M^{-1}$. Hypochromicity in the AFTX-B_1 difference spectrum was large for calf thymus DNA, poly A:poly U and poly A, but quite low for poly A:poly I, poly C, poly U, poly I and the four 2', 3', nucleotide monophosphates (4). Clifford and Rees showed that similar changes occurred in the AFTX-B_1 difference spectrum when the drug was bound to single or double stranded calf thymus DNA. The association between AFTX-B_1 and native DNA did not change T_m nor did it survive passage through a Sephadex G-50 column.

Difference spectra for AFTX-B_1 binding to the DNA nucleotides showed greatest hypochromicity with dG and dA, and very little hypochromicity with dT and dC. Difference spectra of AFTX-B_1 interaction with various purine derivatives showed substantial hypochromicity for 2- and 6-amino purines (5). The above studies indicate that AFTX-B_1 interacts weakly with DNA, and that this interaction probably takes place at purine bases. Furthermore, because T_m is unaffected, there is little chance that AFTX-B_1 intercalates DNA.

Although AFTX-B_1 has been shown to bind to DNA, this interaction does not affect transcription in vitro. In the King and Nicholson study cited above, incubation of E. coli DNA-dependent RNA polymerase with calf thymus DNA in the presence of 2mM AFTX-B_1 had no effect on transcription; whereas incubation in the presence of 10 µg/ml AMD inhibited transcription by 83% (4). Edwards and Wogan demonstrated that incubation of rat liver nuclei with 5-12 µg/ml AFTX-B_1 did not lower the rate of transcription. In contrast, when liver chromatin was isolated from rats previously injected with 0.5 mg/kg AFTX-B_1 and incubated with control liver RNA polymerase, transcription of calf thymus DNA was reduced by 28-46%. When chromatin from control rats was incubated with RNA polymerase from AFTX-treated rats, transcription was unaffected (6). These studies indicate that AFTX-B_1 can only block transcription in vivo, and suggest that a cytoplasmic component is necessary to activate the drug to a form that interacts with the transcriptional template.

Other studies, however, indicate that the RNA polymerase enzyme can be affected by *in vivo* treatment with AFTX-B_1. Saunders *et al.* administered AFTX B_1 (1 mg/kg) to rats and then measured transcription in isolated liver nuclei. ^{3}H-UTP incorporation was inhibited by 50% compared to controls. When nucleolar RNA polymerase and nucleoplasmic RNA polymerase were isolated from the livers of AFTX-treated rats, and used to transcribe denatured calf thymus DNA, the activity of the former enzyme was inhibited by 60% while that of the latter was inhibited by only 10%. Although nucleoplasmic RNA polymerase was not affected by AFTX either *in vivo* or *in vitro* (62.5 µg/ml), its activity was decreased by 90% when 2 µg/ml α-amanitin was applied *in vitro* (7).

The discrepancy in the site of AFTX action notwithstanding, the contrast in the potency of AFTX-B_1 administered *in vivo* instead of *in vitro* suggests that the drug must be activated to inhibit transcription. This interpretation is supported by the finding that labeled AFTX-B_1 administered *in vivo* binds strongly to DNA, RNA and protein. Lijinsky *et al.* showed that when ^{3}H-AFTX-B_1 was injected into rats (0.9 mg/animal), radioactivity remained bound to DNA, RNA and protein fractions of liver, kidney, spleen and small intestine for a period of 1 hr to 8 weeks. Most of the label binding to the four organs appeared within 6-18 hrs, with the liver containing more label on a weight basis than the other three organs. When DNA, RNA and protein were separated by phenol extraction, most label on a

weight basis was bound to protein, while the remaining label was equally divided between DNA and RNA. When the extracted protein was dialyzed against ethanol for 50 hrs, and then against water for 72 hrs, 98.5% of the ^{3}H-radioactivity remained bound (8). Thus, some metabolite of ^{3}H-AFTX-B_1 was tightly bound to DNA, RNA and protein. Unfortunately the nature of the bound label was not determined in this study. This shortcoming, coupled with the fact that the AFTX-B_1 was labeled by exchange with ^{3}H-water raises the problem that much of the label associated with DNA, RNA and protein may not be due to the binding of an AFTX-B_1 derivative.

Some of these reservations have been overcome by <u>in vitro</u> studies of AFTX-B_1 activation. Garner incubated 2 mg of calf thymus DNA, yeast tRNA or rRNA with a microsomal fraction derived from hamster liver, an NADPH generating system and ^{14}C-AFTX-B_1 (0.255 μM). Purification of the nucleic acid in each assay included phenol extraction, precipitation in high salt with ethanol, and washing with ether. On a nucleotide basis, more radioactivity remained associated with calf thymus DNA (1 mole label:30 moles of nucleotides) than to yeast tRNA (1:190) or rRNA (1:330). The label bound to DNA survived passage through a Sephadex G-10 column. When the microsomal fraction was not included in the incubation, no label was bound to the nucleic acids. Incubation of the system with 2 mg poly G, poly A, poly C or poly T resulted in label being more densely bound to poly G (1:260) and poly A (1:1050) (9). Although these

experiments provide little information concerning the nature of the bound label, they do demonstrate that liver microsomes are sufficient to activate AFTX-B_1 into a form that strongly binds to nucleic acids.

Gurtoo *et al.* studied the microsomal activation of AFTX-B_1 in more detail. After establishing that radioactivity from ^{3}H-AFTX-B_1 was bound tightly to calf thymus DNA and rat liver RNA, the authors found that AFTX-B_1 activation was dependent on the presence of an NADPH generating system. When CO_2 or N_2 replaced the gas phase of the reaction, the binding of ^{3}H-radioactivity to DNA fell to 2% or 42%, respectively, of control levels. Addition to the system of β-diethylaminoethyl diphenylpropylacetate HCl (2 mM), an inhibitor of microsomal mixed-function oxidases, reduced binding to DNA by 78% (10). These findings suggest that microsomal mixed-function oxygenases are the agents that activate AFTX-B_1. These enzymes are used to insert a single oxygen atom, derived from molecular oxygen, into aromatic compounds. In addition, they are often NADPH-dependent (11).

Swenson *et al.* have attempted to identify the structure of the AFTX-B_1 derivative bound to RNA. The authors found that when AFTX-B_1 was incubated with hamster or rat liver microsomes and rat liver rRNA, and the RNA purified by phenol extraction, the spectrum of the RNA in the 240 nm to 460 mn range resembled that of AFTX-B_1. Calculations based on the absorption of the complex at 368 nm compared to its absorption at 258 nm showed that one molecule of the AFTX-B_1 derivative was bound per 100 nucleotides. Mild hydrolysis of the

AFTX-RNA complex (0.15 M HCl, 99°C, 90 min) yielded a compound with mass spectroscopic, UV spectroscopic and TLC properties identical with those of 2,3-dihydro-2,3-dihydroxy-AFTX-B_1. At neutral pH the largest differences in the spectrum of the complex compared to that of the hydrolyzate were a shift in the wavelength of maximum absorbance from 368 nm to 365 nm, and a 50% increase in absorbance at 365 nm. Comparison of the spectra of the hydrolyzate and AFTX-RNA complex at pH 7.4 with their spectra at pH 11.5 revealed a bathochromic shift from λ_{max} = 365 nm to λ_{max} = 400 nm in the spectrum of the former compound, but little change (λ_{max} 368 nm → 370 nm) in the spectrum of the latter. The authors suggested that AFTX-B_1 was activated to its 2,3 epoxide by the microsomes, and that this intermediate attacked a nucleophilic group in a G or A residue of RNA (12). This suggestion is supported by other studies which have shown that a number of polycyclic hydrocarbons are converted to (K-region) epoxides by microsomal mixed-function oxygenases, and that these epoxides are carcinogenic (13). Swenson et al. further suggested that the AFTX-B_1 derivative was attached to RNA by its 2-position, and based this interpretation on the fact that an OH group must be at the 2-position of AFTX, as in AFTX-B_{2a} (fig. 1), in order to allow the bathochromic shift in the absorbance spectrum. This property is based on the opening of the two furan rings under basic conditions to form a dialdehyde phenolate ion. If the AFTX-B_1 derivative were attached to RNA by its 2-position, the opening of the rings would presumably not be possible (12).

Moulé and Frayssinet demonstrated that a metabolite of AFTX-B_1 was capable of inhibiting transcription *in vitro*. Incubation of AFTX-B_1 with microsomes derived from rat liver yielded a fluorescent compound (as is AFTX-B_1) with a mobility lower than that of AFTX-B_1 when run on a chloroform-silica gel TLC system. When about 3 µg/ml of this compound was incubated with an *in vitro* transcription system containing *E. coli* RNA polymerase and calf thymus DNA, incorporation of ^{14}C-UTP was inhibited by 50% compared to controls. Incubation of the *in vitro* system with 40 µg/ml AFTX-B_1 had no effect on transcription. Increasing the DNA concentration in the system had no effect on the amount of inhibition caused by the AFTX-B_1 derivative, whether or not the DNA concentration was the limiting factor in the rate of transcription. In contrast, a 50-400% increase in the amount of RNA polymerase caused transcription to recover to 75-100% of control levels. When the AFTX-B_1 derivative was added 2 min after transcription was begun, the time course and level of transcription were that of controls (14). These results imply that the AFTX-B_1 derivative inhibits the initiation of transcription by an interaction with RNA polymerase.

Sarasin and Moulé studied the effects of this AFTX-B_1 derivative on translation *in vitro*. When rat liver polysomes, supernatant factors, amino acids and ^{14}C-leucine were incubated with 20 µg/ml of the derivative, incorporation was inhibited by about 75%. If AFTX-B_1 was used instead of its derivative, translation occurred at control levels (15).

B. Effects of AFTX-B_1 on Transcription and Translation *In Vivo*

AFTX-B_1 produces a number of effects on macromolecular metabolism *in vivo*, including inhibition of RNA synthesis, RNA maturation and protein synthesis and disaggregation of polysomes. These actions are discussed in more detail below.

Lafarge and Frayssinet studied the effects of AFTX-B_1 (1 mg/kg) on ^{14}C-orotic acid incorporation into the liver of partially hepatectomized rats. Incorporation into total nuclear RNA was inhibited less severely, and more reversibly, than incorporation into nucleolar RNA. Incorporation into total nuclear RNA fell by 80% in the livers of animals treated with AFTX-B_1 for two hrs, and recovered to 20% of control levels in 24 hrs. In contrast, incorporation into nucleolar RNA was inhibited by 90% in animals exposed to AFTX-B_1 for 2 hrs, and recovered to only 47% of control incorporation in 24 hrs (16). In HeLa cells, similar results have been reported by Harley *et al*. The authors showed that cultures pulsed with 20 µg/ml AFTX-B_1 for 30 min

had ^{3}H-uridine incorporation into RNA inhibited by 60% within 3-6 hrs. Incorporation recovered to 85% of control values in 24 hrs. In other experiments cells were pulsed with ^{3}H-uridine for 60 min with or without 40 µg/ml of AFTX-B_1 present, and then fractionated into cytoplasmic, nucleoplasmic and nucleolar RNA. Compared to controls, incorporation into each fraction was inhibited by about 50%. The authors claimed that the inhibition of ^{3}H-uridine incorporation was not due to blocking its entry into intracellular pools, although they did not provide any data concerning the specific activity of intracellular UTP (17). It is therefore unclear whether or not AFTX-B_1 affected precursor specific activity. The results of the experiments with HeLa cells indicate that AFTX-B_1 inhibits incorporation into nucleoplasmic and nucleolar RNA more or less equally. This effect is in contrast to that of AMD, which is 50 to 100 times more potent in inhibiting rRNA synthesis than in inhibiting HnRNA and mRNA synthesis (see section II) and implies that the mechanism of AFTX-B_1 action is not the same as that of AMD. Furthermore, the true reversibility of AFTX-B_1 seems doubtful in light of its carcinogenic and mutagenic properties. Although levels of RNA synthesis may recover, the spectrum of RNA synthesis may be qualitatively different.

Besides inhibiting RNA synthesis, AFTX-B_1 also interferes with the maturation of RNA. In the study of Harley *et al.* mentioned above, profiles of RNA from cells treated with 40 µg/ml AFTX-B_1 for 30 min, and then labeled with ^{3}H-uridine for 60 min revealed that

incorporation into 18S RNA and 28-32S RNA was inhibited to a greater extent than incorporation into 45S RNA. These findings suggested that the conversion of 45S RNA into 18S and 28S rRNAs was being blocked. As a test of this hypothesis, the authors measured the labeling of nucleolar RNA by ^{3}H-uridine and ^{14}C(methyl)methionine (17). Labeling of nucleolar RNA with ^{14}C-methionine would be due to the methylation of 45S RNA by S-adenosyl ^{14}C(methyl)methionine (18). Cells were pretreated with AFTX-B_1 (40 µg/ml) for 10 min, and then ^{3}H-uridine and ^{14}C(methyl)methionine were added to the medium for an unspecified amount of time. When the nucleoli of these cells were isolated and their RNA extracted, no difference was found in the ratio of ^{3}H-radioactivity to ^{14}C-radioactivity compared to controls (17). Thus, there was no evidence of an abnormally low level of nucleolar RNA methylation.

Further studies have confirmed that AFTX-B_1 interferes with RNA maturation. Garvican *et al.* followed the fate of ^{3}H-uridine incorporated into the nucleoli of monkey kidney (CV-1) cells in culture. Cells were pulsed with label for 30 min and then chased for 30 min with cold uridine in a medium containing 40 µg/ml AFTX-B_1. Polyacrylamide gel profiles of nucleolar RNA showed a build-up of label in 32S RNA compared to gels of control nucleoli. Furthermore, gels of cytoplasmic RNA derived from drug-treated cells showed a reduction in the amount of label in the 28S RNA peak, but very little reduction in the labeling of the 18S peak (19). These results indicate that AFTX-B_1 inhibits the maturation of 28S RNA at a step past the cleavage

of the 45S precursor to create 32S RNA, and suggest that the drug does not interfere with the maturation of 18S RNA.

Garvican et al. also tested the influence of AFTX-B_1 administration on tRNA maturation. CV-1 cells were labeled for 18 hrs with ^{14}C-uridine (0.5 µCi/ml) and then for 15-40 min with ^{3}H-uridine (15 µCi/ml) in the presence or absence of 40 µg/ml AFTX-B_1. Fractionation of cytoplasmic RNA on 15% polyacrylamide gels revealed two sharp peaks in ^{14}C-radioactivity corresponding to 5S RNA and 4S (t)RNA. Controls labeled for 15 min in ^{3}H-uridine also showed peaks in ^{3}H-radioactivity corresponding to 5S and tRNA in addition to a broad shoulder between the two peaks. Controls labeled for 40 min in the ^{3}H-medium had relatively less ^{3}H-radioactivity in the 5S peak and 4S shoulder, suggesting that some of these RNA species were precursors to tRNA. Cells labeled with ^{3}H-uridine for 40 min in the presence of AFTX-B_1 had a greater proportion of label in the 5S peak and 4S shoulder than their controls. The authors interpreted these results to indicate that AFTX-B_1 slowed the maturation of higher-weight precursors into tRNA (19). Their interpretation would have been more convincing had they demonstrated that label first appearing in the 'pre-tRNA' fractions could be 'chased' into the tRNA peak. Without such a demonstration, the possibility remains that the 'pre-tRNA' species were being degraded.

Moulé demonstrated that the 18S RNA synthesized in the presence of AFTX-B_1 is found in 40S ribosomal subunits; whereas no newly

synthesized 28S RNA is found in 60S subunits. When control rats were injected with ^{14}C-orotic acid, label began to appear in the 40S subunit of liver ribosomes by 30 min, and in the 60S subunit by 50 min. If AFTX-B_1 (1 mg/kg) was administered 3 min after injection of label, radioactivity still appeared in the 40S subunit at the correct time, although at a reduced level. No label appeared in the 60S subunit after 60 min. Dissociation of the 40S subunit with SDS yielded ^{14}C-labeled 18S RNA (20). Further studies by Moulé and Sarasin demonstrated that newly synthesized 40S subunits appeared on polysomes ($\geq$ 3 ribosomes per polysome) 7 hrs after rats were injected with AFTX-B_1 (1 mg/kg) and ^{14}C-orotic acid. The 40S and 60S subunits were released from the polysomes by the addition of 100 μM PURO. When the 60S subunits were purified, there was still no label associated with them (21). These studies clearly indicate that AFTX-B_1 preferentially inhibits the synthesis of large ribosomal subunits over that of small subunits.

In addition to inhibiting transcription, AFTX appears to have a separate effect on translation. In the study of Harley et al., incubation of HeLa cells with 20 μg/ml AFTX-B_1 resulted in a 60% inhibition of ^{14}C-leucine incorporation within 1 hr. Incorporation returned to within 10% of control levels by 3 hrs, and thus recovered faster than the incorporation of ^{3}H-uridine (see above). Furthermore, when the effects on translation were compared for doses of AFTX-B_1 (40 μg/ml, 3 hrs) and AMD (0.2 μg/ml, 30 min) that inhibited uridine

incorporation by about 50%, AFTX-B_1 inhibited ^{14}C-leucine incorporation by 80% while AMD inhibited it by 30% (17). A similar effect was found in CV-1 cells, where exposure of cultures to 40 μg/ml AFTX-B_1 for 3 hrs inhibited ^{3}H-uridine incorporation by almost 100%, and ^{14}C-leucine incorporation by 90%; whereas exposure of cultures to 2 μg/ml AMD for 3 hrs inhibited ^{3}H-uridine incorporation by 100%, and ^{14}C-leucine incorporation by only about 25% (22). Although AFTX-B_1 and AMD may affect the spectrum of RNA synthesis in different ways (see above), the disproportionate effect of AFTX-B_1 on leucine incorporation compared to AMD, and the difference in the kinetics of recovery of leucine incorporation compared to the kinetics of uridine incorporation strongly suggest AFTX-B_1 inhibits protein synthesis independent of its inhibition of RNA synthesis.

The above interpretation is supported by the results of experiments conducted by Sarasin and Moulé. The authors studied the relationship between leucine incorporation and polysome profiles in rats injected with 1 mg/kg AFTX-B_1. Incorporation of ^{14}C-leucine into protein fell to 30% of control values within 2 hrs of drug administration, and recovered to 60% of control values in 7 hrs. However, in contrast to the studies of Harley, Rees and Cohen, the recovery was only transient. By 17-48 hrs after drug administration, incorporation was back down to 20-30% of controls. Analysis of polysome profiles based on absorbance at 260 nm revealed that with increasing time after AFTX-B_1 administration: 1) the total amount of ribonucleoprotein decreased, 2) the relative amount of monosomes, disomes and

ribosomal subunits increased, and 3) the relative amount of polysomes decreased (23). Disruption of polysomes has been reported in a number of studies with AFTX-B_1 (17, 22, 24, 25). However, the kinetics of polysome disaggregation in the Sarasin and Moulé study did not agree with the kinetics of inhibition of leucine incorporation. Although the reduction in functional polysomes could account for the long-term (17-24 hrs) effect of AFTX-B_1 on leucine incorporation, it could not account for the rapid decay and transient recovery of leucine incorporation at earlier times (23). Thus, AFTX-B_1 appears to have two effects on leucine incorporation: 1) an early, transient effect that causes incorporation to first overshoot and then undershoot that predicted on the basis of polysome disaggregation, and 2) a long-term effect explainable on the basis of polysome disaggregation. The cause of the early effect is unknown, but might be explained by changes in the specific activity of the intracellular leucine pool. Although Sarasin and Moulé claimed that AFTX did not influence the entry of ^{14}C-leucine into the precursor pool, they failed to demonstrate that the specific activity of the leucine pool was unchanged by drug treatment (23). The long-term effect of AFTX-B_1 on polysome disaggregation could be caused by a combination of: 1) a reduction of the rate of initiation, 2) a drop in mRNA levels, 3) premature release of ribosomes. Inhibition of mRNA synthesis probably does not account for all the polysomal disaggregation because of the disporportionate effect of AFTX-B_1 on leucine incorporation compared to AMD (see above). Of the two remaining

possibilities, the first seems more likely because at least three inhibitors of RNA synthesis (AMD, cordycepin and 2-mercapto-1(β-4-pyridethyl) benzimidazole) have been shown to inhibit initiation (26). Identification of the processes contributing to polysome disaggregation, however, awaits more refined studies of polysome properties such as ribosomal initiation rates and transit times.

C. Side Effects

Before discussing the side effects of AFTX-B_1, or the other drugs treated in this chapter, a clarification of terms and experimental approaches will be helpful. Side effects are defined as those effects of a drug that occur independent of its primary action. With regard to the drugs being reviewed, their primary actions are defined as the inhibition of RNA or protein synthesis. By contrast, secondary effects are those that do result from the primary action. However, distinguishing between secondary and side effects that occur in an inhibitor experiment may not be a simple problem. Three basic approaches seem possible in sorting out secondary effects and side effects, and are listed below:

1) Administration of inhibitors of dissimilar structure that effect the same primary activity.

2) Administration of structural analogues of an inhibitor that lack the primary inhibitory activity.

3) Administration of an active inhibitor to a system in which the primary activity is already completely blocked, or non-existent.

Effects common to the agents used in the first approach are expected to result from primary or secondary actions. Those effects common to the drugs used in the second approach are expected to be side effects. Changes brought about by addition of the inhibitor in the third approach should be side effects. None of these approaches, however, necessarily detects all the effects in the category being tested. A more complete discussion of these strategies is found in section III of chapter VIII.

The discussion of drug side effects contained in this chapter is limited to those of a biochemical nature. Summaries of electrophysiological side effects are found in the discussion sections of chapters IV and VI.

Because the inhibitory effects of AFTX-B_1 on RNA and protein synthesis probably depend on its activation to a strong electrophile, the specificity of this agent seems doubtful. Indeed the carcinogenic and mutagenic actions of AFTX-B_1 in comparison to other inhibitors of macromolecular synthesis, e.g. AMD, imply the existence of many side effects. Two side effects of AFTX-B_1 have been found in a number of studies: 1) activation of lysosomal enzymes, and 2) inhibition of respiration and oxidative phosphorylation.

Pokrovsky et al. determined the effects of AFTX-B_1 on the level and distribution of 5 lysosomal enzymes isolated from rat liver. The enzymes were acid DNAse, arylsulfatases A and B, β-glucoronidase, β-glucosidase and β-galactosidase. Three hours after rats were

injected with about 12 mg/kg aflatoxin (not pure AFTX-B_1), the total activities of the first three enzymes increased by 168%, 141%, and 121%, respectively, compared to controls. The total activities of these enzymes continued to increase up to 48 hrs after drug administration, and by this time the total activities of the remaining two enzymes were also increased by 2 to 3-fold (27). These results are in agreement with those of Tung *et al.*, who administered aflatoxin (5 μg/g of feed) to chickens over a period of three weeks, and found that total acid phosphatase and β-glucoronidase activities increased by 1 to 2-fold (28). In the Pokrovksy *et al.* study, the increase in enzyme activities was paralleled by an increase in the number of lysosomes seen in sections of livers of drug-treated animals. To test for *in vitro* effects, purified lysosomes were incubated in the presence of 2×10^{-3} M AFTX-B_1 for 30 min, and then centrifuged for 25 min at 10,000 g. The activities of all 5 enzymes increased 3 to 4-fold in the supernatant fraction compared to controls. Unfortunately data pertaining to the total enzyme activities were not provided.

The above studies indicate that AFTX-B_1 can activate lysosomal enzymes *in vivo*. The action of the drug *in vitro* is less clear; it most likely increases soluble enzyme activities by some combination of increased total enzyme activity and increased release of enzymes from lysosomes. If AFTX-B_1 does activate lysosomal enzymes both *in vivo* and *in vitro*, then this action is probably a side effect. This interpretation is based on the fact that AFTX-B_1 does not inhibit transcription

or translation *in vitro* unless activated. Presumably the action of AFTX-B_1 on lysosomes *in vitro* occurs in the absence of this activation, and thus could occur in the absence of the inhibition of RNA synthesis.

AFTX-B_1 also appears to decouple oxidative phosphorylation in mitochondria. Bababunmi and Bassir analyzed the *in vitro* osmotic and ATPase activities of mitochondria isolated from rat liver. In the presence of 3×10^{-3} M AFTX-B_1 mitochondrial swelling reached a maximum in 6 min, and was reversed by the addition of 2 mM ATP. The degree of swelling was dose dependent over AFTX-B_1 concentrations ranging from 3×10^{-6} M to 3×10^{-3} M. In the presence of 2×10^{-4} M AFTX-B_1, mitochondrial ATPase was increased by 90%. The ability of AFTX-B_1 to alter these mitochondrial properties was dependent on the source of the material. Mitochondria isolated from rat kidney showed about one half the sensitivity of liver mitochondria to swelling and increased ATPase activity induced by 2×10^{-4} M AFTX-B_1. Mitochondria from heart or testis showed no swelling or increase in ATPase activity at this drug concentration (29). In a similar study, Bababunmi tested the effect of AFTX-B_1 on mitochondria isolated from rat brain. Mitochondria incubated in the presence of $1\text{-}5 \times 10^{-4}$ M AFTX-B_1 and 2, 4-dinitrophenol (DNP) showed a 42-90% increase in ATPase activity compared to DNP-treated controls. DNP was used to amplify the otherwise low level of mitochondrial ATPase. When AFTX-B_1 was administered *in vivo* to rats at 5 mg/kg, no effect was seen in the ATPase activity of mitochondria isolated from liver, brain or kidney (30). These data suggest that *in vitro* AFTX-B_1 has an action similar to that of DNP, an uncoupler of

oxidative phosphorylation. In contrast, the drug does not appear to affect mitochondria in vivo, suggesting that the activated form of the drug either preferentially binds to other cellular materials, or else is incapable of affecting mitochondrial ATPase levels when the mitochondria are accessible to it.

Doherty and Campbell studied the in vitro effects of AFTX-B_1 on respiration and oxidative phosphorylation in more detial. Oxygen consumption by ADP-stimulated (state 3) mitochondria isolated from rat liver was measured in the presence of 0.1 mM to 0.7 mM AFTX-B_1. Inhibition of oxygen consumption using succinate or glutamate as a substrate ranged from 15 to 45%, and leveled off at 0.5 mM AFTX-B_1 concentration. The inhibition at 0.5 mM AFTX-B_1 was not affected by addition of menadione, which can overcome a block in electron transport between NADH and coenzyme Q. In this case glutamate was a substrate, since succinate enters the respiratory chain at a later step. With succinate as a substrate, inhibition of oxygen consumption was blocked by the addition of N, N, N', N',-tetramethyl-p-phenylene diamine dihydrochloride (TMPD), an agent that can overcome a block in electron transport between cytochrome b and cytochrome c_1. When ascorbate and TMPD were added to mitochondria, in order to maintain TMPD in a reduced state and feed electrons to cytochrome c_1, no inhibition of oxygen consumption was seen on the addition of AFTX-B_1. Thus AFTX-B_1 blocks electron transport between cytochrome b and cytochrome c_1 (site II).

The effect of AFTX-B_1 on oxidative phosphorylation was studied by examining its influence on the ADP:O ratio of mitochondria using

three different types of substrate: 1) glutamate + malate, 2) succinate, 3) ascorbate + TMPD. The first type of substrate energizes phosphorylation at all three sites (FP → CoQ (site I), Cyt b → Cyt c_1 (site II), cyt a + a_3 → O (site III)), while the second energizes phosphorylation at sites II and III, and the third energizes phosphorylation only at site III. AFTX-B_1 (0.5 mM) lowered the ADT:O ratios by 23% and 17% for the first two sites, but did not affect the third site (31). Hence, in vitro administration of AFTX-B_1 blocks respiration at site II, and oxidative phosphorylation at sites I and II.

D. Summary

AFTX-B_1 is a potent hepatocarcinogen that inhibits RNA and protein synthesis in vivo. In order for the drug to inhibit these processes in vitro, it must first be activated by a microsomal fraction, which contains mixed-function oxygenases that presumably epoxidize the drug at the C(2)-C(3) double bond. The activated form of AFTX-B_1 can tightly bind to DNA and RNA in vitro, and presumably it is this binding that mediates the inhibition of transcription or translation in vivo.

AFTX-B_1 inhibits incorporation into RNA and is reversible over a period of about 24 hrs, although the spectrum of RNA synthesis probably does not return to normal. The drug blocks the maturation of 32S ribosomal RNA into 23S RNA, and thus blocks the assembly of 40S ribosomal subunits. In addition AFTX-B_1 inhibits protein synthesis at least in part by disaggregating polysomes. The mechanism of AFTX-B_1-induced polysome disaggregation, and the relationship between this

effect and the others caused by AFTX-B_1 are presently not understood.

Side effects of AFTX-B_1 include activation of lysosomal enzymes and inhibition of respiration and oxidative phosphorylation.

II Actinomycin D

AMD is a potent, irreversible inhibitor of DNA-dependent RNA synthesis in both prokaryots and eukaryots. The activity of AMD is determined by its binding to DNA. This is based on the facts that 1) AMD derivatives with lower DNA binding have a reduced inhibitory effect on transcription, and 2) that in competition studies, inhibition of transcription is decreased by increasing the DNA concentration, but not by increasing the amount of RNA polymerase, nucleotides or cofactors (32). Presumably, AMD inhibits transcription by slowing the movement of RNA polymerase along double stranded DNA (33).

AMD consists of two identical cyclic pentapeptides connected by a tricyclic phenoxazone chromophore (fig. 2). The peptide rings have alternating D- and L-amino acids, except for sarcosine, which does not contain an asymmetric carbon. This feature allows all the amino acid side groups to project toward the outside of the peptide ring. Each ring is cyclized as a lactone.

The chemical structures of AMD necessary for biological activity have been identified. Opening, or removal, of either peptide ring; substitution of Cl or OH for the 2-amino group in the chromophore; or reduction of the quinoidal 3-oxygen of the chromophore all render AMD inactive (32). In contrast, substitution of stearylamino or Br groups at the 7-position of the chromophore, or modification of the amino acid sequence of either or both peptide rings usually lead to only a partial loss of activity (32,34).

A. Binding to DNA

Binding studies have been carried out using many different types of natural and synthetic DNA species. In general, tight ($K \sim 10^6 M^{-1}$) binding occurs only with double stranded DNA. AMD does not bind strongly to single stranded DNA, single or double stranded RNA, or DNA-RNA hybrids (32, 34). Among naturally occurring DNAs, the number of AMD molecules bound roughly parallels the amount of deoxyguanosine (dG) present in the DNA (32, 34). For example, Hyman and Davidson showed that the number of AMD molecules that bound to crab poly d(A-T) accounted for only 60% of the 2% G-C base pairs contained in the DNA, even though the G-C base pairs were evenly distributed (35).

In an effort to elucidate the nature of the AMD binding site, Wells and Larson conducted an investigation of the binding of this drug to a number of synthetic DNA homopolymers. They discovered that AMD bound the most tightly ($K = 3.2 \times 10^6 M^{-1}$), and the most densely to poly d(G-C):poly d(G-C) (1 AMD per 12 nucleotides). In contrast, no binding was detected to poly d(I-C):poly d(I-C), which suggested that the 2-amino group of dG was necessary for AMD binding (36). Deoxyinosine (dI) is dG lacking the 2-amino group. This finding was in agreement with those of Cerami *et al.*, who showed that poly d(A-T):poly d(A-T), which normally did not bind AMD, could be made to bind AMD by the substitution of 2,6 diaminopurine (DAP) for all or some of the adenine (37). DAP differs from adenine by having

an additional amino group at the 2 position. The study of Wells and Larson also showed that AMD bound to most synthetic DNAs containing dG, with a preference for those in which dG was linked on the 3' side to a pyrimidine instead of a purine. One anomalous result from the study was that poly dI (single chain) bound AMD tightly ($K = 1.3 \times 10^{6} M^{-1}$), although at only one site per 111 nucleotides, even though the poly dI had no contaminating dG residues (36).

Of the models proposed for the binding of AMD to DNA, that of Sobell et al. (38) accounts for the most experimental data. The authors studied the structure of AMD co-crystallized with dG by means of X-ray diffraction, and found that 2 dG molecules crystallized with each AMD molecule. The configuration of AMD in this lattice was such that one peptide ring was positioned above, and the other below the chromophore, with both rings perpendicular to the plane of the chromophore (figs. 3A, B). This configuration was stabilized by two hydrogen bonds joining the NH group of the D-valine of one ring to the C=O of the D-valine of the other ring. Each guanosine molecule was positioned so that its purine base was stacked parallel to the AMD chromophore, with one guanosine above the chromophore, and one below it (fig. 3C, D). Each guanosine was hydrogen bonded through its 2-amino group to the C=O of L-threonine in the corresponding peptide ring. Thus, the AMD-dG_2 structure was stabilized by four strong (2.8 - 2.9 Å) hydrogen bonds. Further stabilization appeared to arise from a weak (3.13 - 3.17 Å) hydrogen bond connecting the ring N(3) of each guanine to the NH group

of the corresponding L-threonine, and from the hydrophobic interaction between the isopropyl moiety of each L-methylvaline residue with the sugar residue of the corresponding guanosine.

When two dC residues and the phosphodiester links connecting them to the dG residues were figured into the above model, other stabilizations appeared possible. Hydrogen bonds could have connected the 2-amino group of the AMD chromophore to the phosphate oxygen or to the dC furanose ring oxygen, although in the former case a water bridge might have been necessary.

The essence of the Sobell et al. model lies in the two-fold symmetry of the AMD-dG_2 complex. Although the symmetry is not true crystallographic symmetry (due to the placement of the phenoxazone 2-amino and 3-quinoidal oxygen groups), it determines the ability of AMD to bind to a DNA sequence showing two-fold symmetry. Thus AMD binds to $\frac{GpC}{CpG}$ DNA sequences. Furthermore, the model proposes that the AMD chromophore intercalates the bases of DNA while the peptide rings lie in the narrow groove of the double helix.

The model provides an explanation for other data regarding AMD binding to DNA. It shows that the necessity of the 2-amino group of dG and the 2-amino group of the AMD chromophore for biological activity may be due to their stabilizing the AMD=DNA complex with hydrogen bonds. The need of the quinoidal oxygen may arise from its stabilization of the chromophore planarity (34) which may be necessary for intercalation to occur. The model also accounts for the non-stoichiometric relationship between the number of dG residues in DNA

and the number of AMD binding sites, since AMD is predicted to bind most tightly to GpC sequences in DNA. Whether the model adequately deals with the binding of actinomycins substituted at the 7-position of the chromophore remains to be seen. Such a substitution would seem to block intercalation by steric hindrance.

The manner in which AMD inhibits transcription has been studied in some detail. Studies by Hyman and Davidson have shown that AMD almost exclusively affects the rate of RNA chain propagation, and not the rates of initiation or termination. The authors showed that the <u>in vitro</u> transcription of T7 DNA was inhibited almost completely by AMD concentrations that caused tight binding ($K = 2 \times 10^{6} M^{-1}$) at every 7 ± 2 base pairs. AMD did not inhibit the initiation of transcription, which was measured as the binding of T7 DNA to RNA polymerase immobilized on filters in the presence of ATP and GTP. These two nucleotides are the first transcribed from T7 DNA. Furthermore, when one AMD was bound for every 270 base pairs, transcription was inhibited by 30% and the average chain length, but not the number of chains, was reduced. This result suggested that chain propagation, but not chain termination, was lowered by AMD. After 10 min of transcription at an AMD binding density of one per 270 base pairs, an average of 1800 nucleotides per chain were incorporated, indicating that RNA polymerase (one per chain) had passed several AMD binding sites. This result, combined with the data of Müller and Corothers, suggested that AMD slows chain propagation by blocking the movement

of RNA polymerase (33). Müller and Corothers showed that the potency of AMD derivatives was correlated to their rate constant for dissociation from DNA (39). Hyman and Davidson also showed that AMD binding affected the rate terms of GTP and CTP incorporation, without affecting those of ATP or UTP. These results were consistent with the known preference of AMD binding to DNA containing G residues and were interpreted to mean that AMD slowed CTP and GTP incorporation (33).

B. Inhibition of RNA and Protein Synthesis In Vivo

The in vivo inhibition of transcription caused by a given AMD dose is not the same for all RNA species. In a quantitative study of nucleolar and nucleoplasmic RNA synthesis in cultured mouse L cells, Perry and Kelly showed that on a molecular weight basis the synthesis of 45S, 5S, and tRNA was 50 to 100 times more sensitive to inhibition by AMD than the synthesis of nucleoplasmic RNA (N-RNA). Within each class of RNA molecules, however, the sensitivity to AMD inhibition was positively correlated to the size of the RNA. The data WERE consistent with the interpretation that each rRNA species was transcribed from many sequential copies of the DNA coding for them; whereas N-RNA molecules were individually transcribed. By having rRNA genes sequentially arranged without each having an initiation site, the effective length of rRNA gene transcription is increased, causing the synthesis of rRNA to be disproportionately sensitive to AMD (40).

Besides inhibiting transcription, AMD has been shown to inhibit translation. Singer and Penman (41) found that polyribosomes

isolated from HeLa cells that were labeled for 15 hr and then incubated with 4 μg/ml AMD for an additional 3 hrs sedimented more slowly than non-AMD-treated controls. If HeLa cells were incubated for an additional 1 hr in 1 μg/ml CHX after labeling and AMD treatments, the polysome sedimentation pattern was close to that of controls. This result suggested that AMD slowed the initiation of translation, which caused a decrease in the number of ribosomes per polysome, and that the addition of CHX slowed peptide chain elongation, allowing the steady state number of ribosomes per polysome to increase. Singer and Penman then measured the stability of mRNA in AMD-treated cells by taking advantage of the selective binding of mRNA to poly U immobilized on glass fiber filters. This property is based on the finding that most mRNAs (but not histone mRNA) contain a length (50-200 residues) of poly A at their 3' terminus (42). The sedimentation distribution and level of uridine incorporation into mRNA were unchanged in cells prelabeled for 90 min and then incubated in 4 μg/ml AMD for 20 min, 2 hr, 3.5 hr or 5 hrs, suggesting that mRNA had an average half-life much greater than 5 hrs. This result, in combination with the finding that the sedimentation velocity of polysomes could increase after 3 hr treatment with AMD (in the presence of CHX) suggests that the HeLa cell mRNA remained at control levels, and in undamaged condition after AMD treatment. Thus AMD can decrease the rate of initiation of translation without an attendant decrease in mRNA levels.

These findings have been confirmed in a more quantitative study by Craig, using mouse L cells (26). Cultures treated for 4 hrs

with 1 μg/ml or 2 μg/ml AMD had 40% fewer polysomes (≥ 3 ribosomes per polysome) than controls. The decrease in the polysome profile was greatest for large polysomes (> 8 ribosomes per polysome), and was attended by a 3-fold increase in monosomes. The time course (half-life = 5-6 hrs) and magnitude of the polysome decay closely paralleled that of the inhibition of ^{3}H-leucine incorporation. Cells treated with 1 μg/ml of CHX during the last 45 min of incubation with AMD showed a slightly higher level of polysomes and a lower level of monosomes than controls. These experiments, and those of Singer and Penman (above) indicate that AMD slows the rate of initiation of translation.

C. Side Effects

Compared to AFTX-B_1, AMD might be expected to be a more specific inhibitor of RNA synthesis, because of its high affinity for double stranded DNA. Nevertheless, there have emerged three possible side effects of AMD: a degradation of cellular RNA, an inhibition of respiration and alteration of nucleic acid precursor uptake rates.

Stuart and Farber compared the effects of AMD (2.5 mg/kg body weight) and ethionine (0.153 M/kg body weight) on the content and synthesis of RNA in rat liver. Both agents inhibited RNA synthesis by 90-95% (43). Ethionine was thought to inhibit RNA synthesis by trapping intracellular adenine as S-adenosyl ethionine and lowering the level of intracellular ATP (49); its effect on RNA synthesis was reversed when methionine was administered to the rats (43).

The RNA content of liver cells was analyzed by comparing the ratio of RNA-phosphorous to DNA-phosphorous, because the DNA content of this tissue was not influenced by drug treatment. Both AMD and ethionine induced a steady-state 30% decrease in the RNA content of the liver. AMD caused this level to be reached within 2 hrs, whereas the same level was not reached until 18 hrs after administration of ethionine. This effect was not due to differences in the magnitude or kinetics of inhibition of RNA synthesis caused by the two drugs because they both inhibited RNA synthesis by 90-95% within two hrs of administration. When rats were given ^{14}C-orotic acid and then injected with AMD 2 hrs later, the specific activity of the nuclear RNA rapidly decreased by about 50% compared to controls. In contrast, ethionine did not affect this parameter over the period of 1-24 hrs tested. Examination of ribosomal and "soluble" RNA in these experiments showed that AMD caused a small decrease in their specific activities, while ethionine caused their specific activities to remain almost constant. When rats were given AMD followed 4 hrs later by ethionine, the decrease caused in the specific activity of nuclear RNA was the same as that caused by AMD administration alone (43). Hence, AMD appears to degrade cellular RNA in addition to inhibiting RNA synthesis. In contrast, ethionine can inhibit RNA synthesis without shortening or enhancing the lifetime of RNA. These results suggest that the degradation of RNA is a side effect of AMD.

Schwartz and Garofalo studied in more detail the fate of prelabeled liver RNA in rats treated with AMD. In control experiments

most incorporated ^{14}C-leucine appeared in nuclei 40 min after administration. Labeled RNA was distributed among peaks at 45-34S, 28S, 18S, 5-10S, and 4S when analyzed on sucrose gradients, while very little label was found in the cytoplasm. When AMD was administered 40 min after the label, and its effects assayed 140 min later, more than half the nuclear label seen at 40 min was no longer in the nucleus, yet no additional label appeared in the cytoplasm. In contrast, controls labeled for 180 min showed that about 30% of the nuclear label had been transferred to the cytoplasm, appearing as 28S, 18S and 4S peaks. Optical scans of nuclear and cytoplasmic RNA fractions on sucrose gradients showed a slight loss of 28S and 18S RNA from the nuclei of AMD-treated rats, but no change in the cytoplasmic profile (45). This study suggests that AMD preferentially degrades newly synthesized rRNA and tRNA.

Other studies have shown that AMD also degrades mRNA. Singer and Penman (46) analyzed the half-life of mRNA derived from HeLa cell polysomes by means of its affinity to oligo-dT-cellulose. Of the label incorporated into polysomes prepared in this way, 80% was associated with mRNA and 14% was associated with ribosomes. They labeled control cells for 18 hrs in a medium containing 0.1 μCi/ml ^{14}C-uridine, after which ^{3}H-uridine was added to the medium at a level of 2 μCi/ml. When mRNA was isolated from cells 3-13 hrs after the addition of the ^{3}H-label it showed two different rates of decay. The ^{14}C-labeled mRNA had a half-life of 21 hrs, while the ^{3}H-labeled mRNA had a half-life of 6 hrs. When the experiment was repeated, except that 4 μg/ml of AMD

was added 1 hr after the ^{3}H-label, the ^{14}C-labeled mRNA had a half-life of 12 hrs, while the ^{3}H-labeled mRNA had a half-life of 4.5 hrs. These experiments indicate that AMD can shorten the half-life of mRNA. In addition, however, they raise doubts about the accuracy of the mRNA half-life determinations made in the earlier Singer and Penman (41) study (see section B).

Laszlo et al. have demonstrated that AMD inhibits respiration and anaerobic glycolysis in cultures of human leukemic leucocytes. Cells exposed to a 1-50 µg/ml pulse of AMD for 140 min showed approximately a 50% loss of O_2 consumption and anaerobic CO_2 production. Cells exposed to 50 µg/ml AMD for 3 hrs had ATP levels reduced to 10% that of controls. This dose of AMD lowered amino acid incorporation by about 30% in an hour. In contrast, 10^{-4} M PURO completely blocked amino acid incorporation without affecting O_2 consumption at all (47). These data suggest that AMD does not block respiration through the inhibition of protein synthesis. However, because doses of AMD capable of inhibiting respiration also inhibited uridine incorporation, the inhibition of respiration could not be unambiguously classified as a side effect (47).

Dybing has shown that AMD (1 µg/ml, 1 hr) can alter the uptake of thymidine, uridine and inosine into MH_1C_1 rat hepatoma cultures. Thymidine uptake into the acid soluble pool was increased to 200% of controls, while uridine uptake was increased by 31% and inosine uptake reduced by 61%. The effect of CHX (15 µg/ml) on thymidine uptake was negligible, whereas the combined application of CHX and AMD caused the

same effect as AMD alone (48). In a later study the author demonstrated that 28 µg/ml CHX could inhibit inosine uptake by 53% and block ^{14}C-phenylalanine incorporation by 96%. When cells were exposed to 10^{-6} M AMD in the presence of the above CHX concentration, inosine uptake was inhibited by 84%, while treatment with AMD alone caused an inhibition of only 16% (49). It thus appears that AMD affects thymidine and inosine uptake independent of its action on protein synthesis.

D. Summary

AMD inhibits transcription by binding to double stranded DNA. The binding probably occurs at G-C sequences of the DNA, and is thought to involve intercalation of the AMD-chromophore and placement of the peptide rings in the narrow groove of the double helix. Transcription is presumably inhibited by AMD blocking the movement of RNA polymerase along DNA. AMD also inhibits protein synthesis by blocking initiation, although the relationship between this effect and the inhibition of transcription is not clearly understood.

The side effects of AMD include degradation of cellular RNA, inhibition of respiration and alteration of nucleoside uptake.

III. Puromycin

A. Effect on Protein Synthesis

PURO inhibits protein synthesis in both prokaryots and eukaryots by prematurely terminating nascent polypeptide chains (50) Rabinowitz and Fisher showed that ^{14}C-valine incorporation into Ehrlich ascites tumor cells was decreased by 40-80% during 15 min incubations with 2.5 x 10^{-5} M PURO. Addition of 5 x 10^{-5} M PURO to cells previously labeled for 20 min caused a rapid 70% decline in the specific radioactivity present in the ribosomal fraction of these cells, and an attendant 10-15% increase in the specific activity of non-ribosomal ("soluble") proteins (51).

Allen and Zamecnik showed that ^{14}C-valine labeled peptides were released from a cell free reticulocyte protein synthesis system by the addition of 2 x 10^{-4} M PURO, and that these peptides did not have the same chromatographic and solubility properties as hemoglobin, the major product of the control system. Dinitrophenylation and subsequent hydrolysis of peptides released by PURO showed that they were similar to hemoglobin by containing N-terminal valine. Peptides released by (O-methyl-^{14}C)PURO contained ^{14}C label that was identified as ^{14}C-O-methyl tyrosine after HCl digestion. Dinitrophenylation of peptides prior to HCl digestion did not change the nature of the released ^{14}C-label, indicating that the amino group of O-methyl

tyrosine was probably involved in a peptide bond. Furthermore, the amount of PURO that coprecipitated with the released peptides was equimolar with the calculated number of N-terminal valine residues, suggesting that one PURO molecule was incorporated into each peptide (52).

Nathans later showed that (O-methyl-^{3}H)PURO was incorporated into a TCA precipitable, DNAse and RNAse insensitive fraction of E. coli that yielded labeled O-methyl tyrosine upon digestion with HCl or pronase. Trypsin-chymotrypsin digests of incorporated PURO yielded many radioactive spots when chromatographed, including a spot that corresponded in mobility to ^{3}H-PURO. Carboxypeptidase A treatment of trypsin-chymotrypsin digests did not free any labeled O-methyl tyrosine, suggesting that this moiety of PURO was not incorporated as a free amino acid (53). Thus the amide bond connecting the nucleoside moiety of PURO with the amino acid moiety is resistant to trypsin, chymotrypsin and carboxypeptidase. In contrast, the amino acid moiety of PURO appears to be incorporated by a peptide bond that is sensitive to these enzymes. It was presumed that PURO was the C-terminal residue of the released peptides because it has no carboxyl group with which to make a peptide bond (53).

Smith et al. confirmed that PURO was the C-terminal residue of PURO peptides by incubating an in vitro poly A directed, polylysine synthesizing system, derived from E. coli, with PURO, or ^{32}P-(5'-B-cyanoethyl phosphate)PURO (PCEP), a biologically active derivative

of PURO. Based on chromatographic properties, most peptides released by either drug were the di- and tri-lysyl derivatives. Trypsin digestion of di- and tri-lysyl-PURO yielded dilysine from the former product, and a combination of mono-, di- and trilysine from the latter product. These results suggest that PURO is attached to the C-terminal end of these peptides, since trypsin cannot digest dilysine, and only slowly digests trilysine into mono- and dilysine. Furthermore, if PURO were at an N-terminal, or internal position, then recovery of puromycyl-lysine would have been expected. Studies with ^{32}P-PCEP showed that no ^{3}H-lysine labeled peptides were released without ^{32}P-radioactivity, and that compounds thought to be di-, tri- and tetralysyl-PCEP, based on chromatographic behavior, had molar ratios of ^{3}H- to ^{32}P-radioactivity close to the expected values of 2, 3, and 4, respectively. Removal of the ^{32}P-cyanoethyl phosphate group from dilysyl-PCEP yielded a compound that chromatographed with dilysyl-PURO (54). Thus, all peptides released contained PCEP, and PCEP was incorporated in a manner indistinguishable from that of PURO, once the cyanoethyl phosphate group was removed.

Studies by Traut and Monro showed that PURO could be incorporated by an incomplete cell free system. Ribosomes bearing polyphenylalanyl-tRNA were removed from a poly U directed system and subsequently reacted with PURO. Release of peptidyl-PURO was not dependent on the presence of poly U, and was only partially dependent on GTP and other supernatant fractions. Furthermore, PURO could release peptidyl-PURO from 50S ribosomal subunits alone, if they

were charged with polyphenylalanyl-tRNA (55). Thus the site of PURO action included the 50S (or 60S) ribosomal subunit.

Evidence from the above, and other studies, in addition to consideration of the structure of PURO, suggests that PURO acts as an analogue of aminoacyl-tRNA; the amino nucleoside moiety being analogous to the 3' terminal adenosine of tRNA, and the O-methyl tyrosine moiety being analogous to acylated amino acid (fig. 4). In the case of tRNA, the terminal nucleoside is connected to the amino acid by an acyl linkage, whereas in the case of PURO the two analogous moieties are connected by an amide linkage (fig. 4). Because of these structural similarities, PURO can bind to the ribosomal A site, and be incorporated into the nascent peptide. However, because PURO has no carboxyl group available to participate in a peptide bond, and because PURO has no anticodon to stabilize binding at the P site, the peptidyl-PURO falls off the ribosome (50).

B. Side Effects

PURO causes side effects in carbohydrate and lipid metabolism as well as in respiration and RNA synthesis. These diverse actions may result from it being a structural analogue of adenosine.

Sovik studied the effect of PURO and its derivatives on glycogen synthesis in the isolated rat diaphragm. When the preparation was preincubated in the presence of PURO (270 μg/ml) for 40 min, and labeled for the last 10 min of this period with ^{14}C-glucose, incorporation into glycogen was reduced by 37% compared to controls. This effect was not caused by a decrease in the entry of glucose into the muscle,

an increased breakdown of glycogen or an increased level of glucose-6-phosphate in the muscle (56). Glucose-6-phosphate is known to activate glycogen synthetase (D form) (57). Comparison of the dose-response data for the inhibition of glycogen synthesis with that of protein synthesis showed that the latter effect had a lower PURO threshold (20 µg/ml) than the former (150 µg/ml). Furthermore, a 2¼ hr pulse of 5×10^{-4} M PURO, PAN or 6-dimethylamino PURO (DAP) inhibited glycogen synthesis by about 70%. At the same dose PURO inhibited ^{14}C-amino acid incorporation by over 90%, while the two derivatives inhibited this activity by only 10-20%. These data suggested that PURO inhibited glycogen synthesis independent of its inhibition of protein synthesis. Sovik speculated that PURO and its derivatives modulate glycogen synthesis by converting glycogen synthetase from the D form (dependent on glucose-6-phosphate) to the I form (independent) (56).

This interpretation received support from the work of Appleman and Kemp, who showed that 15 min PURO pulses (0.5 mM) increased the concentration of 3', 5' cyclic adenosine monophosphate (cAMP) in the rat diaphragm by 10-80%. They went on to demonstrate that 1.6 mM PURO completely inhibited cAMP phosphodiesterase activity. These data in combination with those of Sovik suggest that PURO increases muscle glycogen synthesis by inhibiting cAMP phosphodiesterase activity. This action raises the intracellular cAMP concentration, which would then catalyze the conversion of glycogen synthetase from the D to I form through the activation of glycogen synthetase kinase (58).

Consonant with the above results is the finding that PURO increases glycogenolysis in liver. Hoffert and Boutwell administered PURO, PAN or DAP to mice (550 μM/kg body weight) and showed that 1 hr after injection liver glycogen content was decreased by 63, 92, and 95%, respectively. These drugs inhibited ^{14}C-glycine incorporation by 97%, 19%, and 13%, respectively (59). Blatt et al. showed that 2 hr after PURO injection (10 μg/g body weight), the glycogen phosphorylase activity of tadpole liver was increased by 70% (60). The above studies present data that are consistent with the hypothesis that PURO raises cAMP levels in liver by blocking cAMP-phosphodiesterase. Increased cAMP levels should activate phosphorylase kinase, which in turn should convert phosphorylase b to phosphorylase a. This last enzyme catalyzes the digestion of gylcogen to glucose-1-phosphate (57). Whether or not PURO does affect the levels of cAMP in all the above studies, these results strongly suggest that the inhibition of glycogenesis and activation of glycogenolysis are side effects of PURO administration.

Other PURO side effects that may be related to changes in cAMP metabolism are an increase in lipolysis and induction of liver enzyme activity. Korner and Raben showed that 10^{-3} M PURO or PAN blocked the insulin mediated inhibition of release of fatty acids from epididymal fat pads of rats (61). This release is mediated by epinephrine and presumably involves cAMP activation of a protein kinase that activates lipase enzymes (62). Beck et al. administered

PURO (12 mg/kg body weight) to rats, and showed that it caused a huge increase in liver ornithine decarboxylase (ODC) activity. The kinetics of ODC induction were not similar to those of the inhibition of protein synthesis. The latter activity peaked at 1 hr after PURO administration, while the former peaked at 3 hrs, at a time when protein synthesis was normal. This finding, coupled with the fact that dibutyryl-cAMP also induced ODC activity suggests that PURO exerts its effect by increasing cAMP levels (63).

PURO may also exert an influence on mitochondrial function independent of the inhibition of protein synthesis. In EM studies of the brains of mice receiving bitemporal injections of PURO (90 µg total), Gambetti et al. found swollen mitochondria in the entorhinal cortices and ventral hippocampus. The swelling was characterized by a disappearance of the inner matrix, and a diminution of the number and length of cristae. Swollen mitochondria were seen almost exclusively in perikarya, and rarely if ever in dendrites, axons, presynaptic endings or glia. Rats treated with both PURO (90 µg) and acetoxycycloheximide (ACHX) (90 µg) showed a much lower degree of mitochondrial swelling, while those given ACHX (90 µg) alone showed no mitochondrial damage at all. These results suggested that peptidyl-PURO was the agent causing the mitochondrial swelling, because treatment of mice with ACHX in combination with PURO would be expected to block the formation of peptidyl-PURO, and treatment with ACHX alone would not cause release of nascent peptides (see section A). Biochemical studies supported this interpretation by showing that the magnitude

and kinetics of ^{3}H-PURO incorporation (presumably into peptidyl-PURO) paralleled the swelling of mitochondria in PURO-, and PURO plus ACHX treated mice, while the amount of TCA soluble PURO counts was the same in both groups (64). Although Gambetti et al. did not determine the extent to which mitochondrial function was impaired, other workers have found possible side effects of PURO and PAN on respiration and oxidative phosphorylation. Jones and Banks compared the effects of PURO and CHX on oxygen uptake in slices of guinea pig cortex. Incubation of the preparation for 60 min in 100 µg/ml PURO inhibited respiration by 32%, while treatment with CHX (100 µg/ml) or PURO plus CHX (same doses) inhibited respiration by only 7%. Administration of PURO or CHX alone inhibited ^{14}C-valine incorporation by 50-60% (65). These data, like those of Gambetti et al., suggest that the synthesis of peptidyl-PURO, and not the inhibition of protein synthesis, mediates the structural and biochemical changes in mitochondria caused by PURO. Other evidence, however, indicates that PAN may have a direct effect on mitochondrial function. Bartlett et al. administered PAN in the food of rats for 10 days and then tested the ATPase activity of mitochondria isolated from kidneys. Although unstimulated and DNP-stimulated ATPases were little affected, the magnesium-stimulated, and the magnesium-sodium-potassium stimulated ATPases were increased by 41% and 35% respectively. The authors suggested that PAN was inhibiting oxidative phosphorylation or some specialized aspect of ion transport conducted by these mitochondria (66). Whether this effect can be generalized to PURO treatment, and to mitochondria

from other tissues is not as yet clear.

PURO has also been implicated in the inhibition of RNA synthesis. In autoradiographic studies, Jackson and Studzinski found that PURO decreased the incorporation of ^{3}H-uridine into the nuclei of HeLa cells. Cultures were exposed to 100 µg/ml PURO for 30 min, and then to drug and label for an additional 30 min. This treatment caused complete inhibition of amino acid incorporation in other experiments, and in the autoradiographic studies, caused the number of grains found over nucleoli and nuclei to be decreased by 95% and 34% respectively. In similar experiments after a 240 min chase without PURO, cytoplasmic grains were decreased by 72% (67). In a biochemical study, Studzinski and Ellem found that HeLa cells exposed to 3 µg/ml PAN for 72 hrs had their RNA content reduced by about 20%, while their DNA and protein contents were normal. Incorporation of ^{32}P-orthophosphate into rRNA was inhibited by 75% after exposure of cells to 6 µg/ml PAN for 48 hrs. Incorporation into other RNA and into DNA was hardly affected (68). Taken together, the above two studies suggest that PURO and PAN preferrentially inhibit rRNA synthesis, and that this effect is unrelated to the inhibition of protein synthesis. One possible explanation for this, and perhaps all the above side effects, is that PURO, as a structural analogue of adenine, inhibits the metabolism of adenine derivatives such as cAMP, ATP and ADP. Other adenine derivatives with inhibitory properties similar to those of PURO include the methyl xanthines (inhibitors of cAMP phosphodiesterase) (62) and cordycepin (inhibitor of RNA synthesis, and possibly mRNA transport) (69).

C. Summary

PURO inhibits protein synthesis by causing premature release of nascent peptide chains. This property is based on the similarity of the structure of PURO with that of the 3' terminus of aminoacyl-tRNA. The drug is incorporated at the carboxyl end of the peptide chain, but does not have a carboxyl group available for bonding with another amino acid.

Side effects of PURO include inhibition of glycogenesis, RNA synthesis and respiration in addition to stimulation of glycolysis, lipolysis and enzyme activity. These actions may arise from PURO being a structural analogue of adenine.

IV. Cycloheximide

A. Effect on Protein Synthesis

In contrast to PURO, CHX inhibits protein synthesis in eukaryots only, but the mechanism by which this effect occurs has not been fully elucidated. CHX is a member of the group of drugs known as glutarimides, which are characterized by a β(2-hydroxyethyl) glutarimide moiety attached to a ketone that is usually cyclic (fig. 4). The ketone-carbonyl, imide-nitrogen and hydroxyl groups are necessary for biological activity (50).

It is generally believed that CHX slows or stops the movement of ribosomes along mRNA without causing a loss of the nascent polypeptide chain. Colombo, Felicetti and Baglioni showed that a 5 min exposure of intact reticulocytes to 1.2 x 10^{-4} M CHX inhibited the incorporation of ^{14}C-amino acids by about 97% without disaggregating polysomes and without releasing growing peptide chains. CHX (10^{-4}M) inhibited the release of nascent ^{14}C-labeled peptide chains caused by 30 sec exposure to 2.8 x 10^{-4} M PURO by about 50%. However, longer exposure to PURO (5 min) completely removed label from polysomes, suggesting that CHX slows the chain elongation process. Incubation of monosomes, derived from reticulocyte polysomes treated with 10^{-2}M NaF, with 10^{-4}M CHX prevented their reaggregation (70). Thus CHX may affect chain initiation as well as chain elongation.

There is some controversy in the literature as to whether CHX primarily inhibits chain initiation, elongation or termination. Baliga, Pronczuk and Munro, using a cell-free rat liver protein synthesis system showed that 0.1 µg/ml (3.6 x 10^{-7} M) CHX inhibited ^{14}C-leucine incorporation into the complete system by only 20%, yet this same dose inhibited the resumption of ^{14}C-leucine incorporation by about 60% following addition of amino acids to a system previously lacking them. In the latter experiment, reaggregation of polysomes disaggregated by previous withdrawal of amino acids was blocked by 0.1 µg/ml CHX, whereas in the former experiment, stabilization of polysomes was not complete until CHX was used at a dose of 1 mg/ml. This dose of CHX blocked incorporation by 95% (71). Thus CHX appears to inhibit chain initiation at a dose 10^{4} times lower than the dose

that stops chain elongation in this system.

Srinivasan et al. have suggested that CHX preferentially inhibits chain termination in an in vitro system of rat liver polysomes and cell sap. In a dose-response study the authors found that the incorporation of ^{14}C-leucine into cell sap during a 10 min pulse of CHX was a linearly decreasing function of the logarithm of the CHX dose from 5-2000 µg/ml (1.8×10^{-5}M - 7.1×10^{-3}M), whereas the label associated with the ribosomes stayed at control levels up to a dose of 250 µg/ml (8.9×10^{-4} M), and then fell linearly with the logarithm of dose (72). These data are consistent with the scheme that CHX, up to a dose of 250 µg/ml, blocks chain termination, and thus leaves ribosomes labeled at control levels, while at higher levels of CHX, chain initiation or elongation begins to slow down.

CHX appears to inhibit protein synthesis by an interaction with transfer factor II (TF II), a eukaryotic cytoplasmic GTPase that catalyzes the translocation of peptidyl-tRNA from the ribosomal A site to the P site, and moves the ribosome forward one codon along mRNA (73). Baliga, Pronczuk and Munro (71) used an in vitro rat liver system to measure the incorporation of ^{14}C-amino acids, supplied as ^{14}C-aminoacyl-tRNA, into peptides. The system consisted of polysomes supplemented with a crude transfer factor fraction, GTP and glutathione (GSH). When the transferase fraction was treated with 1 mg/ml (3.5×10^{-3}M) CHX, then washed and incubated with the rest of the system, incorporation was reduced to 40-45% of the control level.

However, when 20 mM GSH, 10 mM dithiothreitol, or 20 mM 2-mercaptoethanol were incubated with the transferase fraction, and then washed out, and the transferase and CHX added to the rest of the system, incorporation was potentiated to 63-72% of the control level. This potentiation lasted at least 1 hr. Incubation of polysomes with 20 mM GSH before or during incubation with CHX had no potentiating effect on the level of incorporation. The authors interpreted these results to indicate that GSH, which is a sulfhydryl protein, or the other reducing agents, could activate TF II and thus protect it from attack by CHX. TF II activity has been potentiated by sulfhydryl compounds in another study in which CHX was not used (74). In a subsequent study, Baliga, Cohen and Munro showed that incubation of a rat liver system with ^{3}H-PURO (10^{-6}M) and CHX (3.6×10^{-6}M) for 60 min did not release peptidyl-PURO fragments. If, however, polysomes were preincubated in buffer for 5 min, presumably in order to allow all peptidyl-tRNA to be translocated to the ribosomal P site, CHX did not inhibit the release of peptidyl-PURO (75).

McKeehan and Hardesty measured the incorporation of label supplied as ^{14}C-leucyl-tRNA into nascent globin protein attached to reticulocyte ribosomes. They found that when ribosomes, salts, buffer and 0.20 mM GTP were incubated for 15 min, and then TF I, TF II, ^{14}C-leucyl-tRNA and 10 mM CHX were added for an additional 20 min, the incorporation of label was inhibited by 67% compared to a control that was identical except for the addition of CHX. When TF II was added during the first incubation instead of the second,

the incorporation of label was inhibited by only 30% of another control which was identically treated except for the addition of CHX. The activities of the two controls were identical. Similar results were obtained with ribosomes carrying phenylalanyl-tRNA, when peptide bond formation was measured by the release of phenylalanyl-PURO. When TF II, 1 mM CHX and 0.6 μM PURO were added during the second incubation, release of phenylalanyl-PURO was inhibited by 45% compared to controls. If TF II was added during the first incubation instead of the second, no inhibition of release was found (76).

The results of the experiments cited above concerning TF II show that CHX inhibits protein synthesis *in vitro* by an interaction with the translocase system, and that this interaction can be prevented by protecting TF II with reducing agents, or allowing translocation of peptidyl-tRNA to the ribosomal P site prior to the addition of CHX. It remains unclear, however, whether the deactivation of TF II is the only mechanism by which CHX inhibits protein synthesis *in vivo*. The increased inhibitory effect of CHX on intact cells compared to cell-free systems (50,70) may indicate that CHX inhibits protein synthesis at more than one site.

B. Side Effects (CHX)

CHX has been shown to cause possible side effects in respiration, the uptake of amino acids and nucleic acid precursors, and the synthesis of RNA.

Garber *et al.* studied the effect of CHX on mitochondria isolated from the liver of rat or guinea pig. CHX concentrations of

2-10 mM inhibited state 3 respiration and ATP formation (measured by proton uptake) in mitochondria using substrates such as malate plus glutamate, or β-hydroxybutyrate. These substrates supply electrons that flow down the entire electron transport chain. In contrast, CHX did not inhibit respiration or ATP formation when succinate was used as a substrate which suggests that CHX acts at a point proximal to the entry of succinate in the electron transport chain. Studies with carbonylcyanide p-trifluoromethoxyphenylhydrazine (FCCP), an uncoupler of oxidative phosphorylation, showed that CHX could block the increase in mitochondrial respiration and ATPase activity caused by this agent when malate plus glutamate or β-hydroxybutyrate were substrates. With succinate as a substrate, CHX did not block the FCCP-stimulated increase in respiration and ATP formation. The authors interpreted these results to mean that CHX specifically blocked energy transformation at site I (NADH → coenzyme Q) of electron transfer, and that it might cause a secondary inhibition of respiration at this point (77). Other effects secondary to this inhibition appeared to be inhibition of phosphoenolpyruvate synthesis from malate and α-ketoglutarate (77), gluconeogenesis from pyruvate, lactate or glycerol in rat or guinea pig liver (78), and lipogenesis in rat epididymal fat pads (79).

CHX has been shown to inhibit the uptake of a variety of compounds into plant tissues. MacDonald and Ellis (80) have demonstrated that beet and carrot storage tissue disks, potato tuber disks, wheat roots and pea radicles had chloride uptake inhibited by 41-75% after

exposure to 1 µg/ml CHX for 60 min. In the case of the beet tissue, this effect was distinct from that of PURO (10^{-4} M) because either drug alone could block the development of this activity, but only CHX could inhibit chloride uptake after its development (80, 81). Evans has shown that 3.6-360 µM CHX inhibited uptake of 2, 4-dinitrophenol and glucose into Euglena. The dose-response relationships were peculiar because increasing doses of CHX had a decreasing effect on glucose and DNP uptake. In contrast, phenylalanine or leucine incorporation were increasingly inhibited by larger doses of CHX. Although phenylalanine uptake was inhibited by 50% at the lowest CHX dose, and intracellular phenylalanine and leucine specific activities were not measured (82), these results nevertheless suggest that CHX was not blocking DNP or glucose uptake by inhibiting protein synthesis. This interpretation receives some support from the study of Timberlake and Griffin. These authors showed that the uptake of labeled proline into the water mold Achlya bisexualis was rapidly and completely inhibited by 2.5 µM CHX, and that incorporation of proline into pre-labeled cells was similarly inhibited by CHX. To test if protein synthesis were necessary for proline uptake, the effects of treatment with 150 µM p-fluorophenylalanine (PFPA) were compared with those of treatment with 2.5 µM CHX. These doses were the lowest necessary to cause maximal inhibition of growth. When incorporated, PFPA presumably caused newly synthesized proteins to be non-functional. In contrast to the effect of CHX, PFPA did not decrease proline uptake, suggesting that this activity was not dependent on the synthesis of normal

proteins (83). Clearly, however, the content and position of phenylalanine residues in a protein would determine the extent to which its activity would be modified by PFPA incorporation. Although the authors demonstrated that alkaline phosphatase activity was inhibited by this treatment (83), there is no assurance that the activities of all newly synthesized proteins would be changed.

Ross has shown that CHX can lower the uptake of nucleic acid precursors and inhibit their interconversion. When cocklebur leaf disks were incubated in 2 mM CHX for 4 hrs, protein synthesis was inhibited by 50%, while radioactive orotic acid, uridine or cytidine uptake was inhibited by about 40%. Compared to controls CHX lowered the ratio of radioactive CTP to radioactive UTP in the RNA of leaves labeled with orotic acid or uridine, and raised the ratio for leaves labeled with cytidine. These findings suggested that the interconversion of UTP and CTP was inhibited by CHX. Because this interconversion involves a transamination from glutamine to CTP, Ross suggested that CHX inhibited the reaction by means of its structural similarity to glutamine (84).

CHX has also been shown to inhibit RNA synthesis. Kloet studied the synthesis of RNA in Saccharomyces carlsbergenesis, and found that CHX altered the metabolism of rRNA and sRNA. Yeast protoplasts labeled with ^{14}C-uracil for 45 min in the presence of 10 µg/ml CHX had incorporation lowered by about 70%. Analysis of cellular RNA on sucrose gradients revealed that CHX caused a disproportionate amount of label to remain as high molecular weight

RNA (23S) and as sRNA, even though optical scans of the gradients appeared normal. Labeling of protoplasts with ^{14}C(methyl)methionine under the same conditions inhibited the labeling of RNA by 85%, and produced changes in the distribution of label on gradients similar to those seen with ^{14}C-uracil. Whether or not the difference in the inhibition of uracil and methionine labeling indicates that CHX preferentially blocks the methylation of RNA cannot be resolved, as these differences could have arisen from altered precursor uptake. Purification of ribosomal subunits from yeast labeled with uracil in the presence of CHX for 75 min showed that no label was incorporated into 23S or 16S rRNA. If yeast were prelabeled with uracil in the presence of 5 µg/ml CHX for 45 min, and then chased with cold uracil for 2 hrs (without CHX), then the distribution of labeled RNA on gradients returned to normal. In contrast, exposure of yeast to CHX during the chase led to almost complete loss of labeled RNA (85). Thus, CHX appears to inhibit the synthesis and possibly the methylation of cellular RNA, in addition to blocking the emergence of 23S and 18S RNA into ribosomal subunits. Although the effects of CHX appear to be reversible in 2 hrs, the fate of the RNA formed in the presence of CHX is not clear. Removal of CHX may allow the maturation of high molecular weight RNA into rRNA (and possibly other species); or alternatively, this high molecular weight RNA may be degraded and resynthesized.

Iwabuchi *et al.* have presented evidence that CHX blocks the maturation of rRNA. Exposure of *Dictyostelium discoidium* to 50 or

150 µg/ml CHX completely inhibited ^{14}C-amino acid incorporation within 1.5 hrs, and reduced uracil incorporation by 50% within 2.5 hrs. RNA from controls labeled for 60 min with ^{3}H-uracil and ^{14}C(methyl)methionine had most incorporated radioactivity distributed among 26S, 17S and 4S peaks on sucrose gradients. The peaks in radioactivity corresponded with absorbance peaks in the gradient. In contrast, when cells were pretreated with 100 µg/ml CHX for 30 min, and then labeled for 60 min, the pattern of radioactivity, but not absorbance, on the gradient was changed. A peak of label was found at 28S rather than 26S, and the height of the 17S peak was substantially reduced. When cells were prelabeled for 30 min in the presence of 200 µg/ml CHX, and chased for 30 min in the presence of CHX, the pattern of radioactivity was abnormal, as above. When cells were chased without CHX being present, the pattern became normal (86). Thus CHX appears to block the processing of 28S RNA to 26S RNA, and possibly the maturation of 17S RNA.

McMahon has suggested that in Chlamydomonas reinhardi the inhibition of RNA synthesis caused by CHX is a side effect unrelated to the inhibition of protein synthesis. He compared the effect of blocking protein synthesis with CHX with that of blocking it in temperature sensitive mutants. He found that 7-35 µM CHX completely blocked the incorporation of ^{3}H-argenine into the prctein of an argenine auxotroph. This treatment inhibited the incorporation of ^{3}H-adenine into RNA without significantly affecting the specific activity of the intracellular ATP pool. Other effects of CHX treatment

(2 hrs) included about a 50% reduction in the size of the ATP pool, a stimulation of the degradation of RNA, and an increased rate of cell death. In contrast, blocking protein synthesis by 90% in temperature sensitive mutants had no effect in the size of the ATP pool nor the rate of cell death. The rate of RNA synthesis was increased by about 50% instead of being decreased (87). These results suggest that in Chlamydomonas the effects of CHX other than the inhibition of protein synthesis were side effects.

C. Summary

CHX blocks protein synthesis by interacting with transfer factor II, an enzyme that catalyzes the movement of the ribosome along mRNA. Side effects of CHX include inhibition of the uptake of amino acids and nucleic acid precursors, respiration and RNA synthesis.

Figure 1

The structures of seven of the aflatoxins, from Wogan, 1973 (1).

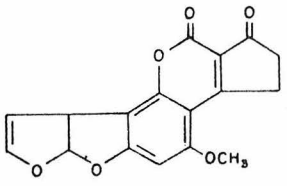

AFLATOXIN B_1

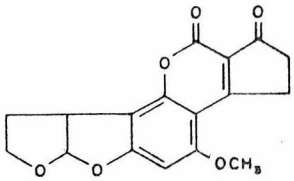

AFLATOXIN B_2

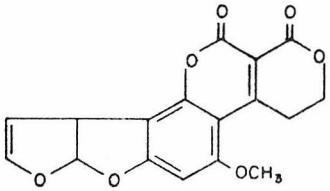

AFLATOXIN G_1

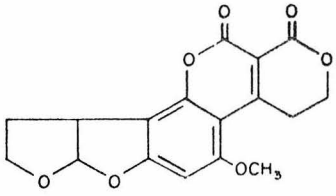

AFLATOXIN G_2

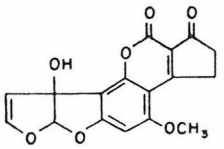

AFLATOXIN M_1

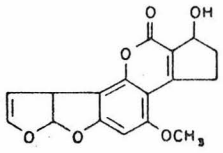

AFLATOXICOL

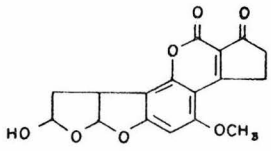

AFLATOXIN B_{2a}

Figure 2

The structure of actinomycin D, from Gale et al., 1972 (34).

Figure 3

Ball and stick models of the structure of AMD (A,B) and an AMD-deoxyguanosine$_2$ complex (C,D); from Sobell et al., 1971 (38). The models show no hydrogen atoms.

A: View of AMD from the plane of the chromophore. Peptide rings lie roughly in the plane of the paper, while the chromophore is perpendicular to the paper. Positions 2 and 3 of the chromophore are to the reader's right. Hydrogen bonds (---) connect the NH_2 group of the D-valine of one peptide ring to the C=O group of the D-valine of the other peptide ring.

B: View of the same structure in A, from slightly above the plane of the chromophore. The molecule has been rotated so that the chromophore is seen to the right of the peptide rings. The 2-NH_2 and 3-quinoidal oxygen groups project toward the reader.

C: The same view of AMD seen in A with the addition of 2 molecules of deoxyguanosine lying above and below the chromophore. Hydrogen bonds connect the 2-NH_2 group of each guanosine with the C=O group of the L-threonine in the peptide ring on the same side of the chromophore.

D: The same structure as in C and the same view as in B.

A

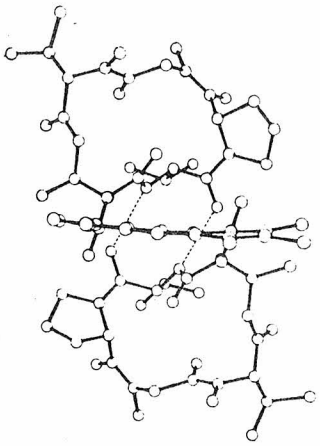

B

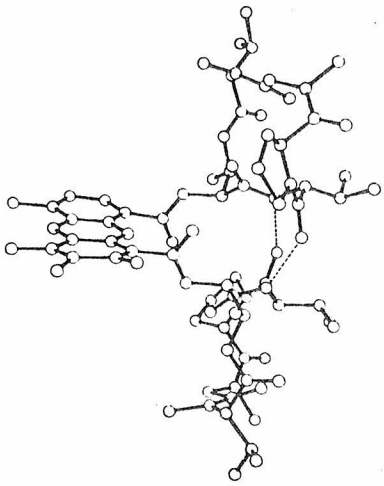

C

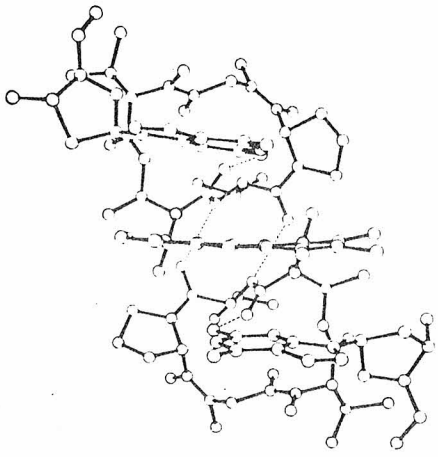

D

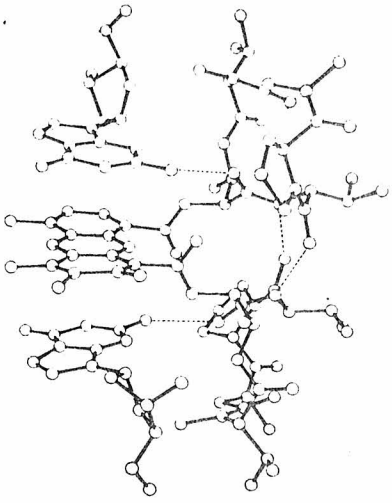

Figure 4

The structures of puromycin, amino acyl-adenosine and cycloheximide; from Gale et al., 1972 (50). Amino acyl-adenosine is the 3' terminus of amino acyl-t-RNA.

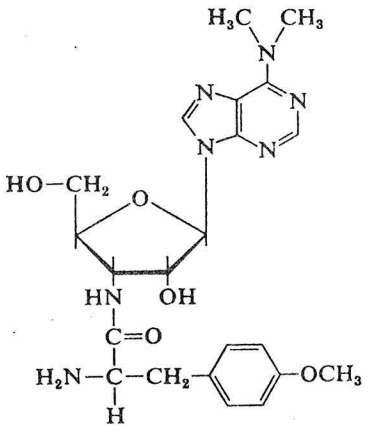

Puromycin

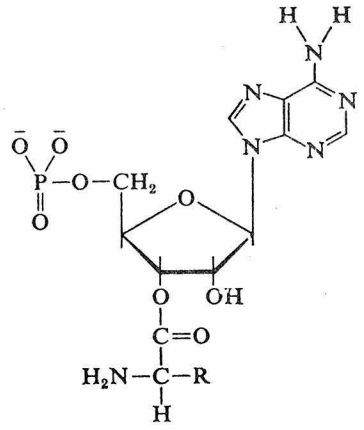

Amino acyl-adenosine

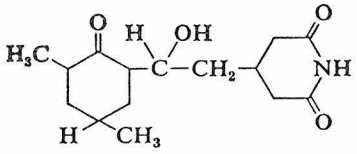

Cycloheximide

REFERENCES

1. Wogan, G. N. In Methods of Cancer Research, Volume VII, ed. H. Busch, Academic Press, New York, 1973. pp 309-344.

2. Ames, B. N., W. E. Durston, E. Yamasaki and F. D. Lee. 1973. Proc. Natl. Acad. Sci. 70: 2281-2285.

3. Sporn, M. B., C. W. Dingman, H. L. Phelps and G. N. Wogan. 1966. Science 151: 1539-1541.

4. King, A. M. Q. and B. H. Nicholson. 1969. Biochem. J. 114: 679-687.

5. Clifford, J. I., and K. R. Rees. 1967. Biochem. J. 103: 467-471.

6. Edwards, G. S. and G. N. Wogan. 1969. Biochim. Biophys. Acta 224: 597-607.

7. Saunders, F. C., E. A. Barker and E. A. Smuckler. 1972. Cancer Res. 32: 2487-2494.

8. Lijinsky, W., K. Y. Lee and C. H. Gallagher. 1970. Cancer Res. 30: 2280-2283.

9. Garner, R. C. 1973. Chem.-Biol. Interactions 6: 125-129.

10. Gurtoo, H. L. and C. V. Dave. 1975. Cancer Res. 35: 382-389.

11. Mahler, H. R. and E. H. Cordes. Biological Chemistry, Second Edition, Harper and Row, New York, 1971. pp 631-641.

12. Swenson, D. H., J. A. Miller and E. C. Miller. 1973. Biochem. Biophys. Res. Comm. 53: 1260-1267.

13. Grover, P. L., A. Hewer and P. Sims. 1972. Biochem. Pharmacol. 21: 2713-2726.

14. Moulé, Y. and C. Frayssinet. 1972. FEBS Letts. 25: 52-56.

15. Moulé, Y. and A. Sarasin. 1973. FEBS Letts. 32: 347-350.

16. Lafarge, C. and C. Frayssinet. 1970. Intl. J. Cancer 6: 74-83.

17. Harley, E. H., K. R. Rees and A. Cohen. 1969. Biochem. J. 114: 289-298.

18. Dalgarno, L. and J. Shine. In The Ribonucleic Acids, ed. P. R. Stewart and D. S. Letham, Springer-Verlag, New York, 1973. pp. 107-134.

19. Garvican, L. and K. R. Rees. 1974. Chem.-Biol. Interactions 9: 429-434.

20. Moulé, Y. 1973. Cancer Res. 33: 514-520.

21. Moulé, Y. and A. Sarasin. 1974. Chem.-Biol. Interactions 9: 1-6.

22. Garvican, L., F. Cajone and K. R. Rees. 1973. Chem.-Biol. Interactions 7: 39-50.

23. Sarasin, A. and Y. Moulé. 1973. FEBS Letts. 29: 329-332.

24. Pong, R. S. and G. N. Wogan. 1969. Biochem. Pharmacol. 18: 2357-2361.

25. Roy, A. K. 1968. Biochim. Biophys. Acta 169: 206-211.

26. Craig, N. 1973. J. Cell Physiol. 82: 133-150.

27. Pokrovsky, A. A., L. V. Kravchenko and V. A. Tutelyan. 1972. Toxicon 10: 25-30.

28. Tung, H.-T., W. E. Donaldson and P. B. Hamilton. 1970. Biochim. Biophys. Acta. 222: 665-667.

29. Bababunmi, E. A. and O. Bassir. 1972. FEBS Letters 26: 102-104.

30. Bababunmi, E. A. 1974. Brain Res. 70: 559-561.

31. Doherty, W. P. and T. C. Campbell. 1973. Chem.-Biol. Interactions 7: 63-77.

32. Reich, E. and I. H. Goldberg. 1964. Progr. in Nucleic Acid Res. and Mol. Biol. 3: 183-234.

33. Hyman, R. W. and N. Davidson. 1970. J. Mol. Biol. 50: 421-438.

34. Gale, E. F., E. Cundliffe, P. E. Reynolds, M. H. Richmond and M. J. Waring. The Molecular Basis of Antibiotic Action, Wiley and Sons, New York, 1972. pp 173-277.

35. Hyman, R. W. and N. Davidson. 1971. Biochim. Biophys. Acta 228: 38-48.

36. Wells, R. D. and J. E. Larson. 1970. J. Mol. Biol. 49: 319-342.

37. Cerami, A., E. Reich, D. C. Ward and I. H. Goldberg. 1967. Proc. Natl. Acad. Sci. 57: 1036-1042.

38. Sobell, H. M., S. C. Jain, T. D. Sakore, G. Ponticello and C. E. Nordman. 1971. Cold Spring Harbor Symp. Quant. Biol. 36: 263-270.

39. Müller, W. and D. M. Corothers. 1968. J. Mol. Biol. 35: 251-290.

40. Perry, R. P. and D. E. Kelley. 1970. J. Cell Physiol. 76: 127-140.

41. Singer, R. H. and S. Penman. 1972. Nature 240: 100-102.

42. Brawerman, G. 1974. Ann. Rev. Biochem. 43: 621-642.

43. Stuart, G. A. and E. Farber. 1968. J. Biol. Chem. 243: 4479-4485.

44. Farber, E., K. H. Shull, S. Villa-Trevino, B. Lombardi and M. Thomas. 1964. Nature 203: 34-40.

45. Schwartz, H. S. and M. Garofalo. 1967. Mol. Pharmacol. 3: 1-8.

46. Singer, R. H. and S. Penman. 1973. J. Mol. Biol. 78: 321-334.

47. Laszlo, J., D. S. Miller, K. S. McCarty and P. Hochstein. 1966. Science 151: 1007-1010.

48. Dybing, E. 1974. Biochem. Pharmacol. 23: 395-402.

49. Dybing, E. 1974. Biochem. Pharmacol. 23: 3045-3051.

50. Gale, E. F., E. Cundliffe, P. E. Reynolds, M. H. Richmond and M. J. Waring. The Molecular Basis of Antibiotic Action, Wiley and Sons, New York, 1972. pp 278-379.

51. Rabinowitz, M. and J. M . Fisher. 1962. J. Biol. Chem. 237: 477-481.

52. Allen, D. W. and P. C. Zamecnik. 1962. Biochim. Biophys. Acta 55: 865-874.

53. Nathans, D. 1964. Proc. Natl. Acad. Sci. 51: 585-592.

54. Smith, J. D., R. R. Traut, G. M. Blackburn and R. E. Monro. 1965. J. Mol. Biol. 13: 617-628.

55. Traut, R. R. and R. E. Monro. 1964. J. Mol. Biol. 10: 63-72.

56. Sovik, O. 1966. Acta Physiol. Scand. 66: 307-315.

57. Lehninger, A. L. Biochemistry, Worth, New York, 1970. pp 499-502.

58. Appleman, M. M. and R. G. Kemp. 1966. Biochem. Biophys. Res. Comm. 24: 564-568.

59. Hoffert, J. F. and R. K. Boutwell. 1963. Arch. Biochem. Biophys. 103: 338-344.

60. Blatt, L. M., J. O. Scamahorn and K. H. Kim. 1969. Biochim. Biophys. Acta. 177: 553-559.

61. Korner, A. and M. S. Raben. 1964. Nature 203: 1287-1289.

62. Jost, J.-P. and H. V. Rickenberg. 1971. Ann. Rev. Biochem. 40: 741-774.

63. Beck, W. T., R. A. Bellantone and E. S. Canellakis. 1973. Nature 241: 275-277.

64. Gambetti, P., N. K. Gonatas and L. B. Flexner. 1968. Science 161: 900-902.

65. Jones, C. T. and P. Banks. 1969. J. Neurochem. 16: 825-828.

66. Bartlett, P., T. Tsujimoto and H. Schaefer. 1965. Life Sciences 4: 1509-1514.

67. Jackson, L. G. and G. P. Studzinski. 1968. Expt. Cell Res. 52: 408-418.

68. Studzinski, G. P. and K. O. Ellem. 1966. J. Cell Biol. 29: 411-421.

69. Darnell, J. E., L. Phillipson, R. Wall and M. Adesnik. 1971. Science 174: 507-510.

70. Colombo, B., L. Felicetti and C. Baglioni. 1965. Biochem. Biophys. Res. Comm. 18: 389-395.

71. Baliga, B. S., A. W. Pronczuk and H. N. Munro. 1969. J. Biol. Chem. 244: 4480-4489.

72. Srinivasan, R., H. Liang, D. S. R. Sarma, R. Kisilevsky and E. Farber. 1971. Biochem. Biophys. Res. Comm. 42: 259-265.

73. Skogerson, L. and K. Moldave. 1968. Arch. Biochem.Biophys. 125: 497-505.

74. Sutter, R. P. and K. Moldave. 1969. J. Biol. Chem. 241: 1698-1704.

75. Baliga, B. S., S. A. Cohen and H. N. Munro. 1970. FEBS Letters 8: 249-252.

76. McKeehan, W. and B. Hardesty. 1969. Biochem. Biophys. Res. Comm. 36:625-630.

77. Garber, A. J., M. Jomain-Baum, L. Salganicoff, E. Farber and R. W. Hanson. 1973. J. Biol. Chem. 248: 1530-1535.

78. Jomain-Baum, M., A. J. Garber, E. Farber and R. W. Hanson. 1973. J. Biol. Chem. 248: 1536-1543.

79. Jomain-Baum, M. and R. W. Hanson. 1975. Life Science 16: 345-352.

80. MacDonald, I. R. and R. J. Ellis. 1969. Nature 222: 791-792.

81. MacDonald, I. R., J. S. D. Bacon, D. Vaughn and H. J. Ellis. 1967. J. Expt. Botany 17: 822-837.

82. Evans, W. R. 1971. J. Biol. Chem. 246:6144-6151.

83. Timberlake, W. E. and D. H. Griffin. 1973. Biochem. Biophys. Res. Commun. 54: 216-221.

84. Ross, C. 1968. Biochim. Biophys. Acta 166: 40-47.

85. de Kloet, S. R. 1966. Biochem. J. 99: 566-581.

86. Iwabuchi, M., Y. Mizukami and M. Sameshima. 1971. Biochim. Biophys. Acta 228: 693-700.

87. McMahon, D. 1975. Plant Physiol. 55: 815-821.

Chapter IV

Effects of Aflatoxin B_1 and Actinomycin D on the Circadian Rhythm of Spontaneous CAP Activity

INTRODUCTION

Most studies investigating macromolecular synthesis as a factor in the maintenance and/or production of circadian rhythms (CRs) have employed the use of inhibitors whose primary effect is on RNA synthesis (actinomycin D, aflatoxin B_1) or protein synthesis (cycloheximide, puromycin). Karakashian and Hastings[1,2] found a loss of circadian rhythmicity in bioluminescent glow when actinomycin D or puromycin were constantly present in cultures of the dinoflagellate, Gonyaulax. Similarly, the CR of photosynthetic capacity in Acetabularia was inhibited by actinomycin D[3,4]. Feldman reported a dose-dependent lengthening of circadian period in the phototactic motility rhythm of Euglena by 0.2-4.0 μg/ml doses of cycloheximide. This range of cycloheximide doses lengthened the CR period by 1-12 hrs, and inhibited phenylalanine incorporation by 19-80 per cent[5]. Strumwasser has shown that the CR in spike output of the neuron R15 in the isolated abdominal ganglion of the mollusc Aplysia californica can be phase advanced during projected night or phase delayed during projected day by intracellular injections of actinomycin D[6]. Macdowall has found that the CR of sap exudation from the plant Nicotiana tobacum has a period that is reversibly lengthened by actinomycin D[7]. In an earlier report, we have shown that the CR of frequency of spontaneous compound action potentials from the isolated Aplysia eye is irreversibly blocked by a 3 hr pulse of the RNA synthesis inhibitor aflatoxin B_1[8]. More recently, Applewhite, Satter and Galston[9] have found that cycloheximide reversibly blocks the CR of leaflet opening in the plant Albizzia at a dose (10^{-4}M) that blocks leucine incorporation by 95 per cent. Threshold

effects on protein synthesis and the CR of leaf movement were caused by similar cycloheximide concentrations ($\sim 10^{-6}$ M). These examples show that the CRs of both unicellular and multicellular organisms are perturbed by inhibitors of macromolecular synthesis, although different CR parameters are affected in different systems. At present, at least 7 different CRs have been shown to be abolished or modified by inhibitors of RNA or protein synthesis.

The modification of CRs by the above agents may be taken to imply a direct role of transcription or translation in the time-keeping mechanism, but conflicting evidence clouds such an interpretation. For example, in anucleate Acetabularia the free-running rhythm of photosynthetic capacity persists for weeks[3,10,11] and is insensitive to actinomycin D, unlike the intact preparation[3,11]. In addition, Bryant raises the possibility that no RNA or protein synthesis is necessary for the maintenance of some CRs since the CR of gas exchange in dry onion seeds occurs in the apparent absence of these processes[12]. More recently, CRs in some systems have been phase shifted by high potassium[13,14] and valinomycin pulses[15]. A model, taking the above data into account, proposes that the membrane is the cellular locus of circadian rhythmicity[16].

The purpose of this paper is to test the sensitivity of the CR of the Aplysia eye to the administration of aflatoxin B_1 (AFTX) and actinomycin D (AMD). AFTX is a potent hepato-carcinogen that is thought to block RNA synthesis[17-19] due to a binding of it, or one of its metabolites, to DNA[19,20]. AMD is a well known inhibitor of DNA-dependent RNA synthesis. The inhibitory properties of this compound arise from its binding to DNA, and thus blocking the movement of RNA polymerase[21].

The molecular biology of the action of these two inhibitors is discussed in more detail in chapter III.

AFTX and AMD were chosen for use in this study because they are both inhibitors of RNA synthesis, yet they have very different structures. It was hoped that the dissimilarity in the drug structures would reduce the possibility of their causing similar side effects. Thus, changes in the eye CR common to both drugs would be presumably due to primary or secondary effects, and not due to side effects.

The isolated Aplysia eye is an advantageous system because it produces an endogenous, highly repeatable CR of large amplitude and low noise. Because the eye is an ensemble of neurons, it may serve as a model for the neuronal loci controlling CRs in other organisms. A foundation of studies on the Aplysia eye already exists[14,22-28] and has been reviewed[29].

In the following study, it is demonstrated that AFTX or AMD applied as 3 hr pulses can inhibit the CR of the eye. The nature of this inhibition is dependent on the dose and phase of drug pulse application. The electrophysiology of the eye during and after drug treatment is shown to be near normal. These results are interpreted with regard to the level at which AFTX and AMD are acting to inhibit the CR of the eye.

MATERIALS AND METHODS

A. Recording of Optic Nerve Activity

Aplysia californica were obtained from the Pacific Biomarine Supply Co., Venice, California. Animals were maintained at 14°C in a circulating seawater system of 1500 gallon capacity. All animals were

exposed to a LD 12:12 light schedule (195 lux at the water surface) for at least three days prior to use.

Eyes were dissected with ∿ 1 cm lengths of optic nerve left attached. Connective tissue around the eye was trimmed as closely as possible to maximize penetration of drug solutions. After dissection, eyes were rinsed in PS-FSW (seawater filtered through 0.22 μ millipore filter and supplemented with 100 units/ml each of penicillin and streptomycin [Microbiological Assoc., Bethesda, MD]). The optic nerve of each eye was then sucked into a recording electrode consisting of a 27 gauge stainless steel hypodermic needle connected to a 2 cm length of tubing (Intramedic PE 10 or 20). In later experiments, a valve was employed to release suction after the eyes were in place.

Recordings were made from each eye submerged in 3.0 ml of PS-FSW, in a separate #2 Nalgene beaker enclosed in a light-tight box. Impulses were amplified by a Tektronix 122 preamplifier and then monitored on a Grass 7B polygraph employing an A.C. EEG amplifier. All recordings were performed in total darkness unless otherwise stated. Temperature in all experiments was maintained at 15° ± 1°C (range).

B. Drugs

Aflatoxin B_1 (AFTX) and actinomycin D (AMD) were obtained from Calbiochem, La Jolla, California. Since AFTX was not easily soluble in PS-FSW about 1/2 mg was first dissolved in 50 μl of dimethyl formamide (DMF) and then part of this solution was added to 10 ml of PS-FSW to reach the desired concentration. AMD was readily soluble in PS-FSW. Concentrations of AFTX and AMD were checked on a Beckman DB spectro-

photometer at 360 and 444 nm respectively. Neither drug at the concentrations used altered the pH of PS-FSW from its normal value. Control eyes were treated with equal amounts (1-5 µl/ml) of DMF dissolved in PS-FSW for AFTX experiments. AMD control eyes received PS-FSW. AFTX, AMD, and their control solutions were applied to eyes as a pulse lasting 3 hr. After a pulse eyes were rinsed 3 times with 3.0 ml of PS-FSW and maintained in PS-FSW for the remainder of the experiment. The 3 rinses were completed within 15 min.

Solution changes were effected by means of tubing (PE 170, Intramedic) connecting the bathing cup to the outside of the light-tight box.

C. Periodogram Analysis

Analysis of raw data, arranged as a sequence of the hourly number of CAPs fired by an eye, was performed by computer using the periodogram method as explained by Strumwasser[30]. Briefly, the periodogram was obtained by arranging each complete data array from several days' optic nerve recording into a matrix whose width was the trial period. For each trial period, the columns of data were averaged and the standard deviation of the column means was expressed relative to the standard deviation of the entire matrix, giving rise to the relative sigma[30]. The relative sigma was plotted as a function of trial period, scanned from 8 hr to 28 hr with 1 hr resolution.

RESULTS

A. Normal Eyes

In constant temperature and darkness the isolated eye of Aplysia

californica spontaneously discharged compound action potentials (CAPs) down the optic nerve.

The frequency of these CAPs expressed a free-running CR. For animals entrained on a L:D 12:12 (12 hr light, 12 hr dark) cycle, the peak of CAP activity in the isolated eye was at projected dawn, circadian time 0 (CTO); the minimum of the activity cycle was reached near projected dusk, CT 12 (Fig. 1). However, the correspondence of activity cycles to the entrainment schedule of the donor animal became less strict as more cycles were recorded, since in constant darkness in PS-FSW, eyes free ran with a period usually less than 24 hr (see Fig. 1 and periodograms[a] in Figs. 2 and 3). The amplitude of the spontaneous CAP frequency rhythm had a lower peak and fewer total CAPs than the previous one (Fig. 2, left).

Fine features of the CAP activity included a CR of CAP amplitude size, and a grouping of CAPs into bursts of 1 to 6 spikes when the eye was active (Fig. 1, right).

If a pair of eyes was taken from the same animal, and each eye was maintained in a separate beaker under identical conditions, a striking similarity in their CRs was observed, as in Fig. 2.

All of the above data are similar to those reported by Jacklet[22, 23], who first described the properties of the Aplysia eye CR.

To quantitate the similarities in eye CRs, the CRs of six pairs of eyes recorded in PS-FSW were compared for times of minimum and maximum activity, amplitude of activity and CR waveform. Each of 4 activity cycles of an eye was compared to the corresponding cycle of its mate. Thus

24 pairs of cycles were analyzed in total. For each pair of cycles, activity minima, determined as the center of the longest CAP interval, occurred within an average of 9 ± 38 (SD) min. Activity maxima, determined from CAP totals every 30 min, occurred within an average of 2 ± 50 min. The amplitude of each cycle was based on its maximum hourly CAP rate, or the total number of CAPs fired in the cycle. Amplitudes were within 16 ± 33 per cent or 18 ± 31 per cent of each other respectively, for each pair of cycles. The similarity of cycle waveforms was determined by computing the linear correlation coefficient of hourly CAP totals for each pair of cycles. The average coefficient was .96 ± .06. The slope of the linear regression obtained while computing the correlation coefficient for each pair of cycles averaged 1.12 ± 0.33. Hence, the CRs of the eyes from the same animal were very similar regarding phase, amplitude and waveform. This property furnishes the basis of using one eye of each pair as a valid control for the other.

B. Drug-Induced Changes in Rhythmicity

Samples of typical results obtained from eyes given a 3 hr pulse of AFTX (16 μg/ml, 5 x 10^{-5}M) or AMD (4 μg/ml, 3 x 10^{-6}M), and their controls are seen in Fig. 3. Drug pulses were administered at various times between the peaks of the first and second activity cycles. Abnormalities in spontaneous CAP activity were classified under the following categories: 1) arhythmicity, 2) reduced amplitude CRs, 3) low amplitude-high frequency oscillations and 4) prolonged activity cycles.

1) Arhythmicity

Following the drug pulse 8 of 20 AFTX-treated eyes (Fig. 3a) and

all 15 AMD-treated eyes (Fig. 3d) showed arhythmic CAP activity which persisted for the duration of the experiment (2 1/2 - 5 days). The level of total CAP activity in arhythmic eyes was lower than that of control eyes during the second and third cycles of control activity, although the damping of activity was less severe in arhythmic eyes. Damping coefficients of AFTX-treated eyes averaged 1.12 ± 0.91 (N = 15) while those of their DMF/PS-FSW controls averaged 0.55 ± 0.14 (N = 15). Damping coefficients of AMD-treated eyes averaged 1.64 ± 0.89 (N = 31) while those of their PS-FSW controls averaged 0.63 ± 0.26 (N = 28). For both groups of drug-treated eyes, the damping coefficient was significantly greater than for their corresponding groups of controls ($p < 0.05$, $p < 0.01$ respectively, t test), while the damping coefficients for the two control groups were not significantly different ($p < 0.3$, t test). Thus AFTX-treated eyes (Fig. 3A) and particularly AMD-treated eyes (Fig. 8E) often showed increasing CAP activity subsequent to the drug pulse.

The amount of inhibition of the CAP activity CR depended on the phase at which AFTX was administered. For all AFTX-treated eyes that became arhythmic, the drug pulse began between CT 3 and CT 15. Other aspects of CAP activity that depended on the phase at which AFTX and AMD were administered are presented in Section D (Phase-Response Relationships).

Some drug-treated eyes in this category also showed delayed activity minima before the onset of arhythmicity (Fig. 3a). Activity minima were considered to be significantly delayed if they occurred more than 85 min after the corresponding minimum in control eyes. This delay is

equivalent to the mean time difference between activity minima for pairs of control cycles plus 2 σ; see Section A (Normal Eyes)[b]. Based on this criterion, 3 AFTX-treated eyes and 4 AMD-treated eyes had activity minima prior to the onset of arhythmicity that were significantly delayed compared to controls. The delays ranged from 87 to 172 min.

2) Reduced Amplitude Circadian Rhythms

Ten of the 20 AFTX-treated eyes showed some circadian rhythmicity after the drug pulse. In 9 of the 10 cases the peaks of activity were lowered and the minima of activity raised, resulting in reduced amplitude CRs (Fig. 3b). Compared to controls, these AFTX-treated eyes were delayed in reaching activity peaks[c]. The magnitude of the phase delays varied from 2-9 hr. Although the magnitude of the delays showed no correlation with the phase of AFTX administration, no reduced amplitude CRs were caused by AFTX pulses given at CT 12 and CT 15. However, the 4 AFTX pulses begun between CT 12 and CT 15 did cause subsequent CAP activity to be arhythmic.

In three cases, activity minima prior to the expression of a reduced amplitude CR were also delayed. The magnitude of these delays was similar to that of the delays in peak activity.

One of the 20 AFTX-treated eyes showed a normal amplitude CR with normal phase (Fig. 3c), although the waveform of the second activity cycle was altered (less steep rising phase) and the activity minima were unusually short (~50 per cent of control) following the drug pulse.

3) Low Amplitude Oscillations of Higher Frequency

Unlike control eyes, which have smooth shaped cycles, AFTX- and

AMD-treated eyes often showed low amplitude oscillations of an estimated 2-6 hr in period. However, periodogram analysis did not reveal any significant differences between control and experimental eyes within this period range. Higher frequency activity appeared whether or not the CR was inhibited following drug treatment (Figs. 3a, 3b, 3c).

4) Prolonged Activity Cycles

In two of the 20 cases AFTX-treated eyes showed an unusually prolonged activity cycle followed by the expression of a normal cycle. The activity cycles following a drug pulse given to one eye at CT 0 and the other eye at CT 12 were extended 22 and 15 hr, respectively, beyond termination of the corresponding control cycle. After activity minima lasting 10 and 14 hr, respectively, a new cycle was expressed by each eye. These cycles peaked 22 and 19 hr later, respectively, than their corresponding control cycles.

C. Dose-Response Relationships

After establishing that the eye CR was modified by AFTX (16 μg/ml) and AMD (4 μg/ml), the dose dependence of CR inhibition was examined. Examples of CAP activity and periodograms for eyes given four different doses of AFTX and AMD during early subjective night (beginning CT 14, CT 11 respectively) are presented in Fig. 4. These data showed the following changes with increasing doses of either drug: 1) a reduction of circadian rhythmicity in CAP activity; 2) a lower overall level of CAP activity; 3) an increase in the level of activity minima. In contrast,

the period of the CR of CAP activity was not dose dependent at doses below those that inhibited the CR.

Dose-response data from eyes represented in Fig. 4, combined with data from other dose-response experiments are plotted in Figs. 5, 6, 7. Fig. 5 demonstrates that the amount of rhythmicity in CAP activity, measured as the sum of the heights of the largest and two adjacent periodogram peaks above a baseline sloping upward to the right (see caption), decreased with larger drug doses. Small periodogram peaks were distributed among trial periods of 14-28 hr (Fig. 4) at all drug concentrations. The dominant period (i.e., the trial period with the dominant peak) of CAP activity did not change except at higher drug concentrations (Fig. 6), where it shifted toward 14-18 hr. This shift was largely due to an artifact arising from periodogram analysis of entire CAP activity records. When periodogram analysis was performed on CAP activity subsequent to drug treatment, and peak heights were determined as above, all drug-treated eyes showed dominant periodogram peaks at 20-25 hr. Thus, the period of CAP activity was not dose dependent, whereas the inhibition of circadian rhythmicity was dose dependent.

Total spike activity following a drug pulse was lowered by increasing doses of AFTX or AMD (Fig. 7). For each eye total CAP activity for the 48 hr following the drug pulse was normalized to the total CAP activity during the 24 hr before the pulse.

An elevation of activity minima occurred in drug-treated eyes with a threshold below that of blocking circadian rhythmicity. For AFTX-treated eyes, activity minima were raised after 8 μg/ml doses (N = 2, Fig. 4e), whereas circadian rhythmicity was fully blocked at 4 μg/ml

(Fig. 4g). Eyes given AFTX doses between 1/2 and 4 µg/ml or AMD doses between 0.10 and 0.50 µg/ml produced normal CRs.

Two differences in the dose-response characteristics of AFTX- and AMD-treated eyes were observed at the doses tested. First, the delay in the appearance of abnormal activity following the drug pulse was shortened with increasing AMD dosage, whereas AFTX-treated eyes showed no change in this delay. Second, activity onsets were delayed (1-4 hr) by higher AMD doses (Fig. 4e-h), but did not show any consistent change with higher AFTX doses (Fig. 4a-d).

D. Phase-Response Relationships

The dependence of the effects of AFTX (16 µg/ml) and AMD (4 µg/ml) on the phase of administration was tested by applying a single 3 hr drug pulse at various times between the peaks of the first and second activity cycles. Paired control eyes were run in all experiments. AFTX pulses delivered 12 hr before projected dawn (Fig. 8d) (N = 2) and AMD pulses delivered 8-24 hr before projected dawn (Figs. 8g, h) (N = 6) maximally inhibited expression of the second activity cycle. Of 11 eyes given an AFTX pulse 15-24 hr before projected dawn (not shown), 5 had the second activity cycle inhibited. As the delay between drug administration and projected dawn of the second cycle was decreased, the second cycle was more completely expressed (Figs. 8a, b, e, f). A reduced amplitude, phase delayed CR followed expression of the second activity cycle for AFTX pulses begun 3-6 hr before projected dawn (Figs. 8a, b) (N = 4). Thus, expression of the second activity cycle was dependent of the phase of drug application.

The delay between drug application and expression of abnormal CAP activity[d] was also phase dependent. An AMD pulse applied 3 hr before projected dawn (Fig. 8e) did not cause abnormal CAP activity until 15 hr after the end of the pulse. When AMD was applied 4 hr earlier (Fig. 8f), the delay was shortened to 3 hr. The same type of relationship held for AFTX-treated eyes.

Two features of CAP activity subsequent to drug application in early subjective day were also seen in recordings of eyes given lower doses during subjective night. They were: 1) the appearance of reduced amplitude rhythms in AFTX-treated eyes (Figs. 8a,b and 4b); 2) a greater delay between AMD application and expression of abnormal activity (Fig. 8e, 4e, f). These data suggest that the eye is less sensitive to either drug during subjective day than during subjective night. If true, this hypothesis would predict that a large drug dose delivered during subjective day would mimic the effects of a smaller dose given in subjective night. Fig. 9 presents data that confirm this hypothesis. Eyes receiving large doses of AFTX (43 μg/ml, N = 2) or AMD (16 μg/ml, N = 2) 1-1/2 hr before projected dawn became arhythmic without revealing subsequent nonzero activity minima. Furthermore, the second activity cycles did not appear to be completely expressed. These effects on CAP activity were similar to those of lower AFTX (16 μg/ml) and AMD (4 μg/ml) doses given 9 and 7 hr before projected dawn (Fig. 8c, f). One striking difference between the high and low dose groups, however, was the elevated level of activity seen in the former.

E. Zeitgeber Experiments

Zeitgeber experiments were conducted to test the reversibility of the drug-induced block of circadian rhythmicity in the eye. Although

there was little indication of spontaneous CR recovery in drug-treated eyes, the possibility that a strong light stimulus could act to initiate or (re)entrain circadian rhythmicity was explored. Light pulses have been used to initiate circadian oscillations in other systems[32]. Since AMD (4μg/ml) pulses always blocked the circadian rhythmicity of optic nerve activity, zeitgeber studies were confined to eyes treated with this drug.

The experiments consisted of administering an AMD pulse to an eye from CT 13 to CT 16 the evening after its first activity cycle. AMD given near this phase caused inhibition of circadian rhythmicity with the least delay (Fig. 8c). The light stimulus (625 lux, 4 hr) was administered in two different ways. In the first type of experiment, a single light pulse beginning at CT 12 was given the day after drug administration (N = 4). In the second type of experiment the zeitgeber was given from CT 0 to CT 4 the morning after the AMD pulse, and repeated 24 hr later (N = 2). In both types of experiments control eyes received a pulse of PS-FSW instead of AMD, followed by the same light regimen given to experimental eyes.

AMD-treated eyes receiving single light pulses remained arhythmic--as judged by periodogram analysis--for the duration of the experiment (46-129 hr) while controls (N = 5) maintained circadian rhythmicity at an average phase delay of 2 hr for 12-60 hr.

One AMD-treated eye given two light pulses subsequently exhibited two low amplitude activity cycles that peaked near the projected zeitgeber onset. Periodogram analysis of the activity following the second zeitgeber revealed a dominant peak at 21 hr trial period; however, the

amplitude of this peak was not sufficiently high compared to unstimulated AMD-treated eyes (N = 7) to conclude that this eye expressed a CR. No circadian rhythmicity was apparent in the other AMD-treated eye given two light pulses. Controls did not live long enough for their activity following the zeitgebers to be analyzed. Clearly more zeitgeber experiments must be done before the reversibility of the CR inhibition caused by AMD can be evaluated.

F. Electrophysiology of Drug-treated Eyes

The electrophysiology of 7 eyes after AFTX treatment (16 µg/ml) and 5 eyes after AMD treatment (4 µg/ml) was tested to see if inhibition of circadian rhythmicity could have been caused by damage to the electrophysiological properties of the eye. AFTX (3 hr, 16 µg/ml) pulses began between CT 1:30 and CT 5 of the first activity cycle. AMD (3 hr, 4 µg/ml) pulses began between CT 3 and CT 4 of the first cycle.

An intracellular investigation of long-term properties of Aplysia eye neurons was not technically feasible at this stage (see 23), so a study of complex but easily recorded activities in the optic nerve was conducted. In these experiments, spontaneous CAP activity as well as phasic and tonic light responses to test light pulses were recorded. All three activities produce CAPs that are conducted down the optic nerve presumably as the result of interactions among receptor, pacemaker and follower cells in the eye[25].

Each light test consisted of two light pulses (40 lux measured at

top of the beakers used for recording eyes, 12 sec) separated by 12 sec of darkness. Eyes received light tests before, during and after drug administration. A phasic light response[22,23], elicited during about the first half of the first light pulse, gradually adapted into a tonic[22,23] response by the end of this pulse. The second light pulse caused a tonic light response with little if any phasic component. Data for phasic light response parameters were obtained from responses to the first light pulse; tonic response data were obtained from the second pulse.

Data obtained from drug-treated eyes receiving light tests were compared quantitatively with paired controls. Seven different parameters were measured. They were the latency, maximum peak to peak CAP amplitude, and frequency of both types of light response; and the maximum peak to peak spontaneous CAP amplitude, measured within 1 hr before each light test. The waveforms of all activities were compared qualitatively. Examples are presented in Figs. 10 and 11. In addition, the spontaneous CAP frequency, expressed as the number of CAPs fired each hour, was compared quantitatively for experiments in which no light tests were applied.

For each eye the value of each parameter measured 1-2 times during and 1-10 times after drug administration was expressed as a percent of the value of that parameter measured just before drug treatment. The difference (D, Tables I-IV) between the normalized value for the experimental eye and its control was calculated for each measurement. Normalized data were pooled in three different ways for light test experiments in order to maximize detection of electrophysiological changes

caused by drug treatment. First, differences between experimental and control measurements for each pair of eyes and each parameter were averaged ($\bar{D}$, Table I) and subjected to a paired t test. Table I presents a summary of the number of eyes found significantly different from their controls ($p < 0.05$) for each parameter. In no case was the number of eyes significantly greater or significantly lower than controls more than half the number of pairs tested.

Second, mean differences computed above for each pair of eyes were averaged for the 7 AFTX-treated eyes and their controls; and for the 5 AMD-treated eyes and their controls. A paired t test was conducted for the AFTX group and for the AMD group. No significant differences between experimental and control eyes were found by this method in either group.

Third, to test for possible time dependence of parameter changes, and to weight the data according to the number[e] of measurements taken, not the number of eyes, the measurement differences from eyes were pooled according to drug treatment and parameter. Differences were averaged ($\bar{D}$, Table II) for measurements taken during drug treatment, for those taken after drug treatment and for both these classes combined. No significant differences were found for AFTX-treated eyes compared to their controls, but 2 were found for AMD-treated eyes. Spontaneous CAP amplitude increased about 13 per cent (Table II, Fig. 11, spontaneous dark activity, traces 3A, C; 7A, C) and tonic light response latency decreased about 10 per cent (Table II, Fig. 11, tonic light response traces 6A, C) compared to controls. These changes were found in data pooled for measurements taken after AMD administration

(Table II), and for measurements taken at all times (not shown).

When waveforms of spontaneous CAP activity and phasic and tonic light responses for experimental and control eyes were compared, one difference appeared in AFTX-treated eyes. In 6 of 7 eyes a multiphasic tonic light response occurred in the presence of AFTX (Fig. 10, tonic light response trace 2A). However, within 1 hr after the drug pulse was rinsed out, the tonic light response waveforms returned to normal (traces 3A, C).

Spontaneous CAP frequency was analyzed in experiments in which no light tests were conducted. In all, 23 pairs of AFTX/control eyes, and 5 pairs of AMD/control eyes were analyzed in a manner similar to those receiving light pulses, except that hourly data were collected only for the activity cycle during which the drug pulse was given, and only for the part of that cycle subsequent to the beginning of the pulse. In addition data were pooled according to the phase of AFTX or AMD application. No changes in spontaneous CAP frequency were caused by drugs applied entirely during the inactive part of the CR (CT 15-CT 21). A summary of eyes significantly different in normalized spontaneous CAP frequency compared to their controls is presented in Table III. A striking percentage of eyes were increased in spontaneous CAP frequency during and after AFTX pulses beginning at CT 3.

The data obtained by averaging the mean differences ($\overline{D}$) of experimental/control pairs of eyes is seen in Table IV. Data obtained by pooling all normalized CAP frequency differences according to phase of drug delivery, and time of measurement are presented in Table V. All data treatments show that almost all eyes receiving an AFTX pulse beginning

at CT 3 were significantly increased in CAP frequency, for the remainder of that activity cycle. AFTX delivered at other phase points caused significant increases in CAP frequency as well, but with less consistency.

DISCUSSION

A. Inhibition of Circadian Rhythmicity

Recordings from eyes given pulses of AFTX (16 µg/ml) or AMD (4 µg/ml) clearly establish that these drugs can irreversibly block the CR of CAP activity in the Aplysia eye (Figs. 3A, D).

Inhibition of circadian rhythmicity seemed to result from a reduction in the amplitude of the circadian oscillation. Dose-response experiments revealed two processes with lower thresholds than the blocking of circadian rhythmicity. They were a reduction in the level of total spontaneous CAP activity (Fig. 5) and an elevation in the level of spontaneous CAP activity minima (Figs. 3c, 4b, e). Both processes could have resulted in a reduction of the amplitude of the CR to zero, without eliminating spontaneous CAP activity altogether. Furthermore, such a mechanism is consistent with the results of periodogram analysis, since with higher doses of AFTX and AMD the dominant periodogram peak was reduced without a shift to other periods.

The inability of AFTX (16 µg/ml) to completely block the CR in some experiments, in contrast to AMD (4 µg/ml), may indicate that this dose of AFTX was at the threshold of blocking a process necessary for

the production of the CR. This interpretation is supported by dose-response data (Fig. 4c) in which halving the AFTX concentration (8 µg/ml) allowed almost complete CR expression, whereas halving the AMD concentration (2 µg/ml) only delayed the block in rhythmicity.

Both drugs also appear to shift the phase of the eye CR. When AFTX (16 µg/ml) failed to abolish circadian rhythmicity, a phase-delayed reduced amplitude rhythm usually resulted (Figs. 3b, 8a, b). In addition, delayed activity onsets following AFTX (Fig. 3a) and AMD (Fig. 4g, h) pulses may evidence phase delays of the CR prior to a complete block of circadian rhythmicity.

The effects of AMD, and to some extent AFTX, on the eye CR are in good agreement with the effects of AMD on two unicellular circadian systems. The luminescence CR of Gonyaulax was inhibited by AMD pulses (8 hr, 0.16 µg/ml) and the delay between AMD application and the inhibition of circadian rhythmicity was dose-dependent. Small delays in the appearance of glow maxima were also observed[1,2]. The CR of oxygen evolution in Acetabularia was inhibited by continuous exposure to AMD (0.27-2.7 µg/ml) and showed a dose-dependent delay in the inhibition of rhythmicity[3,4].

B. Electrophysiology of Drug-Treated Eyes

Significant changes were observed in the electrophysiological properties of eyes treated with AFTX or AMD. AFTX induced multiphasic tonic light responses when present in the bathing medium of the eye, and when applied during an activity cycle at CT 3, it increased spontaneous

CAP frequency for the remainder of the cycle. AMD caused an increase in spontaneous CAP amplitude, and a decrease in tonic light response latency.

The electrophysiological effects caused by AFTX suggest a membrane mediated increase in the excitability of neurons in the eye. Similar results (multiphasic spontaneous CAPs and tonic light responses, increased spontaneous CAP frequency) have been obtained from Aplysia eyes treated with zero or low calcium sea water[25,27]. Under these conditions, eyes expressed CRs with normal period and phase, although the level of CAP activity was increased[27]. These similarities and the transience of AFTX effects suggest that the electrophysiological changes brought about by AFTX administration are side effects that are not related to inhibition of circadian rhythmicity.

To the best of this author's knowledge, no research has been done on the electrophysiological effects of AFTX other than that presented in this study. Histological studies, however, reveal that AFTX pulses (20 µg/ml, 40 µg/ml) induced cytoplasmic granularity in HeLa cells 48 hr after administration. These lesions were fully reversible for 2 hr pulses, but led to cell death within 14 days after administration of 4 hr pulses at 40 µg/ml[17]. Drosophila fed 10 ppm AFTX in their growth medium during the first instar, or during third instar and pupation, revealed abnormally small neurosecretory cells lacking stainable neurosecretory products in the brain and retrocerebral endocrine organs[33].

The changes in spontaneous CAP amplitude and tonic light response latency caused by AMD also suggest increased eye sensitivity. However, the larger CAP amplitudes may merely indicate greater preservation of

these eyes compared to controls, since this parameter tends to decrease in control eyes as well. AMD may be slowing the decline of this parameter as well as others such as CAP frequency; perhaps by some bactericidal action.

The electrophysiological effects of continuous exposure to AMD have been studied in the lobster stretch receptor (2 μg/ml)[34] and the spinal cord of the carpfish Carassius (10 μg/ml)[35]. Normal values of membrane resistance, membrane potential[34] and action potential amplitude were found in preparations maintained for 6 hr[35] and 8-24 hr[34] even though uridine incorporation was inhibited by 90-100 per cent. In vivo studies of AMD applied directly to the nervous tissue being studied have revealed electrophysiological abnormalities. Rats evidenced reduced EEG activity interspersed with spiking discharges 3-5 days after 1 μg of AMD was injected into the hippocampus[36]. Cats injected with 1 μg of AMD in the lumbar subarachnoid space of the spinal cord exhibited spastic paraplegia in their hind legs after 7 to 15 days[37]. Histological examination of mice injected intracerebrally with 20 μg of AMD revealed nuclear swelling and loss of neuronal morphology in the hippocampus and brain stem[38]. The contrast between in vitro and in vivo experiments may be due, at least in part, to higher extracellular concentrations of AMD in the latter studies. More precise control of extracellular AMD concentrations is certainly afforded by in vitro studies.

C. Level of Drug Action

Evaluation of the level at which AFTX and AMD blocked the CR of CAP activity in the Aplysia eye presents some difficulties. The delays in activity onsets caused by both drugs, and the phase-delayed reduced amplitude CRs caused by AFTX suggest some action of these agents at the level of the circadian timing mechanism. However the inhibition of circadian rhythmicity by AFTX and AMD, while consistent with the interpretation that they directly affect the clock mechanism, may be due to blocking the expression (i.e., transduction) of the CR at the intra- or intercellular level. Regarding the intercellular level, the electrophysiological studies in this paper have shown some significant changes in drug-treated eyes. Although these changes are, in my opinion, subtle, they may reflect electrophysiological alterations capable of inhibiting the eye CR.

At the cellular level, the cytotoxic effects of both AFTX and AMD in other systems raises questions of cell death in the Aplysia eye. Although this possibility is not well supported by the electrophysiological studies, the possibility of preferential destruction of circadian pacemaker cells, if such cells exist in the Aplysia eye, cannot be ruled out. It was this possibility that motivated zeitgeber experiments, since a reinitiation of the CR after drug treatment would demonstrate that the circadian oscillator in the eye was not dead. Evaluation of the cytological state of the Aplysia eye after drug treatment awaits further zeitgeber studies and ultrastructural examination.

Footnotes

[a] The periodograms displayed in Fig. 2, and subsequent figures, are used to objectively evaluate the rhythmicity of the corresponding raw data record. A periodogram is a display of the amount of rhythmicity, expressed as a relative sigma, occurring at different periods. The value of the relative sigma at each trial period is determined as in Methods.

In periodogram analysis of the type used in this study, as the value of the trial period increases, the sequence of raw data is divisible into fewer segments, causing the value of the relative sigma to approach 1.0. When the length of the trial period equals the length of the raw data sequence, the relative sigma equals 1.0. Thus, all periodograms have baselines that slope upwards to the right.

Periodogram analysis of control eye records showed a dominant peak located between trial periods of 22 to 24 hr. Because the raw data used in the analysis was a sequence of hourly CAP totals, the periodogram had a resolution of 1 hr. Analysis of the CR by measuring the time between successive cycle peaks (chaper VI) showed the average period to be 23.4 hr.

[b] A criterion of mean ± 2σ is based on the fact that only 4.55 per cent of the population of a normal distribution is expected to lie more than 2σ from its mean[31].

[c] Activity cycles were considered significantly delayed if they peaked more than 2 hr after corresponding control cycles. This delay

is equal to the mean difference between peaks for pairs of control cycles (2 min) plus 2σ (110 min), rounded up to 1/2 hr resolution (see Normal Eyes, Sec. A).

[d]CAP activity for a drug-treated eye was considered abnormal following a pulse if for at least 4 hr the hourly total of CAPs for the control eye was more than 82 per cent above the hourly CAP total for the experimental eye; and the control eye expressed more than 10 CAPs per hr. The 82 per cent difference criterion is equal to the average difference between the peak hourly CAP totals of control cycles (16 per cent) plus 2σ (66 per cent) (see Sec. A, Normal Eyes). This criterion slightly exceeds those calculated from the similarity of control cycle linear regression coefficients (mean + 2σ = 78 per cent) and those calculated from the similarity of the total number of CAPs fired in control cycles (mean + 2σ = 80 per cent) (see Sec. A, Normal Eyes). Both of these statistics are based on averages of all 4 activity cycles for each control eye. If these criteria were based on statistics derived from only second cycle data (N = 6) abnormal CAP activity began during the second cycle in most experiments, then the mean + 2σ criteria become 38 per cent for the linear regression coefficients, 40 per cent for the cycle amplitude and 46 per cent for the total number of CAPs in a cycle. Thus my 82 per cent criterion is the most severe of all computed.

[e]Weighting the data in this manner, however, risks exaggeration of its statistical significance.

TABLE I

EFFECTS OF AFTX & AMD

ON THE ELECTROPHYSIOLOGY OF THE APLYSIA EYE

ACTIVITY →	SPONT. CAP	PHASIC LIGHT RESPONSE			TONIC LIGHT RESPONSE		
PARAMETER	MAXIMUM AMPLITUDE	LATENCY	MAXIMUM AMPLITUDE	FREQUENCY	LATENCY	MAXIMUM AMPLITUDE	FREQUENCY
$\overline{D}$	+ -	+ -	+ -	+ -	+ -	+ -	+ -
AFTX							
#SIG. DIFF.	1 0	1 0	0 1	1 0	0 0	2 0	0 2
TOTAL #	6	5	5	5	6	6	6
AMD							
#SIG. DIFF.	1 0	0 0	0 1	2 1	0 1	0 2	1 0
TOTAL #	4	4	4	4	4	4	4

3-11 light tests were applied to each pair of eyes during and after the drug pulse.

refers to number of pairs of eyes

SIG. DIFF. indicates significantly different at $p < 0.05$ (paired t test)

$$D = \frac{E_A}{E_B} - \frac{C_A}{C_B}$$

E: Refers to experimental eye

C: Refers to control eye

A: Refers to measurement made after drug or control pulse

B: Refers to a measurement made before drug or control pulse for each eye and parameter. This number is used to normalize all measurements made after the pulse by the formulae: $\frac{E_A}{E_B}$ and $\frac{C_A}{C_B}$

TABLE II

THE ELECTROPHYSIOLOGY OF THE APLYSIA EYE

AFTER AMD TREATMENT (POOLED MEASUREMENTS)

ACTIVITY	SPONT. CAP	PHASIC LIGHT RESPONSE			TONIC LIGHT RESPONSE		
PARAMETER	MAXIMUM AMPLITUDE	LATENCY	MAXIMUM AMPLITUDE	FREQUENCY	LATENCY	MAXIMUM AMPLITUDE	FREQUENCY
# pairs of eyes	5	5	5	5	5	5	5
# of Ds	26				27		
$\overline{E}$	0.67				0.82		
$\overline{C}$	0.59	NSD	NSD	NSD	0.92	NSD	NSD
$\overline{D}$ ± S.D.	+0.08±0.15				-0.10±0.21		
P	0.01				0.05		

1-10 light tests were applied to each pair of eyes after the drug pulse.

$D = \frac{E_A}{E_B} - \frac{C_A}{C_B}$; $E = \frac{E_A}{E_B}$; $C = \frac{C_A}{C_B}$

NSD = no significant difference ($p > 0.05$).

P: probability that experimental and control pairs of eyes are different based on paired t test.

See Table I for explanation of other terms.

TABLE III

THE EFFECTS OF AFTX AND AMD
ON THE SPONTANEOUS CAP FREQUENCY OF APLYSIA EYE

Phase of Application / $\overline{D}$	CT 23		CT 00		CT 03		CT 06		CT 09		CT 12	
	+	−	+	−	+	−	+	−	+	−	+	−
During AFTX Pulse												
# Sig. Diff.	0	1	1	0	8	0	1	0	0	0	0	0
Total #	2		3		9		6		3		2	
During AMD Pulse												
# Sig. Diff.	0	1			0	1						
Total #	3		0		2		0		0		0	
After AFTX Pulse												
# Sig. Diff.	0	2	1	1	6	1	2	1	1	0		
Total #			3		8		6		1		0	
After AMD Pulse												
# Sig. Diff.	1	2			0	0						
Total #	3		0		2		0		0		0	
During and After AFTX Pulse												
# Sig. Diff.	0	1	2	0	7	0	2	1	1	0		
Total #	2		3		8		6		1		0	
During and After AMD Pulse												
# Sig. Diff.	1	2			0	1						
Total #	3		0		2		0		0		0	

See Table I for explanation of terms.

No light tests were given in these experiments.

TABLE IV

THE EFFECTS OF AFTX
ON THE SPONTANEOUS CAP FREQUENCY OF THE APLYSIA EYE
(Pooled Means)

Phase of Application	CT 23	CT 00	CT 03	CT 06	CT 09	CT 12
During AFTX Pulse						
# Pairs of Eyes	2	3	9	6	3	2
$\bar{E}$		1.43	0.96			
$\bar{C}$		1.30	0.72			
$\bar{D} \pm$ S.D.	NSD	+0.13±0.02	+0.24±0.09	NSD	NSD	NSD
P		0.02	0.01			
After AFTX Pulse						
# Pairs of Eyes	2	3	8	6	1	0
$\bar{E}$			0.52			
$\bar{C}$			0.39			
$\bar{D} \pm$ S.D.	NSD	NSD	+0.13±0.14	NSD	NSD	NSD
$\bar{P}$			0.02			
During and After AFTX Pulse						
# Pairs of Eyes	2	3	8	6	1	0
$\bar{E}$			0.72			
$\bar{C}$			0.54			
$\bar{D}$	NSD	NSD	+0.18±0.11	NSD	NSD	NSD
P			0.01			

See Tables I and II for explanation of terms.

No light tests were given in these experiments.

TABLE V

THE EFFECTS ON AFTX

ON THE SPONTANEOUS CAP FREQUENCY OF THE APLYSIA EYE
(Pooled Measurements)

Phase of Application	CT 23	CT 00	CT 03	CT 06	CT 09	CT 12
During AFTX Pulse						
# Measurements	8	12	35	24	12	8
$\overline{E}$			0.96		0.57	
$\overline{C}$			0.72		0.44	
$\overline{D} \pm$ S.D.	NSD	NSD	$+0.24 \pm 0.12$	NSD	$+0.13 \pm 0.18$	NSD
P			0.01		0.05	
After AFTX Pulse						
# Measurements	24	36	39	30		
$\overline{E}$	4.63		0.52			
$\overline{C}$	21.72		0.39			
$\overline{D} \pm$ S.D.	-17.09 ± 21.55	NSD	$+0.13 \pm 0.15$	NSD		
P	0.01		0.01			
During and After AFTX						
# Measurements	32	48	74	54	18	
$\overline{E}$	4.93		0.73		0.44	
$\overline{C}$	22.11		0.54		0.32	
$\overline{D} \pm$ S.D.	-17.18 ± 21.45	NSD	$+0.19 \pm 0.15$	NSD	$+0.12 \pm 0.15$	
P	0.01		0.01		0.01	

See Tables I and II for explanation of terms.

No light tests were given in these experiments.

Figure 1

Left: Plot of spontaneous CAP (optic nerve) activity vs. time for the first activity cycle recorded in constant darkness from an isolated Aplysia eye. The value of CAP activity is plotted at each hour of Pacific Daylight Time and represents the total number of CAPs fired for an hour starting at the beginning of the hour plotted. This convention is used in all plots of CAP activity. Dissection occurred 4 hr before the beginning of the record. The donor animal was entrained to an LD 12:12 schedule with light onset at 8 AM (CT 0) (PDT) and light offset at 8 PM (CT 12) (PDT). A complete record of this eye's CAP activity is plotted in fig. 2.

Right: Samples of spontaneous CAP activity recorded at 5 AM (CT 21) (A), 10 AM (CT 2) (B), 5 PM (CT 9) (C), 7 PM (CT 11) (D), and 10 PM (CT 14) (E). Up is negative voltage.

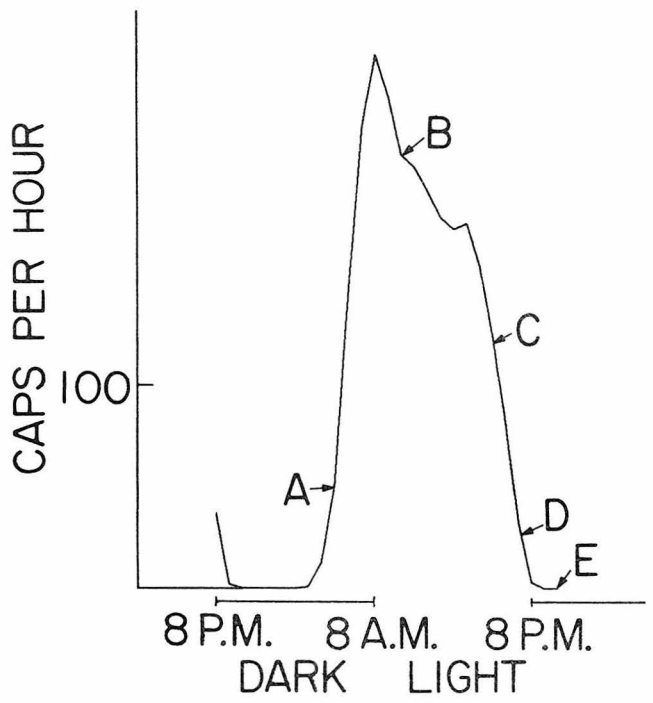
CAPS PER HOUR
100
A
B
C
D
E
8 P.M.
8 A.M.
8 P.M.
DARK
LIGHT

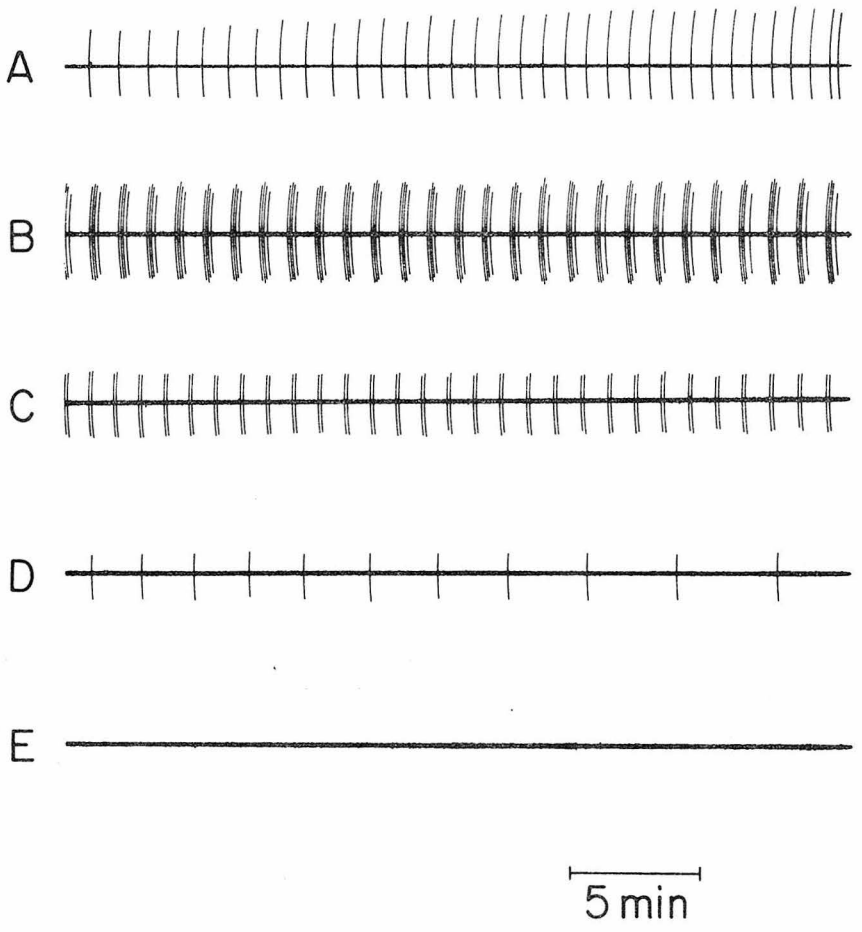
A
B
C
D
E
5 min

Figure 2

Left: A complete record of spontaneous CAP (optic nerve) activity, plotted as CAP frequency vs. time, for two eyes taken from the same animal. Bars represent the projected dark periods (D), and the spaces between them the projected light periods (L) of the donor animal's entrainment schedule. This convention is used in all following CAP activity plots.

Right: Periodograms of entire records to the left, showing a dominant period of 23-24 hr in the CAP activity of both eyes. See Methods for an explanation of periodogram analysis.

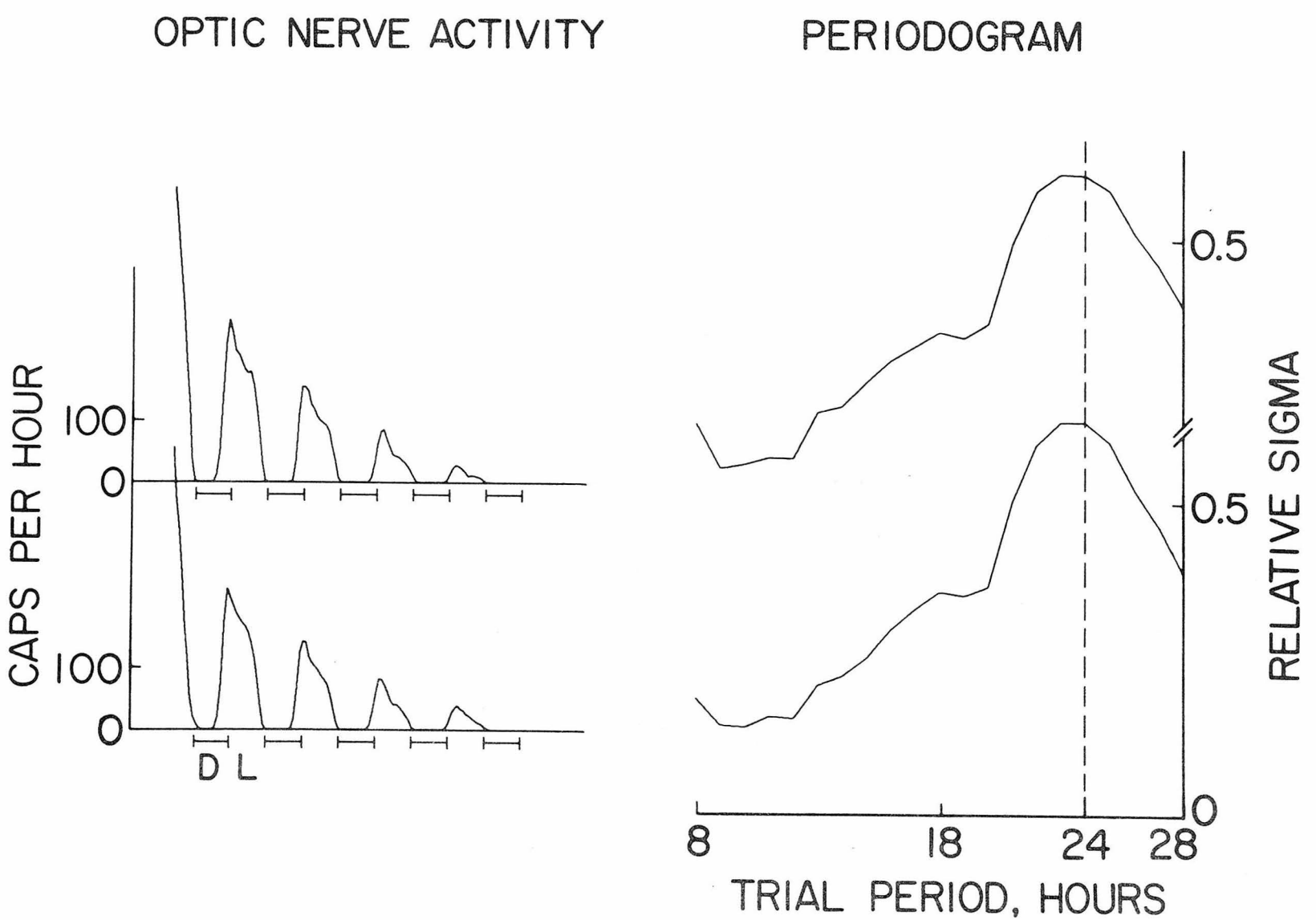
OPTIC NERVE ACTIVITY
PERIODOGRAM
CAPS PER HOUR
100
0
100
0
D L
0.5
0.5
0
RELATIVE SIGMA
8
18
24
28
TRIAL PERIOD, HOURS

Figure 3

Left: Examples of the effects of 3 hr AFTX (16 µg/ml) and AMD (4 µg/ml) pulses on spontaneous CAP (optic nerve) activity. Each group of two records shows CAP activity of a pair of eyes taken from the same animal. The top trace of each pair represents the control eye, which received a 3 hr pulse of DMF/PS-FSW (A,B,C) or PS-FSW (D) instead of a drug pulse. Box (■) shows time at which drug and control pulses were applied.

A) An example of circadian rhythmicity inhibited by an AFTX pulse.

B) An example of a phase-delayed, reduced amplitude CR following AFTX pulse.

C) An example of the failure of an AFTX pulse to block circadian rhythmicity.

D) An example of circadian rhythmicity blocked by an AMD pulse.

Right: Periodograms of each complete record to the left. Periodogram peak height at 23 hr trial period is sensitive to changes in the circadian rhythmicity of CAP activity.

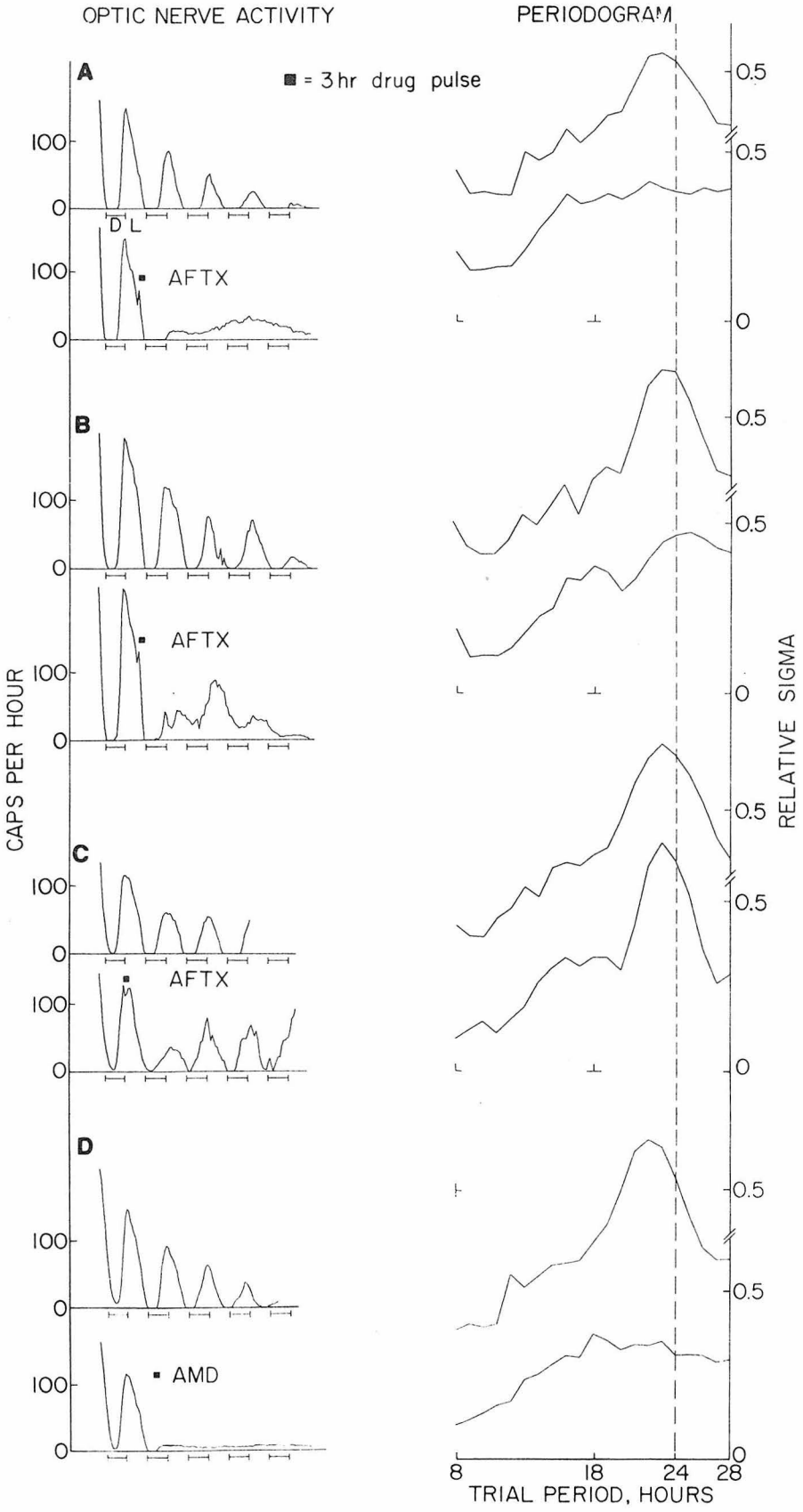
OPTIC NERVE ACTIVITY
PERIODOGRAM
■ = 3 hr drug pulse
A
B
C
D
D L
AFTX
AFTX
AFTX
AMD
100
0
0.5
CAPS PER HOUR
RELATIVE SIGMA
8
18
24
28
TRIAL PERIOD, HOURS

Figure 4

Left: Spontaneous CAP activity (dark activity) of eyes receiving various doses of AFTX or AMD. Pairs A,B; C,D; E,F; and G,H were from the same animal. No paired control eyes were run in these experiments. All AFTX pulses began at CT 14 and all AMD pulses at CT 11. Box (■) shows the time a 3 hr drug pulse was given.

Right: periodograms of each complete record to the left.

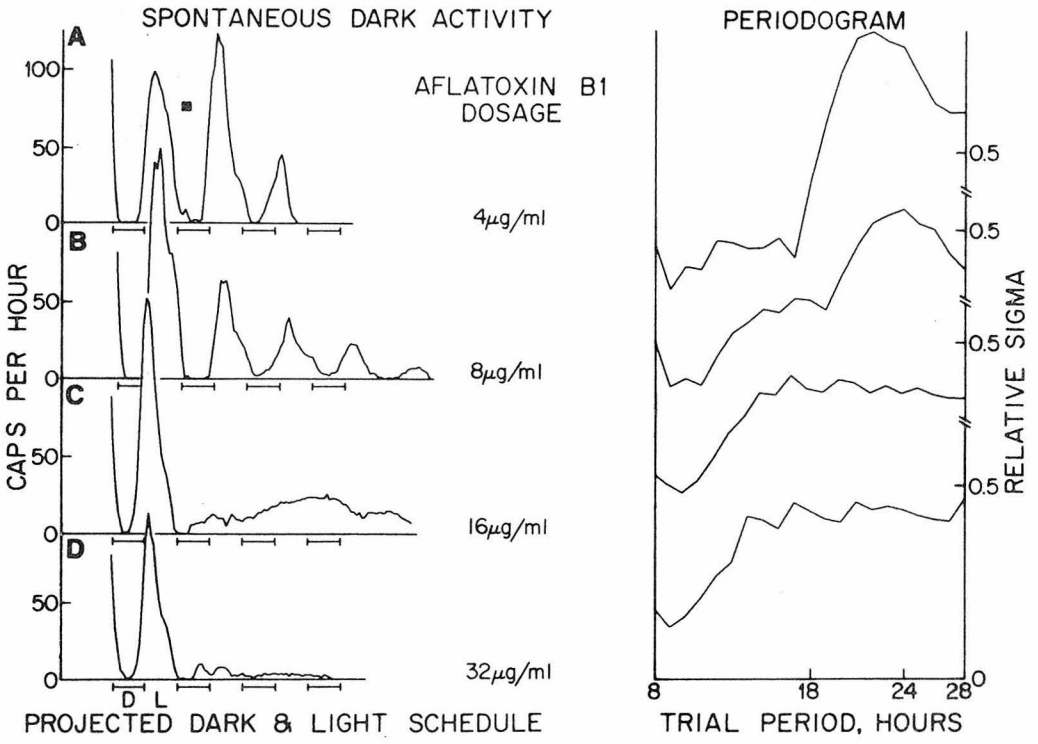
SPONTANEOUS DARK ACTIVITY
PERIODOGRAM
AFLATOXIN B1
DOSAGE
A
B
C
D
4μg/ml
8μg/ml
16μg/ml
32μg/ml
CAPS PER HOUR
100
50
0
D L
PROJECTED DARK & LIGHT SCHEDULE
0.5
RELATIVE SIGMA
8
18
24
28
TRIAL PERIOD, HOURS

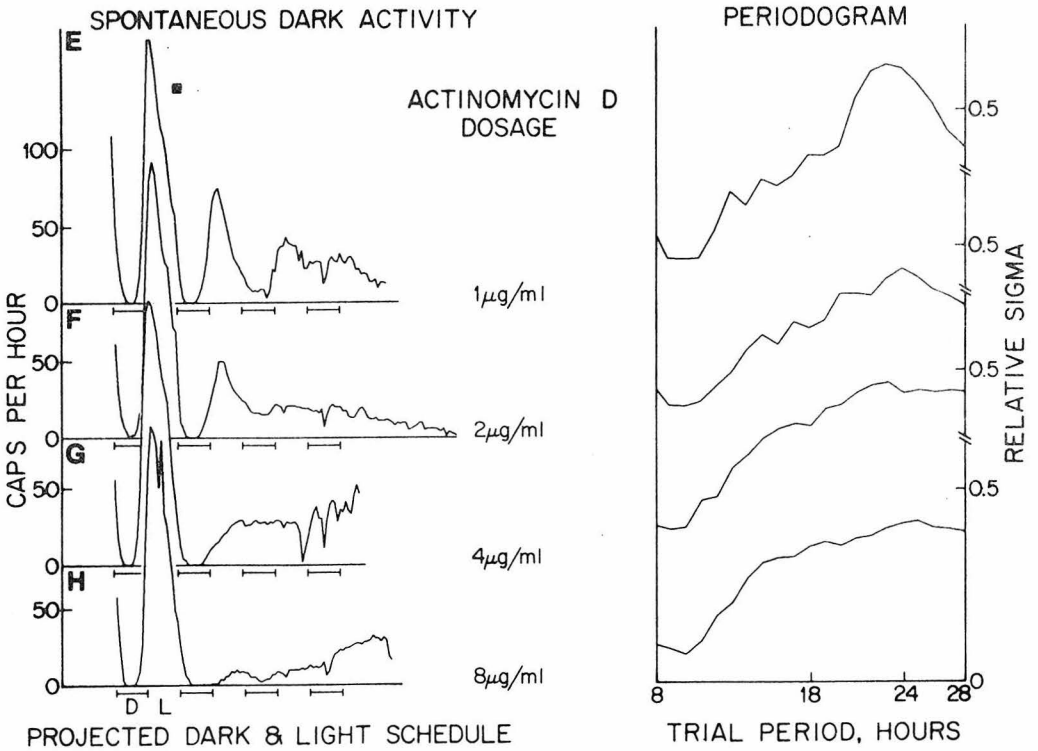
SPONTANEOUS DARK ACTIVITY
PERIODOGRAM
ACTINOMYCIN D
DOSAGE
E
F
G
H
1μg/ml
2μg/ml
4μg/ml
8μg/ml
CAPS PER HOUR
100
50
0
D L
PROJECTED DARK & LIGHT SCHEDULE
0.5
RELATIVE SIGMA
8
18
24
28
TRIAL PERIOD, HOURS

Figure 5

Plot of periodogram peak height vs. drug concentration. Peak height is measured relative to a baseline connecting the relative σ of each periodogram at 8 hr trial period with its relative σ at 28 hr trial period. The value of the largest periodogram peak height found in this way is summed with the values of the two adjacent points. All drug pulses were delivered between CT 8 and CT 14 of the first activity cycle. Each point represents one eye; 11 eyes received AFTX and 8 received AMD pulses. Data from the 8 eyes represented in fig. 4 are included. No paired controls were run in these experiments.

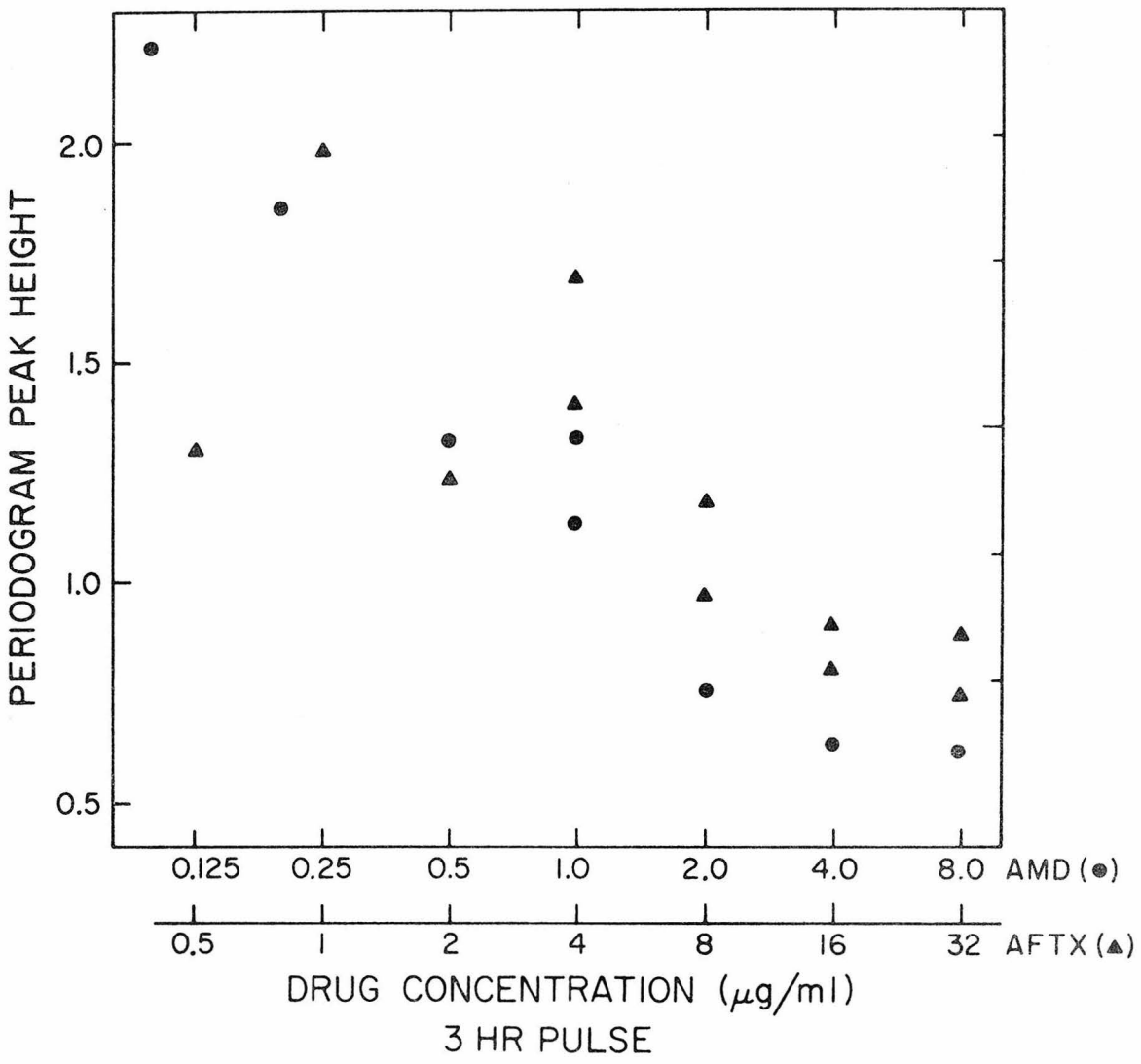
PERIODOGRAM PEAK HEIGHT
2.0
1.5
1.0
0.5
0.125
0.25
0.5
1.0
2.0
4.0
8.0
AMD (●)
0.5
1
2
4
8
16
32
AFTX (▲)
DRUG CONCENTRATION (μg/ml)
3 HR PULSE

Figure 6

Plot of the dominant period of spontaneous CAP activity vs. drug concentration. The dominant period is the trial period at which the largest periodogram peak occurs. See caption of fig. 5 for details of peak height measurement. These data are derived from the same population of eyes plotted in fig. 5. Each point represents one eye.

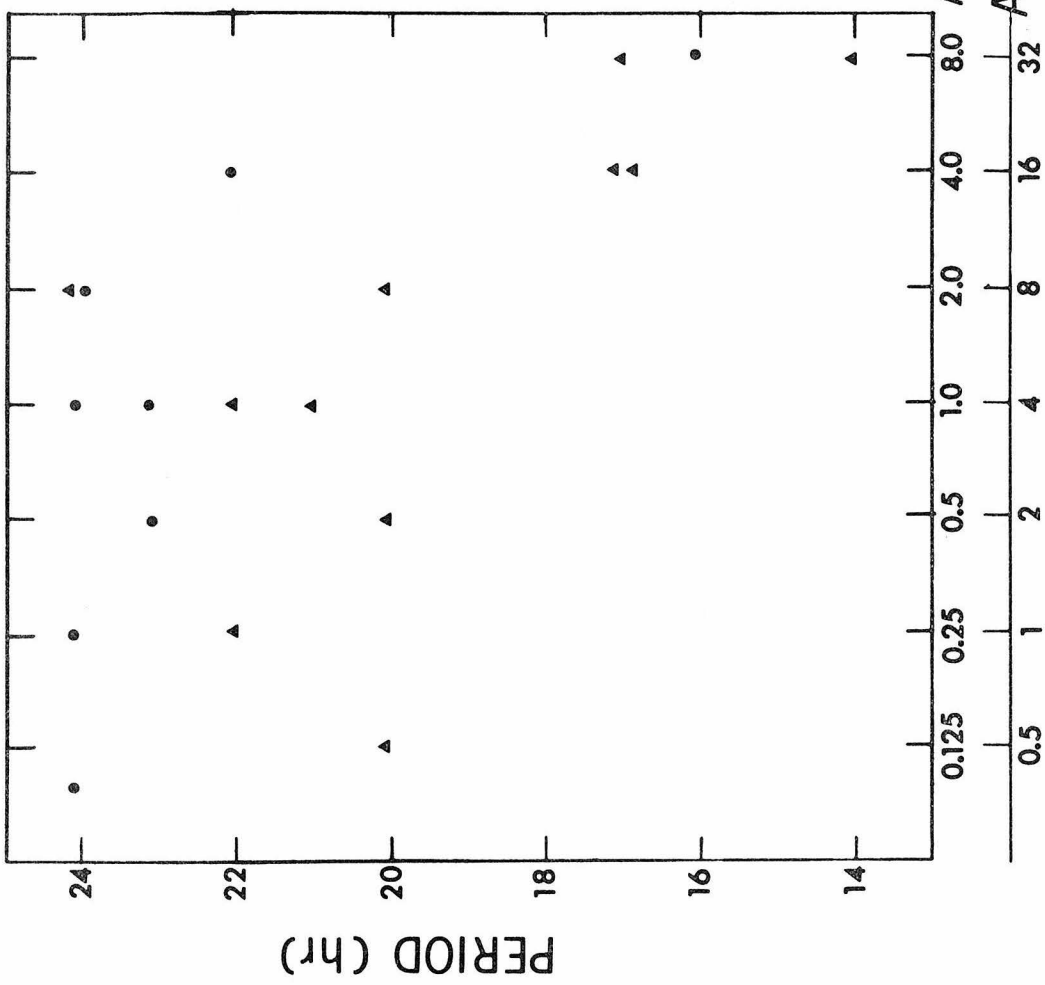
PERIOD (hr)
24
22
20
18
16
14
0.125
0.25
0.5
1.0
2.0
4.0
8.0
AMD (•)
0.5
1
2
4
8
16
32
AFTX (▲)
DRUG CONCENTRATION (ug/ml)
3 HR PULSE

Figure 7

Plot of the normalized number of CAPs fired by eyes after drug treatment vs. drug concentration. Normalization is accomplished by summing the number of CAPs fired in the 48 hr period following drug treatment, and dividing this number by twice the number of CAPs fired during the first activity cycle. These data are taken from the same population of eyes plotted in fig. 5 and 6. Each point represents one eye.

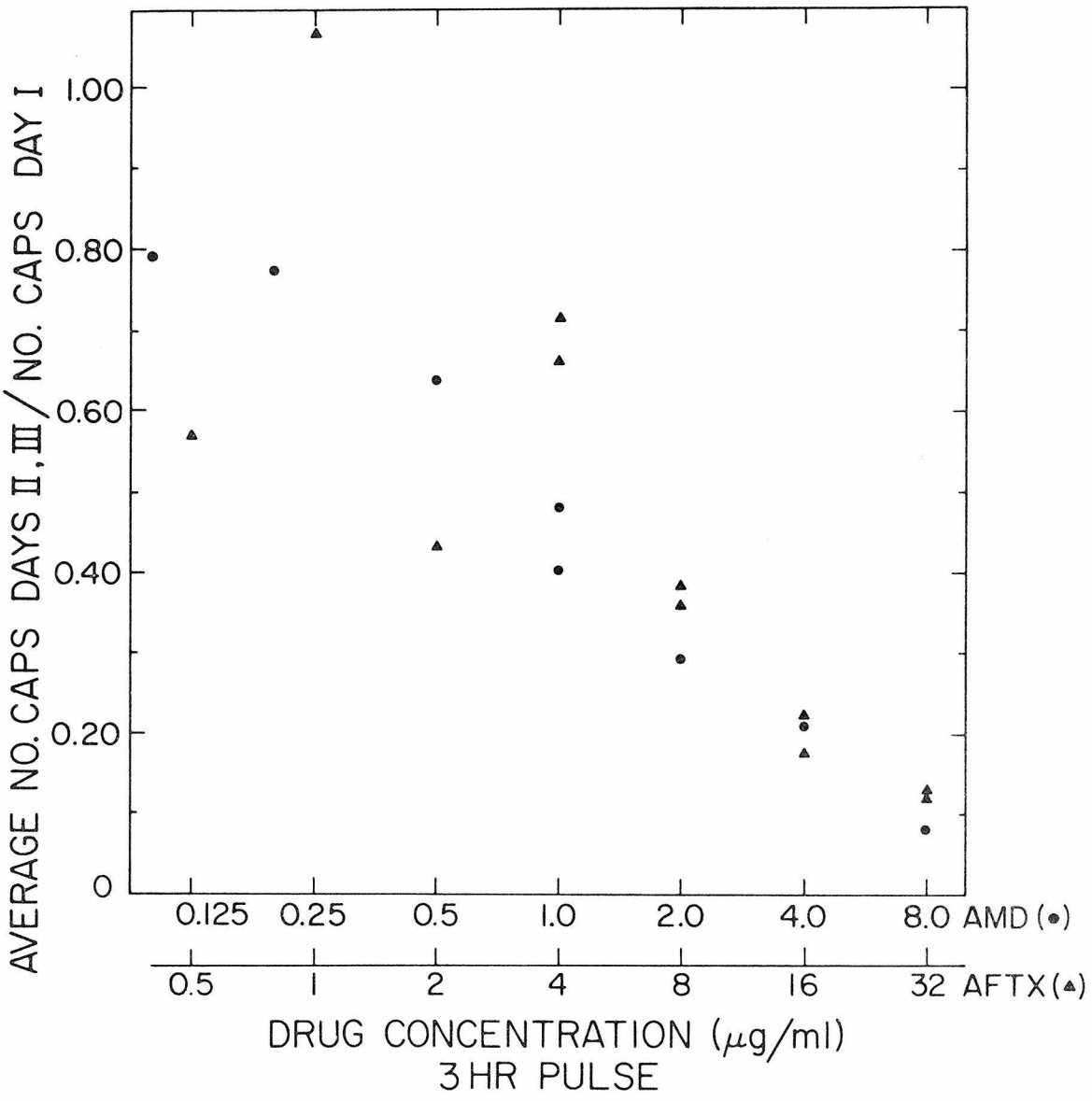
AVERAGE NO. CAPS DAYS II, III / NO. CAPS DAY I
1.00
0.80
0.60
0.40
0.20
0
0.125
0.25
0.5
1.0
2.0
4.0
8.0 AMD (•)
0.5
1
2
4
8
16
32 AFTX (▲)
DRUG CONCENTRATION (μg/ml)
3 HR PULSE

Figure 8

Examples of spontaneous CAP activity (spontaneous dark activity) from experiments in which the phase of AFTX (16 µg/ml) and AMD (4 µg/ml) pulse administration was varied. Each plot represents two or more experiments conducted under the same conditions. Each experiment had a paired control run simultaneously (not shown). Dashed lines enclose the period between projected dusk (CT 12) of the first activity cycle and projected dawn (CT 0) of the second. The number at the right of each record represents the time, in hours, between the beginning of the drug pulse and projected dawn of the second activity cycle.

SPONTANEOUS DARK ACTIVITY

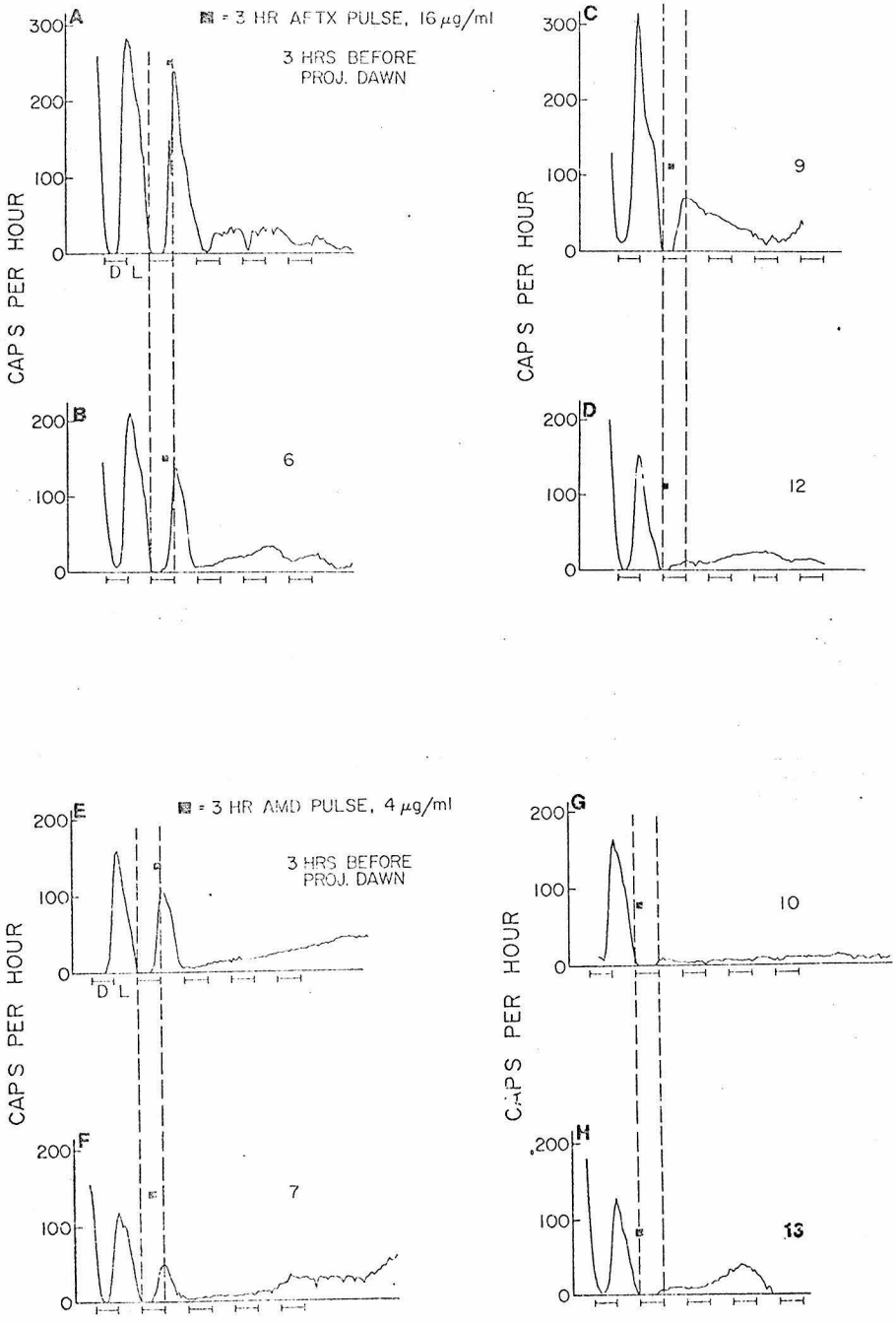

Figure 9

Plot of spontaneous CAP frequency vs. time for eyes receiving high doses of AFTX (43 µg/ml) or AMD (16 µg/ml). Drugs were applied as 3 hr pulses beginning at CT 22:30 of the second activity cycle (■). The two records in this figure represent eyes taken from the same animal. No control eyes were run. The gap in the right-hand portion of the upper record indicates that 2 hr of data were lost because a polygraph pen ran out of ink.

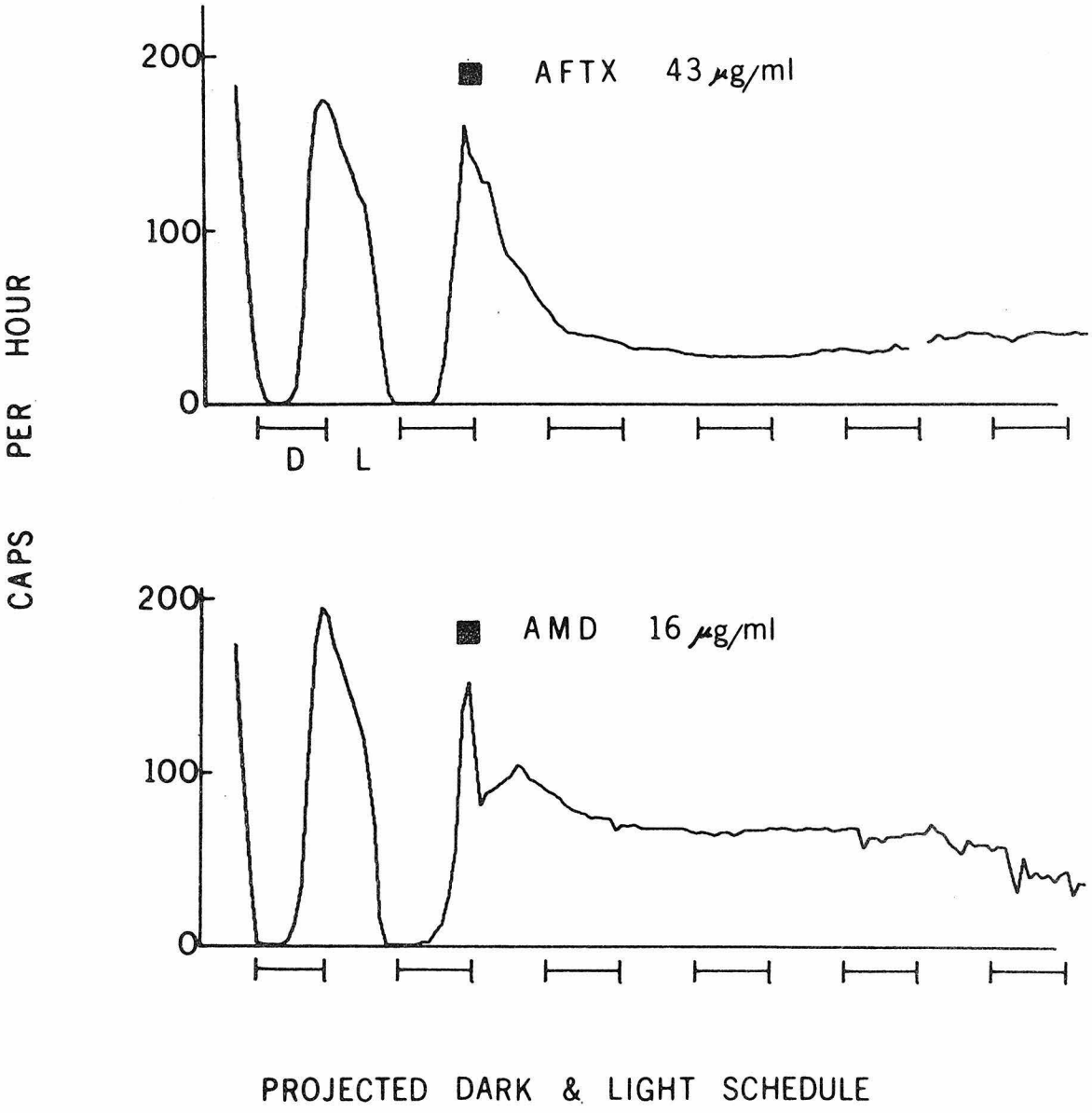
CAPS PER HOUR
200
100
0
AFTX 43 µg/ml
D L
200
100
0
AMD 16 µg/ml
PROJECTED DARK & LIGHT SCHEDULE

Figure 10

Top: Plot of spontaneous CAP activity (spontaneous dark activity) of an eye receiving a 3 hr AFTX pulse (16 µg/ml) at CT 1:30 of the first activity cycle, and a paired control eye that received a DMF/PS-FSW pulse instead. Recordings were made from eyes maintained in separate beakers housed in the same cooling dish and light-tight box. Both eyes received light tests at various times (indicated by circled numbers) during the experiment.

Below: Examples of spontaneous CAP activity, phasic light responses and tonic light responses recorded before (1), during (2) and after (3-6) the administration of an AFTX (A) or control (C) pulse. All recordings were made by means of a single suction electrode onto the optic nerve. Signals were amplified by a Tektronix 122 preamplifier then fed into an EEG amplifier of a Grass 7B polygraph and then recorded. Half-amplitude band-pass filters were set at 0.3 Hz (low) and 50 Hz (high). Down is negative voltage.

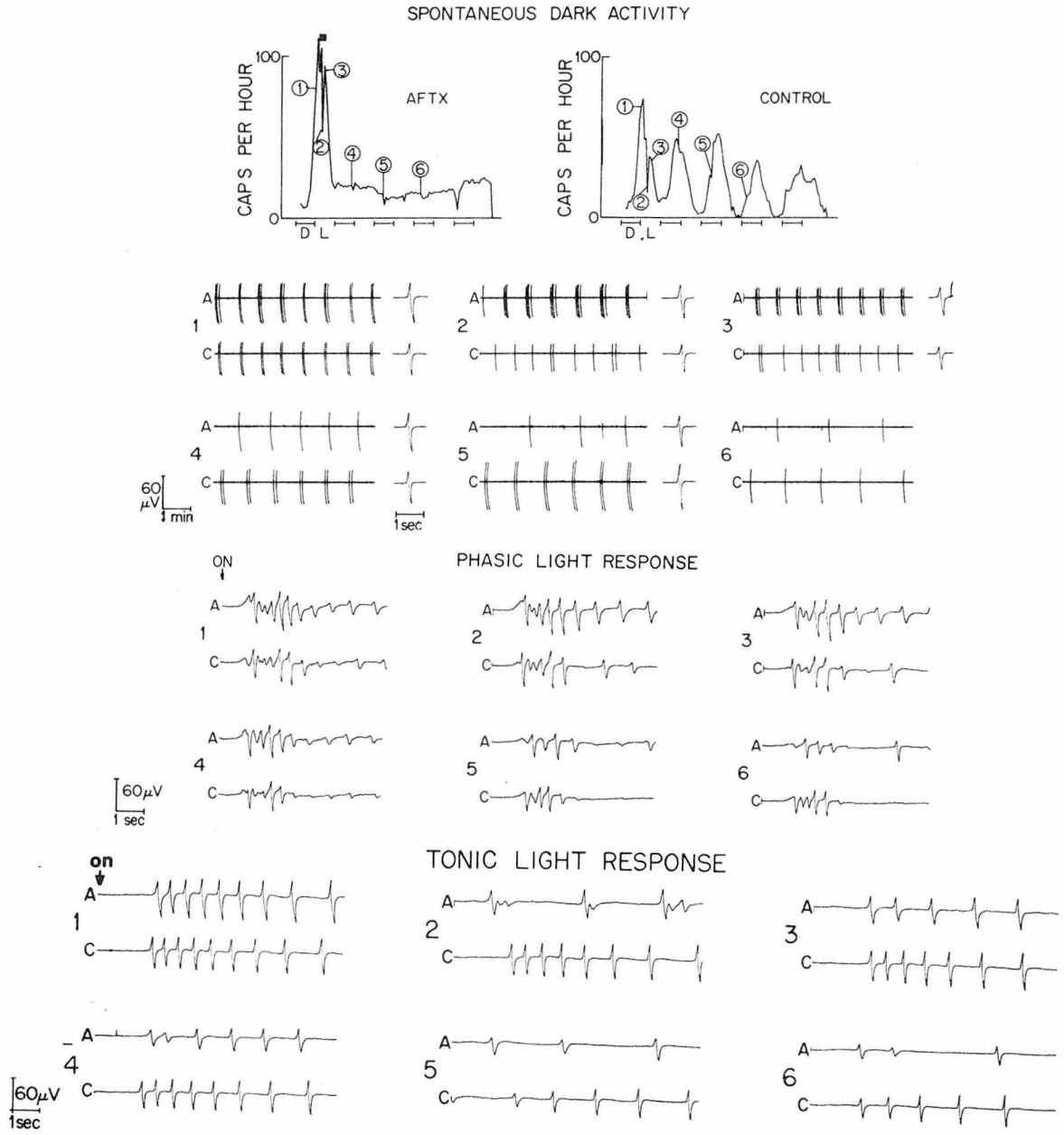
SPONTANEOUS DARK ACTIVITY
CAPS PER HOUR
100
0
AFTX
CONTROL
D
L
A
C
1
2
3
4
5
6
60 μV
1 min
1 sec
ON
PHASIC LIGHT RESPONSE
60μV
1 sec
on
TONIC LIGHT RESPONSE
60μV
1sec

Figure 11

Top: Plot of spontaneous CAP activity (spontaneous dark activity) of an eye receiving a 3 hr pulse of AMD (4 µg/ml) at CT 4 of the first activity cycle, and a paired control eye that received PS-FSW instead. Other details are the same as those in fig. 10.

Below: Examples of recordings as described in fig. 10, except that A refers to recordings from AMD-treated eye. Numbers 3-7 refer to recordings made after the AMD or control pulse was rinsed out.

SPONTANEOUS DARK ACTIVITY

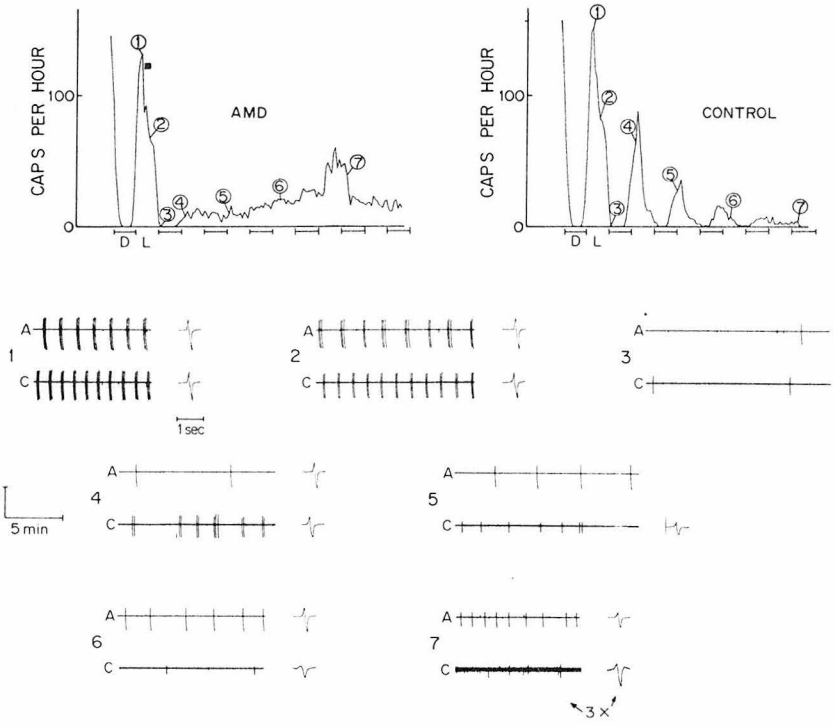

PHASIC LIGHT RESPONSE

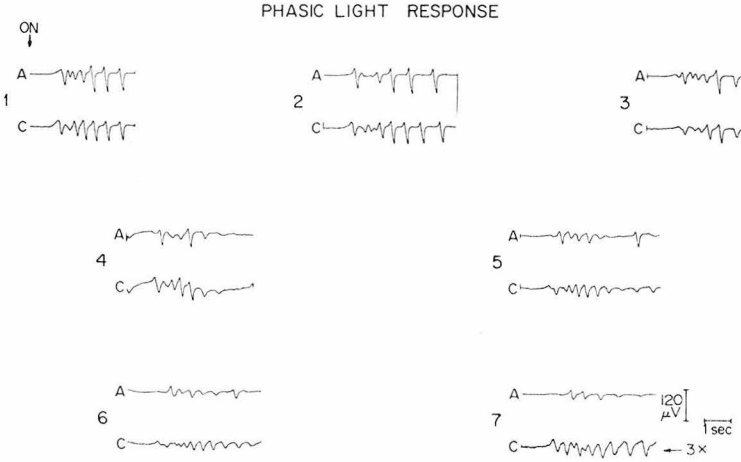

TONIC LIGHT RESPONSE

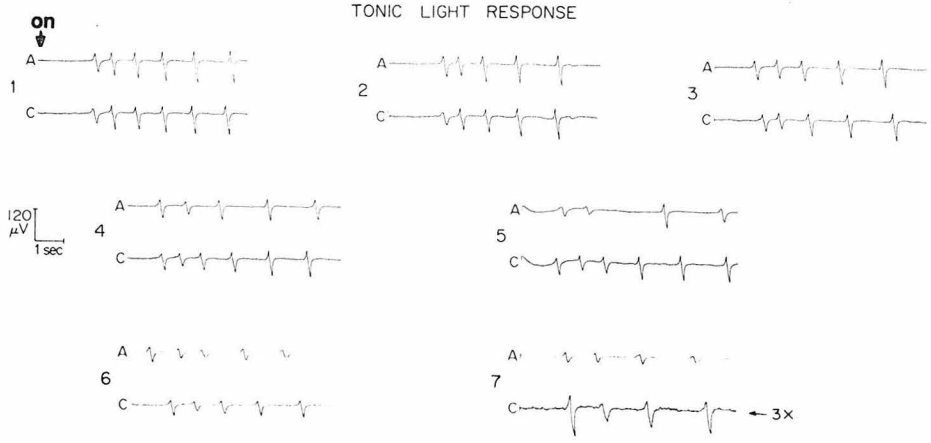

REFERENCES

1. Karakashian, M. W., and J. W. Hastings. 1962. Proc. Nat. Acad. Sci. USA 48: 2130-2137.

2. Karakashian, M. R., and J. W. Hastings. 1963. J. Gen. Physiol. 47: 1-12.

3. Van den Driessche, T. 1966. Biochim. Biophys. Acta 126: 456-470.

4. Schweiger, H. G. In International Symposium on Circadian Rhythmicity, Wageningen, Netherlands. Pudoc, Wageningen, 1972. pp. 157-174.

5. Feldman, J. F. 1967. Proc. Nat. Acad. Sci. USA 57: 1080-1087.

6. Strumwasser, F. In Circadian Clocks. J. Aschoff, ed. North-Holland, Pub. Co., Amsterdam, 1965. pp. 442-462.

7. Macdowall, F. D. H. 1964. Canad. J. Botany 42: 115-122.

8. Rothman, B. S., and F. Strumwasser. 1973. Fed. Proc. 32: 365.

9. Applewhite, P. B., R. L. Satter, and A. W. Galston. 1973. J. Gen. Physiol. 62: 707-713.

10. Sweeney, B. M., and F. T. Haxo. 1961. Science 134: 1361-1363.

11. Sweeney, B. M., C. F. Tuffli, Jr., and R. H. Rubin. 1967. J. Gen. Physiol. 50: 647-659.

12. Bryant, T. R. 1972. Science 178: 634-636.

13. Bünning, E., and I. Moser. 1973. Proc. Nat. Acad. Sci. USA 70: 3387-3389.

14. Eskin, A. 1972. J. Comp. Physiol. 80: 353-376.

15. Bünning, E., and I. Moser. 1972. Proc. Nat. Acad. Sci. USA 69: 2732-2733.

16. Njus, D., F. M. Sulzman, and J. W. Hastings. 1974. Nature 248: 116-120.

17. Harley, E. H., K. R. Rees, and A. Cohen. 1969. Biochem. J. 114: 289-298.

18. Sporn, M. B., C. W. Dingman, H. L. Phelps, and G. N. Wogan. 1966. Science 151: 1539-1541.

19. Clifford, J. I., and K. R. Rees. 1966. Nature 209: 312-313.

20. Neely, W. C., J. A. Landsden, and J. R. McDuffie. 1970. Biochemistry 9: 1862-1866.

21. Gale, E. F., E. Cundliffe, P. E. Reynolds, M. H. Richmond, and M. J. Waring. The Molecular Basis of Antibiotic Action. Wiley, New York, 1972.

22. Jacklet, J. W. 1969. Science 164: 562-563.

23. Jacklet, J. W. 1969. J. Gen. Physiol. 53: 21-42.

24. Jacklet, J. W., and J. Geronimo. 1971. Science 174: 299-302.

25. Audesirk, G. 1973. Brain Res. 59: 229-242.

26. Sener, R. 1972. The Physiologist 15: 262.

27. Jacklet, J. W. 1973. J. Comp. Physiol. 87: 329-338.

28. Eskin, A. 1971. Z. vergl. Physiol. 74: 353-371.

29. Strumwasser. F. 1973. The Physiologist 16: 9-42.

30. Strumwasser, F. In Mammalian Hibernation III. K. C. Fisher, A. R. Dawe, C. P. Lyman, E. Schönbaum, and F. E. South, eds. Amer. Elsevier, New York, 1967. pp. 110-139.

31. McNemar, Q. Psychological Statistics. Wiley & Sons, New York, 1962. p. 31.

32. Bruce, V. G. 1960. Cold Spr. Harb. Symp. Quant. Biol. 25: 29-48.

33. Kirk, H. D., A. B. Ewen, H. E. Emson, and D. G. R. Blair. 1971. J. Invert. Pathol. 18: 313-315.

34. Edstrom, J. E., and W. Grampp. 1965. J. Neurochem. 12: 735-741.

35. Bonderson, C., A. Edstrom, and A. Bevis. 1967. J. Neurochem. 14: 1032-1034.

36. Nakajima, S. 1969. J. Comp. Physiol. Psychol. 67: 457-461.

37. Koenig, H., and C. Lu. 1967. Trans. Am. Neurol. Assoc. 92: 250-252.

38. Appel, S. H. 1965. Nature 207: 1163-1166.

Chapter V

The Biochemical Effects of Aflatoxin B_1 and Actinomycin D on the Eye

I Introduction

In the previous chapter it was demonstrated that the circadian rhythm of compound action potential (CAP) frequency in the isolated eye of Aplysia californica could be inhibited by the 3 hr pulse application of aflatoxin B_1 (AFTX) or actinomycin D (AMD) at the dose of 16 µg/ml and 4 µg/ml, respectively. The purpose of the experiments presented in this chapter is to test the biochemical potency of the above drug dosages on the incorporation of uridine and leucine into the isolated Aplysia eye.

AFTX and AMD have been reported to be inhibitors of RNA and protein synthesis in many other systems (1-5). The mechanism of AFTX action on RNA synthesis is poorly understood. Some evidence suggests that AFTX, or one of its metabolites, binds to DNA, and presumably interferes with RNA polymerase (4-6). Other evidence suggests that AFTX interferes with the maturation of RNA (3). AMD interferes with transcription by tightly binding to double stranded DNA, and thus slowing or blocking the movement of RNA polymerase along the DNA molecule (1, 2). The manner in which AFTX and AMD interfere with protein synthesis is not clearly understood at present. A more detailed discussion of the molecular biology of AFTX and AMD is presented in chapter III.

II Materials and Methods

Eyes were dissected in the same manner used in chapter IV to prepare eyes for the recording of spontaneous CAP activity. However,

after dissection, instead of mounting each eye on a suction electrode, a surgical thread with an identifying tag was tied to its optic nerve. Four eyes prepared in this way were suspended by the thread in 1.0 ml of PS-FSW in a Nalgene #00 beaker. Eyes remained in this pre-label medium in constant darkness for about 36 hr at $14^{\circ}C \pm 0.5^{\circ}C$ (range). Drug and control pulses were prepared and administered as in chapter III except that all solution changes took place by means of a Pasteur pipette in room light (170 lux). Eyes were exposed to this light for a maximum of 3 min.

A. Double Label Experiments

All eyes were labeled in a medium consisting of: (mM): 423 NaCl, 9.7 KCl, 13.3 $CaCl_2$ 49 $MgCl_2$, 28 Na_2SO_4, 5 Tris buffer, pH 7.7; 100 units/ml each of penicillin and streptomycin, 10 µCi/ml L-(U-^{14}C)leucine (312 mCi/mM), 50 µCi/ml (5-^{3}H)uridine (~50 Ci/mM) (Schwarz-Mann) and 20 µl/ml 0.05 M NaOH to neutralize the .01 M HCl in which the ^{14}C-leucine was dissolved. Eight eyes were labeled together in 1.0 ml of medium, for a period lasting 7 to 9 hr. After the label was rinsed out, eyes were kept in PS-FSW for 1 hr prior to grinding. Eyes were cut from their optic nerves and were ground at $0^{\circ}C$ in a glass homogenizer with 3 x 50 µl rinses of 0.01 M phosphate buffer, pH 7.0. Grinders were then rinsed with 2 x 50 µl aliquots of 0.01 M phosphate buffer, pH 7.0, containing 1% sodium dodecyl sulfate (SDS) to aid in removing material from the glass surfaces. The SDS rinses were added to the homogenate.

The homogenate was suspended in 0.5 ml 5% trichloroacetic acid (TCA) at 0°C and 100 µl of 3 mg/ml bovine serum albumin (BSA) was added as a carrier. The suspension was then adjusted to 5% TCA concentration by adding 350 µl cold 10% TCA. Suspensions were allowed to sit at 0°C for 30 min and were then centrifuged at 12,350 g for 10 min. The first TCA supernatant was removed and counted in Aquasol (New England Nuclear, Boston, Mass.). The pellet was washed with 5% cold TCA and recentrifuged. The second TCA supernatant was removed and the pellet dissolved overnight in 1.0 ml of NCS tissue solubilizer (Amersham/Searle, Arlington Heights, Illinois), then added to 10 ml toluene PPO/POPOP scintillation fluid in a counting vial. Two hundred µl of 4 M NH_4OH was added to the counting fluid to prevent luminescence (7). Counts remaining in grinders were determined by rinsing the inside of each grinder with 1.0 ml of NCS tissue solubilizer. The NCS from each grinder was then prepared for counting as above. Samples were counted on a Beckman LS-230 liquid scintillation counter at 39% ^{3}H and 73% ^{14}C counting efficiency for the precipitate and grinder contents and 30% ^{3}H- and 59% ^{14}C-counting efficiency for the supernatant.

TCA precipitates in some experiments (see tables II, III) were collected by drying each homogenate on a glass fiber filter (Whatman GFA), and rinsing with about 25 ml of 5% cold TCA. Homogenates in these experiments did not contain SDS. The total volume of the TCA rinse was determined and a 1.0 ml aliquot was counted as above

in 10 mls of Aquasol. Filters were dried at 60°C and then extracted overnight in scintillation vials containing 1.0 ml of NCS tissue solubilizer. Ten ml toluene PPO/POPOP scintillation fluid and 200 µl 4 M NH_4OH were later added to the vial.

B. Single Label Experiments

In other labeling studies the specific activity of TCA insoluble eye material was determined. Eyes were dissected and labeled as above with the following exceptions: 1) they had shorter lengths of optic nerve remaining after dissection, 2) they were labeled in groups of 4 in 0.5 ml of a medium containing ^{14}C-leucine but not ^{3}H-uridine; 3) all solutions were changed in the dark by means of plastic tubing connecting the inside of the beakers with the outside the light-tight box in which the eyes were kept. After labeling, eyes were rinsed three times in PS-FSW and maintained in PS-FSW for 1 hr. Each was then ground in 6 x 50 µl rinses of .001 M phosphate buffer, pH 7.0, at 0°C. The homogenate was centrifuged at 12,350 g for 10 min, after which the supernatant was removed and stored for pool activity experiments (see appendix II). The pellet was resuspended in 300 µl of .01 M leucine, adjusted to 7% TCA by the addition of 50 µl 50% TCA, and allowed to sit for 30 min at 0°C. The suspension was recentrifuged, and the supernatant discarded. The pellet was resuspended in .01 M leucine in 7% TCA and recentrifuged. The supernatant was again discarded, while the pellet was extracted overnight in 200 µl 1 M NaOH. The NaOH soluble eye material was cleared by

centrifugation at 3500 g for 15 min. Protein content of a 100 µl sample was determined by the method of Lowry et al. (8). Radioactivity was determined by lyophilizing 100 µl of the 1200 µl sample generated in the Lowry assay, dissolving it in 10 ml NCS-toluene-PPO/POPOP scintillation fluid, and counting as above.

III Results

The incorporation of ^{3}H-uridine and ^{14}C-leucine into TCA insoluble material was determined using a protocol similar to that used in studies of the CR of CAP activity. Briefly, eyes were dissected during subjective day and maintained in darkness in PS-FSW. A 3 hr drug or control pulse was administered at CT 13 the following evening. Drug pulses administered near this phase caused inhibition of the eye CR with the least delay (ch. IV , figs. 8C, H). After the pulse, eyes were rinsed for a period of 1, 9, 49, or 73 hr in PS-FSW and then labeled for 7-9 hr. Eyes were then rinsed in PS-FSW for 1 hr, and then individually homogenized. The radioactivity in TCA insoluble and TCA soluble fractions of the eye was then determined.

To first establish that eyes from the same animal were valid experimental/control pairs, eyes were labeled 1 hr (N = 4 pr.) and 49 hr (N = 4 pr.) after receiving a control pulse of PS-FSW. The ratio of incorporation of each eye with that of its mate (table I) showed minimal variation, measured by standard deviation, when incorporation was expressed as the ratio of TCA insoluble counts in the homogenate (I_h), corrected for insoluble counts left in the grinder

(I_g) to the total TCA soluble counts (S). Thus incorporation = $\frac{I_h + I_g}{S}$. By expressing incorporation relative to soluble counts, some correction was presumably made for differences in the size of eyes and their uptake of label. Grinders contained about 16% of the ^3H and ^{14}C counts found in I_h; and about 70% of the grinder counts were estimated to be TCA insoluble based on recovery of incorporated ^{14}C counts from grinders rinsed with 1 M NaOH. Other control experiments are presented in appendix I A, B.

The results of AFTX (16 µg/ml) and AMD (4 µg/ml) studies are presented in tables II and III and plotted in fig. 1. Both drugs had similar effects on uridine incorporation; at 1 and 9 hr after the drug pulse incorporation was significantly lowered to about 40% control levels while at 49 and 73 hr incorporation was recovered to 80-100% of control values. Leucine incorporation was significantly inhibited in AFTX-treated eyes at all time points, while AMD-treated eyes evidenced incorporation below, but not significantly different from controls. Inhibition of leucine incorporation showed some recovery in later time points for eyes treated with either drug.

The lowered levels of incorporation found in experimental eyes was the result of fewer TCA insoluble counts ($I_h + I_g$) and not the result of an increase in TCA soluble counts (S). In fact, in three cases the number of TCA soluble counts in experimental eyes was significantly lower than in controls. Eyes labeled 1 or 9 hr after an AFTX pulse or 1 hr after an AMD pulse had 22-27% fewer TCA soluble ^3H counts than their controls (paired t test, all $p < 0.02$). The

number of TCA soluble ^{14}C counts was not changed by drug treatment.

The amount of radioactivity in control TCA soluble and TCA insoluble fractions decreased as label was given at later times. All control data (tables I, II, III) for the first two time points were averaged together, and compared to the average control data from the last two time points. TCA soluble and insoluble ^{3}H counts were lowered by 8% and 15% respectively in the latter data. TCA soluble and insoluble ^{14}C counts were both lowered by 38%. These changes had little effect on the ratio of TCA insoluble to TCA soluble counts for either label.

One peculiarity of control data was that the variability of incorporation values among all experiments (tables I, II, III) was greater than the variability within each experiment. Although control eyes tended to give larger incorporation values with older batches of label, differences in technique could not be ruled out as a possible cause of variability of control incorporation values.

In an effort to improve upon the accuracy of measuring leucine incorporation, and as a check on the method used above, experiments were conducted in which the specific activity of TCA insoluble material, expressed as ^{14}C counts per mg protein, was determined for control and drug-treated eyes. Unlike the above method, measurement of incorporation by specific activity does not depend on quantitative recovery of TCA insoluble material (see appendix I D).

To test the similarity of specific activity determinations of eyes from the same animal, a series of control experiments was conducted.

The repeatability of the specific activity determination within each pair of eyes (table IV) showed substantial improvement over the previous method (table I). Other pertinent control experiments are found in appendix I C, D.

Results of specific activity measurements (table IV) showed that leucine incorporation 49 hr after an AMD pulse was significantly decreased compared to controls. The percent inhibition of leucine incorporation was in good agreement ($p < 0.8$, t test) with the value obtained by the previous method (table III). Eyes labeled 49 or 73 hr after an AFTX pulse were not significantly different from controls (table IV). Although the ratios of experimental to control incorporation were higher at both time points than the ratios obtained by the previous method (table II), the results of the two methods were not significantly different ($p < 0.2$ at 49 hr, $p < 0.5$ at 73 hr, t test).

IV Discussion

A. Inhibition of Uridine and Leucine Incorporation

The main purpose of the biochemical studies was to test whether drug doses used to inhibit circadian rhythmicity in the eye had significant effects on uridine and/or leucine incorporation. This requirement has been met for uridine incorporation measured 1 or 9 hr after a pulse of either drug; for leucine incorporation measured 1, 9, 49 or 73 hr after an AFTX pulse and 49 hr after an AMD pulse.

Some correspondence between inhibition of uridine or leucine

incorporation and inhibition of circadian rhythmicity (ch. IV) was observed. Both AFTX and AMD similarly affected the level and time course of uridine incorporation at doses that inhibited circadian rhythmicity. In addition, AFTX caused irreversible inhibition of both leucine incorporation and circadian rhythmicity.

Other properties of incorporation and circadian rhythmicity after drug treatment did not correspond. Uridine incorporation returned close to control levels when measured at 49 hrs and 73 hrs after the end of AFTX or AMD pulses; whereas circadian rhythmicity was irreversibly blocked by these drug treatments. The effect of AFTX on uridine incorporation in the eye is similar to its effect in other systems. In the rat, 500 μg/kg doses of AFTX given by intraperitoneal injection caused the incorporation of ^{14}C-orotic acid into liver RNA to decline to 33% of control levels when measured 2 hrs after drug administration. When incorporation was measured 24 hrs after administration, it was at control levels (9). In Hela cells exposed to 20 μg/ml AFTX for 30 min, uridine incorporation declined to about 45% of control levels 6 hrs after drug administration, and recovered to about 85% of control levels 24 hrs after administration (3). In contrast to AFTX, AMD is thought to be an irreversible inhibitor of RNA synthesis, presumably because of its tight binding (binding constant, K is $\sim 10^6$ M^{-1}) (1) to DNA. However, the inhibition of uridine incorporation caused by AMD in some systems appears reversible (10, 11), although these findings may be artifacts

of cell division or cell death. Such an artifact may explain the unexpected recovery of uridine incorporation in the Aplysia eye. Furthermore, the reversibility of uridine incorporation after AFTX or AMD administration in the Aplysia eye does not eliminate the possibility that the spectrum of RNA molecules being synthesized is not normal (11, 12). This possibility may explain why the inhibition of uridine incorporation did not correspond to the inhibition of circadian rhythmicity.

In contrast to the similarities in uridine incorporation, leucine incorporation was considerably lower following AFTX pulses than following AMD pulses. The disproportionate effect of AFTX on leucine incorporation is consistent with results found in other systems, and is thought to arise from a direct effect of AFTX on polyribosomes (3, 13). Although inhibition of leucine incorporation in some studies is reversible within 6-24 hrs after AFTX administration (3, 14), a report that polyribosomes isolated from rat liver as long as 5 days after AFTX administration were disaggregated (15) suggests that the machinery of protein synthesis may not really return to normal. This effect may explain why leucine incorporation was irreversibly inhibited in the Aplysia eye.

Since leucine incorporation following AMD pulses was significantly inhibited at only one time point, analysis of the kinetics inhibition was not possible without more data.

Interpretation of incorporation experiments requires two additional caveats. First, the specific activity of label in precursor

pools may change as a result of drug treatment, and thus cause disproportionate changes in incorporation compared to changes in synthesis of RNA or protein (11, 16). An attempt was made to measure the average specific radioactivity of intracellular leucine in the eye. Unfortunately, the method employed was not developed to the point of demonstrating similar specific activities in pairs of control eyes. The details of this study are presented in appendix II.

The second caveat concerns the problem that incorporation in the whole eye may not accurately reflect incorporation in the structures that produce the CR. This possibility is supported by the fact that 80% of the neurons in the Aplysia eye are photoreceptor cells that most likely do not act as circadian oscillators (17, 18). Some improvement may be gained in this area by conducting incorporation experiments on eye fragments. Sener, in this laboratory, has shown that when only 20% of the retina remains attached to the optic nerve, a normal CR is still expressed (19). Since the base of the eye is enriched in secondary (non-receptor) neurons relative to the rest of the retina (17), incorporation into the base of the eye may better represent incorporation into the circadian oscillator. In addition to this approach, autoradiograpy of labeled eyes should allow identification of the sources of incorporation.

Appendix I - Supplementary Control Experiments

A. Incorporation of Label into RNA and Protein

Experiments were designed to test whether or not ^{3}H-uridine and ^{14}C-leucine were incorporated into RNA and protein, respectively, by taking advantage of the sensitivity of RNA to base hydrolysis (20) and the sensitivity of protein to pronase digestion (21). TCA-insoluble material from double-labeled control eyes was used in these experiments. Labeling occurred from CT 17 to CT 1, 1½ days after dissection. The preparation of this material is described in Methods (Double Label Experiments).

In base hydrolysis experiments, the TCA-insoluble material from each of 8 eyes was dissolved in 1.0 ml of 0.3 M NaOH and incubated at 37°C for 90 min. Each solution was neutralized by the addition of 0.5 ml 0.6 M HCl, and brought to a final TCA concentration of 5% by the addition of 0.17 ml of 50% TCA. The resultant suspensions were kept at 0°C for 30 min. and then centrifuged at 12,350 g for 10 min. The supernatants and pellets were separated and counted as in Methods. This procedure yielded 97 ± 1% (N=8) of the total ^{3}H-radioactivity and 5 ± 1% (N=8) of the total ^{14}C-radioactivity in the supernatant fractions.

In pronase experiments, the TCA insoluble material from each of 8 eyes was suspended in 1.0 ml of 0.05 M Tris buffer, pH 7.8, containing 1 mg/ml pronase (Calbiochem), and incubated at 37°C for 19 hr. Each suspension was adjusted to a final TCA concentration

of 5% by the addition of 0.11 ml of 50% TCA and centrifuged and counted as above. The supernatant fractions contained 80 ± 8% (N=8) of the total ^{14}C-radioactivity and 3 ± 2% (N=8) of the total ^{3}H-radioactivity.

Although each procedure rendered the proper insoluble radioactivity into soluble form, chemical identification of the solublized labels would have unambiguously identified the nature of the incorporated label. Base hydrolysis of the TCA insoluble material should have yielded a mixture of 2'-OH and 3'-OH-^{3}H-UMP (20). HCl hydrolysis of TCA insoluble material (or pronase solublized material) should have yielded ^{14}C-leucine, which could have been identified by the chromatographic properties of its dinitrophenyl derivative, as described in appendix II.

B. The Source of Incorporation

A check for microbial sources of incorporation was accomplished by measuring the incorporation of ^{3}H-uridine and ^{14}C-leucine into 4 eyes that were homogenized together both before and after labeling, and comparing the magnitude of this incorporation with that of 4 eyes homogenized together only after labeling. Presumably, the incorporation into the former group would be due to microbial sources, since homogenization of eyes before labeling should inhibit their incorporation of label, while providing a nutrient medium for the growth of microbes less susceptible to homogenization.

The two groups of 4 eyes were prepared as in Methods for double-labeled control eyes. Each eye in one group had its mate in

the other group. At the time of labeling (CT 17 to CT 1, 1½ days after dissection), one group of eyes was ground together in 200 µl of PS-FSW in a glass homogenizer, to which was then added 0.5 ml of double-label medium (see Methods). The other group of 4 intact eyes was incubated in a number 00 Nalgene beaker in a solution of 200 µl PS-FSW and 0.5 ml double-label medium. At the end of the labeling period, material from the former group was rehomogenized in the medium already present in the grinder, while the latter group of (intact) eyes was transferred to a different grinder, and homogenized in its labeling medium. Each homogenate was transferred to a separate centrifuge tube, to which was added 100 µl of 3 mg/ml BSA as a carrier, and 100 µl of 50% TCA. Each grinder was rinsed with 2 x 0.5 ml aliquots of 5% TCA, which were then pooled with the appropriate homogenate. The two homogenates were kept at 0°C for 30 min., and then centrifuged at 12,350 g for 10 min. The resultant supernatant fractions were removed and counted as in Methods, while the pellets were resuspended in 1.5 mls of 5% TCA (0°C). This step was repeated 3 more times so that the supernatants contained negligible amounts of ^{3}H- and ^{14}C-radioactivity. The pellets were counted as in Methods (Double Label Experiments).

The pellet derived from the former group of eyes contained 7% of the ^{3}H-radioactivity and 2% of the ^{14}C-radioactivity found in the pellet derived from the latter group. If microbes were incorporating significant amounts of label, then a larger amount of

incorporation might have been expected in the former group of eyes. This interpretation, however, does not take into account the possibility that homogenization of eyes could have also damaged the microbes present in the tissue, causing a reduction in the level of microbial incorporation. The damage could have resulted directly from the homogenization, or indirectly through the release of toxic material such as lysosomes.

An additional test of microbial incorporation would have been to compare incorporation of normally treated eyes with that of eyes given eukaryotic-specific inhibitors of RNA and protein synthesis. Camptothecin and anisomycin have been shown to inhibit eukaryotic RNA (22) and protein (23) synthesis, respectively, in other systems; they are also inhibitors of uridine (24) and leucine (25) incorporation, respectively, in Aplysia. Incorporation of ^{3}H-uridine or ^{14}C-leucine that was resistant to these drugs would determine a maximum level of microbial (plus mitochondrial) incorporation.

C. Specific Activity of Delensed vs. Intact Eyes

To see if the repeatability of specific activity determinations could be further improved, the effect of delensing eyes before fractionation was tested. A large contribution of unlabeled protein from the lens could cause "noise" or insensitivity in the specific activity analysis. Pairs of control eyes were dissected and labeled with ^{14}C-leucine as in Methods (Single Label Experiments). This population was separated into 8 groups of 4 eyes, so that for each

group of eyes there was a corresponding group containing their mates. After labeling, all eyes were delensed, and the four eyes in each group were homogenized together. Homogenates were otherwise treated as in Methods (Single Label Experiments). The protein specific activity of a group of eyes was compared to the protein specific activity of the group of their mates. The ratios of specific activities of each pair of corresponding groups averaged 0.97 ± 0.07 (N=4 pairs of groups). The ratio of specific activities of pairs of intact eyes (table IV) averaged 0.99 ± 0.08 (N=6 pairs of eyes). Thus, no substantial improvement was gained in the repeatibility of specific activity determinations among pairs of eyes by delensing them.

Comparison of the specific activity delensed eyes with that of intact eyes substantiated the hypothesis that the lens contained the majority of the protein in the eye. The 8 groups of delensed eyes had an average specific activity that was 3.6 times greater than the average specific activity of 12 intact control eyes (table IV). Both groups of eyes were labeled from CT 17 to CT 1, 1½ days after dissection in single label medium. Based on this finding, the lens should contain 72% of the total eye protein[a].

D. Sensitivity to Changes in Amount of Protein

The sensitivity of specific activity determinations to the amount of material present in an eye sample was tested on 5 different concentrations of the same sample of NaOH soluble eye material. This material was obtained from control eyes labeled from CT 17 to

CT 1 with single label medium. The material was diluted approximately 2:3, 3:8, 1:6 and 1:8 with 1 M NaOH. Protein specific activity was determined for 100 µl aliquots of the undiluted material, and the four diluted samples, as described in Methods (Single Label Experiments).

A plot of ^{14}C-leucine incorporation versus protein concentration for each of the 100 µl samples is presented in figure 2, along with a least squares fit line. These data indicate that the specific activity measured for a sample is not influenced by the amount of material present in the sample.

To check that protein and incorporated radioactivity were distributed proportionately between recovered material and material left in the grinders, the specific activity of TCA insoluble material from four intact eyes was compared to the specific activity of the TCA insoluble material remaining in the four grinders used to homogenize the eyes. Each grinder was rinsed overnight with 100 µl of 1 M NaOH. The rinses were pooled and neutralized with 400 µl of 1 M HCl and otherwise treated as described in Methods (Single Label Experiments). The TCA insoluble material recovered from the grinders contained 10% of the radioactivity and 7.5% of the protein found in all four eye samples. If the material recovered from the grinders had been combined with the four eye samples, their specific activity would have increased by only 2.4%. Thus, although the incorporated activity and protein may not be distributed proportionately between the sample and the grinder, the loss of material onto grinder surfaces

does not appear to significantly alter the specific activity of an eye sample.

FOOTNOTES

a The calculation is as follows:

Let: R_c = Retinal CPM

R_p = Retinal Protein

L_c = Lens CPM

L_p = Lens Protein

Since the retina has a specific activity that is 3.6 times greater than that of the whole eye:

$$\frac{R_c}{R_p} = 3.6 \frac{R_c + L_c}{R_p + L_p}$$

which simplifies to:

$$\frac{L_p}{R_p} = 2.6 + 3.6 \frac{L_c}{R_c}$$

The above expression can be written as the inequality:

$$\frac{L_p}{R_p} \geq 2.6$$

which can be transformed in a few steps to the final expression.

$$\frac{R_p}{L_p} \leq \frac{1}{2.6}$$

$$\frac{R_p + L_p}{L_p} \leq \frac{1}{2.6} + 1$$

$$\frac{L_p}{R_p + L_p} \geq \frac{2.6}{3.6} = 0.72$$

Thus the lens contains at least 72% of the total eye protein.

Appendix II--Leucine Pool Studies

A. Introduction

The purpose of the studies presented in this appendix was to measure the average intracellular specific activity of ^{14}C-leucine in the Aplysia eye. By measuring this parameter, incorporation of ^{14}C-leucine into control and drug-treated eyes could be corrected for any changes in average pool activities.

The method of Reiger and Kafatos (16) was used for leucine specific activity determinations. It is based on the reaction of ^{14}C-leucine of unknown specific activity with ^{3}H-2,4-dinitrofluorobenzene (^{3}H-DNFB) of known specific activity to yield N-2,4-dinitrophenylleucine (DNP-leucine) labeled with both ^{3}H- and ^{14}C-radioactivity (figure 3). The ratio of ^{14}C-radioactivity to ^{3}H-radioactivity recovered as DNP-leucine by thin layer chromatography (TLC) is then used to calculate the specific activity of the ^{14}C-leucine. Since some of the ^{14}C-leucine in a tissue sample is of extracellular origin, and may have a specific activity very different from the intracellular pool, some correction must be made in the above calculation. This is accomplished by labeling the extracellular space with ^{3}H-inulin, a polysaccharide impermeable to cellular membranes (16). By knowing the ratio of ^{3}H-inulin radioactivity to ^{14}C-leucine radioactivity in the medium, and demonstrating that the extracellular space is equally accessible to both labels, the amount of extracellular ^{14}C-leucine can be calculated from the amount of ^{3}H-inulin recovered from the tissue.

This method is advantageous because: 1) it requires little specialized equipment, 2) if enough radioactivity can be recovered it is sensitive to low amounts of leucine, 3) it does not require quantitative recovery of leucine.

B. Materials and Methods

1) Labeling of Eyes

All eyes used in pool activity studies were control eyes labeled from CT 17 to CT 1, 1½ days after dissection. Eyes were labeled in a medium containing 5 μCi/ml (U-^{14}C) leucine (312 mCi/mM, Schwartz-Mann, Orangeburg, N.Y.) and in some cases 0.6 mg/ml (^{3}H-methoxy)inulin (45 Ci/mg, ICN, Irvine, Calif.). For more details on the labeling medium and procedure, see Methods, Single Label Experiments in this chapter. After labeling, eyes were rinsed 2-5 times in PS-FSW over a period of 1 hr. Each eye was then ground in 6 x 50 μl rinses of 0.001 M phosphate buffer, pH 7.0, at 0°C. The homogenate was centrifuged for 10 min at 12,350 g, and the supernatant stored frozen until used for specific activity determinations.

2) Dinitrophenylation of Samples

The reaction mixture for samples used in one dimensional chromatography consisted of 100 μl supernatant, 200 μl of 0.2 M Na_2HPO_4 (pH 9.08) and 100 μl of 25 μM/ml non-radioactive DNFB and 50 μl of an aqueous solution containing a known amount of ^{3}H-leucine (46 Ci/mM). The DNFB solution was made fresh for each experiment by dissolving 46 mg DNFB in 10.0 mls 100% ethanol.

The reaction mixture for sea water samples analyzed by one dimensional chromatography contained 500 µl of sample, 100 µl of 25 µM/ml non-radioactive DNFB, 50 µl of ^{3}H-leucine, 200 µl of 0.2 M Na_2HPO_4 and 37.5 µl of 0.5 M NaOH. The base was needed to keep the reaction mixture at pH 9.0, which was necessary for the dinitrophenylation to take place (data not shown). Addition of Na_2HPO_4 to the reaction mixture caused a precipitate to form. This material did not appear to interfere with the reaction nor the chromatography of the dinitrophenylated sample, although recovery of DNP-leucine was slightly reduced.

The reaction mixture for samples run on two dimensional chromatography contained the same ingredients used in the mixture for one dimensional chromatography of eye supernatants, except that 100 µl of 2.5 µM/ml ^{3}H-DNFB ($\sim$ 20 µCi/µM) was used instead of non-radioactive DNFB. The ^{3}H-DNFB solution was made fresh for each experiment by evaporating 100 µl of (^{3}H-3,5)DNFB (0.5 mCi/ml benzene, 30 Ci/mM, Amersham) in a conical test tube under reduced pressure. The tube was then repeatedly filled and emptied with about 1 ml of fresh 2.5 µM/ml non-radioactive DNFB dissolved in 100% ethanol. The specific activity of the ^{3}H-DNFB prepared in this way was checked by counting a 20 µl sample in 10 ml of toluene-PPO-POPOP scintillation fluid. In some experiments, 50 µl of exogenous ^{14}C-leucine (0-5975 DPM, 312 mCi/mM) was added to the reaction mixture.

Regardless of the contents of the reaction mixture, it was incubated at 37°C for 16-24 hrs in the dark.

3) Purification of DNP-Leucine

Upon completion of the reaction, each sample was lyophilized at room temperature in dim light. The resultant powder was taken up in 200 µl of 0.2 M $NaCO_3$ (pH 11.44) and extracted with two rinses of 0.5 ml diethyl ether, which were then discarded. The aqueous fraction was acidified by addition of 100 µl concentrated HCl, and extracted with two rinses of 0.5 ml ether. The combined acid-ether extracts were evaporated under reduced pressure, taken up in 100 µl ether, mixed with ∿ 5 µg each DNP-leucine, DNP-isoleucine, DNP-valine and DNP-phenylalanine (Nutritional Biochemicals Corp., Cleveland, Ohio), and stored in a freezer until chromatographed. These non-radioactive carriers were added to help visualize the separation on thin layers. DNP-isoleucine, DNP-valine and DNP-phenylalanine are the DNP-derivatives of naturally occurring amino acids that chromatograph most closely to DNP-leucine (26).

a) Two-Dimensional Thin-Layer Chromatography

DNP-leucine was separated from other acid-ether soluble compounds by means of chromatography on plastic backed silica gel thin layers (20 cm x 20 cm x 0.25 mm; Brinkmann, Westbury, N.Y.) according to the method of Brenner et al. (26). The solvent for the first dimension was prepared by mixing 100 mls toluene (spectral grade), 30 mls pyridine (spectral grade), 60 mls 2-chloroethanol and 60 mls of 0.8 N NH_4OH. The organic phase of this mixture was separated and stored for chromatography while the aqueous phase was combined with 1.3 volumes of 0.8 N NH_4OH and used to moisten the thin layers. This procedure involved

exposing the thin layers to vapors of the aqueous mixture for at least 2 days prior to chromatography. Without this preparation, the mobility of the DNP-amino acid carriers was greatly reduced in the first dimension of chromatography.

Prior to chromatography, each thin layer was attached to a 20 cm x 20 cm glass plate by wetting the plastic backing with water. About 1 cm of the right and left edges of each thin layer were scraped clean of sorbent with a platinum spatula in order to obtain a flat solvent front during chromatography. Without this precaution, the solvent flowed more quickly at the edges of the thin layer than in the center. The sample was applied to the lower left corner of the thin layer and quickly dried by means of a mild current of air directed by a length of Tygon tubing. The air flow was directed in order to cause minimal drying of the rest of the thin layer. The tube containing the sample was rinsed with 50 µl of ether, and this rinse applied on top of the sample spot, and dried. The thin layer was placed in a 4-plate chamber and developed by ascending chromatography. The plate was removed from the chamber and dried in a fume hood for 45 min.

Prior to development of the thin layer in the second dimension, it was turned 90°, and the lower 1 cm edge of exposed plastic backing cut with a scissors. The new right and left edges were scraped as above. The plate was developed twice in a solvent containing 80 mls benzene (spectral grade), 20 mls pyridine (spectral grade) and 2 mls glacial acetic acid. The thin layer was then separated from the glass plate and dried overnight in a fume hood.

b) One Dimensional Thin Layer Chromatography

One dimensional TLC was performed on thin layers that were not specially pretreated, except that the right and left edges were scraped as above. As many as 8 samples were applied to the layer at a spacing of 2 cm. Thin layers were developed two times in the benzene:pyridine: glacial acetic acid solvent system used above.

4) Counting of Radioactivity

The positions of the carrier DNP-amino acids on chromatograms were visible because of their yellow color. The spot was removed by circumscribing it with a platinum spatula, and then scraping the silica gel within the spot into a trough constructed of aluminum foil. The sorbent was transferred to a scintillation vial, to which was added 10 mls of toluene-PPO-POPOP-NCS-NH_4OH scintillation fluid (see Methods, Double Label Experiments in this chapter). The sorbent was extracted overnight, producing a slight yellow color in the counting fluid. Radioactivity was counted at 34% efficiency for ^{3}H-radioactivity and 68% efficiency for ^{14}C-radioactivity. The spillover of ^{3}H-radioactivity into the ^{14}C channel was 3%, while the spillover of ^{14}C-radioactivity into the ^{3}H channel was 20%.

In the experiment using ^{3}H-inulin and ^{14}C-leucine to label eyes, 100 µl samples of PS-FSW rinses of eyes after labeling were counted in 10 mls Aquasol (New England Nuclear, Boston, Mass.) at 36% efficiency for ^{3}H-radioactivity and 72% efficiency for ^{14}C-radioactivity. The spillover of ^{3}H-radioactivity into the ^{14}C channel was 1.5%, while the spillover of ^{14}C-radioactivity into the ^{3}H channel was 16%.

C. Results and Discussion

1) Quantitative Analysis of the ^{14}C-Leucine Content of Eye Supernatants--One Dimensional TLC

Recovery and separation of DNP-leucine from other products in the dinitrophenylated supernatant of the eye was tested in a group of 8 eyes labeled for 8 hrs with ^{3}H-inulin and ^{14}C-leucine. After labeling, eyes were rinsed 3-5 times with PS-FSW over a period of 1 hr (see section 4 for more details of the rinse procedure), and then each eye homogenized separately in 300 µl of 0.001 M phosphate buffer, pH 7.0. (Each homogenate was centrifuged at 12,350 g for 10 min.) An analysis of the radioactivity found in the supernatant fraction of each eye is presented in the first two columns of table V. Although the medium in which the eyes were labeled contained 5.2 times more ^{3}H-radioactivity (DPM) than ^{14}C-radioactivity (DPM), in the supernatant the ^{3}H-radioactivity represented only 10% $\pm$ 01% (N=8) of the ^{14}C-radioactivity. Thus, little ^{3}H-inulin radioactivity remained in the eye after a 1 hr rinse with PS-FSW. This point will be considered in more detail in section 4.

Supernatant samples were reacted with non-radioactive DNFB, extracted with ether and analyzed by one dimensional TLC. Included in each sample applied to the thin layers were four non-radioactive DNP-amino acids (DNP-phenylalanine, DNP-valine, DNP-leucine and DNP-isoleucine) and a known amount of ^{3}H-leucine (0.29 µCi). These additions served as visual and radioactive markers for the separation of DNP-derivatives on TLC.

A schematic representation of the separation achieved by one dimensional TLC is shown in the left-hand part of figure 3, and an analysis of the radioactivity found in the TLC spots is presented in the top half of table VI. Spot 1 was thought to be 2,4 dinitrophenol (DNP-OH) because of its position on the chromatograms (26), its intense yellow color, and the fact that it did not appear when the carrier DNP-amino acids were chromatographed without being mixed with an eye supernatant. DNP-OH would be an expected reaction product of excess DNFB under basic conditions. Spots 2 and 3 were identified as DNP-phenylalanine and DNP-valine, respectively, because of their positions on chromatograms (26). Spot 4 was identified as DNP-leucine because of its position on the chromatograms, and because it contained 83% of the ^{3}H-radioactiivty and 79% of the ^{14}C-radioactivity found in spots 2-5. Controls showed that no ^{3}H-radioactivity derived from ^{3}H-inulin appeared on the chromatogram. Spot 5 was identified as DNP-isoleucine because of its slightly greater mobility than DNP-leucine in the second dimension (26). The positions of the five spots on two dimensional TLC were in agreement with those expected on the basis of the above assignments (26).

Analysis of the radioactivity found in the one dimensional chromatograms (table V) showed that much of the ^{14}C-radioactivity in the supernatants was not ^{14}C-leucine. Because a known amount of ^{3}H-leucine was added to each supernatant sample, the per cent recovery of leucine as DNP-leucine was calculated. Recovery was 40% $\pm$ 04% (N=8) based on the assumption that all the added ^{3}H-radioactivity was ^{3}H-leucine.

This figure is in good agreement with the 40-50% recovery found by Reiger and Kafatos (16). By correcting the amount ^{14}C-DNP-leucine recovered for the efficiency of recovery, the total amount of ^{14}C-leucine in the supernatant was calculated (third column, table V). These data showed that only 14% ± 10% (N=8) of the radioactivity in the aqueous soluble fraction of the eyes was ^{14}C-leucine (fourth column, table V).

The nature of the remaining 86% of the ^{14}C-radioactivity is not very clear. An additional 4%[a] of the total radioactivity was found in spots 2, 3 and 5 (table VI). Another 17% ± 02% (N=4)[b] probably remained in the acidified aqueous phase of the sample (see Materials and Methods). No label was expected to have been lost during the basic ether extractions[b] nor during the lyophilization of the reaction mixture[b]. Hence, the most likely step at which label could have been removed was the acidification of the aqueous phase of the sample. Presumably, the radioactivity was lost as $^{14}CO_2$, derived from $^{14}CO_3^=$ or a decarboxylation reaction. The reason for such a transformation of label, if true, is not at all clear.

2) Analysis of ^{14}C-Leucine Specific Activity by Two Dimensional TLC

Duplicate 100 µl samples of the supernatants analyzed by one dimensional TLC were also analyzed by two dimensional TLC. Eight samples were reacted with 0.25 µM of ^{3}H-DNFB, run on two dimensional TLC, and analyzed for ^{3}H- and ^{14}C-radioactivity. The distribution of ^{14}C-radioactivity among the 5 spots was very similar to that found

after one dimensional TLC (table VI). Calculations based on the expected amount of ^{14}C-leucine in the supernatants (third column, table V) compared with the amount of ^{14}C-DNP-leucine recovered after two dimensional TLC (second column, table VII) showed that DNP-leucine was recovered with an efficiency of 34% ± 04% (N=8; fifth column, table VII). Thus, the one dimensional TLC system was as good as the two dimensional system for separating and recovering DNP-leucine. Preliminary experiments showed, however, that the one dimensional system was not useful for specific activity determinations, because a large amount of non-specific ^{3}H-radioactivity (from ^{3}H-DNFB) was associated with spots 4 and 5 (data not shown).

Analysis of the distribution of ^{3}H-radioactivity on two dimensional TLC showed a much different distribution compared to that of the ^{14}C-radioactivity (table VI). A huge amount of ^{3}H-radioactivity (0.71 - 0.94 μCi), but no ^{14}C-radioactivity was found in spot 1, supporting the interpretation that it contained DNP-OH. As expected, ^{3}H-radioactivity was associated with the other spots as well, suggesting that endogenous valine (spot 3), phenylalanine (spot 2), isoleucine (spot 5) and leucine (spot 4) were being detected. It is of interest to note that the ratio of ^{3}H-radioactivity in spots 2, 3 or 5 compared to the ^{3}H-radioactivity in spot 4 was fairly constant in the 8 eyes analyzed. The ratio of ^{3}H-radioactivities between spots 5 and 4 is in good agreement with the findings of Reiger and Kafatos, who showed that spot 5 had 108-133% of DNP-radioactivity associated with spot 4 (16). This feature will be cited later on in section 3.

^{3}H-radioactivity not associated with ^{14}C-radioactivity was found to the right (spot 4R), the left (spot 4L) and below (spot 4B) the DNP-leucine spot (table VI). The nature of this radioactivity is presently unclear. It was not due to background radiocativity all over the thin layer, because analysis of six rectangular spots to the right of spot 4R in the chromatogram of eye number 3 showed that the level of ^{3}H-radioactivity varied from 9% to 36% of that in spot 4. These spots had about the same areas as spot 4R, and contained no ^{14}C-radioactivity (data not shown).

One possible explanation is that other DNP-derivatives chromatographed near DNP-leucine. Brenner et al. have shown that DNP-norleucine and DNP-α-amino-n-caprylic acid migrate close to spot 4. The former compound would be expected to appear near the intersection of spots 4B and 4L, while the latter would be expected near the top of spot 4L (26). The presence of these or other compounds in the dinitrophenylated supernatant might be responsible for some of the ^{3}H-radioactivity found around spots 4 and 5. Alternative explanations are that the ^{3}H-radioactivity was due to the decomposition of DNP-leucine, or that some of the tritium associated with DNP-leucine exchanged with the solvent or sorbent during chromatography.

These difficulties notwithstanding, calculations were made for the amount and specific activity of the ^{14}C-leucine present in the eye supernatant. Based on the specific activity of the ^{3}H-DNFB (19.05 μCi/μM) used in this experiment, the amount of DNP-leucine recovered

from 100 µl of supernatant varied from 8.3 µµM to 22.6 µµM (fourth column, table VII). If correction was made for the calculated efficiency of DNP-leucine recovery (fifth column, table VII) and the fact that the sample represented 1/3 of the entire supernatant, then the amount of free leucine in the eye was 42 ± 18 µµM (sixth column, table VII). Because of the uncertainty in the origin of the ^{3}H-radioactivity surrounding spot 4, which was 30-43% of the ^{3}H-radioactivity in this spot on the basis of area (table VI), the amount of leucine could have averaged as little as 24 µµM. Calculation of the specific activity of the ^{14}C-leucine was 30.8 ± 17.9 µµCi/µµM (seventh column, table VII) with no correction for background ^{3}H-radioactivity, or averaged as high as 54.0 µµCi/µµM with the correction. These pool activities represent a 6 to 10 fold dilution of the ^{14}C-leucine present in the medium (312 mCi/mM).

3) Test of the Sensitivity of the Method to Changes in Specific Activity

For pool activity measurements to be useful, they must be sensitive to changes in the specific activity of ^{14}C-leucine. One way to test this property is to add various amounts of high specific activity ^{14}C-leucine (312 mCi/mM) to identical supernatant samples, and assay the effect on the calculated specific activity. This test was conducted on eight 100 µl samples taken from the combined supernatants of eight eyes. Samples were reacted with 0.25 µM of ^{3}H-DNFB (20.56 µCi/µM) in the presence of 0-5975 DPM of exogenous ^{14}C-leucine.

Radioactivity found in spots 4 and 5, which were scraped together as one spot, was analyzed and the results plotted in figure 5. These data show that the specific activity of the sample varies linearly with the amount of exogenous ^{14}C-leucine added. This result would be expected if the amount of radioactive leucine added did not significantly contribute to the concentration of endogenous leucine. If the concentration of exogenous leucine were significant, then the plot would not be linear, and would asymptotically approach the specific activity of the exogenous ^{14}C-leucine. This clearly is not the case in figure 5.

The intercept of the least-squares line with the ordinate indicates the specific activity of the sample with no exogenous ^{14}C-leucine added was 2.64 μμCi/μμM. Because about half of the ^{3}H-radioactivity recovered from spot 4 plus 5 was expected to be from DNP-isoleucine (table VI), the true value of the specific activity of the sample was more likely 5.28 μμCi/μμM. This value is certainly lower than that calculated in the previous experiment (30.8 μμCi/μμM). The reason for this discrepancy is unclear.

Further information can be gained from the slope of the line, which was 0.00451 μμCi/μμM per DPM added. This number means that the specific activity of the samples changed by 1 μμCi/μμM for every 101 μμCi of ^{14}C-leucine added[c], indicating that each sample contained 101 μμM of endogenous leucine plus isoleucine. If correction was made for the fact that half the 101 μμM was DNP-isoleucine (table VI), and that the supernatant represented 1/3 of an eye, then the amount

of leucine per eye was 152 μμM. Correction for background ^{3}H-radioactivity would raise the specific activity to 9.6 μμCi/μμM, and lower the size of the pool to 86.6 μμM per eye. Although these figures are 3-6 fold different from those calculated in the previous experiment, the method appears to be adequately sensitive to changes in specific activity.

4) Test of Inulin as an Extracellular Marker

To test the usefulness of ^{3}H-inulin as a marker for extracellular space, the kinetics of its release from the eye were compared with those of ^{14}C-leucine. If the extracellular space is equally accessible to ^{3}H-inulin and ^{14}C-leucine, and the uptake and release of ^{14}C-leucine from cells is low enough, then the kinetics of the release of the labels should be the same. Thus, the ratio of ^{3}H-radioactivity to ^{14}C-radioactivity should stay constant as the eye is rinsed after labeling. If this property can be demonstrated, then the amount of extracellular ^{14}C-leucine in the eye supernatant can be calculated from the amount of ^{3}H-inulin in the supernatant.

The kinetics of ^{3}H-inulin and ^{14}C-leucine release were tested in a group of 8 eyes during the 1 hr period following removal of the labeling medium. This medium contained 5.21 times more ^{3}H-radioactivity (DPM) as ^{14}C-radioactivity (DPM) (see Materials and Methods). The group of eyes used in this experiment were those whose supernatants were analyzed for ^{14}C-leucine content and specific activity (tables V, VI, VII). Eyes number 1 and 2 were each labeled alone in a beaker

containing 0.5 ml of medium. Eyes number 3, 5, 7 were incubated together in 0.5 ml of medium in another beaker, while in still another beaker eyes number 4, 6, 8 were labeled in 0.5 mls of medium. Pairs 1,2; 3,4; 5,6; and 7,8 were each taken from one of four animals. At the end of the 8 hr labeling period the medium in each beaker was replaced by 1.0 ml of PS-FSW. This rinse (rinse 1) was removed within 2 min, and repeated after 7 min (rinse 2), 25 min (rinse 3), 48 min (rinse 4) and 60 min (rinse 5) for eyes 1 and 2. The other eyes were rinsed with 1.0 ml of PS-FSW after 2 min (rinse 1), 9 min (rinse 2) and 60 min (rinse 3). All rinses were filtered through a 0.65 μ millipore filter to remove any radioactive cellular debris.

Analysis of the radioactivity found in 100 μl samples of each rinse showed that the kinetics of release of ^{3}H-radioactivity and ^{14}C-radioactivity were not the same (table VIII). During the first rinse, 0-2 min after removal of the label, the ratio of ^{3}H-radioactivity to ^{14}C-radioactivity was 10-33% below that in the medium. Later rinses showed a greater drop in this ratio, and during the last 12 min of the 1 hr rinse period it was 81% below that of the medium (eye number 2, rinse 5). In all four groups of eyes, the ratio decreased with time.

To test whether the efflux of ^{14}C-radioactivity from the eye was due to release of ^{14}C-leucine, 500 μl samples were reacted with 2.5 μM of non-radioactive DNFB and analyzed by one dimensional TLC. A known amount of ^{3}H-leucine was added to the reaction mixture in order to assay the recovery of leucine as DNP-leucine. The efficiency

of recovery was 29% ± 8% (N=14), a 28% reduction in recovery compared to 100 µl supernatant samples.

The results of these experiments indicated that almost all the ^{14}C-radioactivity rinsed from the eye was ^{14}C-leucine (table IX). The calculation of slightly greater than 100% ^{14}C-leucine content was probably caused by the ^{3}H-leucine not being 100% pure. This would cause the efficiency of DNP recovery to be underestimated, and thus cause the amount of ^{14}C-DNP-leucine to be overestimated.

Calculation of the ratio of ^{3}H-inulin to ^{14}C-leucine rinsed from the eyes (table IX) still indicated that the kinetics of release of the two labels were not the same. Thus, ^{3}H-inulin cannot be used as a reliable marker of the extracellular space of the eye. This finding is in contrast to those of Reiger and Kafatos, who claimed that the ratio of inulin radioactivity to leucine radioactivity did not change very much from that in the medium when silkmoth galea were rinsed ten times over a period of 10 min (16).

The possible reasons for the increased release of ^{14}C-leucine relative to ^{3}H-inulin include: 1) unequal retention of the compounds in the extracellular space, 2) release of intracellular leucine into the extracellular space, and 3) hydrolysis of ^{14}C-labeled proteins in the extracellular space. The third possibility seems the least likely because the amount of hydrolysis necessary to reduce the ^{3}H to ^{14}C ratio during the first rinse would be expected to completely dominate the ratio in the last rinse, unless the amount of hydrolysis also decreased with similar kinetics. The first possibility also seems

unlikely because the ratio of ^{3}H-radioactivity to ^{14}C-radioactivity would be expected to eventually increase. The data clearly show that the ratios decreased with time. One way of distinguishing between the first two possibilities might be to determine the specific activity of the ^{14}C-leucine in the rinses. If some of the ^{14}C-leucine in the extracellular space was of intracellular origin, then its specific activity might be expected to be lower than that in the medium. If the ^{14}C-leucine diffused more quickly from extracellular space than ^{3}H-inulin, then its specific activity should not change.

5) Comparison of ^{14}C-Leucine Specific Activities and Incorporation in Pairs of Eyes

Calculations of leucine specific activities in the supernatants of the eight eyes (seventh column, table VII) showed a 2-3 fold difference in the values obtained for eyes from the same animal (eighth column, table VII). In contrast, the incorporation into eyes from the same animal (ninth column, table VII) was quite similar (tenth column, table VII). The dissimilarities in the specific activity calculations were thus the major cause of the dissimilarities in the protein synthesis calculations (eleventh and twelfth columns, table VII), which were obtained by dividing incorporation by the leucine specific activity.

Possible explanations for the dissimilarity in leucine specific activities in eyes from the same animal include: 1) the measurements were contaminated by extracellular leucine, 2) the specific activity of

leucine measured 1 hr after the labeling period did not reflect the specific activity during the labeling period, 3) hydrolysis of ^{14}C-labeled proteins distorted the measurements, 4) the average leucine specific activity and the average incorporation were not representative of the same distribution of cells in the eye.

Some support for hypothesis 1 is found in table V, where there is a greater correspondence in the amount of ^{3}H-inulin in each pair of eyes than there is in the amount of ^{14}C-leucine. If more of the ^{14}C-leucine in eyes 2, 4, 6 were of extracellular origin than in eyes 1, 3, 5, then the even numbered eyes would have a higher apparent specific activity than the odd numbered ones, as found in the seventh column of table VII. This explanation does not account for the data for eyes 7 and 8.

Whatever the explanation for the dissimilarity in specific activities, there is evidence of a systematic error in the experiment. Eyes 3, 5, 7 all had lower specific activities than their mates, eyes 4, 6, 8. Since these odd-numbered eyes were labeled together in one beaker, and these even-numbered eyes labeled together in another beaker, some dissimilarity in the labeling or rinsing of the two groups may have caused a systematic effect on the apparent leucine specific activity. Clearly, this experiment should have been repeated, and time permitting it would have been repeated.

Footnotes

[a] Spots 2, 3 and 5 contained 27% of the radioactivity in spot 4, which was 14% of the radioactivity in the supernatant. Hence, 27% x 14% = 4%.

[b] Based on data from a set of 4 eyes treated similarly.

[c] $\frac{0.0045\ \mu\mu Ci/\mu\mu M}{DPM} = \frac{1\ \mu\mu Ci/\mu\mu M}{101\ \mu\mu Ci} = \frac{1}{101\ \mu\mu M}$

TABLE I

Incorporation of [^{3}H]uridine and [^{14}C]leucine in Pairs of Control Eyes

	Treatment	Delay of Label (hr)	No. Pairs of Eyes	[^{3}H]uridine Incorporation* Average ± S.D.	[^{14}C]leucine Incorporation* Average ± S.D.
A	PS-FWS	1	4	0.158 ± 0.014	0.415 ± 0.060
B	PS-FSW			0.150 ± 0.005	0.469 ± 0.079
$\overline{R}$				1.05 ± 0.08	0.90 ± 0.15
P				< 0.3	< 0.3
A	PS-FSW	49	4	0.166 ± 0.028	0.327 ± 0.057
B	PS-FSW			0.185 ± 0.035	0.364 ± 0.036
$\overline{R}^{\dagger}$				0.91 ± 0.16	0.90 ± 0.12
P$^{\#}$				< 0.4	< 0.2

*Incorporation for each eye is computed as $\frac{I_h + I_g}{S}$; where I_h is the TCA insoluble counts in the homogenate, I_g is the estimated TCA insoluble counts left in the grinder, and S is the TCA soluble counts in the homogenate.

†$\overline{R}$ is the average of the incorporation ratios determined for each pair of eyes. One eye of each pair is in group A, and the other in group B.

$$R = \left(\frac{I_h + I_g}{S}\right)_A \Big/ \left(\frac{I_h + I_g}{S}\right)_B$$

#P is the probability that incorporation in group A is different from that in group B, determined by a paired t test.

TABLE II

Incorporation of [^{3}H]uridine and [^{14}C]leucine in AFTX-treated and Control Eyes

	Treatment	Delay of Label (hr)	No. Pairs of Eyes	[^{3}H]uridine Incorporation Average ± S.D.	[^{14}C]leucine Incorporation Average ± S.D.
A	† AFTX	1	4	0.035 ± 0.011	0.093 ± 0.042
B	†DMF/PS-FSW			0.136 ± 0.007	0.317 ± 0.033
$\overline{R}$				0.26 ± 0.08	0.30 ± 0.14
P				< 0.01	< 0.01
A	† AFTX	9	4	0.045 ± 0.009	0.052 ± 0.019
B	†DMF/PS-FSW			0.131 ± 0.012	0.193 ± 0.016
$\overline{R}$				0.35 ± 0.07	0.27 ± 0.10
P				< 0.01	< 0.01
A	AFTX	49	4	0.114 ± 0.014	0.168 ± 0.028
B	DMF/PS-FSW			0.120 ± 0.010	0.298 ± 0.039
$\overline{R}$				0.96 ± 0.18	0.57 ± 0.13
P				< 0.9	< 0.02
A	AFTX	73	4	0.150 ± 0.016	0.194 ± 0.049
B	DMF/PS-FSW			0.158 ± 0.036	0.323 ± 0.041
$\overline{R}$				0.99 ± 0.27	0.60 ± 0.12
P				< 0.9	< 0.01

See Table I for explanation of row and column headings.

† In these experiments TCA precipitates were collected on glass fiber filters instead of by centrifugation (see Methods, Single Label Experiments).

TABLE III

Incorporation of [^{3}H]uridine and [^{14}C]leucine in AMD-treated and Control Eyes

	Treatment	Delay of Label (hr)	No. Pairs of Eyes	[^{3}H]uridine Incorporation Average ± S.D.	[^{14}C]leucine Incorporation Average ± S.D.
A †	AMD	1	3*	0.069 ± 0.004	0.160 ± 0.018
B †	PS-FSW			0.141 ± 0.009	0.202 ± 0.007
$\overline{R}$				0.47 ± 0.01	0.79 ± 0.12
P				< 0.01	< 0.2
A	AMD	9	4	0.043 ± 0.009	0.155 ± 0.018
B	PS-FSW			0.101 ± 0.008	0.214 ± 0.053
$\overline{R}$				0.43 ± 0.09	0.74 ± 0.13
P				< 0.01	< 0.1
A	AMD	49	3*	0.092 ± 0.007	0.137 ± 0.035
B	PS-FSW			0.118 ± 0.011	0.205 ± 0.024
$\overline{R}$				0.77 ± 0.10	0.67 ± 0.16
P				< 0.2	< 0.1
A	AMD	73	3*	0.114 ± 0.010	0.170 ± 0.016
B	PS-FSW			0.129 ± 0.014	0.174 ± 0.023
$\overline{R}$				0.88 ± 0.05	0.99 ± 0.12
P				< 0.1	< 0.8

* Indicates the data from a pair of eyes was dropped because of abnormal control incorporation. See Table I for explanation of row and column headings.

† In this experiment, TCA precipitates were collected on glass fiber filters instead of by centrifugation (see Methods, Single Label Experiments).

TABLE IV

Incorporation of [^{14}C]leucine into Control, AFTX-treated and AMD-treated Eyes Determined by Protein Specific Activity

	Treatment	Delay of Label (hr)	No. Pairs of Eyes	[^{14}C]leucine Incorporation cpm/μg protein x 10^{-1} Average ± S.D.
A	PS-FSW	1	6	128 ± 009
B	PS-FSW			130 ± 006
$\overline{R}$*				0.99 ± 0.08
P				< 0.6
A	AFTX			72.7 ± 21.0
B	DMF/PS-FSW	49	4	90.1 ± 12.5
$\overline{R}$				0.81 ± 0.22
P				< 0.1
A	AFTX	73	4	76.8 ± 11.5
B	DMF/PS-FSW			89.0 ± 15.5
$\overline{R}$				0.89 ± 0.25
P				< 0.5
A	AMD	49	8	34.3 ± 07.5
B	PS-FSW			57.8 ± 16.9
$\overline{R}$				0.63 ± 0.18
P				< 0.01

*$\overline{R}$ is average of ratios of protein specific activity determined for each pair of eyes. One eye of each pair is in group A, and the other in group B.

$$R = \frac{\text{Specific Activity (Eye in A)}}{\text{Specific Activity (Mate in B)}}$$

TABLE V

Analysis of Radioactivity from the Aqueous Soluble Fraction of Eyes Labeled with ^{3}H-Inulin and ^{14}C-Leucine

Column	1	2	3	4
Eye No.	^{3}H*	^{14}C*	^{14}C-Leu**	%^{14}C-Leuϕ
1	1358	11416	1895	17
2	1894	17798	5503	31
3	1662	15668	2263	14
4	1748	22038	5942	27
5	2684	23094	1654	07
6	2464	27166	2443	09
7	3056	28818	1802	06
8	2578	23042	1176	05

* 2 times the DPM in a 50 µl sample of supernatant taken before the addition of ^{3}H-leucine.

** DPM of ^{14}C-leucine in 100 µl of supernatant, corrected for losses based on the recovery of a known amount of ^{3}H-leucine as ^{3}H-DNP-leucine.

ϕ $\frac{^{14}C\text{-LEU}}{^{14}C} \times 100$

TABLE VI

Analysis of Radioactivity in Dinitrophenylated Eye Supernatants After One and Two Dimensional TLC

	SPOT NUMBER@						
I-Dimen.¢	1	2	3	4R	4L	4B	5
^{3}H*	---	01±01**	06±02	---	---	---	05±02
^{14}C*	---	11±09**	08±03	---	---	---	08±03
II-Dimen.¢							
^{3}H*	$3.43x10^{5} \pm 1.48x10^{5}$	131±49	167±36	60±28	73±41	43±14	102±23
^{14}C*	0	0	01±01	02±04	01±02	04±02	11±04

* Numbers are per cent DPM recovered relative to DPM recovered from spot 4 (DNP-leucine) ± standard deviation. N=8 unless otherwise designated. On one dimensional TLC, spot 4 had 24,461 ± 2,288 DPM ^{3}H-radioactivity and 1,117 ± 749 DPM ^{14}C-radioactivity (N=8). The ^{3}H-radioactivity was derived from ^{3}H-leucine. On two dimensional TLC spot 4 had 592 ± 228 DPM ^{3}H-radioactivity and 886 ± 535 DPM ^{14}C-radioactivity (N=8). The ^{3}H-radioactivity was derived from ^{3}H-DNFB.

** N=4

¢ Samples run on one dimensional TLC were reacted with 2.5 μM cold DNFB. This caused intense coloring of spot 1 (dinitrophenol), which severely quenched scintillation counting. Samples run on two dimensional TLC were reacted with 0.25 μM ^{3}H-DNFB (19.05 μCi/μM), which did not cause serious quenching of scintillation counting.

@ Figure 4 shows typical positions of spots on one and two dimensional TLC. On two dimensional TLC, spots 4, 4B and 5 had almost equal areas, while spots 4R and 4L had about double this area.

TABLE VII

Analysis of the Specific Activity of ^{14}C-Leucine in the Aqueous Soluble Fraction of Eight Eyes

Column	1	2	3	4	5	6	7	8	9	10	11	12
Eye No.	^{3}H-DPM	^{14}C-DPM	μμCi Rec.	μμM Rec.	% Rec.	μμM Tot.	$\frac{\mu\mu Ci}{\mu\mu M}$	R	$\frac{\mu\mu Ci}{\mu g}$	R	$\frac{\mu\mu M}{\mu g}$	R
1.	352	598	272	8.4	32	26.3	32.4		847		26.1	
								0.49		1.00		2.04
2.	525	1823	831	12.5	33	37.5	66.3		847		12.8	
3.	948	777	353	22.6	35	65.2	15.6		778		49.9	
								0.38		0.95		2.50
4.	763	1636	744	18.2	28	66.0	40.9		816		20.0	
5.	707	507	230	16.9	44	38.1	13.6		729		53.6	
								0.36		0.88		2.47
6.	362	723	329	8.6	30	28.9	38.1		828		21.7	
7.	732	562	255	17.5	32	55.3	14.6		859		58.8	
								0.58		1.13		1.94
8.	348	457	208	8.3	40	21.0	25.1		760		30.3	

Explanation of Columns

1, 2 } DPM of radioactivity found in spot 4.
3 μμCi of ^{14}C-radioactivity recovered =
4 μμM of DNP-leucine recovered
5 Per cent of DNP-leucine recovery based on amount of label in the third column, table V
6 Estimated total μμM of DNP-leucine based on amount recovered and per cent recovery
7 Specific activity of leucine in supernatant calculated as rec. μμCi ÷ rec. μμM
8,10,12 Ratio of numbers in preceeding column
9 Incorporation into eye in units of μμCi per μg protein per 8 hrs.
11 "Protein synthesis" in units of μμM of leucine incorporated per μg protein per 8 hrs; computed as the ratio of the value in column 9 to the value in column 7.

TABLE VIII

Rinses of Eyes Labeled with ^{3}H-Inulin and ^{14}C-Leucine

Rinse No.	Eye 1			Eye 2			Eyes 3,5,7			Eyes 4,6,8		
	^{3}H*	^{14}C*	R**	^{3}H	^{14}C	R	^{3}H	^{14}C	R	^{3}H	^{14}C	R
1	---	---	---	337879	72190	4.68	197328	56839	3.47	206333	55924	3.69
2	12615	6186	2.04	39386	10939	3.60	24763	8490	2.92	28627	9874	2.90
3	1465	966	1.52	3478	1761	1.98	6957	2930	2.37	5213	2570	2.03
4	334	313	1.07	340	538	0.63						
5	---	---	---	206	418	0.49						

* Numbers refer to DPM in a 100 µl sample of a 1.0 ml rinse passed through a 0.65 µ filter.

** Ratio of ^{3}H-DPM to ^{14}C-DPM.

TABLE IX

DNFB Analysis of Rinses of Eyes Labeled with ^{3}H-Inulin and ^{14}C-Leucine

Rinse No.	Eye 1			Eye 2			Eyes 3,5,7			Eyes 4,6,8		
	^{14}C*	$\%^{14}C$**	R$^{\phi}$	^{14}C	$\%^{14}C$	R	^{14}C	$\%^{14}C$	R	^{14}C	$\%^{14}C$	R
1	---	---	---	389605	108	4.34	287723	101	3.43	301518	108	3.42
2	33013	107	1.91	56836	104	3.46	39306	93	3.15	47437	96	3.02
3	4370	90	1.68	8187	93	2.12	12258	84	2.84	10487	82	2.49
4	1669	107	1.00	1862	69	0.91						
5	---	---	---	1970	94	0.52						

* Total DPM recovered as ^{14}C-DNP-leucine from a 500 µl sample; corrected for losses based on the recovery of a known amount of ^{3}H-leucine as ^{3}H-DNP-leucine. Samples are from the same rinses analyzed in table VIII.

** Per cent of ^{14}C-radioactivity in rinse (table VIII) accounted for as ^{14}C-DNP-leucine calculated as $\frac{^{14}C\text{-DPM (table IX)}}{^{14}C\text{-DPM (table VIII) X 5}}$

ϕ Ratio of the ^{3}H-radioactivity (table VIII) to 1/5 of the ^{14}C-radioactivity (table IX).

Figure 1

Percent control incorporation ($\bar{R}$ in tables II, III) of ^{3}H-uridine and ^{14}C-leucine in eyes treated with AFTX (16 µg/ml) or AMD (4 µg/ml) pulses, plotted as a function of the time between the end of the drug pulse and the middle of the labeling period. Eyes were dissected and kept in PS-FSW for about 36 hr and then given a drug pulse from CT 13 to CT 16. A label pulse, lasting 7-9 hr began 1, 9, 49 or 73 hr after the drug pulse was terminated. Bars represent standard deviation on both sides of $\bar{R}$. (*) indicates data in which incorporation of drug-treated eyes was significantly different ($p < 0.05$, paired t test) from paired controls.

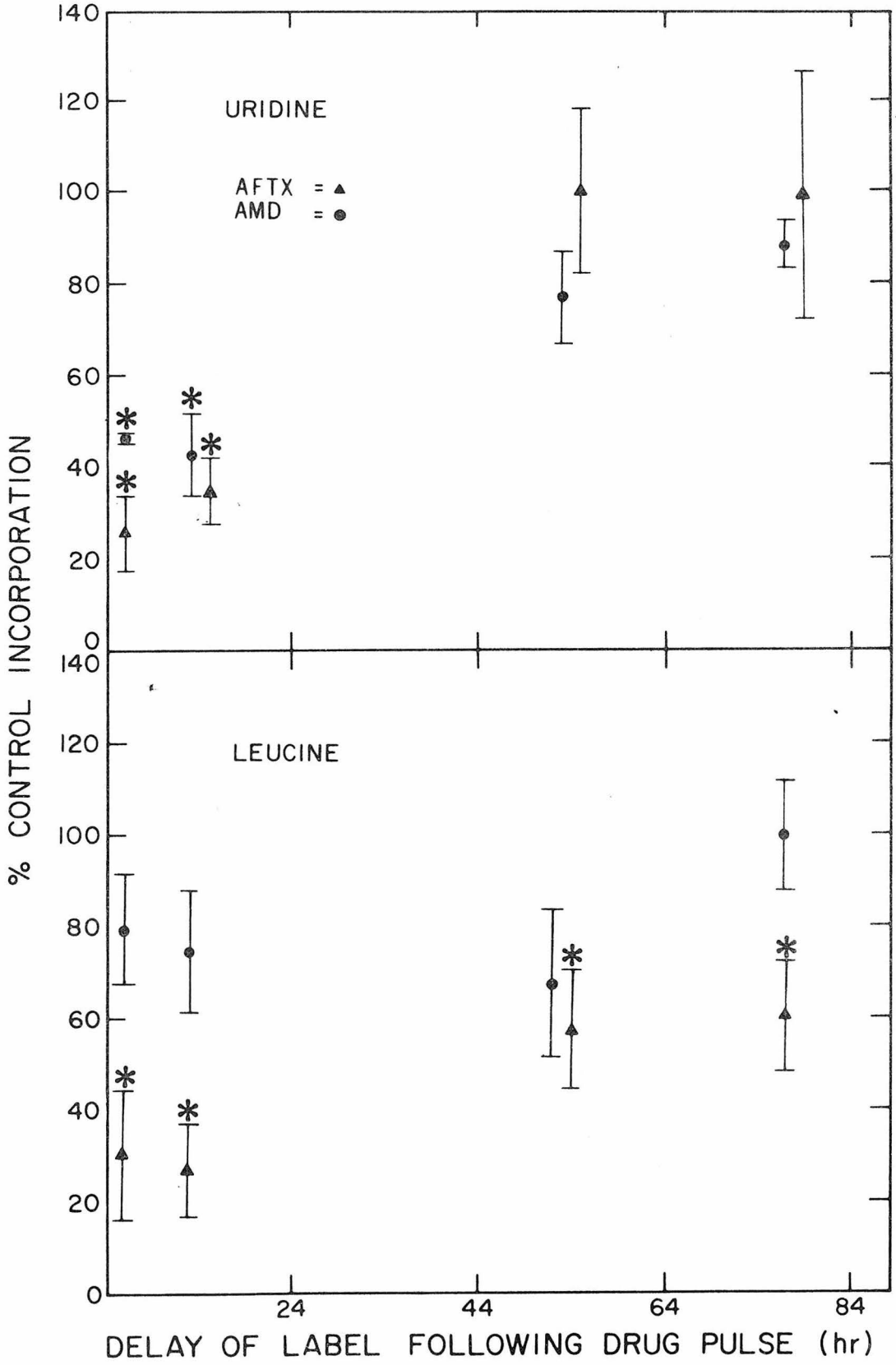
URIDINE
AFTX = ▲
AMD = ●
LEUCINE
% CONTROL INCORPORATION
0
20
40
60
80
100
120
140
24
44
64
84
DELAY OF LABEL FOLLOWING DRUG PULSE (hr)

Figure 2

Plot of incorporated ^{14}C-leucine radioactivity vs. protein concentration of five 100 µl samples of TCA insoluble eye material dissolved in 1 M NaOH. A sample of NaOH solubilized eye material, and 4 dilutions of this solution, were analyzed as in appendix ID. The line is a least squares fit to the data points, and is described by the equation $Y = 159X - 526$, where Y is the total ^{14}C-radioactivity, and X is the protein concentration, in µg/ml, of the 100 µl sample of NaOH soluble eye material (see Methods, Single Label Experiments). The correlation coefficient of the correspondence between Y and X is 0.995 (Pearson product-moment).

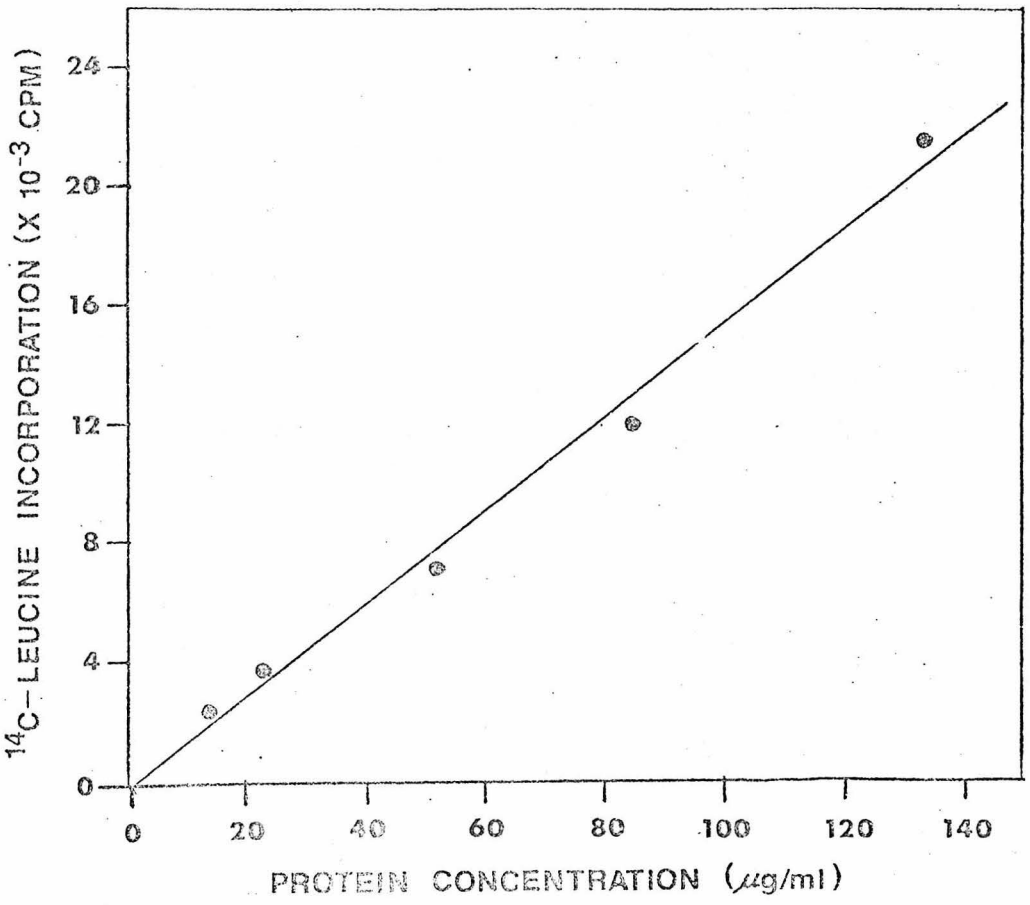
^{14}C– LEUCINE INCORPORATION (X 10^{-3} CPM)
0
4
8
12
16
20
24
0
20
40
60
80
100
120
140
PROTEIN CONCENTRATION (μg/ml)

Figure 3

The reaction of 2,4-dinitrofluorobenzene (DNFB) with a free amino acid to form an N-2,4-dinitrophenyl amino acid (DNP-amino acid). In some experiments, the DNFB was labeled in the 3 and 5 positions with ^{3}H (*). In all experiments, the reaction mixture contained leucine, uniformly labeled with ^{14}C (*).

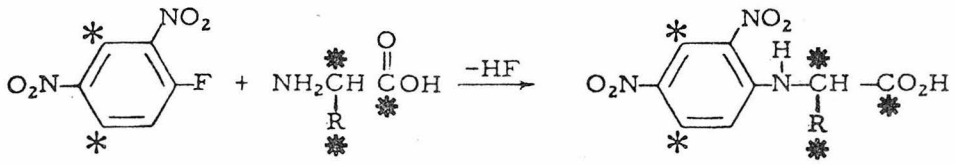

Figure 4

Schematic representation of the separation of DNP-derivatives by chromatography on silica gel thin layers.

Left: Separation achieved by two dimensional TLC. With the thin layer oriented for development in the first dimension, 1 cm of sorbent was removed from the right and left edges (— — —). A dinitrophenylated sample containing carrier DNP-amino acids was applied to the lower left hand corner of the thin layer (●). The chromatogram was developed in the organic phase of toluene: pyridine: 2-chloro-ethanol: 0.8 N NH_4OH (100:30:60:60) and dried. The layer was turned 90° so that the chromatographed spots were at its bottom, 1 cm of sorbent was removed from the new right and left edges (-----), and the exposed plastic backing at the bottom of the plate was removed. The thin layer was developed two times in benzene: pyridine: glacial acetic acid (80:20:2). Numbered areas surrounded by solid lines represent yellow, elliptical-shaped spots on the chromatogram. Spots were identified as DNP-OH (#1), DNP-phenylalanine (#2), DNP-valine (#3), DNP-leucine (#4) and DNP-isoleucine (#5). Numbered rectangular areas (.....) were scraped from chromatograms after removal of spots 1-5.

Right: Separation achieved by one dimensional TLC. Thin layers, spotted with as many as 8 dinitrophenylated samples plus carrier DNP-amino acids, were developed two times in benzene: pyridine: glacial acetic acid (80:20:2).

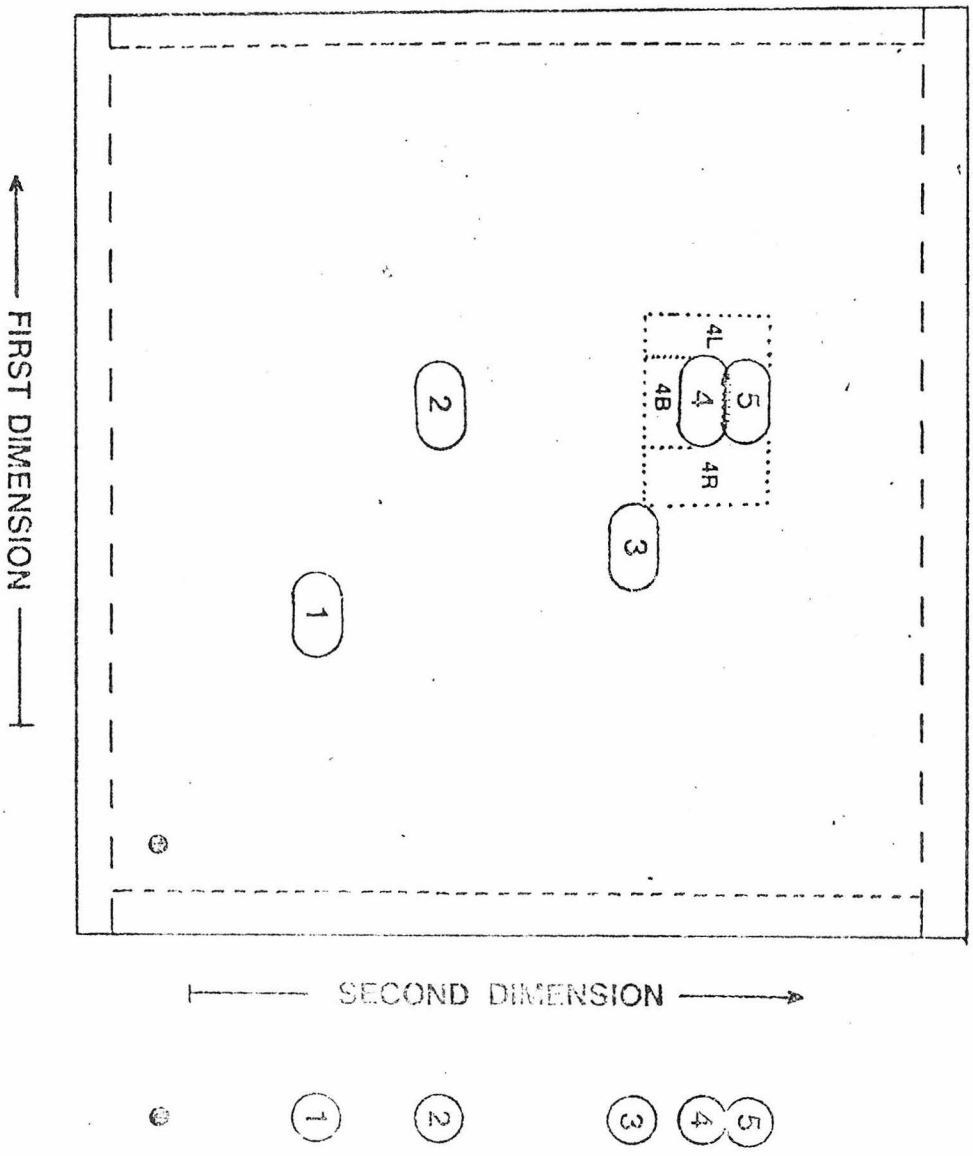
FIRST DIMENSION
SECOND DIMENSION
1
2
3
4L
4
4B
5
4R
1
2
3
4
5

Figure 5

Plot of the specific activity of ^{14}C-leucine in 8 eye supernatant samples vs. the amount of exogenous ^{14}C-leucine (312 mCi/mM) added to them. The samples were identical except for the added ^{14}C-leucine. Each sample was dinitrophenylated in a mixture containing 0.24 μM of ^{3}H-DNFB (20.56 μCi/μM), and analyzed by two dimensional TLC. The line is a least squares fit to the 8 data points; and is described by the equation $Y = 0.00451X + 2.64$, where Y is ^{14}C-leucine specific activity in units of μμCi/μμM, and X is ^{14}C-radioactivity in units of DPM. The correlation coefficient of the correspondence between Y and X is 0.996 (Pearson product-moment).

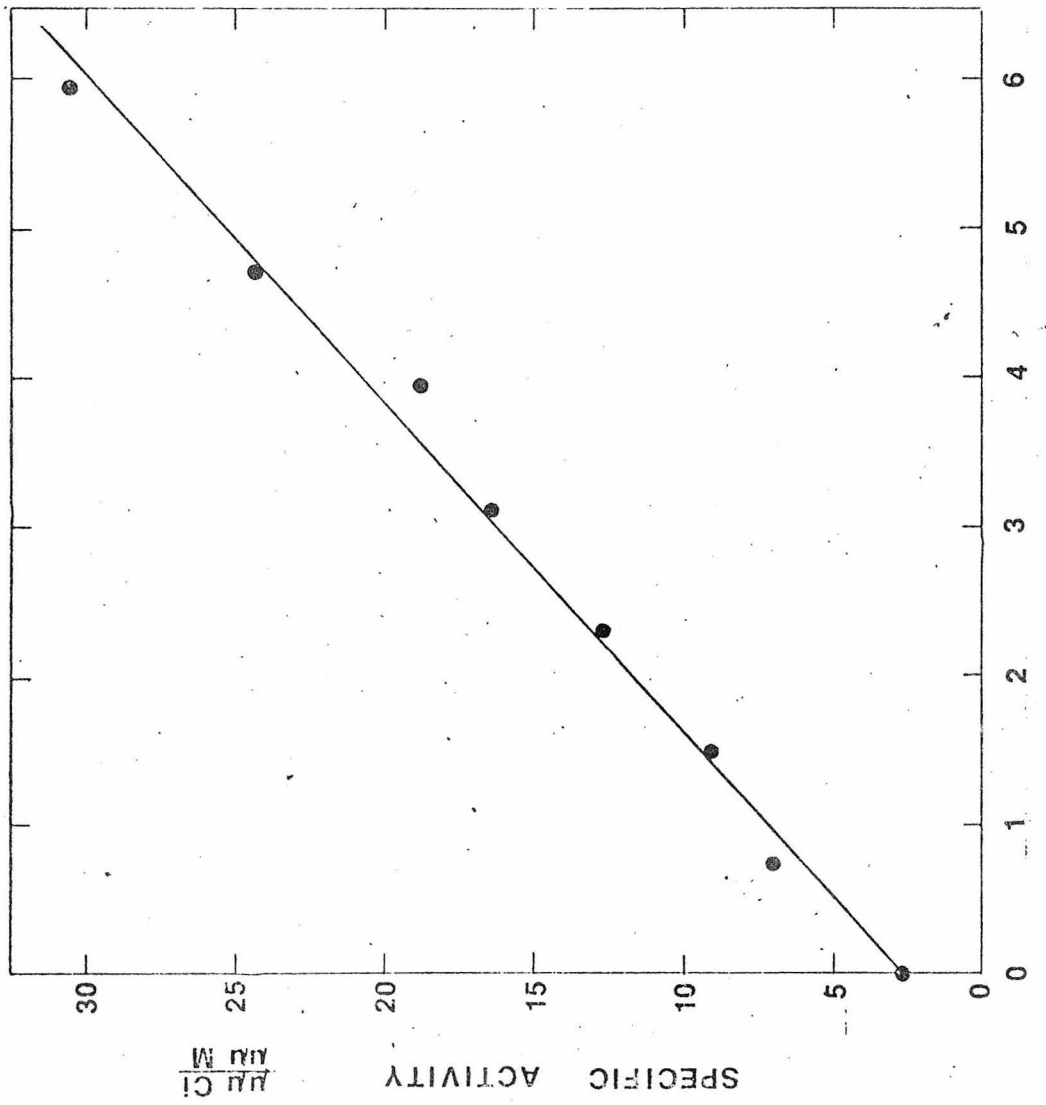
SPECIFIC ACTIVITY
μμ Ci / μμ M
0
5
10
15
20
25
30
0
1
2
3
4
5
6
DPM ADDED X 10^{-3}

REFERENCES

1. Gale, E. F., E. Cundliffe, P. E. Reynolds, M. H. Richmond and M. J. Waring. The Molecular Basis of Antiobiotic Action, Wiley & Sons, New York, 1972. pp 173-277.
2. Reich, E., and I. H. Goldberg. 1964. Prog. Nucleic Acid Res. 3: 183-235.
3. Harley, E. H., K. R. Rees, and A. Cohen. 1969. Biochem. J. 114: 289-298.
4. Sporn, M. B., C. W. Dingman, H. L. Phelps, and G. N. Wogan. 1966. Science 151: 1539-1541.
5. Clifford, J. I., and K. R. Rees. 1966. Nature 209: 312-313.
6. Neeley, W. C., J. A. Landsden, and J. R. McDuffie. 1970. Biochemistry 9: 1862-1866.
7. Ward, S., D. L. Wilson, and J. J. Gilliam. 1970. Anal. Biochem. 38: 90-97.
8. Lowry, O. H., N. J. Rosenbrough, A. L. Farr, and R. J. Randall. 1951. J. Biol. Chem. 193: 265-275.
9. Lafarge, C., and C. Frayssinet. 1970. Intl. J. Cancer 6: 74-83.
10. Benedetto, A., C. Delfini, S. Puledda, and A. Sebastiani. 1972. Biochim. Biophys. Acta. 287: 330-339.
11. Sawicki, S. G., and G. C. Godamn. 1972. J. Cell Biol. 55: 299-309.
12. Schluederberg, A., R. C. Hendel, and S. Chavanich. 1971. Science 172: 577-579.
13. Garvican, L., F. Cajone, and K. R. Rees. 1973. Chem.-Biol. Interactions 7: 39-50.

14. Clifford, J. I., and K. R. Rees. 1967. Biochem. J. 120: 65-75.

15. Pong, R. S., and G. N. Wogan. 1969. Biochem. Pharmacol. 18: 2357-2361.

16. Reiger, J. C., and F. C. Kafatos. 1971. J. Biol. Chem. 246: 6480-6488.

17. Jacklet, J. W., and J. Geronimo. 1971. Science 174: 299-302.

18. Audesirk, G. 1973. Brain Res. 59: 229-242.

19. Strumwasser, F. 1973. The Physiologist 16: 9-42.

20. Berry, R. W. 1969. Science 166: 1021-1023.

21. Nomoto, M., Y. Narahashi, and M. Murakami. 1960. J. Biochem. 48: 593-602.

22. Schultz, A. G. 1973. Chem. Rev. 73: 385-405.

23. Vazquez, D. T. Staehelin, M. L. Celma, E. Battaner, R. Fernandez-Muñoz, and R. E. Monro. In Inhibitors, Tools in Cell Research, ed Th. Bucher and H. Sies. Springer-Verlag, New York. 1969. pp. 100-123.

24. Wilson, D. L. Personal Communication 6/73. Unpublished results.

25. Schwartz, J. H. V. F. Castellucci, and E. R. Kandel. 1971. J. Neurophysiol. 34: 939-953.

26. Brenner, M., A. Niederwieser and G. Pataki. In: Thin Layer Chromatography, ed E. Stahl, Springer-Verlag, New York, 1965, pp 414-427.

Chapter VI

Effects of Puromycin and Cycloheximide on the Circadian Rhythm of Spontaneous CAP Activity

I Introduction

In chapter IV it was demonstrated that 3 hr pulse application of the RNA and protein systhesis inhibitors aflatoxin B1 or actinomycin D could block the circadian rhythm (CR) of spontaneous compound action potential (CAP) activity in the isolated Aplysia eye without eliminating spontaneous CAP activity. Because the inhibition of the CR was essentially irreversible, it was difficult to determine the level at which the drugs were affecting the CR. Possible explanations for inhibiting the CR included stopping the circadian clock, inhibiting the transduction of the CR and destruction of hypothetical circadian pacemaker cells.

Pulse application of reversible agents might yield more interpretable results concerning the level at which the CR was affected if, after being washed out, they allowed the CR to be expressed. Since puromycin (PURO) and cycloheximide (CHX) are known to be reversible inhibitors of protein synthesis in other systems (1,2), their effects on the Aplysia eye CR were studied.

These drugs have changed the phase and period of free-running CRs in other systems. PURO pulses (8 hrs, 10^{-5}M) caused small (2 hr) but significant phase delays in the CR of luminescence in the marine dinoflagellate Gonyaulax. When administered continuously, PURO (2×10^{-5}M) blocked the expression of this CR without entirely inhibiting luminescence (3). Feldman showed that the length of the free-running period of the phototactic motility CR in cultures of

Euglena was dependent on the concentration of CHX (0.2-4.0 mg/ml) to which they were continuously exposed. When CHX was removed from the cultures after 1-3 days, their free-running period became normal but they remained out of phase with controls (4).

This chapter presents the results of dose-response, phase-response and electrophysiological studies on the effects of PURO and CHX pulses administered to the isolated Aplysia eye, and establishes that the drugs cause phase shifts in the CR of spontaneous CAP activity.

II Materials and Methods

A. Recording of CAP Activity

Spontaneous CAP activity was recorded in a manner identical with that described in chapter III. In brief, CAP activity was recorded by means of a suction electrode placed on the optic nerve of each eye. Eyes were kept submerged in 3.0 ml of PS-FSW in separate beakers and maintained at 15 ± 1°C (range). PS-FSW is sea water filtered through a 0.22 μ millipore filter and supplemented with 100 units per ml each of penicillin and streptomycin. Eyes were kept in constant darkness unless otherwise stated. Signals from the optic nerve were amplified by a Tektronix 122 preamplifier and then recorded on a Grass 7B polygraph employing A.C. EEG type amplifiers.

B. Drug Solutions

Puromycin HCl and cycloheximide were obtained from Calbiochem, La Jolla, Calif. Puromycin aminonucleoside (PAN) was obtained from

Nutritional Biochemicals, Inc., Cleveland, Ohio. All three drugs were soluble in PS-FSW at the desired concentrations. Solutions of PURO were adjusted to the pH of PS-FSW (~7.8) by the addition of small volumes of 0.1 M NaOH when necessary. Solutions of PAN and CHX were adjusted to the pH of PS-FSW by the addition of small volumes of 0.1 M HCl. The concentrations of PURO and PAN solutions were checked on a Beckman DB spectrophotometer at 276 nm.

The solution inside each beaker was changed by means of tubing (PE 170, Intramedic) connecting the beaker to the outside of a light-tight box. When a drug or control solution was removed, each eye was rinsed with three changes of 3 mls PS-FSW, and then maintained in PS-FSW for the duration of the experiment.

III Results

A. Normal Eyes

The details of the CR of normal *Aplysia* eyes were described fully in chapter IV. Aspects of this data pertinent to the experiments presented in this chapter are reviewed below.

In constant darkness and temperature the isclated *Aplysia* eye spontaneously discharges CAPs down the optic nerve. The frequency of these CAPs follows a free-running CR with a period of about 22-24 hrs when determined by periodogram analysis at 1 hr resolution. CAP activity during the first cycle of the CR peaks near projected dawn, circadian time 0(CT 0), of the donor animal's LD 12:12 entrainment

schedule, and reaches a minimum near projected dusk (CT 12). When a pair of eyes is taken from the same animal and optic nerve recordings are made from each eye in separate beakers, a striking similarity in their CRs is observed.

To quantitate these similarities, the CRs of 6 pairs of eyes were recorded in PS-FSW and compared for CR amplitude, phase and waveform. Each cycle in one eye was compared to the corresponding cycle of its mate. Each eye was analyzed for 4 cycles. Activity maxima, determined from CAP totals every half hour, occurred within an average of 2 ± 55 min. (SD). Other data showed a close correspondence between pairs of cycles with respect to their amplitudes and waveforms. The complete data concerning these similarities are presented in chapter IV.

Other information not related to the similarities of CRs was extracted from the CAP activity records of these six pairs of eyes. The free-running period of the CR, based on the time intervals between successive half-hourly CAP activity peaks, averaged 23.42 ± 1.48 hrs for all 36 intervals. The damping coefficient of the CR, based on the decline in peak hourly CAP activity in successive activity cycles, averaged 0.67 ± 0.17 for all 36 pairs of successive cycles.

B. Dose-Response Relationships

Twelve hr pulses of PURO (5-134 µg/ml) or CHX (10-2000 µg/ml) were administered to eyes to determine the spectrum and range of

effects on the CR of CAP activity. All pulses began on the second subjective night after dissection, at CT 17. The effects on CAP activity were classified as: 1) those occurring during the drug pulse, 2) those occurring 0-7 hrs after the end of the pulse, and 3) those occurring from 7 hrs after the pulse to the end of the experiment. The changes in CAP activity caused by either drug had different dose-response characteristics during each of the three periods. The nature and dose-dependence of the changes during each period are discussed below.

1) <u>During the Pulse</u>

The waveform of the second CAP activity cycle and the level of CAP activity were changed during pulses of PURO or CHX. PURO doses of 20 µg/ml (fig. 1B) and 50 µg/ml (fig. 1C) increased the steepness of the falling phase of the second activity cycle. The slope of this falling phase was expressed as the change in hourly CAP frequency from the peak of the second activity cycle to the end of the drug pulse divided by the difference in time between these two points and normalized to the peak hourly CAP frequency of the first activity cycle. The slope of the falling phase during PURO pulses of 20 µg/ml (fig. 1B) and 50 µg/ml (fig. 1C) was 1.9 times as steep as the corresponding slope during the 5 µg/ml PURO pulse (fig. 1A). The time at which the second activity cycle peaked was not affected by PURO doses between 5 and 50 µg/ml. The second activity cycle, however, was almost completely inhibited during a PURO pulse of 125 µg/ml (fig. 5A) or 134 µg/ml (fig. 1D).

CHX pulses caused changes in the waveform of the second activity cycle similar to those caused by PURO pulses. The steepness of the decline in CAP activity from the peak of the second activity cycle to the end of the CHX pulse was related to the concentration of CHX administered. This decline in CAP activity should not be confused with the falling phase of the second activity cycle beginning 1-2 hrs after termination of the CHX pulse. The slope of decline in CAP activity for the eyes given CHX pulses of 100 µg/ml (fig. 1F), 1000 µg/ml (fig. 1G) and 2000 µg/ml (fig. 1H) were 3.5, 8.0 and 35 times steeper, respectively, than the slope of the eye treated with a CHX pulse of 25 µg/ml (fig. 1E). The eye given a 10 µg/ml pulse of CHX (not shown) had a slope 1.8 times steeper than the eye given the 25 µg/ml pulse. A delayed activity peak was expressed during the CHX pulse in two of three eyes given a 1000 µg/ml pulse (fig. 1G) and in the eye given a 2000 µg/ml pulse (fig. 1H). The second activity cycle peaked at normal times during CHX pulses of 500 µg/ml and less.

The average CAP activity during the pulse was depressed by 50% to almost 100% in eyes given PURO concentrations ranging from 50-134 µg/ml compared to eyes given lower PURO doses (5-20 µg/ml) (fig. 2). CAP activity for each eye was quantitated by computing the average hourly CAP frequency during the pulse divided by the peak hourly CAP total for the first activity cycle. This procedure allowed the CAP activity that occurred during the pulse to be normalized to the level of previous CAP activity.

In contrast to the depressed CAP activity seen during PURO pulses of 50-134 μg/ml in concentration, the level of CAP activity during CHX pulses (10-2000 μg/ml) was not changed except at 2000 μg/ml, where it was increased by about 40% (fig. 2). Most of the increase in CAP activity occurred during the last half of the 2000 μg/ml CHX pulse (fig. 1H), and thus gave the second activity cycle an abnormal appearance.

2) Zero to Seven Hours After the Pulse

Within 7 hours of the removal of a PURO (50-134 μg/ml) or CHX (10-2000 μg/ml) pulse, CAP activity that had been decreasing during the pulses cycled from a relative minimum to a relative maximum and then began to decline again (figs. 1C-H). The end of this 7 hr period corresponds to the end of the third projected light period (CT 12). The cycling of CAP activity during this period is referred to as a "rebound" because its rising phase represents a reversal in the normal direction of CAP activity changes at this phase of the CR. One of two eyes treated with a 20 μg/ml PURO pulse showed a shoulder in the falling phase of the second activity cycle during this period (fig. 1B). The other eye, and eyes given 10 μg/ml (not shown, N=2) and 5 μg/ml (fig. 1A, N=1) PURO pulses did not show a shoulder or rebound.

The amount of CAP activity expressed by each eye during the "rebound" period was quantitated by computing the average hourly CAP frequency during this period divided by the peak hourly CAP

frequency of the first activity cycle. The results of this analysis (fig. 3) showed that CHX-treated eyes produced about 2 times more CAP activity during the rebound period than PURO-treated (5-50 μg/ml) eyes. Eyes given larger doses of PURO (125, 134 μg/ml; N=1 each) expressed unusually high CAP activity during the rebound (figs. 5A and 1D). This effect may reflect a correspondence between the depression of CAP activity during a high PURO pulse (figs. 1D, 2) and the increase in CAP activity during the rebound (figs. 1D, 3). However the linear correlation coefficient calculated for the correspondence between CAP activity during the drug pulse and CAP activity during the rebound period was -0.42 for PURO-treated eyes (N=11) and -0.26 for the CHX-treated eyes (N=8) (Pearson Product Moment). Thus the inverse relationship between CAP activity during higher concentration PURO pulses and CAP activity during the rebound period is not reflected in the data obtained from eyes given lower PURO doses, nor in the CHX dose-response data.

3) More Than Seven Hours After the Drug Pulse

By 7 hrs after the end of PURO or CHX pulses, the CAP activity of most eyes that had expressed a rebound had reached another relative minimum (figs. 1D, E, F). From this point in time, most eyes expressed a CR of CAP activity that was phase shifted from the projected light-dark schedule of the donor animal by an amount dependent on the drug and dose administered previously. The expression of this CR was different in PURO-treated eyes compared to CHX-treated eyes.

In the former group, a falling phase (figs. 1B, C, D) - distinct from the falling phase of the rebound - sometimes preceded by a rising phase (figs. 1C, D) occurred during the third projected night. This falling phase appeared to be in phase with the CR subsequently expressed. In contrast, eyes given CHX pulses did not express a falling phase during this period (figs. 1E, F, G) except for the eye given a 2000 μg/ml dose (fig. 1H).

The expression of an additional falling phase in CAP activity of PURO-treated eyes during the third projected night may imply that PURO caused phase advances in the Aplysia eye CR, whereas CHX caused phase delays. However, for reasons explained in the following section, the effects of PURO and of CHX pulses were both tentatively considered to be phase delays.

The magnitude of the phase delay caused by either drug was dependent on the dose administered. The phase delay of each activity cycle peaking on or after the third projected dawn (first dashed vertical line of each record in fig. 1) was estimated by the time between the peak in half-hourly CAP frequency for that particular cycle and the preceding projected dawn. This estimate was then revised by adding or subtracting any phase advance or delay, respectively, between the peak in half-hourly CAP activity for the first cycle and the first projected dawn. The phase delays calculated for each cycle were then averaged together for each eye. Thus, phase delays were determined relative to a CR projected from each eye's first activity cycle assuming a 24 hr free-running period.

Phase delays computed in this way were probably a bit below their actual value since the eye free-runs with a period of 23.4 hrs (see Normal Eyes) on the average. Phase delays were considered significant if they were greater than 2 hrs (see footnote C, ch. IV). A graph of the phase delays caused by different doses of PURO or CHX is presented in figure 4. With increasing CHX dose above 500 µg/ml the phase of the CR was increasingly delayed. This relationship lends credence to the interpretation that CHX caused phase delays. The phase delays caused by PURO pulses had essentially an "all or none" relationship with the dose, with a threshold of 20 µg/ml. These data therefore do not help resolve the question of whether PURO pulses caused phase advances or delays.

The CRs expressed subsequent to the rebound period were also examined for changes in waveform, period, and damping. In many cases the CR waveform was changed by drug treatment. The level of activity minima was raised in most eyes treated with 10-134 µg/ml PURO pulses (fig. 1B, C, D) or 500-2000 µg/ml CHX pulses (fig. 1G, H); whereas it was unaffected by lower doses of either drug (fig. 1A, E, F). In addition to the changes in the CR waveform at activity minima, activity cycles were less smooth (figs. 1A-D, G, H). A similar increase in CAP acitvity "noise" occurred in eyes after treatment with aflatoxin B1 or actinomycin D pulses (ch. IV). CAP activity "noise" was seen following all PURO pulses (5-134 µg/ml, figs. 1A-D) and following CHX pulses of 500-2000 µg/ml (figs. 1G, H).

The period of the CR after drug treatment was not changed by PURO or CHX treatment. Starting at dusk of the third projected dark period, the interval of time (i.e., the period) between successive peaks in half-hourly CAP frequency was determined for each eye. When peak intervals were averaged according to PURO or CHX dose, no differences were found in any group compared to control eyes (see Normal Eyes) (all $p > 0.05$, t test). When intervals were averaged according to drug without regard to dose, still no significant differences were found between drug-treated and control eyes (N=36 intervals)(PURO: $p < 0.1$, N=25; CHX: $p > 0.5$, N=20; t test).

The damping coefficient of the CR after drug treatment was significantly increased in a few cases. Starting at dusk of the third projected dark period, the damping coefficient between each successive pair of cycles was determined for each eye by dividing the peak hourly CAP rate of the later cycle by the peak hourly CAP rate of the earlier one. Damping coefficients were averaged according to drug and dose. The damping coefficients averaged from the data of two eyes receiving a 20 µg/ml pulse (fig.1B), and from the data of an eye receiving a 25 µg/ml (fig. 1E) or 100 µg/ml (fig. 1F) CHX pulse were significantly increased by 44, 32, and 31%, respectively, ($p < 0.01$, N=6 pairs of successive cycles; $p < 0.05$, N=4; and $p < 0.05$, N=4, respectively, t test) compared to control eyes (N=36, see Normal Eyes). Damping coefficients pooled according to drug treatment without regard to dose were not significantly different

from control damping coefficients (PURO: $p < 0.1$, N=35; CHX: $p < 0.5$, N=27; t test).

C. The Effect of Varying the Duration of the PURO Pulse

In an attempt to decide whether 12 hr PURO pulses (20-134 µg/ml) caused phase advances or phase delays in the CR, the effects of 125 µg/ml PURO pulses begun at CT 17 of the second subjective night and lasting 12 (N=1), 9.5 (N=1) or 6 hrs (N=3) were compared. It was hoped that by decreasing the length of the PURO pulse, the magnitude of the phase shift, be it an advance or a delay, would also decrease.

Decreasing the length of the PURO pulse caused the subsequent rebound peak and CAP activity peaks to occur at earlier times (fig. 5). The eyes receiving the 12 hr, 9.5 hr and 6 hr PURO pulses (fig. 5A, B, C) showed rebounds that peaked at CT 5:30, 4:30 and 0:30 respectively. Figure 5C is representative of the 3 eyes that received a 6 hr PURO pulse at CT 17. Thus rebound peaks occurred within 2 hrs after the pulse was washed out.

Decreasing the length of the PURO pulse caused the CAP activity peaks to occur at earlier times. The phase shifts caused by the pulses were computed as in dose-response experiments (section IIIB). If PURO pulses caused phase delays, these delays averaged 14.0, 11.0, and 3.75 hrs, respectively, for decreasing PURO pulse durations (fig. 5). Alternatively, the phase advances were computed as 10.0, 13.0 and 20.25 hrs, respectively. Because the computed phase delays

decreased with PURO pulse duration, the effect of PURO pulses beginning at CT 17 was tentatively classified as a phase delay of the CR.

D. Phase-Response Relationships

The phase dependence of PURO pulse administration was tested on a population of 15 experimental and 15 control eyes. In each experiment, a pair of eyes dissected from the same animal between CT 5 and CT 8 was used. One eye received a 6 hr PURO pulse at a concentration of 125 μg/ml (0.23 mM) while its mate received an equimolar (64 μg/ml) pulse of PAN at the same time. PURO and PAN pulses were delivered at seven different phase points of the CR, spanning the 46 hr period from CT 10, a few hrs after dissection, to CT 7:30, near the end of the second activity cycle.

PAN was chosen as a control agent because it is a cleavage product of PURO, lacking the o-methyl tyrosine moiety, that does not inhibit protein synthesis (5). Eyes treated with PAN expressed normal CR's.

A relatively high dose of PURO was chosen to increase the chances of causing large phase shifts. The shortening of the PURO pulse length in these experiments, compared to dose-response experiments, and the possibility of phase-dependent sensitivity of eyes to drug pulses both increased the chances of getting small, uninterpretable phase shifts. The effects of PURO pulses administered at each phase point were classified according to effects that occurred during the PURO pulse, those that occurred during the rebound period

0-7 hrs after the end of the pulse, and those that occurred more than 7 hours after the PURO pulse. The phase dependence of changes in CAP activity taking place in each of these three periods is discussed in detail below.

1) During the PURO Pulse

The effects of PURO during the pulse were analyzed by comparing the CAP activity of PURO-treated eyes with that of their paired, PAN-treated controls. The average hourly CAP rate of each eye during a 6 hr PURO or PAN pulse was normalized to its peak hourly CAP rate during the first activity cycle, except for eyes given pulses at the two earliest phase points (CT 10, CT 17:30 of the day of dissection). Since pulses beginning at these times occurred before the first activity cycle peak, the CAP activity taking place between CT 9 and CT 10 on the day of dissection was used to normalize CAP activity during a PURO or PAN pulse.

The results of the above analysis revealed that PURO inhibited spontaneous CAP activity. Eight eyes that received a PURO pulse beginning at CT 17-17:30 or CT 1:30 before either the first or second activity cycle, had average hourly CAP activities during the pulse that were 13-70% of the corresponding activity in their controls. In contrast, 7 eyes given PURO pulses at the other phase points (CT 10-10:30, CT 5) showed average CAP activity during the pulse that was 81-127% of the corresponding control activity with two exceptions that were 36% and 197% of their respective controls.

Thus PURO pulses occurring during activity cycles depressed CAP activity (fig. 6B), while those occurring at the very end of an activity cycle (fig. 6A) or during the inactive part of the CR tended to have little effect on CAP activity.

2) Zero to Seven Hours After the PURO Pulse

An analysis of CAP activity from 0 to 7 hrs after the termination of a PURO or PAN pulse was performed, in a manner similar to that above, to investigate the relationship between the phase of PURO administration and the magnitude of the rebound occurring in this period. No clear relationship was discovered, except that in two cases no rebound occurred after a PURO pulse. One of the eyes in this category received a PURO pulse at CT 10 before the first activity cycle (not shown) and the other received the pulse at CT 10:30 before the second cycle (fig. 6B). All other eyes given PURO pulses evidenced a rebound (fig. 6A). No PAN-treated controls showed a rebound.

3) More Than Seven Hours After the PURO Pulse

At the end of the rebound period, seven hours after the termination of the pulse, the CAP activity of each PURO-treated eye began to follow a CR that was phase shifted. The magnitude and direction of the phase shift in each experiment were determined by comparing the CR of the PURO-treated eye with that of its PAN-treated control. The magnitude of the phase difference between corresponding activity cycles of experimental and control eyes was computed as the time interval between their half-hourly CAP frequency peaks. The

direction designated for the phase shift was that which gave the smaller magnitude phase shift. Thus, the example in fig. 6A represents a phase delay of 4 hrs, and the example in fig. 6B represents a phase advance of 4 hrs. The directions of phase shifts assigned by this criterion are arbitrary, and thus remain tentative until confirmed by supplementary experiments.

The relationship between the phase of PURO pulse administration and the magnitude and direction of the resultant phase shift is plotted with solid lines in fig. 7. The position of the horizontal bars relative to the abscissa represents the phase at which the 6 hr PURO pulse was administered, while their position relative to the ordinate represents the average resultant phase shift. The vertical bars span the range of observed phase shifts.

These data reveal that PURO pulses administered entirely during subjective day caused phase advances, while those given slightly before (CT 10-10:30) or entirely during subjective night caused phase delays. Projected dawn separates the phases at which maximal phase delays and maximal phase advances were obtained.

In addition, the phase shifts caused by PURO pulses administered at times about 24 hrs apart are similar in magnitude and direction. Thus the phase-response curve is itself an example of a CR; in this case a CR of the sensitivity of eyes to phase shifts induced by PURO pulses.

The phase response data plotted in solid lines in figure 7 are in good agreement with those plotted in dashed lines. The latter

before, during and after drug administration. A phasic light response (7, 9), elicited during the first half of the first light pulse, gradually adapted into a tonic response by the end of this pulse. The second light pulse caused a tonic light response with little or no phasic component. Data concerning the phasic light response were obtained from responses to the first light pulse; those concerning the tonic light response were obtained from the second pulse.

Data derived from recordings of light responses and spontaneous CAP activity from experimental and control eyes were compared quantitatively. The latency, maximum peak to peak CAP amplitude and CAP frequency were measured for both the phasic and tonic light responses. In addition, the maximum peak to peak amplitude and frequency of spontaneous CAP activity were measured every hour for the entire length of each experiment. Spontaneous CAP waveforms were usually recorded at higher paper speeds immediately before light tests were conducted. Waveforms of light responses and spontaneous CAP activity were compared qualitatively between experimental and control eyes. Figures 8 and 9 show examples of light response and spontaneous CAP activity waveforms recorded at various times before, during and after eyes were treated with PURO, CHX or PS-FSW pulses.

For each eye the value of each light response parameter measured during and after drug administration was expressed relative to the value of that parameter measured just before drug treatment. Because there was usually no spontaneous CAP activity occurring at

the beginning of the drug pulse (CT 17; figs. 8, 9, spontaneous CAP activity trace 2), the values of spontaneous CAP amplitude and frequency occurring at the peak of the first activity cycle were used to normalize their respective parameters measured during and after drug treatment.

The difference between each normalized parameter value for an experimental eye, and the corresponding value of its control was calculated. Normalized data were pooled in two different ways to maximize the detection of electrophysiological changes caused by drug treatment.

In the first method, differences between normalized experimental and control measurements for each pair of eyes were averaged according to parameter and evaluated by a paired t test. Table I presents a summary of the number of eyes found significantly different from their controls ($p < 0.05$) for each light response parameter. Data from light tests administered 1-2 times during and 3-8 times after the pulse have been averaged for each eye.

Data obtained from hourly measurements of spontaneous CAP amplitude and frequency were analyzed by the first method also. However because of the relatively large number of measurements made of spontaneous CAP activity parameters,differences between the corresponding normalized values of each experimental and control eye measurement were averaged according to the time at which the data were collected. Thus the electrophysiological data for each parameter were averaged according to those collected during the pulse,

those collected 0-7 hrs after the pulse, and those collected more than 7 hrs after the pulse. The number of eyes significantly different from their controls with respect to spontaneous CAP amplitude and frequency during each of these periods is presented in table II.

Analysis of electrophysiological parameters (tables I, II) by the first method revealed that in no case were all the experimental eyes of a category significantly different in the same direction from their controls. A category is represented by the data within each box in tables I, II. In ten of twenty-four categories, some eyes were significantly greater than their controls while others were significantly lower. In 8 categories, half or more of the eyes analyzed were significantly different from their controls in the same direction. However, on an individual eye basis, there were no correlations between changes in one parameter and changes in another.

In order to evaluate whether or not the distribution of changes between pairs of experimental and control eyes represented an overall significant change among all pairs of eyes in each category, a second method of analysis was used. In this approach the <u>mean</u> differences between each pair of eyes were averaged together in each category. The results of this analysis are presented in table III for light response parameters, and in table IV for spontaneous CAP activity parameters. Of all 36 light response categories (6 parameters x 2 drugs x 3 periods of time) significant differences between experimental and control eyes were found in only 2 categories.

First, there was a 23% increase in the tonic light response amplitude of PURO-treated eyes measured more than 7 hrs after the end of the drug pulse (table III). Second, there was a 32% increase in the tonic light response frequency in CHX-treated eyes during the period from 0 to 7 hrs after the pulse (table III; fig. 9, tonic light response trace 4). Of all 12 spontaneous CAP categories (2 parameters x 2 drugs x 3 periods of time), significant differences between experimental and control eyes were found in only one. There was a 67% increase in the spontaneous CAP frequency of PURO-treated eyes during the period from 0 to 7 hrs after the pulse (table IV; fig. 8, spontaneous CAP activity trace 5).

Qualitative examination of recordings from drug-treated eyes did not reveal any systematic changes in the waveforms of light responses compared to controls. However recordings of spontaneous CAP activity during CHX pulses showed that the duration of CAP activity bursts was reduced by about 33% (fig. 9, spontaneous CAP activity trace 3). Soon after the CHX pulse was removed, the burst duration began to increase (fig. 9, spontaneous CAP activity trace 4) and returned to normal by 3 hrs.

IV Discussion

A. Nature of the Phase Shift

The data presented in this study clearly show that PURO and CHX pulses (figs. 1, 5, 6) phase shifted the CR of spontaneous CAP activity in the Aplysia eye. The phase shift in the CR of each eye

caused by a drug pulse persisted for the duration of the experiment and showed no sign of reversal. This finding is upheld by the fact that the free-running period did not change in phase shifted eyes.

The results of this study have not allowed unambiguous interpretation of the direction of phase shifts caused by PURO and CHX. The direction of phase shifts could not be assigned on the basis of transients, because the CR reached its steady state phase without expressing transient phase shifts of intermediate values. Thus the direction of phase shifts was assigned on the basis of dose-response and duration-response studies.

In dose-response studies, where 12 hr PURO or CHX pulses were begun at CT 17, all phase shifts were interpreted as phase delays. For CHX-pulsed eyes, this interpretation is supported by the fact that increasing CHX concentrations caused increasing delays in the occurrence of activity cycle peaks subsequent to the pulse (figs. 1E-H, 4). For eyes whose phase was significantly shifted by PURO administration (20 µg/ml-134 µg/ml), the slope of the relationship between dose and the magnitude of the computed phase shift could not be evaluated (fig. 4). However, the results of experiments in which the length of PURO pulses beginning at CT 17 was varied demonstrated that activity peaks appeared at earlier times following shorter duration pulses (fig. 5). These data support the interpretation that PURO pulses caused phase delays in dose-response experiments.

In phase-response experiments, the direction of the phase shift was arbitrarily determined as that which yielded the smaller magnitude shift. For eyes receiving 6 hr PURO pulses (125 μg/ml = 0.23 mM) beginning at CT 17, the phase change was assigned as a delay, and was thus in agreement with the interpretation of PURO pulse lengthening experiments.

Regardless of the directions assigned to phase shifts in these experiments, their magnitudes were proportionately larger than those caused by PURO or CHX pulses in other systems. PURO pulses (8 hrs, 10^{-5} M) applied at 3 different phases to Gonyaulax cultures caused maximally about 2 hr phase delays in the CR of bioluminescence (3). CHX pulses (2 mg/ml) lasting from 1-3 days increased the length of the free-running period of the phototactic mobility CR in cultures of Euglena from about 24 to about 30 hrs, and thus caused the CR to be phase delayed by 2-18 hrs (4). In contrast, 12 hr PURO (20-134 μg/ml) or CHX (2000 μg/ml) pulses applied to the Aplysia eye caused phase delays of 12 to 16 hrs (fig. 4), while 6 hr PURO pulses caused phase delays and advances of maximally about 6 hrs. Thus the magnitudes of the maximum phase shifts caused by PURO or CHX pulses were close to the length of the pulses delivered.

B. The Electrophysiology of Drug-Treated Eyes

Significant changes were observed in the electrophysiology of eyes treated with 12 hr pulses of PURO (20 μg/ml) or CHX (500 μg/ml) when compared with the electrophysiology of control eyes. PURO caused an increase in spontaneous CAP frequency and an increase in tonic

light response amplitude. CHX caused an increase in the tonic light response frequency and a decrease in the duration of spontaneous CAP bursts. These effects are discussed in detail below.

1) PURO Effects

Eyes receiving 20 µg/ml PURO pulses revealed an increase in the frequency of spontaneous CAP activity during the period from 0-7 hrs after the end of the pulse. The increase in spontaneous CAP frequency is attributable to the expression of what appears to be part of a CAP activity cycle during this period (figs. 1B; 8 top, under arrow 5), and is most likely not due to a rebound, as seen following higher concentration PURO pulses (figs. 1D, 5A, 6B).

PURO-treated eyes also showed an increase in the maximum tonic light response amplitude at times more than 7 hrs after the end of the pulse. This effect may reflect an increased excitability of PURO-treated eyes during this period. Alternatively, it may reflect greater preservation of PURO-treated eyes compared to controls, since the tonic light response amplitude may merely be decreasing less rapidly in PURO-treated eyes.

Other studies of isolated nervous tissue have demonstrated that PURO lowers the amplitude of action potentials, possibly because of a direct effect on the neuronal membrane. After a 6 hr exposure to solutions containing 0.17 mM PURO, the height of extracellularly recorded CAPs in the isolated spinal cord of the fish Carassius was decreased by 25%. CAPs recorded from spinal cords exposed to 0.17 mM PAN for 6 hrs were normal in amplitude (5). Similar results

were found with the isolated rabbit vagus nerve treated for 1 hr in solutions containing 0.2-1.0 mM PURO. CAP amplitudes were reduced by about 10-40% depending on dose, and showed partial recovery within 30 min after the PURO was washed out of the bathing medium. In addition, the after-potential and post-tetanic hyperpolarization were reversibly diminished by PURO. In contrast, 1 mM PAN did not change the CAP amplitude, after-potential nor post-tetanic hyperpolarization in 1 hr (10). In isolated rat superior cervical ganglia, 1 hr PURO (0.09-0.54 mM) pulses depressed reversibly the amplitude of post-ganglionic potentials by about 40-70% in a dose-dependent manner. In contrast to other studies, however, PAN (0.19-0.96 mM) depressed CAP height by 24-35% in 1 hr, and was not reversible (11).

The results found in these experiments may be due to a direct effect of PURO on the membrane. In one of the above cases, PURO doses that depressed electrical activity also inhibited protein synthesis by almost 100%. However, acetoxycycloheximide (ACHX) pulses also almost completely blocked protein synthesis without depressing electrical activity (5). Furthermore, if CHX (10) or ACHX (5) pulses were given in combination with PURO, electrical activity was still depressed. These results imply that the inhibition of protein synthesis was not the cause of the depression in CAP amplitude. Furthermore, they suggest that the release of peptidyl-puromycin fragments was not involved in the depression of the CAP amplitude because doses of ACHX or CHX capable of inhibiting protein

synthesis should have also inhibited the incorporation of PURO into peptides (12). Studies of human and rabbit erythrocytes treated with 0.7 mM PURO for 2 hrs showed that their sensitivity to hyposmotic lysis and their permeability to ^{22}Na were both increased (13). Taken together, the results of the above experiments suggest that PURO depresses electrical activity in neurons by increasing the permeability of the membrane. This effect appears to be independent of effects on protein synthesis caused by PURO.

Some depressive effects of PURO on spontaneous CAP activity were found in the present study. In electrophysiological experiments, where 20 µg/ml (0.04 mM) PURO pulses were administered, 2 of 6 eyes showed a significant decrease in spontaneous CAP amplitude, and 3 of 6 eyes showed a significant decrease in spontaneous CAP frequency (table II; fig. 8, spontaneous CAP activity trace 3). In dose-response experiments, PURO doses of 125 µg/ml (0.23 mM) and 134 µg/ml (0.25 mM) almost completely inhibited spontaneous CAP activity (figs. 1D, 2, 5A) during the pulse, and in one of two cases lowered the spontaneous CAP amplitude (not shown).

2) CHX Effects

Eyes receiving 12 hr pulses of CHX (500 µg/ml) in electrophysiological experiments showed an increase in the tonic light response frequency during the period from 0-7 hrs after the end of the pulse (fig. 9, tonic light response trace 4), and a decrease in the duration of spontaneous CAP bursts during the pulse (fig. 9, spontaneous CAP activity trace 3). These findings suggest that

CHX caused an increase in the excitability of the Aplysia eye. This interpretation is further supported by the fact that one eye given a pulse of CHX at 2000 µg/ml showed increased spontaneous CAP activity during the pulse (figs. 1G, 2).

The effects of CHX or ACHX on the electrophysiological properties of other isolated preparations tend to be less severe than those of PURO. Incubation of the Carassius spinal cord for 6 hrs in a solution containing 1 µg/ml ACHX caused no change in CAP amplitude even though methionine incorporation was inhibited by 95% (5). Similarly, after exposure to solutions containing 1 mM CHX for 1 hr, the rabbit vagus nerve exhibited normal CAP amplitude and after-potentials. No indication was given, however, concerning the effect of CHX on post-tetanic hyperpolarization (10). Three hr pulses of CHX (0.18 mM) or ACHX (0.08 mM) irreversibly depressed the size of post-ganglionic CAPs by 26% in the rat superior cervical ganglion. These doses almost completely inhibited the incorporation of valine into ganglionic protein (11).

The variability in the results of PAN and CHX pulses delivered to several different systems demonstrates that the electrophysiological effects of inhibitors should be evaluated for the particular system being used.

C. Level of Drug Action

The results of this study clearly establish that the CR of spontaneous CAP activity was expressed following PURO or CHX pulses. The existence of a CR after drug administration avoids some of the

problems encountered when the effects of aflatoxin B1 and actinomycin D were interpreted in chapter IV. Since the CR was inhibited following some aflatoxin B1 pulses and all actinomycin D pulses, the possibility that the drugs were killing circadian pacemaker cells could not be eliminated. There is little chance, however, that PURO or CHX pulses phase shift the CR by killing cells involved in the free-running clock mechanism.

The electrophysiological changes caused by PURO (20 μg/ml) pulses do not seem to be the cause of the phase shift in the CR. The increase in the frequency of spontaneous CAP activity during the period from 0 to 7 hrs after the pulse appears to be the rising phase of an activity cycle that was already phase shifted. The increase in the tonic light response amplitude also occurred after the phase was shifted.

The changes in the electrophysiological properties of eyes caused by 500 μg/ml CHX pulses are less easily explained. The decrease in CAP burst duration coincident with the CHX pulse, and the increase in the tonic light response frequency during the period from 0 to 7 hrs after the pulse may both reflect transient electrophysiological changes capable of causing a phase shift in the CR.

The similarities in the effects of PURO pulses and high potassium pulses (6) on spontaneous CAP activity suggest that PURO

and high potassium pulses affect identical or closely related processes in the Aplysia eye. The two treatments had four effects in common. First, spontaneous CAP activity was inhibited by high potassium pulses and by higher concentration (50-134 μg/ml) PURO pulses. The two treatments differed, however, in the manner in which they brought about the inhibition. During the first few minutes of a high potassium pulse the frequency of spontaneous CAP activity increased as the amplitude decreased down to noise level. In contrast, PURO pulses decreased the frequency and amplitude of spontaneous CAP activity.

Second, rebounds occurred following the removal of high potassium or PURO pulses. Again, however, the details of the effects of the two treatments are different. High potassium rebounds showed relatively more CAP activity in relatively less time (about 2 hrs) than PURO rebounds.

Third, the relationship between the duration of the pulse and the magnitude of the phase shift was similar for high potassium-treated and PURO-treated eyes. For eyes administered high potassium pulses beginning at CT 13:30 and lasting about 0.5 to 9 hrs (Eskin, 1972(6); fig. 7) the duration of the pulse almost equalled the magnitude of the phase delay. For eyes given PURO pulses beginning at CT 17 and lasting 6-12 hrs, the pulse duration and phase shift magnitude were similar, but not as similar as in the high potassium experiments.

Fourth, the phase-response curves obtained from high potassium or PURO experiments were strikingly similar.

At present the mechanisms by which high potassium and PURO pulses phase shift the circadian clock remains unresolved. However, both treatments seem to have two properties in common.

First, they seem to depolarize neurons. High potassium treatment does this by lowering the potassium gradient across the cellular membrane. PURO probably causes depolarization of neurons by increasing the permeability of their membranes.

Second, both treatments inhibit protein synthesis. PURO interrupts protein synthesis by prematurely terminating growing polypeptide chains (14). The effects of PURO on the incorporation of leucine in the isolated Aplysia eye are presented in chapter VII. The manner in which high potassium pulses affect protein synthesis is not clearly understood. However, Ram, in this laboratory, showed that leucine incorporation into the isolated parietovisceral ganglion of Aplysia was reduced by 50% during 4 hr pulses of high potassium (90 mM) medium (15).

Of the two effects listed above, I feel that the inhibition of protein synthesis mediates the phase shifts in the Aplysia eye CR caused by high potassium or PURO pulses because: 1) 20 µg/ml PURO pulses phase delayed the CR without significantly depressing spontaneous CAP activity during the pulse and without causing rebounds; and 2) both PURO and CHX pulses phase shifted the CR, and both PURO and CHX lowered leucine incorporation in the Aplysia eye by about 50% (see chapter VII).

TABLE I

The Effects of Puromycin and Cycloheximide on the Electrophysiology of the Aplysia Eye

Activity	Phasic Light Response						Tonic Light Response					
Parameter	Latency		Maximum Amplitude		Frequency		Latency		Maximum Amplitude		Frequency	
$\bar{D}$	+	−	+	−	+	−	+	−	+	−	+	−
PURO												
# SIG.DIF.	2	0	4	0	2	1	2	2	3	0	1	2
TOTAL #	6		6		5		6		6		6	
CHX												
# SIG.DIF.	0	1	0	1	1	0	0	0	0	1	1	0
TOTAL #	3		3		3		3		3		3	

3-9 Light Tests were applied to each pair of eyes during and after the drug pulse.

refers to number of pairs of eyes.

Sig. Dif. indicates significantly different at $p<0.05$ (paired t test).

$$D = \frac{E_A}{E_B} - \frac{C_A}{C_B}$$

E: refers to experimental eye

C: refers to control eye

A: refers to a measurement made after the drug of control pulse

B: refers to a measurement made before drug or control pulse for each eye and parameter. This measurement is used to normalize all measurements made after the pulse by the formulae:

$$\frac{E_A}{E_B} \text{ and } \frac{C_A}{C_B}$$

TABLE II

The Effects of Puromycin and Cycloheximide on the Electrophysiology of the Aplysia Eye Spontaneous CAP Activity

Drug	Puromycin				Cycloheximide			
Parameter	Maximum Amplitude		Frequency		Maximum Amplitude		Frequency	
$\bar{D}$	+	-	+	-	+	-	+	-
During Pulse								
# SIG. DIFF.	1	2	1	3	1	1	1	1
TOTAL #	6		6		4		3	
0-7 Hrs After Pulse								
# SIG. DIFF.	5	0	3	0	0	1	2	0
TOTAL #	6		6		3		3	
> 7 Hrs After Pulse								
# SIG. DIFF.	3	1	1	1	1	2	0	1
TOTAL #	5		5		3		3	

Spontaneous CAP amplitudes and frequencies were measured every hour throughout each experiment.

See table I for explanation of terms.

TABLE III

The Effects of Puromycin and Cycloheximide on the Electrophysiology of the Aplysia Eye Light Response Parameters (Pooled Means)

Activity	Phasic Light Response			Tonic Light Response		
Parameter	Latency	Maximum Amplitude	Frequency	Latency	Maximum Amplitude	Frequency
PUROMYCIN						
*7 Hrs After Pulse						
# pairs of eyes	4	4	4	4	4	4
$\overline{E}$					1.28	
$\overline{C}$					1.04	
$\overline{D} \pm SD$	NSD	NSD	NSD	NSD	0.24±.09	NSD
P					0.02	
CYCLOHEXIMIDE						
**0-7 Hrs After Pulse						
# pairs of eyes	3	3	3	3	4	4
$\overline{E}$						1.27
$\overline{C}$						0.96
$\overline{D}$	NSD	NSD	NSD	NSD	NSD	0.31±.14
P						0.05

*3-6 light tests were applied to each eye 7 hrs after the PURO pulse.

**1-2 light tests were applied to each pair of eyes 0-7 hrs after the CHX pulse.

$$D = \frac{E_A}{E} - \frac{C_A}{C_B} \; ; \; E = \frac{E_A}{E_B} \; ; \; C = \frac{C_A}{C_B}$$

P: probability that experimental and control eyes were not different based on paired t test.

NSD = no significant difference ($p > 0.05$, paired t test).

All numbers have been rounded to the nearest .01.

TABLE IV

The Effects of Puromycin and Cycloheximide on the Electrophysiology of the Aplysia Eye Spontaneous CAP Activity (Pooled Means)

Drug	Puromycin		Cycloheximide	
Parameter	Maximum Amplitude	Frequency	Maximum Amplitude	Frequency
During Pulse				
# Pairs of Eyes	6	6	4	4
$\overline{E}$				
$\overline{C}$				
D	NSD	NSD	NSD	NSD
P				
0-7 Hrs After Pulse				
# Pairs of Eyes	6	6	3	3
$\overline{E}$		0.25		
$\overline{C}$		0.15		
D	NSD	0.10±.07	NSD	NSD
P				
>7 Hrs After Pulse				
# Pairs of Eyes	5	5	3	3
$\overline{E}$				
$\overline{C}$				
D	NSD	NSD	NSD	NSD
P				

All numbers have been rounded to the nearest 0.01.

See table III for explanation of terms.

Figure 1

Spontaneous CAP activity of eyes receiving various doses of PURO or CHX. Drugs were administered as a 12 hr pulse (■) beginning at CT 17 of the second projected night. Records A, B; C, D; F, G; were obtained from a pair of eyes taken from the same animal. No paired controls were run in these experiments. Vertical dashed lines are drawn at projected dawn of the donor animal's LD 12:12 entrainment schedule, which is represented by the bars (dark period) and spaces (light period) along the abscissa.

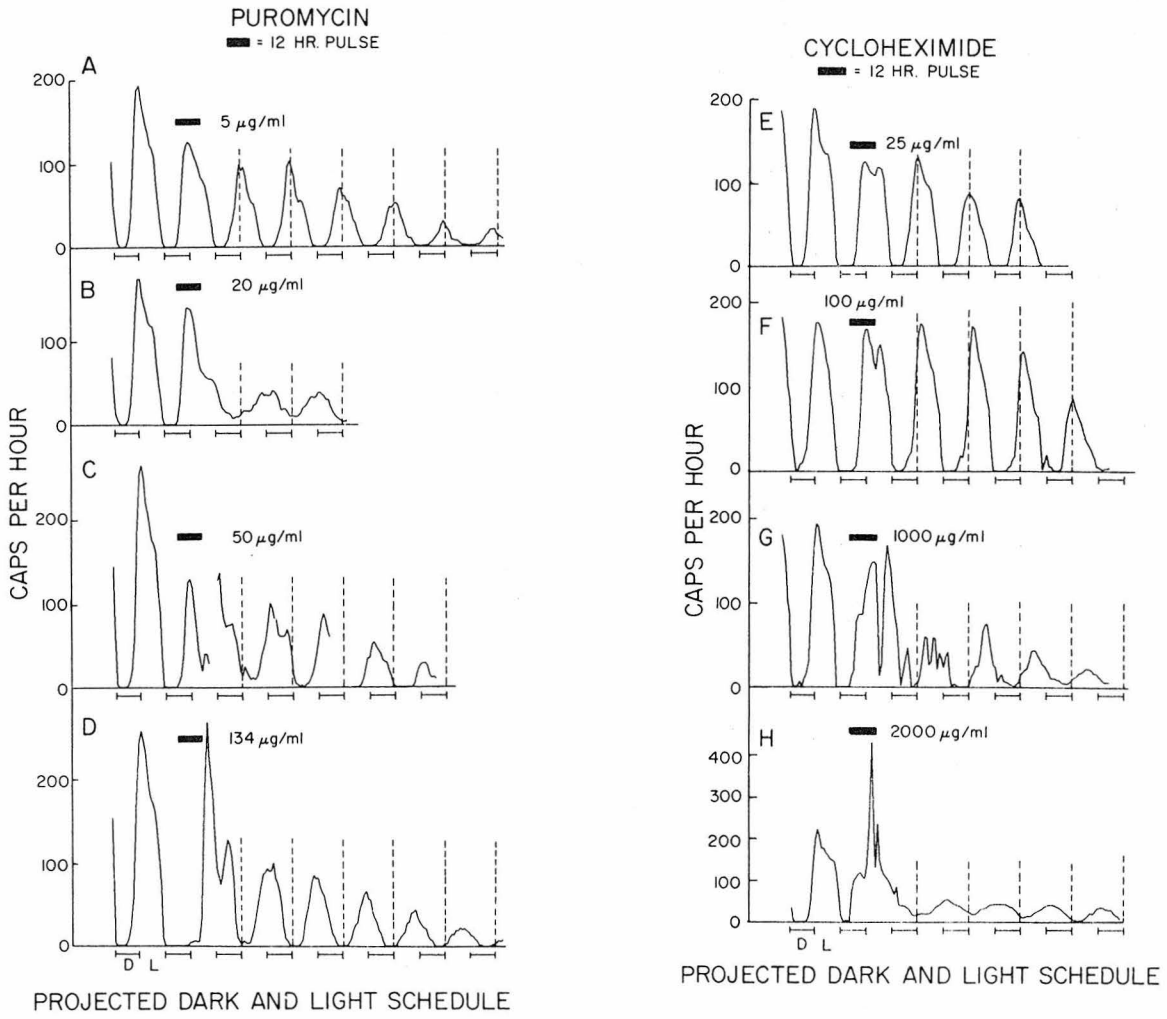
PUROMYCIN
= 12 HR. PULSE
A
5 μg/ml
B
20 μg/ml
C
50 μg/ml
D
134 μg/ml
CAPS PER HOUR
200
100
0
D L
PROJECTED DARK AND LIGHT SCHEDULE
CYCLOHEXIMIDE
= 12 HR. PULSE
E
25 μg/ml
F
100 μg/ml
G
1000 μg/ml
H
2000 μg/ml
400
300
CAPS PER HOUR
PROJECTED DARK AND LIGHT SCHEDULE

Figure 2

Plot of normalized hourly CAP frequency during a drug pulse vs. drug concentration. Hourly CAP frequency during a 12 hr PURO or CHX pulse was averaged and then divided by the peak hourly CAP frequency from the first activity cycle. Drug doses are plotted on a logarithmic scale. Each point (●) represents data obtained from one eye. The results from 11 PURO and 8 CHX experiments are displayed.

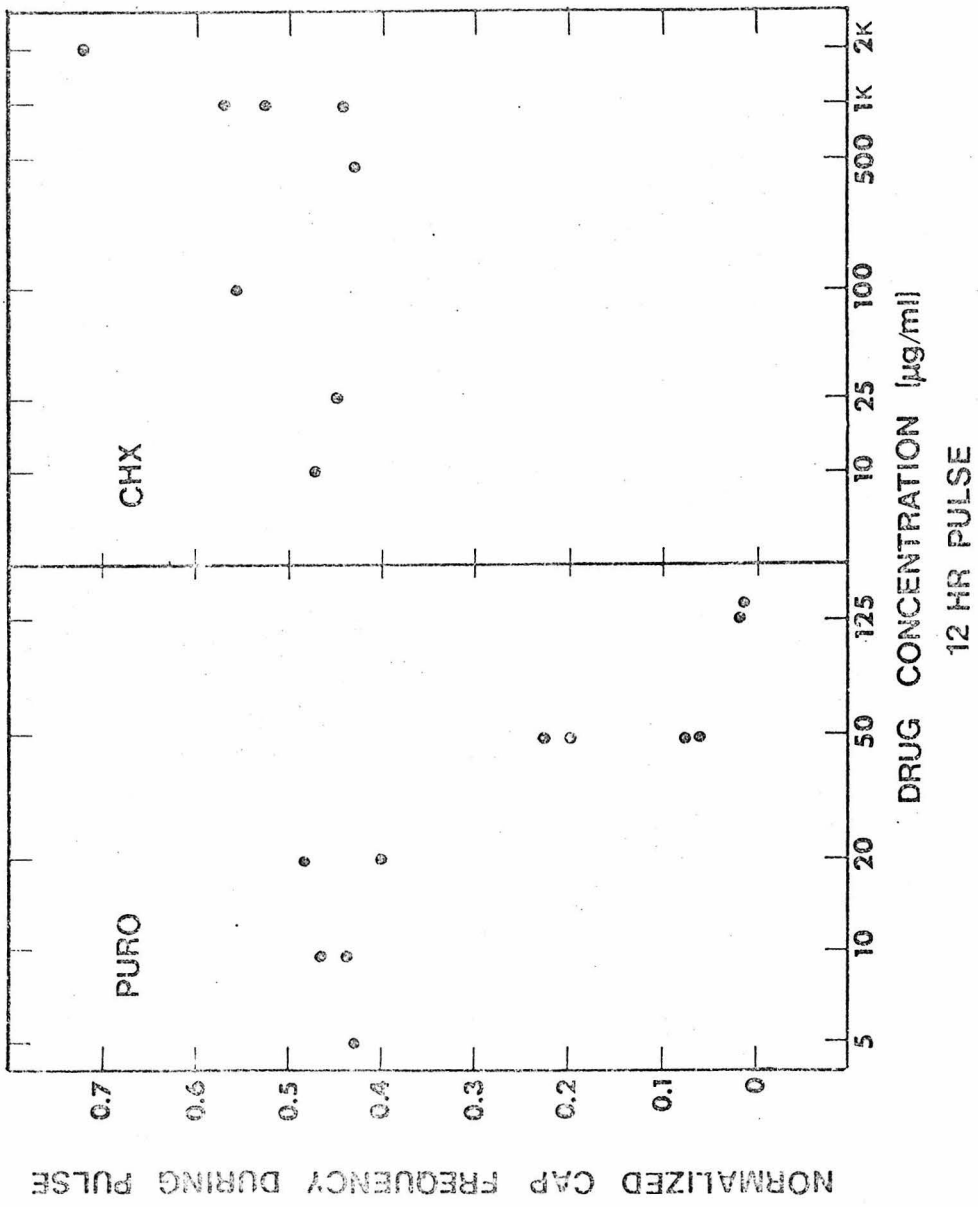
NORMALIZED CAP FREQUENCY DURING PULSE
0.7
0.6
0.5
0.4
0.3
0.2
0.1
0
PURO
CHX
5
10
20
50
125
10
25
100
500
1K
2K
DRUG CONCENTRATION (µg/ml)
12 HR PULSE

Figure 3

Plot of normalized CAP frequency during the period from 0 to 7 hrs after a drug pulse vs. drug concentration. Hourly CAP activity during this period was averaged and normalized as in figure 2. Drug doses are plotted on a logarithmic scale. Each point (●) represents data obtained from one eye. These data are derived from the population of eyes whose data are plotted in figure 2.

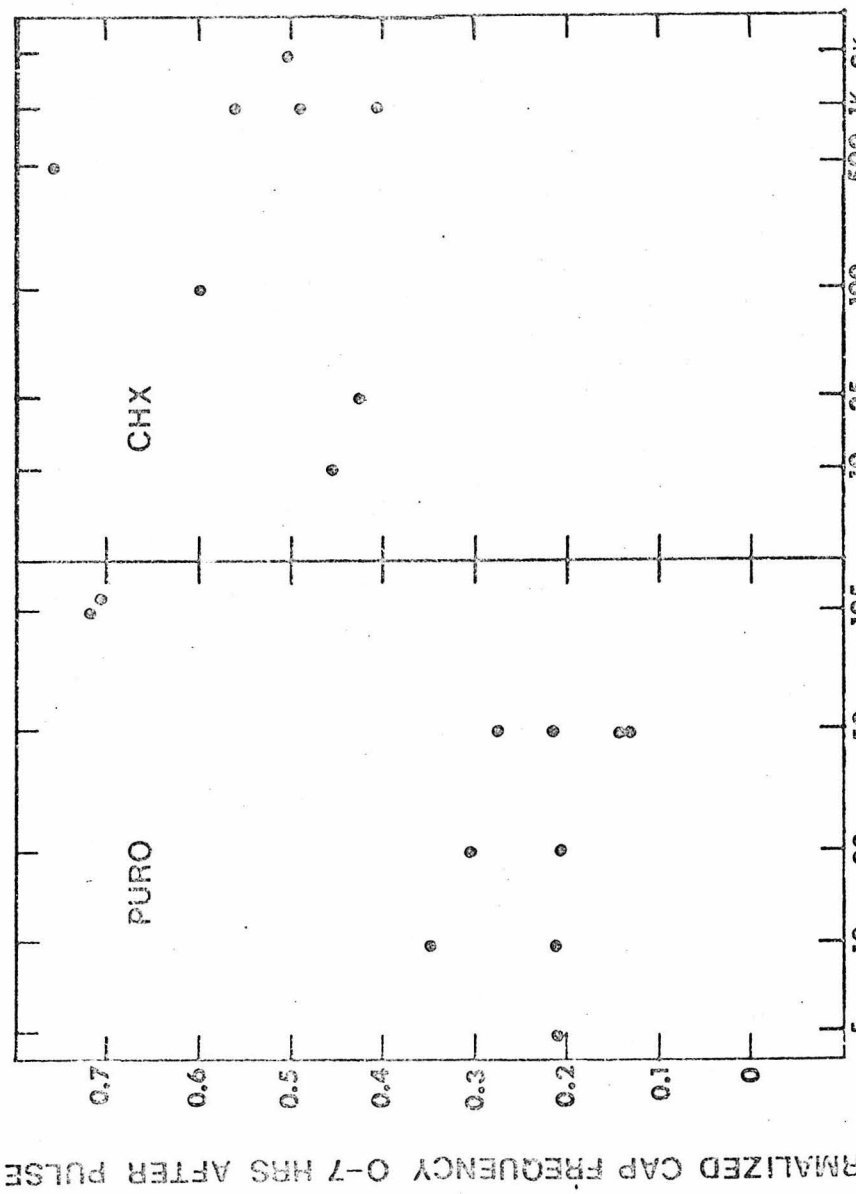
CHX
PURO
0.7
0.6
0.5
0.4
0.3
0.2
0.1
0
5
10
20
50
125
10
25
100
500
1K
2K
DRUG CONCENTRATION (µg/ml)
12 HR PULSE
NORMALIZED CAP FREQUENCY 0-7 HRS AFTER PULSE

Figure 4

Phase delay in the CR subsequent to the drug pulse vs. drug concentration. The phase delay of each activity cycle occurring on or after the third projected dawn was estimated relative to a CR projected from the peak of each eye's first activity cycle assuming a 24 hr free-running period. See text for exact procedure. Drug doses are plotted on a logarithmic scale. Each point (●) represents the data obtained from one eye. These data are derived from the population of eyes whose data are plotted in figures 2 and 3.

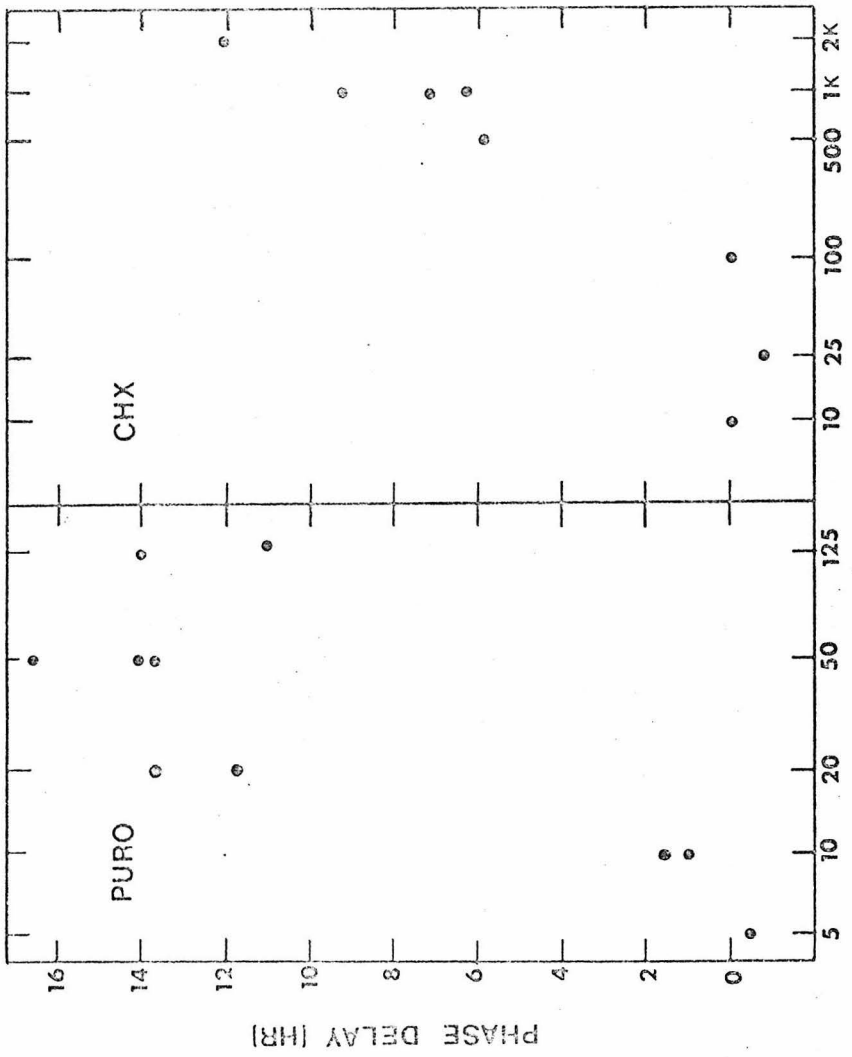
PHASE DELAY (HR)
0
2
4
6
8
10
12
14
16
PURO
CHX
5
10
20
50
125
10
25
100
500
1K
2K
DRUG CONCENTRATION (µg/ml)
12 HR PULSE

Figure 5

Spontaneous CAP activity of eyes receiving 125 µg/ml doses of PURO as pulses lasting 12, 9.5 or 6 hrs. All pulses began at CT 17 of the second projected night. Vertical dashed lines are drawn at projected dawn of the donor animal's LD 12:12 entrainment schedule. Box (■) represents the PURO pulse.

PUROMYCIN PULSES 125 µg/ml

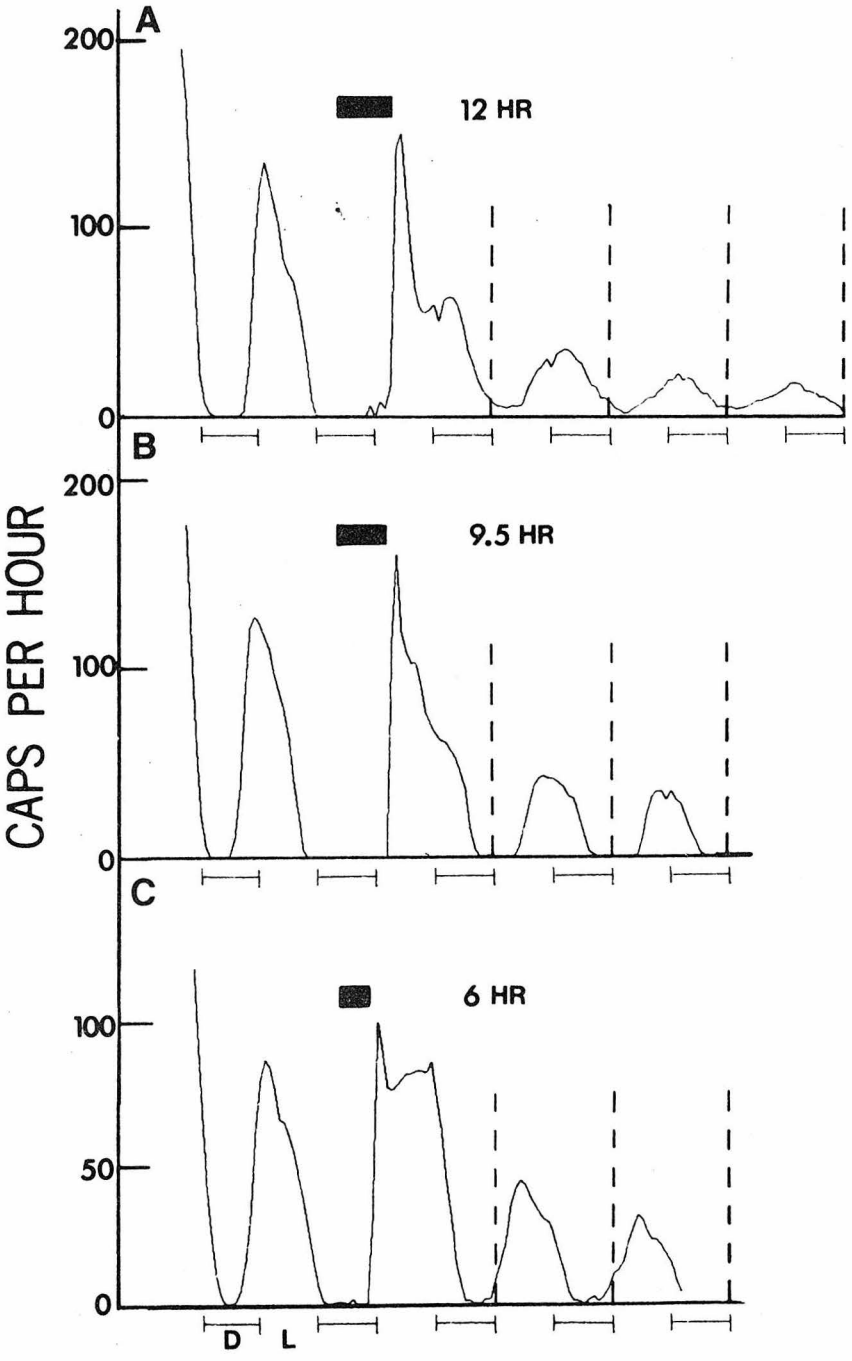

PROJECTED DARK & LIGHT SCHEDULE

Figure 6

Spontaneous CAP activity of eyes receiving a 6 hr pulse of PURO (125 µg/ml) or PAN(64 µg/ml). A: an example of a 4 hr phase delay caused by a PURO pulse begun at CT 10:30 on the first subjective day after dissection. B: an example of a 4 hr phase advance caused by a PURO pulse begun at CT 1:30 on the second subjective day following dissection. Box (■) represents the PURO or PAN pulse.

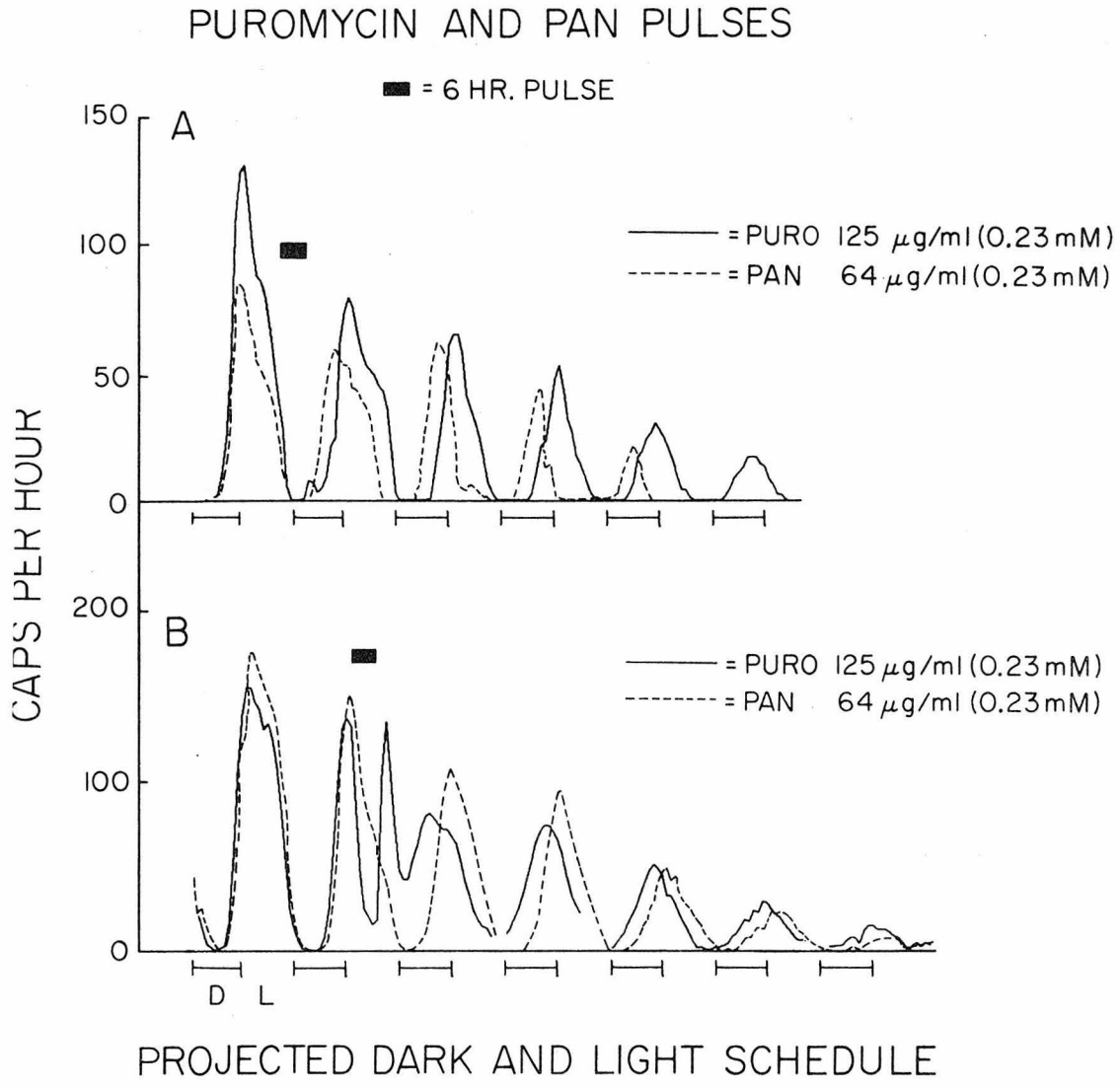
PUROMYCIN AND PAN PULSES
= 6 HR. PULSE
A
B
= PURO 125 μg/ml (0.23 mM)
= PAN 64 μg/ml (0.23 mM)
= PURO 125 μg/ml (0.23 mM)
= PAN 64 μg/ml (0.23 mM)
CAPS PER HOUR
150
100
50
0
200
100
0
D L
PROJECTED DARK AND LIGHT SCHEDULE

Figure 7

Solid lines: Phase shifts caused by 6 hr pulses of PURO (125 μg/ml) vs. the phase at which the pulses were applied. Position of horizontal bars relative to the projected dark and light schedule (abscissa) shows phase at which 6 hr PURO pulse was applied. Position of horizontal bar relative to the ordinate represents the average phase shift caused by PURO pulses. Phase differences between corresponding half-hourly cycle peaks were pooled and averaged for eyes given a PURO pulse at the same time. At each data point, the first number of each pair indicates the number of eyes from which data were obtained. The second number represents the number of phase differences averaged together. The vertical bar spans the range of phase differences. Dashed lines: Partial representation of data collected by Eskin (6), who administered 4 hr pulses of high potassium (107 mM) sea water to isolated Aplysia eyes at different phases of their free-running CR. Eskin's data are plotted in the same manner as those of PURO-treated eyes except that phase shifts are first averaged for each eye, and then mean phase shifts are averaged together for a population of similarly treated eyes. A complete plot of Eskin's data is presented in chapter II, figure 15.

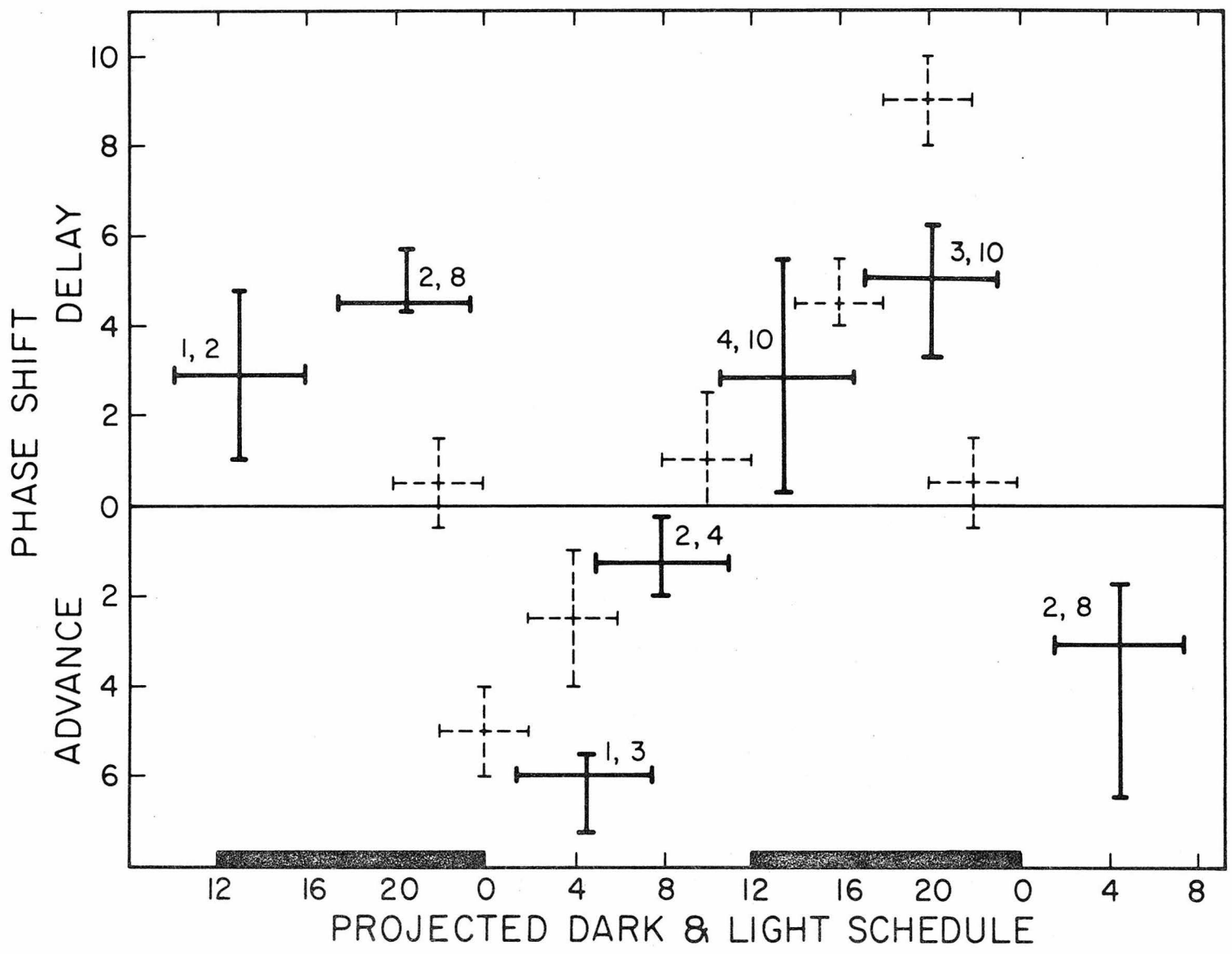
PHASE SHIFT
DELAY
ADVANCE
10
8
6
4
2
0
2
4
6
1, 2
2, 8
4, 10
3, 10
2, 4
1, 3
2, 8
12
16
20
0
4
8
12
16
20
0
4
8
PROJECTED DARK & LIGHT SCHEDULE

Figure 8

Top: Plot of spontaneous CAP activity of an eye that received a 12 hr pulse of PURO (20 µg/ml) beginning at CT 17 of the second subjective night (——) and a control eye that received a 12 hr pulse of PS-FSW at the same time (----). Both eyes were taken from the same animal. Recordings were made from eyes maintained in separate beakers housed in the same cooling dish and light-tight box. Both eyes received light tests at various times(indicated by arrows) during the experiment. Numbered arrows refer to recordings shown below. Box (■) shows when PURO and PS-FSW pulses were administered.

Below: Examples of spontaneous CAP activity, phasic light responses and tonic light responses recorded before, 1, 2; during, 3; and after, 4-8; the administration of a PURO (P) or control (C) pulse. Recordings from each eye were made by means of a single suction electrode attached to the optic nerve. Signals were amplified by a Tektronix 122 preamplifier, fed into an EEG type amplifier of a Grass 7B polygraph and then recorded. Half-amplitude band-pass filters were set at 0.3 Hz (low) and 250 Hz (high). Down is negative voltage.

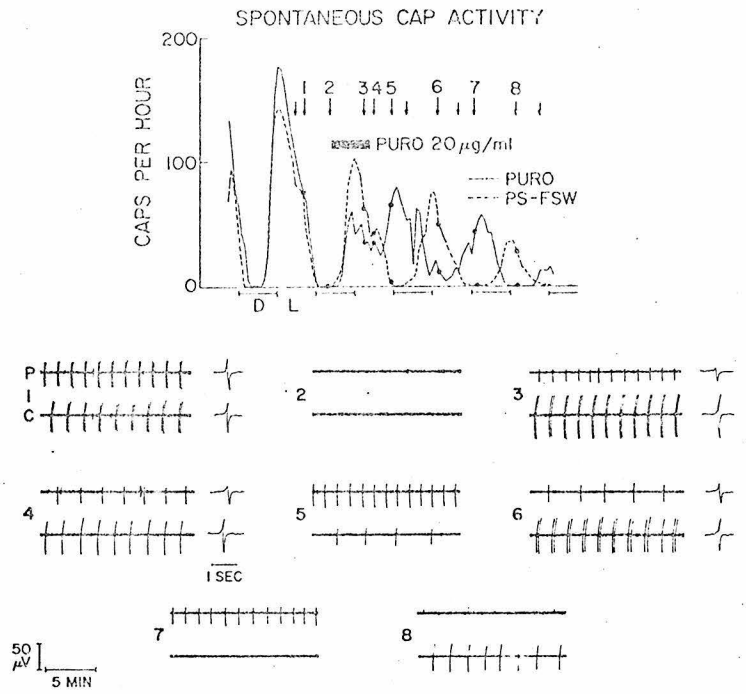
SPONTANEOUS CAP ACTIVITY
200
100
0
CAPS PER HOUR
1 2 345 6 7 8
PURO 20 μg/ml
PURO
PS-FSW
D L
P
I
C
2
3
4
5
6
1 SEC
7
8
50 μV
5 MIN

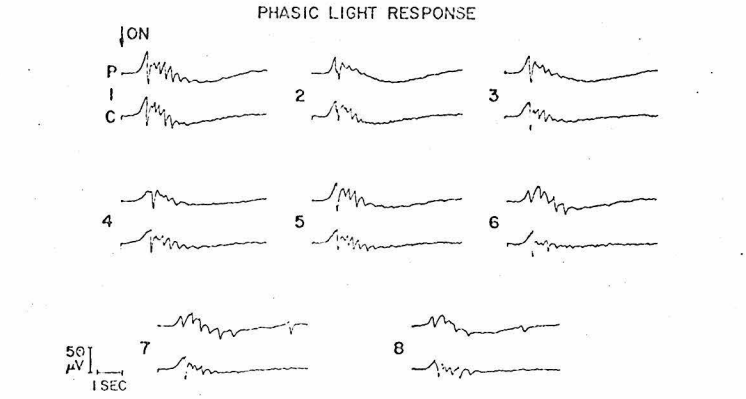
PHASIC LIGHT RESPONSE
ON
P
I
C
2
3
4
5
6
50 μV
1 SEC
7
8

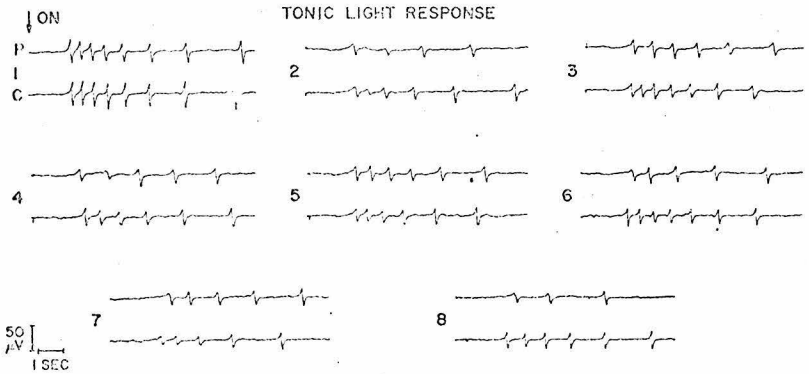
TONIC LIGHT RESPONSE
ON
P
I
C
2
3
4
5
6
50 μV
1 SEC
7
8

Figure 9

Top: Plot of spontaneous CAP activity of an eye that received a 12 hr pulse of CHX (500 µg/ml) beginning at CT 17 of the second subjective night (——) and a control eye that received a 12 hr pulse of PF-FSW at the same time (----). Box (■) represents CHX and PS-FSW pulses. Other details are the same as in figure 8.

Below: Examples of recordings as described in figure 8, except that CHX refers to recordings made from CHX-treated eyes, and CON refers to recordings from control eyes. Numbers 4-7 refer to recordings made after the CHX or PS-FSW pulse was rinsed out.

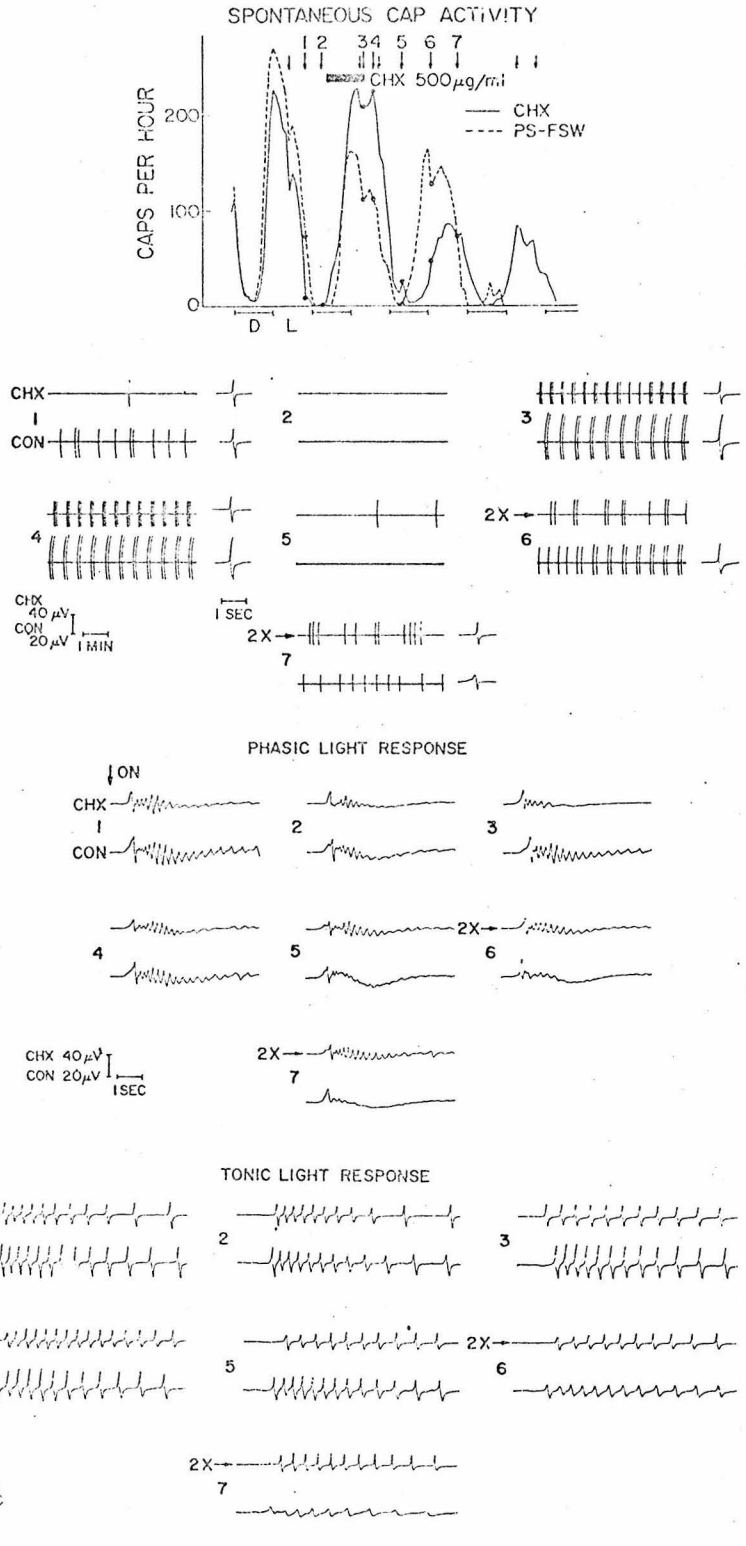
SPONTANEOUS CAP ACTIVITY
1 2 3 4 5 6 7
CHX 500µg/ml
CHX
PS-FSW
CAPS PER HOUR
200
100
0
D L
CHX
CON
1
2
3
4
5
2X
6
7
CHX 40 µV
CON 20 µV
1 MIN
1 SEC
PHASIC LIGHT RESPONSE
ON
CHX 40 µV
CON 20 µV
1 SEC
TONIC LIGHT RESPONSE
ON
CHX 40 µV
CON 20 µV
1 SEC

REFERENCES

1. Mueller, G. C., K. Kajiwara, E. Stubblefield and R. R. Reuckert. 1962. Cancer Research 22: 1084-1090.

2. Yeh, S. D. J., and M. E. Shils. 1969. Biochem. Pharmacol. 18: 1919-1926.

3. Karakashina, M. W., and J. W. Hastings. 1963. J. Gen. Physiol. 47: 1-12.

4. Feldman, J. F. 1967. Proc. Natl. Acad. Sci. 57: 1080-1087.

5. Bondeson, C., A. Edstrom and A. Beviz. 1967. J. Neurochem 14: 1032-1034.

6. Eskin, A. 1972. J. Comp. Physiol. 80: 353-376.

7. Jacklet, J. 1969. J. Gen. Physiol. 53: 21-42.

8. Audesirk, G. 1973. Brain Resh. 59: 229-242.

9. Jacklet, J. 1969. Science 164: 562-563.

10. Dahl, N. A. 1969. J. Neurobiol. 2: 169-180.

11. Paggi, P. and G. Toschi. 1971. J. Neurobiol. 2: 119-128.

12. Baliga, B. S., S. A. Cohen and H. N. Munro. 1970. FEBS Letters 8: 249-252.

13. Burka, E. R., S. K. Ballas and S. M. Sabesin. 1975. Blood 45: 21-27.

14. Gale, E. F., E. Cundliffe, P. E. Reynolds, M. H. Richmond, and M. J. Waring. The Molecular Basis of Antibiotic Action, Wiley and Sons, New York, 1972. pp 278-379.

15. Ram, J. R. 1974. Brain Resh. 76: 281-296.

Chapter VII

Biochemical Effects of Puromycin and Cycloheximide on the Eye

I Introduction

In chapter VI it was demonstrated that 12 hr pulses of PURO (20-134 µg/ml), or CHX (500-2000 µg/ml) applied to the isolated Aplysia eye caused phase delays in its CR of spontaneous CAP activity. In addition, analysis of the phase-response curve determined for the effects of 6 hr PURO (125 µg/ml) pulses, and the similarity of this curve with the phase-response curve determined by Eskin (1) for 4 hr high potassium pulses applied to the Aplysia eye, suggested that PURO was affecting the circadian clock of the eye at a point close to, or identical with, that affected by high potassium. Two effects that were probably common to both PURO and high potassium treatment were: 1) the depolarization of neurons, and 2) the inhibition of protein synthesis. Either effect could thus be the cause of the phase shifts in the eye CR brought about by PURO or high potassium pulses.

The purpose of this chapter is to explore the effects of PURO and CHX pulses on protein synthesis in the Aplysia eye. PURO and CHX inhibit protein synthesis by creating lesions at or near the ribosomal level. The two drugs, however, have dissimilar structures (fig. 1), and interfere with translation by completely different mechanisms. PURO inhibits protein synthesis by prematurely terminating nascent polypeptide chains, whereas CHX appears to inhibit protein synthesis by reducing the activity of transfer factor II, an enzyme that catalyzes ribosomal translocation along mRNA (2). A more

detailed discussion of the mechanisms by which PURO and CHX inhibit protein synthesis is presented in chapter III.

In this chapter the effects of 12 hr PURO and 12 hr CHX pulses on leucine incorporation in the Aplysia eye are analyzed by a double label SDS-polyacrylamide gel system. The advantages of this system are that over 93% of the incorporated label can be solubilized, and run on the gel, and that the incorporated material is separated according to molecular weight. Two questions are asked concerning the effects of the two drugs. First, do the lowest doses of PURO (20 µg/ml) and CHX (500 µg/ml) capable of phase shifting the CR decrease the level, or change the gel pattern of incorporated label? Second, do PURO pulses (125 µg/ml) have a reversible effect on the level or gel pattern of incorporated label? The results of this study indicate that during 20 µg/ml PURO or 500 µg/ml CHX pulses, leucine incorporation is lowered by about 50%. Furthermore, during a 125 µg/ml PURO pulse, leucine incorporation is inhibited by about 85%, and the gel label pattern severely altered. The changes caused by 125 µg/ml PURO pulses appear to be almost completely reversible.

II Materials and Methods

A. Labeling of Eyes

Eyes were labeled in a manner similar to that used in single label experiments described in chapter V (Methods). The labeling medium was essentially PS-FSW, buffered at pH 7.8 with 5 mM tris, containing either ^{3}H- or ^{14}C-leucine. Four eyes taken from 2 animals

were labeled in each experiment. Two experimental eyes, each from a different animal, were labeled together in 0.5 ml of a medium containing 3.2 nM/ml L-(4,5-^{3}H)leucine (2.9 Ci/mM), which was obtained by diluting L-(4,5-^{3}H)leucine (46 Ci/mM, Schwartz-Mann) with cold L-leucine. Two control eyes were labeled together in 0.5 ml of a medium containing 3.2 nM/ml of L-(U-^{14}C)leucine (312 mCi/mM, Schwartz-Mann). Eyes were labeled for a period lasting 5 or 8 hrs, depending on the type of experiment.

B. Preparation of Gel Samples

After labeling, eyes were rinsed for about 5 min in 3 changes of 1.0 ml PS-FSW. A ^{3}H-labeled experimental eye and its ^{14}C-labeled control were freed of optic nerve and any remaining connective tissue, and ground together in a glass homogenizer at 14°C. Each pair of eyes was ground together in 20 µl of a grinding solution, which consisted of 0.04 M sodium phosphate buffer, pH 7.2, containing 10% glycerol, 0.2% sodium dodecyl sulphate (SDS), 0.0015% bromphenol blue, and 0.2% 2-mercaptoethanol. The grinder was rinsed with 2 x 20 µl aliquots of grinding buffer and the rinses pooled with the homogenate. The homogenate was stored frozen for as long as a week. Before being applied to gels, samples were heated at 65°C for 30 min, and then centrifuged at 8,000 g (4°C) for 15 min. The supernatant was separated from the pellet, and the pellet frozen until it was washed and counted for radioactivity at a later time.

In all experiments, the ^{3}H- or ^{14}C-radioactivity remaining in the pellet was at most 7% of the total incorporated radioactivity in

the supernatant, which was computed as 3 times the respective ^{3}H- or ^{14}C-radioactivity fixed in the appropriate gel. This calculation was based on the fact that 1/3 of the supernatant (20 µl/60 µl) was applied to a gel (see below).

C. Gel Techniques

The general procedure for gel electrophoresis was that of Shapiro et al., 1967 (3). The gel solution consisted of 0.1 M sodium phosphate buffer, pH 7.2, containing 5% acrylamide, 0.135% methylene bisacrylamide 0.2% SDS, 0.075% ammonium persulphate and 0.00075% tetramethylethylenediamine (TEMED). The gel solution was pipetted into glass tubes of 3 mm inner diameter to a height of 6 cm. After the gel solution hardened, a 20 µl aliquot of sample supernatant was placed in the tube to cover the top of the gel. The tube was then filled to the top with reservoir buffer (0.1 M sodium phosphate buffer, pH 7.2, containing 0.2% SDS). Gels were electrophoresed at room temperature at 20 V for 4-5 hrs. The position of the tracking dye (bromphenol blue) and length of each gel were recorded. Gels were removed from their glass tubes and fixed for 2 days in 3 changes of 12.5% TCA. Each gel was cut into about 50 slices of about 1.25 mm in width by means of an "egg slicer" consisting of a frame of parallel stainless steel wires that fit into a slotted teflon trough. Each slice was extracted overnight in a scintillation vial containing 5 mls of a toluene PPO-POPOP scintillation fluid supplemented with 10% NCS tissue solublizer (Amersham-Searle) and 2% 4M NH_4OH, as described by Ward, Wilson and Gilliam (4). Sample pellets were counted

in 5 mls of the same fluid.

Radioactivity was assayed on a Beckman LS 200B liquid scintillation counter at 32% ^{3}H and 57% ^{14}C counting efficiencies. ^{3}H spillover into the ^{14}C channel was 4%, and ^{14}C spillover into the ^{3}H channel was 19.6%. All samples were counted for 10 min.

III Results

A. Control Eyes

The gel patterns of label incorporated into eyes taken from the same animal were compared to see if one eye was a valid control for the other. Two pairs of eyes were labeled from CT 6:30 to CT 14:30, two days after dissection. One eye of each pair was labeled with ^{3}H-leucine, while the other was labeled with ^{14}C-leucine. Each pair of eyes was then ground together, and electrophoresed on a SDS-polyacrylamide gel system. The ^{3}H- and ^{14}C gel patterns derived from one of two such experiments are presented in figure 2.

The pyramid shaped gel pattern, peaking at about 40,000 (40 K) daltons, and showing little incorporation below 12 K daltons is typical of the Aplysia eye. The molecular weights of proteins in the gel have been determined relative to the migration of known molecular weight protein standards. The mobility of a protein on the gel, relative to the tracking dye (bromphenol blue), varied linearly with the logarithm of its molecular weight in the range from 12 K to 68 K daltons (see appendix I).

The gel patterns of the ^{3}H-labeled and the ^{14}C-labeled eyes

were almost identical. This finding is reflected in figure 2B, where the ratio of ^{3}H to ^{14}C counts in each gel slice are presented. The ratios were computed for raw ^{3}H- and raw ^{14}C-counts corrected for background (11.8, 11.4 cpm respectively). Ratios were not calculated for slices that had fewer than 25 raw ^{3}H- or ^{14}C- cpm. Figure 2B shows the flat ratio pattern expected for two eyes having similar gel incorporation patterns. The small increase in the ratio computed for the first few gel slices was not seen in the ratio pattern computed for the other identically treated pair of eyes.

The ratios of total ^{3}H-cpm (corrected for ^{14}C spillover) to ^{14}C cpm found in the 2 control gels are presented in table I. The two ratios are below the ratio of 5.22 predicted on the basis of ^{3}H and ^{14}C counting efficiencies and specific activities assuming equimolar incorporation of ^{3}H-leucine and ^{14}C-leucine .

B. Threshold Studies

The effects of 12 hr PURO (20 µg/ml, 37 µM) and 12 hr CHX (500 µg/ml, 1.8 mM) pulses on the gel pattern of label incorporated into eyes were determined. Eyes received drug pulses about 1 1/2 days after dissection, from CT 17 to CT 5. These doses, when applied as 12 hr pulses at the same phase in dose-response experiments (chapter V), were the minimal concentrations needed to phase-shift the eye CR. Experimental eyes received a 7 hr drug pulse followed by a 5 hr pulse of medium containing the same drug concentration and ^{3}H-leucine. Control eyes received a 7 hr pulse of PS-FSW followed by a 5 hr pulse

of medium containing ^{14}C-leucine. Two pairs of eyes were used in 20 µg/ml PURO pulse experiments, and two pairs were used in 500 µg/ml CHX pulse experiments. Each pair of eyes was ground together and electrophoresed on a gel.

The gel patterns of incorporated label were changed by the PURO and by the CHX pulses. Because the changes in the incorporation patterns were small, only the ratio patterns of the gels are presented in figure 3A, B. The ratio pattern helps to visualize small differences between the gel patterns of experimental and control eyes. Figures 3A, B show that the shape and level of the ratio patterns are changed by PURO or CHX treatment. There is a pronounced decrease in the ratio values of the gel at molecular weights above 75 K daltons in PURO-treated eyes. A less steep decrease is seen in CHX-treated eyes (fig. 3A).

The ratios of total ^{3}H-cpm to total ^{14}C-cpm in each of the two gels of PURO-treated eyes and each of the two gels of CHX-treated eyes are presented in table I. Relative to their paired ^{14}C-labeled controls, PURO and CHX-treated eyes incorporated about half the amount of ^{3}H-leucine than did ^{3}H-labeled control eyes.

C. <u>The Kinetics of PURO Inhibition</u>

A series of experiments was designed to test the reversibility of changes in the gel pattern of incorporated ^{3}H-leucine caused by administration of PURO pulses to eyes. In an effort to increase the chance of seeing large changes in the gel pattern of eyes labeled

after a PURO pulse compared to the gel pattern of eyes labeled during a PURO pulse, all experimental eyes received a 125 µg/ml pulse of PURO. The pulse was administered from CT 17 to CT 5, one day after dissection. Two experimental eyes were labeled with ^{3}H-leucine during the last 5 hrs of the PURO pulse; two were labeled for 8 hrs beginning 2 hrs after the end of the pulse; two were labeled for 8 hrs beginning 12 hrs after the pulse and two were labeled for 8 hrs beginning 20 hrs after the pulse. Paired control eyes were labeled with ^{14}C-leucine at the same time their corresponding experimental eyes were labeled with ^{3}H-leucine.

The effect of 125 µg/ml PURO pulses on the gel pattern of ^{3}H-leucine incorporated during the drug pulse was very striking compared to the pattern of ^{14}C-labeled controls. As seen in figure 4A, ^{3}H-leucine incorporation was strongly inhibited at molecular weights above 12 K daltons. The ratio patterns (fig. 4B) revealed that the inhibition of ^{3}H-leucine incorporation increased with the apparent molecular weight of the labeled material. The ratio of total ^{3}H-cpm to total ^{14}C-cpm in the two gels of eyes labeled during a 125 µg/ml PURO pulse was only 15% of that computed for control gels. The decrease in the ratio was significant at the 95% confidence level (table II).

Eyes labeled from 2 to 10 hrs after the removal of a PURO pulse showed a dramatic recovery of ^{3}H-leucine incorporation. The ratio patterns (fig. 5A) showed a prominent peak between about 72 K and 109 K molecular weights, and a minor peak at about 20 K and

possibly at 38 K. The decreasing incorporation seen at high molecular weights during the PURO pulse was no longer present. In addition, the ratio of total ^{3}H-cpm to total ^{14}C-cpm recovered to a level close to that of control eye pairs (table II). Eyes labeled from 12 to 20 hrs (fig. 5B) after the end of the PURO pulse, and from 20 to 28 hrs (fig. 5C) after the pulse, had ratio patterns that showed a peak at about 20 K daltons, but that no longer had a peak at 72 K - 109 K daltons. There was little additional change in the ratio of total ^{3}H-cmp to total ^{14}C-cpm (table II) compared to the ratios calculated for eyes labeled 2 to 10 hrs after the end of the PURO pulse.

IV Discussion

A. Control Vs. Control Eyes

The similarity in the gel incorporation patterns of a ^{3}H-labeled eye and a ^{14}C-labeled eye taken from the same animal demonstrates that one eye is a valid control for the other. The variability in the ratios of total ^{3}H-cpm to total ^{14}C-cpm in the two control vs. control gels (table I) was similar to the variability in the ratios of leucine incorporation values computed for control vs. control experiments of chapter V (see chapter V , table I). When expressed as a relative error (standard deviation/mean) the variability of the former set of experiments was ± 21.5%, while the variability of the latter set was ± 16.7%. These two relative errors are not significantly different (F test).

The mean of the two ratio values computed for control vs.

control experiments was 20% below the value expected on the basis of equimolar ^{3}H-leucine and ^{14}C-leucine incorporation. A similar discrepancy was found by Ram (5), in this laboratory, when analyzing gels of aqueous soluble material from Aplysia parietovisceral ganglia that were simultaneously labeled with ^{3}H-leucine and ^{14}C-leucine. He found the ratio of total ^{3}H-cpm to total ^{14}C-cpm to be as much as 64% below the value calculated on the basis of specific activities and counting efficiencies. Some, but not all of the discrepancy could be explained by the existence of a volatile ^{3}H-labeled component in the medium containing ^{3}H-leucine. The nature of the remaining discrepancy was not resolved.

Some evidence suggests that the lowering of the ratio values in control vs. control gel experiments was due to the ^{3}H-leucine being radiochemically impure. Experiments were designed to measure the ratio of ^{3}H-leucine-cpm to ^{14}C-leucine-cpm in a medium composed of equal volumes of a ^{3}H-leucine medium and a ^{14}C-leucine medium. An aliquot of the combined medium was dinitrophenylated (as in chapter V , appendix II), extracted into the organic phase of an aqueous: ether system, and chromatographed on silica gel TLC. The ratio of ^{3}H-cpm to ^{14}C-cpm in the DNP-leucine spot of the TLC plate was 18% lower than the ratio of the untreated medium. If the medium was first evaporated before being counted, the ratio was lowered by only 8%. The ratio of the ^{3}H-cpm to ^{14}C-cpm in the aqueous fraction was 116% higher than that in the untreated medium. These results suggest that the ^{3}H-leucine used in the medium was about 82% radiochemically pure,

assuming 100% ^{14}C-leucine radiochemical purity. The cause of the lack of purity could be radiolysis, since the specific activity of the stock ^{3}H-leucine was very high (46 Ci/mM).

A 20% loss of stock ^{3}H-leucine purity could account for the lowered ratio of total ^{3}H-cpm to total ^{14}C-cpm found in control vs. control gels. Dilution of the stock ^{3}H-leucine with cold leucine to make the labeling medium would lower the specific activity of the medium by 20% of the expected value. An alternative, but less likely, explanation is that the amount of cold leucine used in the dilution was too high.

B. Threshold Studies

The data presented in this chapter have shown that the minimal doses of PURO and CHX capable of phase shifting the CR of the eye also influenced the level and gel pattern of incorporated ^{3}H-leucine. Both of these changes are reflected in the ratio histograms of eyes treated with 20 µg/ml PURO pulses or 500 µg/ml CHX pulses. Both drug treatments caused the level of the ratio pattern to drop to about half that of control eyes at molecular weight regions below 75K daltons, and to decline to even lower values at molecular weight regions above 75K daltons. The decline in the ratio pattern of PURO-treated eyes was more severe than that of the CHX-treated eyes. The decline in the ratio patterns suggests that synthesis of proteins larger than 75K daltons is more extensively inhibited than the synthesis of lower molecular weight proteins.

Preferential inhibition of higher molecular weight protein synthesis is consistent with the mechanism of PURO action, but not with that of CHX action. Since PURO inhibits protein synthesis by prematurely terminating nascent polypeptide chains (2), the probability of a peptide being terminated by PURO should depend, at least in part, on the number of amino acid residues it contains. The mechanism of PURO action, however, does not provide an explanation for the flat ratio pattern seen at molecular weights below 75K daltons. If CHX were inhibiting protein synthesis by slowing the initiation, elongation or termination of growing peptide chains (2), the incorporation of label should be equally inhibited at all regions of the gel. Thus, the slight decline in the ratio pattern of CHX-treated eyes remains unexplained.

The decrease in the ratio of total ^{3}H-cpm to total ^{14}C-cpm in these PURO and CHX experiments was not statistically significant, possibly because of the low sample size. Thus the lowering of the ratio levels, and the slope in the ratio patterns must be regarded as qualitative changes until more experiments are conducted.

C. Kinetics of PURO Inhibition

The level and shape of gel ratio patterns changed as a function of the time eyes were labeled relative to the delivery of a 125 µg/ml PURO pulse. The ratio pattern of eyes labeled during the last 5 hrs of the PURO pulse showed inhibition of leucine incorporation at all molecular weights above 12 K. The amount of inhibition increased with molecular weight. This effect appears similar to that seen

with eyes labeled during 20 µg/ml PURO pulses, except that the ratio pattern in the latter case sloped downwards at molecular weights above 75 K daltons instead of 12 K daltons. More severe inhibition of the synthesis of lower molecular weight proteins should result from increasing the dose of PURO, since the average number of amino acids incorporated between PURO-induced termination events should be lowered. The rise in the ratio pattern at low molecular weights probably results from leucine incorporation into some combination of peptidyl-PURO molecules and normal proteins. Identification of peptidyl-PURO would be possible in similar experiments by using labeled PURO.

An inhibition of incorporation into high molecular weight material with an attendant increase in low molecular weight incorporation was found by Wilson (6) in the gel pattern of neuron R2 of Aplysia, when the isolated PVG was labeled for the last 19.5 hrs of a 21.5 hr pulse of 1 mg/ml PURO. The increase of incorporation into low molecular weight material was most likely caused by the production of peptidyl-PURO.

Eyes labeled 2 to 10 hrs after the end of the PURO pulse had incorporation ratios that were close to control levels, and ratio patterns which showed a major peak between 72 K and 109 K daltons. This peak may be related to the rebound in spontaneous CAP activity seen from 0 to 7 hrs after the end of 125 µg/ml PURO pulses in dose-response experiments (chapter VI). If true, this hypothesis would predict that eyes labeled from 2 to 10 hrs after the end of a 20 µg/ml PURO pulse would not have a peak at the 72 K to 109 K region of the

ratio histogram, since in dose-response experiments, eyes pulsed with this concentration of PURO showed no rebound in spontaneous CAP activity (chapter VI).

Eyes labeled from 12 to 20 hrs, or from 20 to 28 hrs after the end of the 125 µg/ml PURO pulse had ratios of total ^{3}H-cpm to total ^{14}C-cpm that were close to the ratios in control vs. control experiments, and ratio patterns showing a peak at 20 K daltons. This peak was the only feature of the ratio pattern that differed from the ratio pattern in control vs. control experiments. Hence, with the exception of the 20 K dalton peak, the effects of PURO on leucine incorporation appeared reversible within 12 hrs after its removal.

The existence of a 20 K dalton peak in the ratio pattern of eyes labeled 12-20 hrs or 20-28 hrs after the end of the PURO pulse suggests two alternative interpretations. First, the peak may represent an effect of PURO on protein synthesis that is not readily reversible. If so, a peak at 20 K daltons might occur in the ratio pattern of eyes labeled from 28 to 36 hrs after the end of the PURO pulse. Alternatively, the 20 K dalton peak may be due to a difference in the spectrum of proteins synthesized by eyes whose CRs are out of phase. This interpretation is based on the finding that eyes given 125 µg/ml PURO pulses in dose-response experiments (chapter VI) expressed CRs that were phase delayed by about 12 hrs. If this interpretation were true, then the ratio pattern of eyes labeled 28-36 hrs after the

end of the PURO pulse would have a trough at the 20 K dalton region. Furthermore, control eyes labeled 12 hrs out of phase would be expected to have different gel patterns at the 20 K dalton region.

The effects of PURO on the magnitude of amino acid incorporation have been reversible in other in vivo systems. Mueller et al. found that ^{14}C-leucine incorporation into HeLa cells was completely inhibited during 2 hr and 4 hr pulses of PURO (10 µg/ml), and that the rate of incorporation returned to 75% and 50%, respectively, of control values during the 6-8 hrs following removal of the drug (7). Williamson and Schweet showed that reticulocytes incubated for 10 min in the presence of 2.5×10^{-4} M PURO did not incorporate ^{14}C-valine, but that after the drug was removed, the incorporation rate measured over the next 30 min was at the control value (8). Although these experiments show that the inhibition of incorporation caused by PURO can be reversed, they give no indication of the spectrum of proteins being synthesized. Small changes in this spectrum would surely not have been detected in these studies. The reservations raised in chapter V regarding the interpretation of incorporation experiments are applicable in this chapter as well. Briefly, changes in the level and shape of ratio patterns derived from double labeled gels may, in part, be due to changes in the specific activity of intracellular leucine pools, and not the result of changes in the level of protein synthesis. In addition, changes in the gel pattern of label incorporated into the eye may not reflect changes in the pattern of incorporation at the circadian oscillator of the eye.

APPENDIX I

Behavior of Molecular Weight Standards on SDS-polyacrylamide Gels

The mobility of protein standards on the gel system used in this chapter was determined to allow assignment of molecular weight values to ^{3}H- and ^{14}C-leucine radioactivity incorporated in the Aplysia eye. SDS-polyacrylamide electrophoresis has been shown by Weber and Osborn to separate proteins by molecular weight (9), presumably because the anionic detergent (SDS) coats the protein in solution, and thus causes its mobility in the gel through a positive electrical field to be dependent on size alone. The authors showed that the mobility of protein standards, relative to bromphenol blue, was a linear function of the logarithm of the standard's molecular weight. The standards ranged from 11,000 (11 K) to 220,000 (220 K) daltons in molecular weight. Since the sample buffer used in these studies contained a reducing agent (2-mercaptoethanol), protein subunits linked by disulfide bonds were separated.

Four protein standards were electrophoresed on the gel system used in this chapter. The standards were bovine serum albumin, molecular weight 68 K (10); human gamma globulin, molecular weights 50 K and 23.5 K, respectively, for the heavy and light subunits (11); horse heart cytochrome C, molecular weight 11.7 K (9); and bovine pancreas insulin, molecular weights 3.5 K and 2.2 K, respectively, for the B and A subunits, calculated from their amino acid sequences

presented in (12). The four standards were run four times each on gels; each standard was run two times on a gel by itself, and two times on a gel containing all four standards. When run separately, 4 µg of each standard, dissolved in 20 µl sample buffer, was applied to a gel and run as in Methods of this chapter. When all four standards were run together 1 µg each was applied in a total sample volume of 20 µl.

After electrophoresis, the position of the tracking dye (bromphenol blue) on each gel, and the length of each gel were noted. Gels were then removed from their glass tubing, and stained overnight in a solution of water:methanol:acetic acid (10:10:2) containing 0.5% Coomassie Brilliant Blue stain. Gels were destained in water: methanol:acetic acid (65:25:10) and stored in 7.5% acetic acid, 5% methanol. The positions of the dye band(s), and length of the gel were noted. The mobility of the band(s) in each gel was calculated by the formula:

$$\text{Relative Mobility} = \frac{\text{length of gel before staining}}{\text{migration of tracking dye}} \times \frac{\text{migration of standard}}{\text{length of gel after staining}}$$

The length of each gel after staining and storage was very close to its length before staining.

The results of the relative mobility calculations for the four protein standards are presented in table III. No systematic differences

were seen between the relative mobilities of standards run separately, and standards run together. The average of the four relative mobility determinations for each standard is plotted relative to the known molecular weight of the standard in figure 6. Also included in figure 9 is a line, which is a least squares fit to the four relative mobility determinations made for each standard, except insulin. The insulin data were not used in the least squares calculation because the molecular weight of the peptide(s) that ran as a single band could not be unambiguously assigned. Thus, it could not be determined whether insulin ran as 3.5 K and 2.2 K subunits whose bands could not be separately resolved, or a single 5,700 molecular weight species, or some combination of the two possibilities.

The data plotted in figure 9 show that proteins from 12 K to 68 K daltons in molecular weight have mobilities, relative to bromphenol blue, that are a linear function of the logarithm of their molecular weights. This finding is in good agreement with that of Ram in this laboratory. Ram used the same gel system to electrophorese material from the Aplysia PVG (5).

For proteins below 12 K daltons in molecular weight, the molecular weight determination is unreliable. A loss of molecular weight resolution in proteins of high mobility was seen by Wilson (6) and Dunker and Reuckert (13) using 5% polyacrylamide gels. Fortunately, very little incorporated radioactivity in the Aplysia eye runs with an apparent molecular weight below 12 K daltons.

Some problems are encountered in applying the curve determined for purified protein standards to the assignment of molecular weight to incorporated radioactivity in the eye. The first problem is that the protein standards may not have the same relative mobilities when electrophoresed together with an eye sample. Although this possibility was not tested, Ram, in this laboratory, using the same gel system, showed that protein standards did retain their mobility properties when electrophoresed with aqueous soluble extracts from the Aplysia PVG (12). Second is the problem that not all proteins of known molecular weight have mobilities that are closely predicted by the standard curve. Shapiro et al. (3), and later Dunker and Reuckert (13) showed that the mobility of ribonuclease A was below that expected on the basis of molecular weight determinations by other methods. Furthermore, Glossman and Neville (14) have shown that glycoproteins tend to migrate through the gel more slowly than predicted on the basis of known molecular weight. The third problem is the possibility of banding artifacts. Reports by Brewer (15) and by Mitchell (16) have demonstrated that certain purified proteins yield multiple bands upon electrophoresis. Apparently residual ammonium persulfate in the gel can cause an oxidation of sulfhydryl or other groups in the protein, and thus slightly change its electrophoretic mobility.

Because the three abovementioned problems have not been exhaustively tested in the gel system used in this chapter, the

molecular weight values assigned to incorporated material should be considered as approximations.

TABLE I

Total CPM in Gels From Threshold Studies

	Experiment Experiment	Hrs of Label	Total ^{3}H-CPM*	Total ^{14}C-CPM*	Ratio# $^{3}H/^{14}C$	Average Ratio# ± SD	Per Cent Control	P@
I.	Cont. vs Cont.							
	1.	8	11810	3338	3.54			
						4.18 ± 0.90	100	-
	2.	8	11513	2388	4.82			
II.	PURO - 20 µg/ml							
	1.	5	4396	2191	2.01			
						1.95 ± 0.08	47	< 0.1
	2.	5	6495	3424	1.90			
III.	CHX - 500 µg/ml							
	1.	5	4697	2281	2.06			
						1.86 ± 0.28	44.5	< 0.1
	2.	5	3595	2169	1.66			

*Corrected for ^{3}H and ^{14}C background of 11.8 and 11.4 cpm/slice, respectively; and for 19.6% spillover of ^{14}C into ^{3}H channel.

#Experiment number 1 in each group is represented by a ratio histogram in the figures of this chapter.

@P is determined by the use of a t test comparing the average experimental vs. control ratio with the average control vs. control ratio.

Control vs. control experiments were labeled from CT 6:30 to CT 14:30, 2 days after dissection.

PURO vs. control and CHX vs. control experiments had drug pulse and control pulse administered from CT 17 to CT 5, 1½ days after dissection, and were labeled during the last 5 hrs of the drug pulse or control pulse.

TABLE II

Kinetics of PURO Inhibition

	Experiment	Hrs of Label	Total ^{3}H-CPM	Total ^{14}C-CPM	Ratio $^{3}H/^{14}C$	Average Ratio ± SD	Per Cent Control	P
I.	Cont. vs Cont.*							
	1.	8	11810	3338	3.54	4.18 ± 0.90	100	-
	2.	8	11513	2388	4.82			
II.	During Pulse#							
	1.	5	1966	3354	0.59	0.63 ± 0.06	15	< 0.05
	2.	5	2261	3388	0.67			
III.	After Pulse 2-10 Hrs							
	1.	8	13640	3566	3.83	4.10 ± 0.38	98	> 0.9
	2.	8	17916	4102	4.37			
IV.	After Pulse 12-20 Hrs							
	1.	8	15059	3724	4.04	4.08 ± 0.05	97	> 0.9
	2.	8	13429	3264	4.11			
V.	After Pulse 20-28 Hrs							
	1.	8	6866	1981	3.47	4.12 ± 0.92	99	> 0.9
	2.	8	12202	2560	4.77			

*Repeated from table I.

#Experimental eyes in groups II to V were pulsed with 125 µg/ml PURO from CT 17 to CT 5, 1½ days after dissection. Eyes in group I were labeled during last 5 hrs of drug or control pulse.

Other details as in table I.

TABLE III

Mobility of Molecular Weight Standards

on SDS-Polyacrylamide Gels

Standard	BSA	Gamma-G-H	Gamma-G-L	Cyto C	Insulin
Molecular Weight	68 K	50 K	23.5 K	11.7 K	5.7 K: 3.5 K + 2.2 K
Relative Mobility ± SD	0.560 ± 0.002	0.628 ± 0.003	0.893 ± 0.012	1.092 ± 0.003	1.310 ± 0.009
N	4	4	4	4	4

Figure 1

Structures of PURO, amino acyl-adenosine and CHX. Amino acyl-adenosine is the 3' terminal nucleoside of amino acyl-tRNA. Figures taken from Gale et al., 1972 (2).

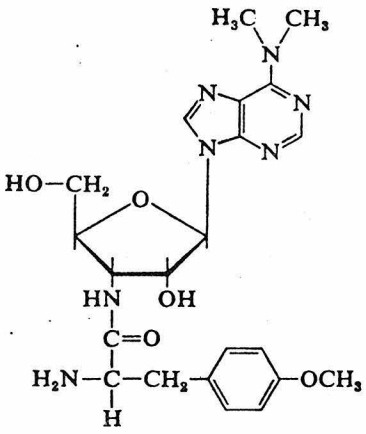

Puromycin

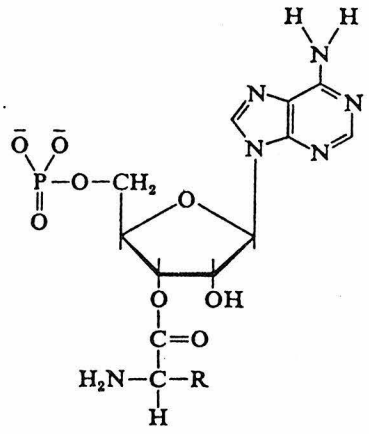

Amino acyl-adenosine

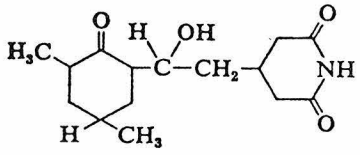

Cycloheximide

Figure 2

A: Gel incorporation pattern for a pair of control eyes labeled from CT 6:30 to CT 14:30, 2 days after dissection. Both eyes were taken from the same animal; one eye was labeled in a medium containing ^{3}H-leucine while the other was labeled in a medium containing ^{14}C-leucine. Eyes were homogenized together and electrophoresed on a gel, which was then fixed and sliced. Raw ^{3}H (■) and ^{14}C (□) radioactivity in each slice was then determined. Molecular weight scale was determined from the mobility of protein standards (fig. 6, table III), which varied linearly with the logarithm of their molecular weight in the range from 12 K daltons to 68 K daltons. Slice number 1 is at the top of the gel.

B: Histogram of the ^{3}H-cpm to ^{14}C-cpm ratio computed for each slice of the gel represented in part A. Background radioactivity was subtracted before the ratios were computed. However, spillover of ^{14}C radioactivity into the ^{3}H channel was not subtracted, causing the ratio histogram to be uniformly raised by a value of 0.2. No ratio has been computed for slices having fewer than 25 raw ^{3}H-cpm or ^{14}C-cpm.

CONTROL

LABEL: CT 6:30 – CT 14:30

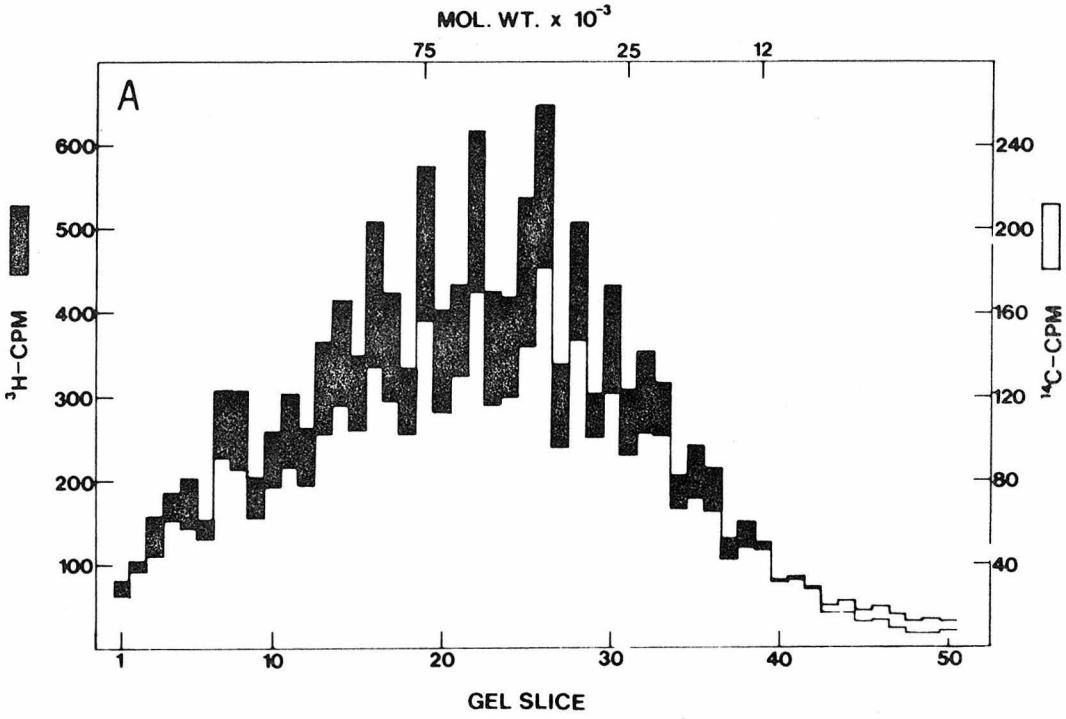

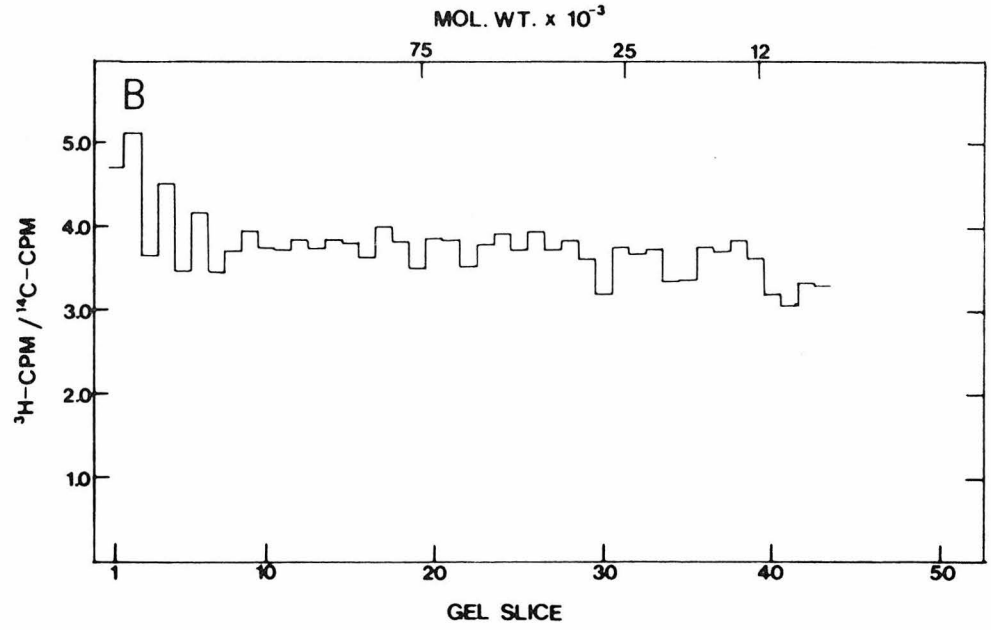

Figure 3

A: Ratio histogram derived from the gel incorporation pattern of a pair of eyes from the same animal. One eye was treated with a 20 µg/ml pulse of PURO from CT 17 to CT 5, 1½ days after dissection, and labeled with ^{3}H-leucine during the last 5 hrs of the PURO pulse. The other eye was treated with PS-FSW from CT 17 to CT 0, and then labeled with ^{14}C-leucine from CT 0 to CT 5. Gel had a total of 47 slices. Other details are presented in figures 2A and 2B.

B: Ratio histogram derived from gel of ^{3}H-labeled experimental eye treated with 500 µg/ml CHX, and ^{14}C-labeled control. Gel had a total of 50 slices. Other details as in part A.

DRUG PULSE: CT 17 – CT 5

LABEL: CT 0 – CT 5

PUROMYCIN, 20 μg / ml

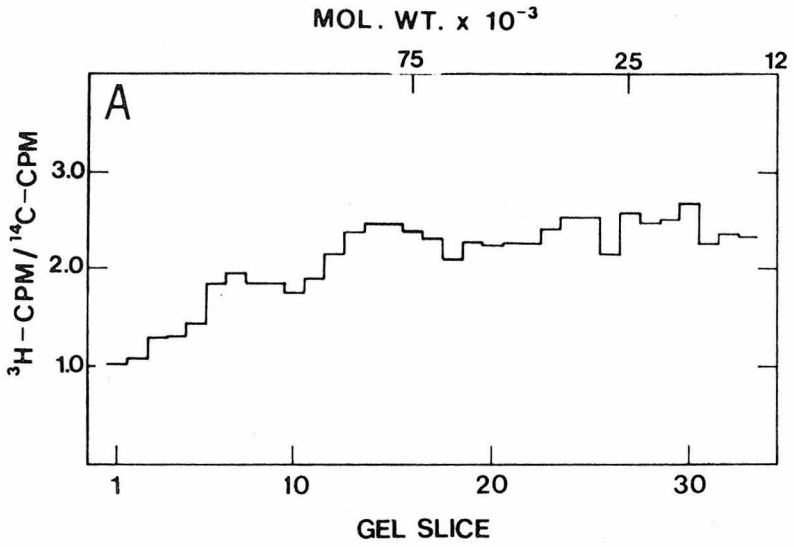

CYCLOHEXIMIDE, 500 μg / ml

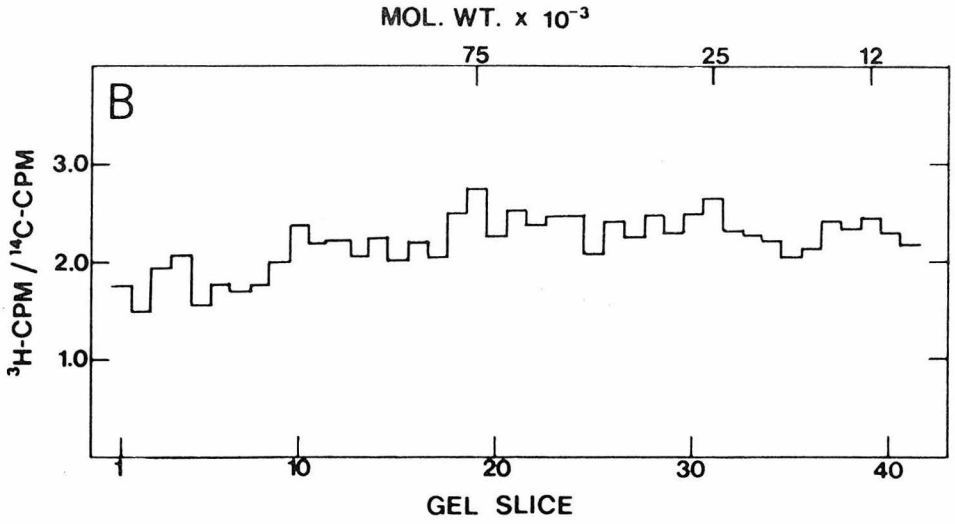

Figure 4

A: Gel incorporation pattern of a pair of eyes from the same animal. One eye was treated with a 125 µg/ml pulse of PURO from CT 17 to CT 5, 1½ days after dissection, and was labeled with ^{3}H-leucine during the last 5 hrs of the PURO pulse. The other eye was treated with PS-FSW from CT 17 to CT 0, and was then labeled from CT 0 to CT 5 with ^{14}C-leucine. Other details as in fig. 2A.

B: Ratio histogram derived from gel incorporation pattern shown in part A. Other details as in fig. 2B.

PUROMYCIN, 125 µg/ml: CT 17–CT 5

LABEL: CT 0–CT 5

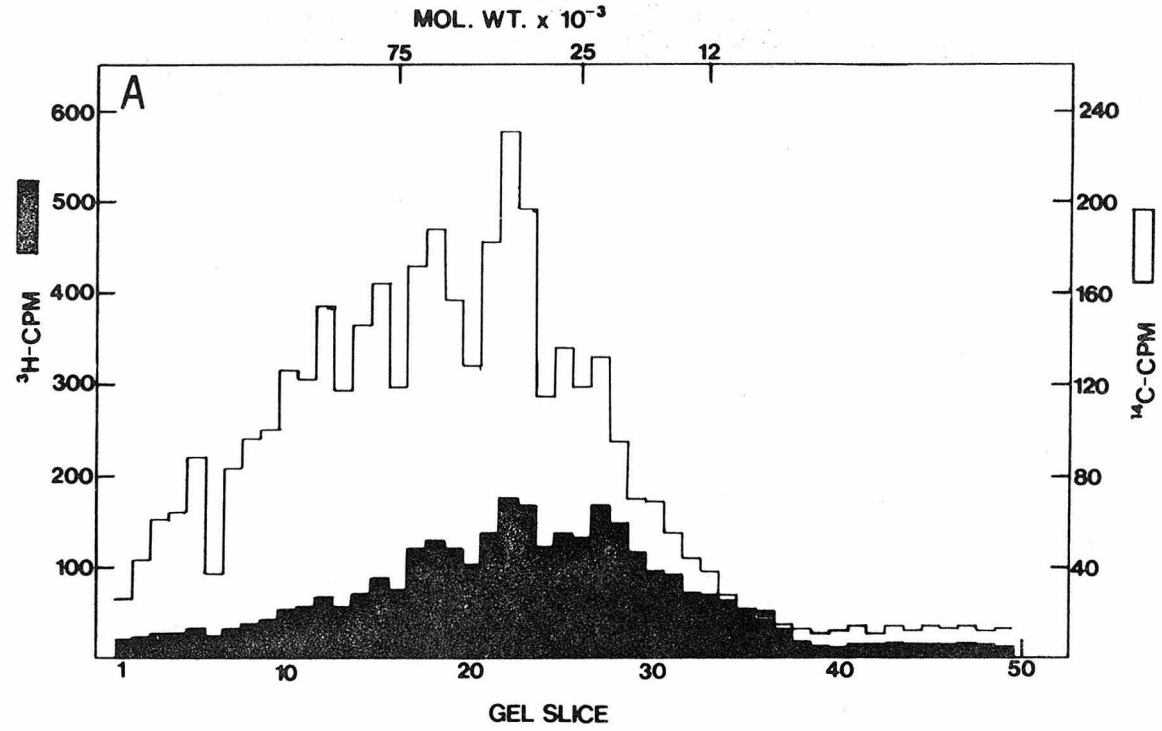

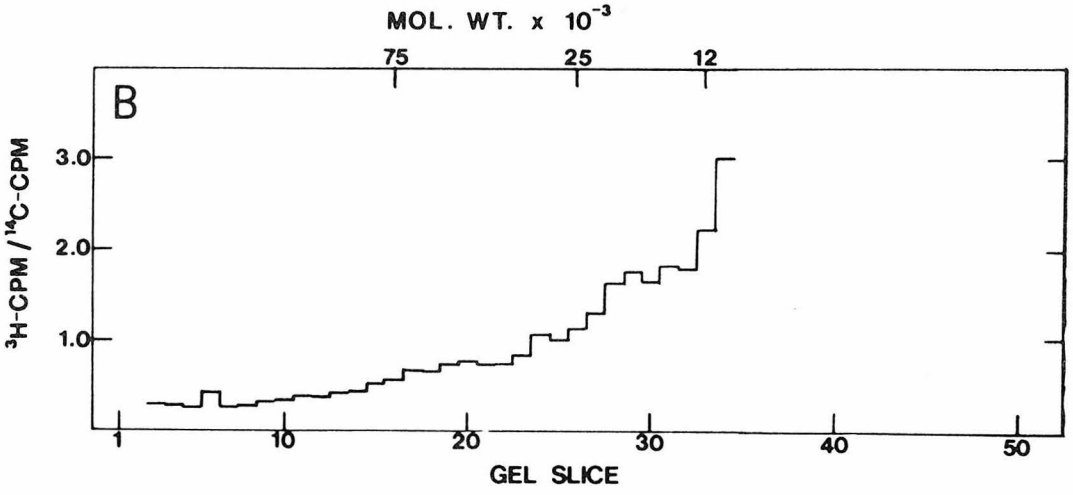

Figure 5

Ratio histograms derived from gel incorporation patterns of a pair of eyes labeled 2-10 hrs, A; 12-20 hrs, B; or 20-28 hrs, C; after the end of a PS-FSW or 126 µg/ml PURO pulse administered from CT 17 to CT 5, 1½ days after dissection. One eye of each pair was treated with PURO, and subsequently labeled with ^{3}H-leucine. The other eye was treated at the same time with PS-FSW, and subsequently labeled with ^{14}C-leucine. The gels each had a total of 49, 48, and 48 slices, respectively. Other details as in fig. 2B.

PUROMYCIN, 125 μg/ml: CT 17 – CT 5

LABEL ADMINISTRATION:

HOURS AFTER END OF DRUG PULSE

RATIO HISTOGRAM

2–10 HRS

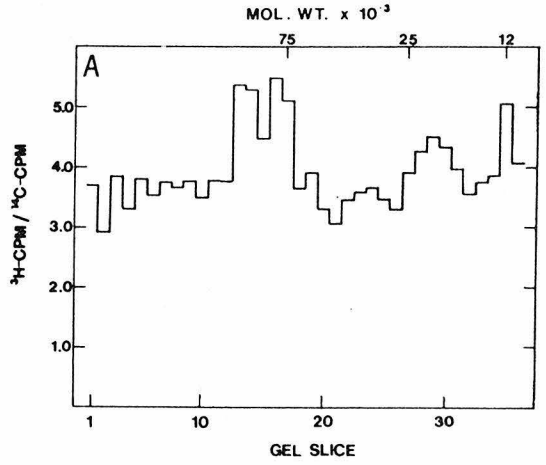

12–20 HRS

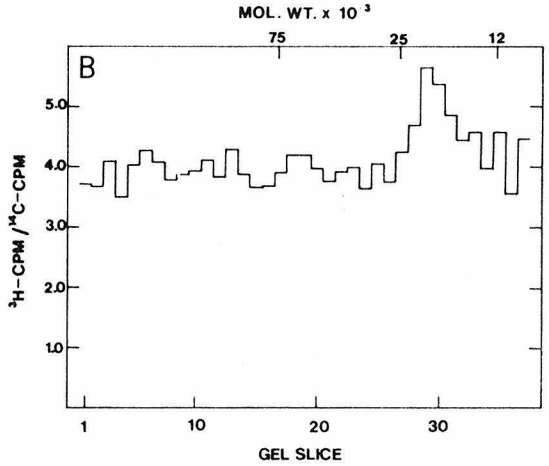

20–28 HRS

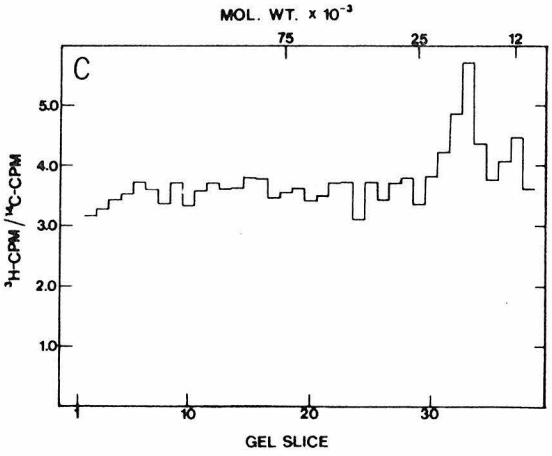

Figure 6

Plot of molecular weight (logarithmic scale) versus mobility on SDS-polyacrylamide gels relative to bromphenol blue for protein standards of known molecular weight. Protein standards represented by each point (●) are: bovine serum albumin, molecular weight 68 K daltons (A); human gamma globulin, heavy subunit, molecular weight 50 K daltons (B); human gamma globulin, light subunit, molecular weight 23.5 K daltons (C); horse heart cytochrome C, molecular weight 11.7 K daltons (D); bovine pancreas insulin, molecular weight 5.7 K daltons (E); bovine pancreas insulin, heavy subunit, molecular weight 3.5 K daltons (F); and bovine pancreas insulin, light subunit, molecular weight 2.2 K daltons (G). The position of points A-D relative to the abscissa represents the average of four mobility determinations. Since insulin ran on gels as a single band, points E-G represent two different interpretations of this result. Insulin may behave as an intact molecule (E) or as two subunits (F,G) that could not be resolved from each other. The position of points E-G relative to the abscissa is the same, and represents the average of four mobility determinations for the single insulin band.

The line is a least squares fit to all 16 mobility determinations for points A-D, and is described by the equation: $Y = -1.397X + 2.602$, where Y is the logarithm (base 10) of molecular weight in units of 1 K daltons, and X is mobility relative to bromphenol blue. The correlation coefficient of the correspondence between Y and X is 0.998 (Pearson product-moment).

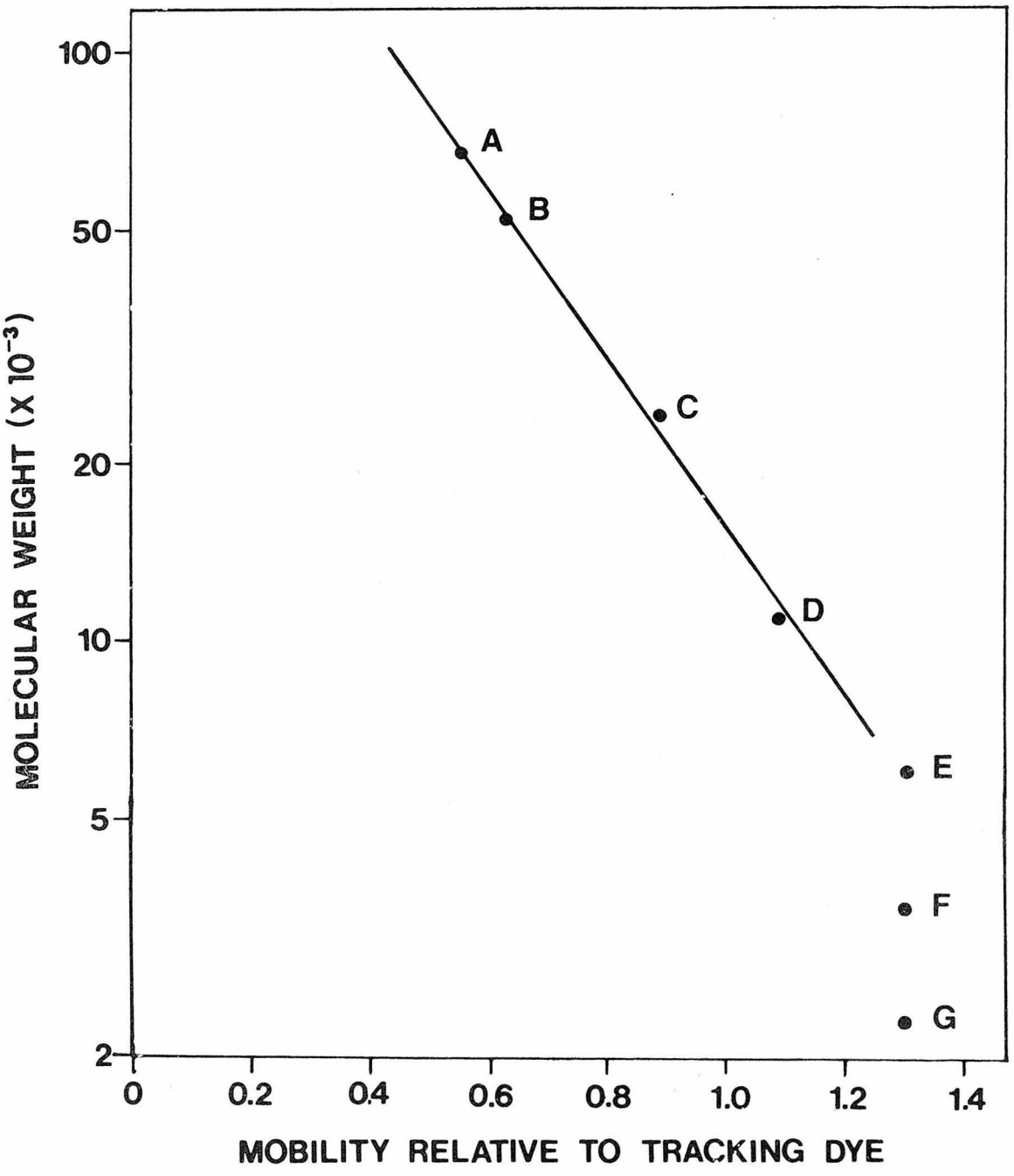
100
50
20
10
5
2
MOLECULAR WEIGHT (X 10⁻³)
A
B
C
D
E
F
G
0
0.2
0.4
0.6
0.8
1.0
1.2
1.4
MOBILITY RELATIVE TO TRACKING DYE

REFERENCES

1. Eskin, A. 1972. J. Comp. Physiol. 80: 353-376.

2. Gale, E. F., E. Cundliffe, P. E. Reynolds, M. H. Richmond, and M. J. Waring. The Molecular Basis of Antibiotic Action, Wiley and Sons, New York, 1972. pp. 278-379.

3. Shapiro, A. L. E. Vinuela, and J. V. Maizel. 1967. Bioch. Biophys. Res. Comm. 28: 815-820.

4. Ward, S. D. L. Wilson, and J. J. Gilliam. 1970. Anal. Biochem. 38: 90-97.

5. Ram, J. L. 1974. Thesis, California Institute of Technology. pp. 193-204.

6. Wilson, D. L. 1971. J. Gen. Physiol. 57: 26-40.

7. Mueller, G. C., K. Kajiwara, E. Stubblefield and R. R. Rueckert, 1962. Cancer Res. 22: 1084-1090.

8. Williamson, A. R. and R. Schweet. 1964. Nature 202: 435-437.

9. Weber, K. and M. Osborn. 1969. J. Biol. Chem. 244: 4406-4412.

10. Castellino, F. J. and R. Barker. 1968. Biochemistry 7: 2207-2217.

11. Edelman, G. M., W. E. Gall, M. J. Waxdal and W. H. Konigsberg. (ed.) 1972.

12. Sober, H. H. (ed.) 1970. Handbook of Biochemistry, Chemical Rubber Co., Cleveland, Ohio. pp. C263-C264.

13. Dunker, A. K. and R. R. Rueckert. 1969. J. Biol. Chem. 244: 5074-5080.

14. Glossmann, H. and D. M. Neville, Jr. 1971. J. Biol. Chem. 246: 6339-6346.

15. Brewer, J. M. 1967. Science 156: 256-257.

16. Mitchell, W. M. 1967. Biochem. Biophys. Acta 147: 171-174.

THESIS SUMMARY

The purpose of the experiments presented in this Ph.D. thesis was to test the dependence of the CR of the isolated Aplysia eye on the synthesis of macromolecules (RNA and protein). The test of this dependence required a method of altering the rates of RNA and protein synthesis. The most feasible approach was to use drugs that blocked the production of these macromolecules. An alternative, and perhaps more desirable approach of creating a more specific lesion by using mutants conditionally defective in RNA or protein synthesis was not possible because the genetics of Aplysia have not yet been worked out, and no such mutants are available in this species.

In an inhibitor experiment a pulse of AFTX, AMD, PURO or CHX was administered to an eye. AFTX and AMD were known to be inhibitors of RNA and protein synthesis, while PURO and CHX were known to be inhibitors of protein synthesis (chapter III). The effects of these drugs on the CR, biochemistry and electrophysiology of eyes were assayed so that the dependence of the CR on macromolecular synthesis could be tested according to the three criteria proposed in chapter I:

1) establishing that the inhibitors affected the time-keeping mechanism (circadian oscillator) underlying the CR,

2) demonstrating that the doses of the drugs capable of modifying the circadian oscillator (CO) could also significantly decrease the level of macromolecular synthesis,

3) showing that the modification of the CO was not a result of inhibitor side effects.

The following is a summary of the findings contained in this Ph.D.thesis, and a discussion of their relevance to the above criteria.

I. Modification of the Circadian Oscillator

The effect of an inhibitor on a CO cannot be measured directly. Although it has been demonstrated that single cells are capable of producing CRs, the intracellular components of the CO have not been identified in any circadian system. Thus, the state of the CO must be inferred from the state of the overt CR(s) or its response to entraining stimuli. It is generally accepted that the steady-state phase and period of the free-running CR are determined by the CO, in part because these properties can be conserved when the expression of the overt CR(s) is temporarily blocked. Hence, changes in the steady-state phase or period of the CR are inferred to reflect changes in the underlying "clock" mechanism (chapter I).

The structure of the CO of the Aplysia eye is not well understood. Although the CO is located, at least in part, at the base of the eye, identification of its cellular components has not been accomplished. At present it is not known whether the CO consists of a single circadian cell, a population of circadian cells or a population of non-circadian cells interacting to produce a CR. Hence, assays of the state of the CO were limited to recording of the CR of CAP activity from the optic nerve (chapter II).

The effects of AFTX and AMD on the CR of the eye could not be unambiguously interpreted as arising from modifications of the CO. In about half the AFTX experiments, and in all the AMD experiments, a 3 hr pulse of drug (16 µg/ml, 4 µg/ml, respectively) caused irreversible inhibition of the CR. Dose-response experiments showed that this inhibition resulted from the combined decrease of CR maxima and increase of CR minima. These results, coupled with periodogram analysis of dose-response experiments, suggested that the CR was blocked without a significant change in the free-running period. Although the blocking of the CR was consistent with the disruption of CO activity, the possibility of the two drugs interfering with the coupling between the CO and CR could not be eliminated. In the other AFTX experiments, a phase-delayed reduced-amplitude CR followed drug administration. Furthermore, in some AFTX and AMD experiments a delayed CAP activity onset appeared before inhibition of the CR. The phase and onset delays suggested that prior to, or in the absence of, CR inhibition, the CO of the eye was being affected. Thus, the transduction, if not the underlying mechanism, of the CR was inhibited by AFTX and AMD (chapter IV).

The results of experiments conducted with PURO and CHX indicated that these agents were capable of modifying the state of the CO. During a 12 hr pulse of PURO (5-134 µg/ml) CAP activity was depressed in a dose dependent manner, whereas during a 12 hr pulse of CHX (25-2000 µg/ml) beginning at the same time the level of CAP activity

was little affected except at the highest dose. From 0 to 7 hrs after the removal of PURO (50-134 µg/ml) or CHX (25-2000 µg/ml), a rebound of CAP activity occurred. Subsequent to this rebound, phase delays of 12-16 hrs were expressed in eyes treated with 20-134 µg/ml of PURO, and phase delays of 6-12 hrs were expressed in eyes treated with 500-2000 µg/ml CHX. A phase-response curve determined for the effects of 6 hr PURO (125 µg/ml) pulses was similar to that found by Eskin (1) for the application of high potassium pulses to the eye. PURO or CHX treatment, however, did not change the free-running period of the eye. These results indicated that PURO and CHX affected the CO, and that PURO acted at a step close to, or identical with, that affected by high potassium treatment (chapter VI).

II. Biochemical Effects of Inhibitors

Biochemical assays were generally conducted on eyes treated with the minimal dose of inhibitor necessary to affect the CR. These experiments were performed in a manner similar to those in which the effects of inhibitors on the CR were assayed.

To test the biochemical effects of AFTX (16 µg/ml) and AMD (4 µg/ml) on the eye, incorporation of ^{3}H-uridine and ^{14}C-leucine into TCA insoluble material was measured 1-9, 9-17, 49-57 and 73-81 hrs after administration of a 3 hr drug pulse (chapter V). Drug pulses were begun at CT 13, because phase response studies revealed that AFTX pulses had the best chance of inhibiting the CR when delivered at this phase (chapter IV). The biochemical experiments demonstrated

that AFTX and AMD inhibited uridine incorporation by about 50-75% during the first 17 hrs after removal of the drug pulse. At 49-57 hrs, and 73-81 hrs after the pulse, uridine incorporation was the same as that of controls. In AFTX-treated eyes, leucine incorporation was inhibited by 40-70% from 1-81 hrs after the end of the drug pulse; whereas in AMD-treated eyes, this incorporation was inhibited by about 20% at 49-57 hrs after the pulse. At all other times that uridine and leucine incorporation were measured, they were not significantly different from controls. These data demonstrated that doses of AFTX and AMD capable of inhibiting the CR also significantly inhibited uridine and leucine incorporation. Of the biochemical effects of the two drugs, only the inhibition of leucine incorporation appeared irreversible, and this was the only effect that corresponded to the irreversible inhibition of the CR caused by the two drugs (chapter V).

The biochemical effects of PURO and CHX were tested on leucine incorporation by means of electrophoresis of SDS-solubilized eye material onto 5% polyacrylamide gels. The gel system had the advantages of solubilizing over 93% of the incorporated material, and separating it according to molecular weight. In each experiment, a drug-treated eye was labeled with ^{3}H-leucine, while its control was labeled with ^{14}C-leucine; then both eyes were homogenized together and run on a single gel.

The effects on leucine incorporation were determined for eyes given 12 hr PURO (20 µg/ml) or 12 hr CHX (500 µg/ml) pulses begun at CT 17 (chapter VII). In dose-response studies, these doses were the

minimum that caused significant phase delays in the CR for 12 hr pulses delivered at the same phase (chapter VI). When the label was administered to eyes during the last 5 hrs of a PURO or CHX pulse, total incorporation was lowered by about 50%. The distribution of label in the gels of PURO-treated eyes showed increasing inhibition of incorporation with increasing molecular weight above 75 K daltons. For CHX-treated eyes, incorporation was inhibited equally at all molecular weights.

The reversibility of the effects of PURO on leucine incorporation was also studied. Eyes labeled during the last 5 hrs of a 12 hr PURO (125 µg/ml) pulse had total incorporation lowered by 85%. The distribution of label in the gels showed increasing inhibition of incorporation with increasing molecular weight above 12 K daltons. When eyes were labeled 2-10 hrs after the end of the PURO pulse, incorporation returned close to control levels, although the distribution of label in the gel showed increased incorporation at 72 K - 109 K daltons and at 20 K daltons relative to controls. Eyes labeled 12-20 hrs or 20-28 hrs after the end of the PURO pulse also had levels of total incorporation close to that of controls, but had increased incorporation at the 20 K dalton region of the gels. These experiments indicated that the minimal doses of PURO and CHX capable of phase shifting the CR inhibited leucine incorporation by about 50%. Furthermore, they demonstrated that the inhibition of leucine incorporation caused by PURO was almost completely reversible within 12 hrs after removal of the drug (chapter VII).

Interpretation of the biochemical effects of the four inhibitors required two caveats. First, changes in the intracellular specific activity of precursor pools could have influenced the rates of uridine and leucine incorporation independent of the rates of RNA and protein synthesis. Second, the inhibition of incorporation into the whole eye might not have been quantitatively or qualitatively the same as the inhibition of label into cell(s) comprising the CO (chapters V, VII).

The above reservations notwithstanding, it is tempting to point out that leucine incorporation was inhibited by about 50%, when measured during the last half of PURO and CHX pulses or soon after AFTX pulses. This correspondence hints at the possibility that leucine incorporation must be inhibited by about 50% for the CO to be affected. If a guess is to be made as to why AMD inhibited leucine incorporation by only 20%, a change of the intracellular pool activity is a reasonable choice. Reiger and Kafatos have shown that the intracellular specific activity of leucine in the galea of silkmoths increased by about 75% over a period of 6 hrs after the administration of 60 µg/ml of AMD for 1 hr (2). If the same effect took place in the Aplysia eye, then protein synthesis would have really been inhibited by 54%[a].

III. Side Effects of Inhibitors

Side effects of a drug are those effects that occur independent of the drug's primary action. In contrast, secondary effects are those that do result from this action. The primary actions of the drugs used in this study are defined as the inhibition of RNA and protein

synthesis. In some respects this definition is offered with reservation, since the mechanisms by which AFTX inhibits RNA and protein synthesis, and by which CHX and PURO inhibit RNA synthesis, is not well understood. This reservation also applies to the inhibition of protein synthesis by AMD, since this effect is most likely a secondary effect of inhibition of RNA synthesis. In contrast, the inhibition of RNA synthesis by AMD, and the inhibition of protein synthesis by PURO and CHX are clearly primary effects (chapter III). Nevertheless, the above definition does not appear to seriously affect the validity of the forthcoming discussion, and is thus provided for the sake of simplicity.

Part of demonstrating that the CR of the eye is dependent on macromolecular synthesis required that the effects of the inhibitors on the CR not be due to side effects. However, distinguishing between secondary effects and side effects in an inhibitor experiment is not often a simple problem. In chapter III three experimental approaches to this problem were proposed. The two approaches used in this study are discussed below:

1) Administration of inhibitors of dissimilar structure that affect the same primary activity. Effects common to all inhibitors would be implicated as primary or secondary effects, assuming that the drugs have no side effects in common. Effects not common to all would be possible side effects. This approach is useful in identifying primary and secondary effects, but cannot unambiguously identify side effects. Although the drugs may inhibit the same primary activity, qualitative and quantitative differences in their actions may produce some secondary effects not common to all.

2) Administration of structural analogues of an inhibitor that lack the primary inhibitory activity. Effects common to the analogues and inhibitor would be implicated as side effects, although not all side effects would be detected. Because of qualitative and quantitative differences in the side effects caused by these agents, some side effects would not be common to all.

Approach number 1 has been used in these studies to demonstrate that the modifications of the CR of the eye caused by the inhibitors were due to primary or secondary effects. Four inhibitors of dissimilar structure were administered to the eye, each capable of affecting the CR at a dose that inhibited macromolecular synthesis. These data suggested that the production of the CR was dependent on macromolecular synthesis with the provision that the four drugs did not have side effects in common at the electrophysiological or biochemical levels.

The electrophysiological properties of eyes were tested by recording spontaneous CAP activity and responses to 12 sec light pulses at various times before, during or after the administration of a drug pulse. Eight electrophysiological parameters were measured and compared quantitatively between experimental and control eyes. They were the latency, amplitude and frequency of both the phasic and tonic light responses, and the amplitude and frequency of spontaneous CAP activity. AFTX induced multiphasic tonic light responses during the drug pulse, and when applied near the peak of spontaneous CAP activity, increased spontaneous CAP frequency by 35% for the remainder of the activity cycle. AMD caused a 13% increase in spontaneous CAP

amplitude and a 10% decrease in tonic light response latency subsequent to its removal. PURO increased the amplitude of the tonic light response by 23% when measured more than 7 hrs after the end of the pulse. CHX caused a 32% increase in the tonic light response frequency measured 0-7 hrs after the end of the pulse, and a 33% decrease in the duration of spontaneous CAP bursts during the pulse (chapters IV and VI).

The results of these experiments showed that the drugs had very mild effects on the electrophysiological properties of the eye, and suggested that they were not modifying the CR due to toxic effects. Had the drugs altered the CR by reducing the population of cells in the eye, greater changes in the light responses and possibly spontaneous CAP activity would have been expected. Furthermore, these experiments suggested that the CR was not modified by electrophysiological side effects, because each drug caused different electrophysiological changes in the eye.

It also seems unlikely that the four drugs would have had biochemical side effects in common, although the possibility of common side effects can never be ruled out entirely. If one side effect is to be chosen as that most likely to be common to the four drugs, it is the inhibition of respiration. AFTX (3), AMD (4), CHX (5) and possibly PURO (6) inhibit respiration in other systems (chapter III). It is highly unlikely, however, that inhibition of respiration caused the CR modifications, because the electrophysiological properties of

neurons are highly dependent on respiration. A study by Giacobini has shown that the impulse amplitude and frequency of the isolated stretch receptor organ of the crayfish are very sensitive to the application of inhibitors of respiration, glycolysis, oxidative phosphorylation and citric acid cycle enzymes. In almost all cases, impulse activity was more sentitive to the inhibitor than was oxygen uptake. In contrast, Giacobini found no effect on impulse activity when 125-250 µg/ml of PURO or 1-2.5 µg/ml of AMD were applied to the stretch receptor for 9-12 hrs (7). It would therefore be reasonable to expect that if modification of the CR were caused by inhibition of respiration, then this side effect would cause similar electrophysiological changes in the eyes treated by the drugs. Clearly, this interpretation could be further tested by measuring oxygen consumption in eyes treated with AFTX, AMD, PURO or CHX, and by administration of inhibitors of respiration to the eye.

Approach number 2 has been used to a limited extent in these studies. PAN was administered as a control for PURO, and although it is a structural analogue of PURO, it did not affect the CR. Had it caused a similar phase shift to that caused by PURO without inhibiting protein synthesis, then this effect would have been due to a side effect. Similar approaches should have been possible with structural analogues of the other inhibitors used, for example AFTX-B_2, aflatoxicol, 2-deamino,2-chloro (or hydroxy) AMD, deoxyCHX (chapter III).

IV. Perspectives

The results of these Ph.D. thesis studies have shown that:

1) AFTX, AMD, PURO and CHX were capable of modifying the CR of the eye.

2) With regard to PURO and CHX, a strong case can be made that these modifications reflected changes in the underlying mechanism of the circadian clock; whereas in the case of AFTX and AMD this interpretation is clearly weaker.

3) Doses of AFTX and AMD capable of blocking the CR significantly inhibited the incorporation of uridine and leucine into the eye, while doses of PURO and CHX that could phase shift the CR inhibited leucine incorporation into the eye. The effect of PURO and CHX on uridine incorporation was not tested.

4) The drugs did not appear to modify the CR by means of causing electrophysiological or biochemical side effects.

These findings strongly suggest that the production of the CR of the isolated Aplysia eye is dependent on macromolecular synthesis. With respect to the field of circadian rhythms, these studies represent the most thorough evaluation of the dependence of CRs on macromolecular synthesis to date. Unfortunately, they do not elucidate the manner in which macromolecular synthesis is involved in the production of the CR. The solution to this problem awaits the identification of specific biochemical lesions that cause changes in the underlying properties of the CR. A combined genetic and biochemical approach would appear to be best suited for this task.

Footnote

[a] $\frac{\text{80\% control incorporation}}{\text{175\% control specific activity}}$ = 46% control protein synthesis = 54% inhibition.

REFERENCES

1. Eskin, A. 1972. J. Comp. Physiol. 80: 353-376.
2. Reiger, J. C. and F. C. Kafatos. 1971. J. Biol. Chem. 246: 6480-6488.
3. Doherty, W. P. and T. C. Campbell. 1973. Chem-Biol. Interactions 7: 63-77.
4. Laszlo, J., D. S. Miller, K. S. McCarty and P. Hochstein. 1966. Science 151: 1007-1010.
5. Gambetti, P., N. K. Gonatas and L. B. Flexner. 1968. Science 161: 900-902.
6. Garber, A. J., M. Jomain-Baum, L. Salganicoff, E. Farber and R. W. Hanson. 1973. J. Biol. Chem. 248: 1530-1535.
7. Giacobini, E. 1966. Acta Physiol. Scand. 66: 34-48.